STRUCTURAL AND MECHANISTIC INSIGHTS INTO HYDROLYTIC ENZYMES / INHIBITORS WITH SPECIAL REFERENCE TO ASPARTIC PROTEASES

A Thesis

Submitted To The

University Of Pune

For The Degree Of

Doctor Of Philosophy

(In Biotechnology)

by

VINOD V. P.

DIVISION OF BIOCHEMICAL SCIENCES

NATIONAL CHEMICAL LABORATORY

PUNE -411 008 (INDIA)

SEPTEMBER 2006

IN THE FOND MEMORIES OF

MY FATHER……

Research is to see what everybody else has seen,
and to think what nobody else has thought.

-Albert-Szent-Gyorgi (1893-1986) U. S. Biochemist.

TABLE OF CONTENTS

ACKNOWLEDGEMENT

To my extreme delight, I would like to evince my whole-hearted gratitude and indebtedness to my mentor ***Dr. (Mrs.) Mala Rao****, for introducing me to the fascinating realm of Molecular Biochemistry. I sincerely thank her for her excellent guidance, teaching, encouragement, benign attention, and for helping me out in most stressful times, both scientific and personal, which helped me to think positively and remain optimistic. Her scientific temperament, innovative approach, dedication towards her profession and down to earth nature has inspired me the most. Although this eulogy is insufficient, I preserve an everlasting gratitude for her.*

I express my profound gratitude to ***Dr. S. Sivaram****, Director, NCL, for allowing me to carry out my research in a prestigious and well-equipped laboratory. I also thank him for his constant support, encouragement and inspiration given to me through out the work. I am grateful to* ***Dr. Murali Sastry*** *for introducing me to the field of Nanotechnology and giving an opportunity to work in his area of research. I am also grateful to* ***Dr. (Mrs.) Vasanti Deshpande, Dr. Absar Ahmad, Dr. Sushuma Gaikwad*** *and* ***Dr. Vijayamohanan*** *for their encouragement and support.*

With much appreciation, I would like to mention the role of ***Dr. Milind S. Patole*** *and* ***Umasankar*** *for their help in my research works on cloning. I extend my thanks to* ***Rasesh, Badri, Sachin*** *and* ***Lokesh Sir*** *for the lighter moments shared. I am thankful to* ***Dr. Mahesh J. Kulkarni,*** *for his constant encouragement and help in MALDI experiments.*

I find words inadequate to express the appreciation of my affectionate seniors ***Dr. Chandravanu Dash*** *and* ***Dr. Jui Pandhare*** *for their constructive comments and suggestions, ceaseless inspiration, advice, and munificent support at all the time. Special thanks are to my seniors* ***Dr. Sudeep George, Dr. Anand Gole, Dr. Ashvani,*** *and friends* ***Sumant, Hrushi, Selvakannan, Girish, Sudheer*** *and* ***Maggie*** *for their help and inspiration. I extend my sincere thanks to* ***Mr. Ajish Kumar, K. S.*** *and* ***Vivek J. P*** *for their selfless support and encouragement.*

Thanks are also due to my lab mates ***Anish, Sharmili, Aarohi, Ajit, Nitin, Nilesh, Gyan, Priyanka, Dr. Rachna Pandey*** *and* ***Neha*** *for the cordial and friendly atmosphere in the lab.*

I express my gratitude to ***Mrs. Indira Mohandas*** *for her timely help rendered during the course of work. I am thankful to* ***Mr. R. Lambharte*** *for his untiring help in routine chores.*

I am grateful to ***Department of Science and Technology*** *(DST)* ***Govt. of India****,* ***Biotechnology Society of India*** *(BSI),* ***Research Foundation of NCL, India*** *(RF-NCL),* ***Federation of Asian and Oceanian Biochemists and Molecular Biologists*** *(FAOBMB),* ***International Union of Biochemistry and Molecular Biology*** *(IUBMB), and* ***Deutsche Forschungsgemeinschaft*** *(DFG, Germany) for the encouragement given in terms of awards.*

The fellowship awarded by ***University Grants Commission*** *(UGC)* ***Govt. of India*** *is gratefully acknowledged.*

I owe my deepest gratitude to ***my parents, brother, sister-in-law, my lovable nephew Kudus*** *and* ***Anamika*** *for their eternal support and understanding of my goals and aspirations. Without them, I would not have been able to complete much of what I have done and become who I am. They are the light that shines my way and the drive for my ever-persistent determination. Without their enduring support and encouragement, it would not have been possible to embark upon this journey in life.*

It gives me great strength and belief in presence of ***Almighty****, because of his blessing it was possible to bring the completion of my research endeavours in the best possible way. I bow to the divine strength and wish it would dwell throughout my life.*

Vinod V. P.

CERTIFICATE

Certified that the work incorporated in the thesis

STRUCTURAL AND MECHANISTIC INSIGHTS INTO HYDROLYTIC ENZYMES / INHIBITORS WITH SPECIAL REFERENCE TO ASPARTIC PROTEASES

submitted by **Mr. Vinod V. P.** was carried out under my supervision at the Division of Biochemical Sciences, National Chemical Laboratory, Pune, India. Material obtained form other sources has been duly acknowledged in the thesis.

September 2006

Dr. (Mrs.) Mala Rao
(Research Guide)

DECLARATION BY THE CANDIDATE

I declare that the thesis entitled **"STRUCTURAL AND MECHANISTIC INSIGHTS INTO HYDROLYTIC ENZYMES / INHIBITORS WITH SPECIAL REFERENCE TO ASPARTIC PROTEASES"** Submitted by me for the degree of Doctor of Philosophy is the record of work carried out by me under the guidance of **Dr. (Mrs.) Mala Rao** and has not formed the basis for the award of any degree, diploma, associateship, fellowship, titles in this or any other university or other institute of higher learning.

I further declare that the material obtained from other sources has been duly acknowledged in the thesis.

September-2006 **Vinod V. P.**

ABBREVIATIONS

3-APTS	3-aminopropyltrimethoxysilane
AAS	Atomic absorption spectrometry
ACN	Acetonitrile
AIDS	Acquired immuno deficiency syndrome
ATBI	Alkalo-thermophilic *Bacillus* inhibitor
ca	Circa
DAEE	Bis (2-(4-aminophenoxy) ethyl) ether
DCM	Dicholoromethane
DEAE	Diethylaminoethyl
DNSA	Dinitrosalicylic acid
DOX	Doxorubicin
E. coli	*Escherichia coli*
EDAX	Energy dispersive analysis of X-rays
F-Prot	Fungal aspartic proteases
FTIR	Fourier transform infrared spectroscopy
GST	Glutathione S- transferase
Hb	Hemoglobin
HIV	Human immunodeficiency virus
IC_{50}	50 % inhibitory concentration
ICM-MS	Intact cell matrix assisted laser desorption/ionization mass spectrometry
IGT-I	Insulin-like growth factor-I
IHF	Integration host factor
Int	Integrase
IUBMB	International union of biochemistry and molecular biology
MALDI	Matrix assisted laser desorption / ionization
MTCs	Magnetic targeted carriers
ODA	Octadecylamine
OPH	Organophosphorous hydrolase
OPTA	o-Phthalaldehyde
PCR	Polymerized chain reaction
pI	Isoelectric point
rp-HPLC	Reverse phase- high performance liquid chromatography
SA	Sinapinic acid
SDS-PAGE	Sodium dodecyl sulfate polyacrylamide gel electrophoresis
SEM	Scanning electron microscopy
TEM	Transmission electron microscopy
TFA	Trifluoroacetate
TS	Transition state
UV-Vis	Ultraviolet-visible
VDE	Violaxanthin de-epoxidase
Xis	Excisionase
XRD	X-ray diffraction
Xyl I	Xylanase from *Thermomonospora* sp.

ABSTRACT

"A molecule has no function in isolation - but once it interacts with another molecule, it can exhibit a variety of functions. Biomolecular interactions are often described according to the molecules that interact, their individual structures and the structure of the complex as well as the kinetics, forces, energetics and mechanism involved in it".

Enzymes are the catalytic cornerstones of metabolic activities of a living thing and most of the reactions in living organisms are being catalyzed by these molecules. Hence it can rightly be called the catalytic machinery of living systems. Man has directly or indirectly used enzymes in his daily life almost since the beginning of human history. Enzyme focused research is of favourite not only to biological community, but also with process designers, engineers and researchers working in other scientific fields. Apart from basic approach, enzymes are widely studied from an industrial point of view. Enzymes have been used since the dawn of mankind in cheese manufacturing and indirectly via yeasts and bacteria in food manufacturing. Isolated enzymes were first used in detergents in the year 1914, their protein nature proven in 1926 and their large-scale microbial production started in 1960s. The past few decades of the twentieth century have witnessed spectacular advances and betterment of living standards due to the beneficial integration of enzyme technology with scientific progress and rapid translation of laboratory findings into practical technologies and commercial-scale manufacturing processes. The hydrolases are a group of enzymes, which catalyze the bond cleavage by using water molecule. Studies on hydrolytic enzymes were always been of key interest to researchers due to its significant industrial applications and vital roles in human patho-physiology.

The present investigation is focused to understand the molecular mechanism of aspartic proteases, xylanases, their interactions with inhibitors and nanoparticles for its possible

industrial and biomedical applications. The present work has been organized under the following headings.

1) General introduction
2) Inhibition of xylanase by peptidic aspartic protease inhibitors
    i) Structural and mechanistic insights into the inhibition of xylanase by an aspartic protease inhibitor from an extremophilic *Bacillus* sp.
    ii) Slow-tight binding inhibition of xylanase by the specific aspartic protease inhibitor pepstatin
3) Biochemical studies on the enhancement of xylanase activity in presence of amino acids.
4) Molecular cloning and expression of an aspartic protease inhibitor in *Escherichia coli*
5) Development of gold nanoparticle based bioconjugates using fungal aspartic protease
    i) Gold nanoparticles assembled on amine-functionalized Na-Y zeolite: A biocompatible surface for enzyme immobilization.
    ii) Fabrication, characterization and enzymatic activity of fungal protease-gold nanoparticle membrane bioconjugate.

Chapter-1

General Introduction

This chapter presents an overview of the research carried out on hydrolytic enzymes, especially on proteases and xylanases with special emphasis on their occurrence, properties and industrial applications.

Chapter-2

Inhibition of Xylanase by peptidic aspartic protease inhibitors

Specific enzyme inhibitors for target enzymes are not only useful probes of the kinetic and chemical mechanisms of enzyme-catalyzed reactions, but their action mechanism provides background information for the development of specific bioactive compounds. This chapter describes the inhibition mechanisms and evaluates the kinetic parameters

associated with the interactions of xylanase, as a model system for hydrolytic enzymes, with aspartic protease inhibitors.

Part-1 Structural and mechanistic insights into the inhibition of xylanase by an aspartic protease inhibitor from an extremophilic *Bacillus* sp.

This section of the chapter describes the evaluation of the kinetic parameters of the slow-tight binding inhibition of xylanase by a peptidic inhibitor, *Alkalo Thermophilic Bacillus Inhibitor* (ATBI), from an extremophilic *Bacillus* sp. The steady-state kinetics revealed time-dependent competitive inhibition of xylanase by ATBI, consistent with two-step inhibition mechanism. The inhibition followed a rapid equilibrium step to form a reversible enzyme-inhibitor complex (*EI*), which isomerizes to the second enzyme-inhibitor complex (*EI**), which dissociates at a very slow rate. The rate constants determined for the isomerization of *EI* to *EI**, and the dissociation of *EI** were 13 ± 1 x 10^{-6} s^{-1} and 5 ± 0.5 x 10^{-8} s^{-1}, respectively. The K_i value for the formation of *EI* complex was 2.5 ± 0.5 μM, whereas the overall inhibition constant K_i* was 7 ± 1 nM. The conformational changes induced in xylanase by ATBI were monitored by fluorescence spectroscopy and the rate constants derived were in agreement with the kinetic data. Thus, the conformational alterations were correlated to the isomerization of *EI* to *EI**. ATBI binds to the active site of the enzyme and disturbs the native interaction between the histidine and lysine, as demonstrated by the abolished isoindole fluorescence of o-phthalaldehyde-labeled xylanase. The experimental results revealed that the inactivation of xylanase is due to the disruption of the hydrogen-bonding network between the essential histidine and other residues involved in catalysis and a model depicting the probable interaction between ATBI or OPTA with xylanase has been proposed.

Part-2 Slow-tight binding inhibition of xylanase by the specific aspartic protease inhibitor pepstatin

This part of the chapter describes the inhibition mechanism of xylanase by pepstatin, a specific inhibitor towards aspartic proteases. The kinetic analysis revealed competitive inhibition of xylanase by pepstatin with an IC_{50} value 3.6 ± 0.5 μM. The progress curves

were time dependent, consistent with a two-step slow tight binding inhibition. The inhibition followed by a rapid equilibrium step to form a reversible enzyme-inhibitor complex (*EI*), which isomerizes to the second enzyme-inhibitor complex (*EI**), which dissociates at a very slow rate. The rate constants determined for the isomerization of *EI* to *EI**, and the dissociation of *EI** were 15 ± 1 x 10^{-5} s^{-1} and 3.0 ± 1 x 10^{-8} s^{-1}, respectively. The K_i value for the formation of *EI* complex was 1.5 ± 0.5 μM, whereas the overall inhibition constant K_i* was 28.0 ± 1 nM. Pepstatin binds to the active site of the enzyme and disturbs the native interaction between the histidine and lysine, as demonstrated by the abolished isoindole fluorescence of o-phthalaldehyde-labeled xylanase. The experimental results revealed that the inactivation of xylanase is due to the interference in the electronic microenvironment and disruption of the hydrogen-bonding network between the essential histidine and other residues involved in catalysis and a model depicting the probable interaction between pepstatin with xylanase has been proposed.

Chapter-3

Biochemical studies on the enhancement of xylanase activity in presence of amino acids

This chapter describes the enhancement of xylanase activity from an alkalothermophilic *Thermomonospora* sp. by glycine. The xylanase activity increased seven-fold at alkaline pH in presence of glycine and its pH optimum shifted from 7 to 8 without using any protein engineering techniques. The steady state kinetics reveals that glycine in the reaction mixture increases the K_m and K_{cat} values of the enzyme from 3.6 to 8.2 mg / ml and 7.8 × 10^4 to 1.08× 10^5 min^{-1} respectively. Analysis of the enzyme conformation in presence of glycine using fluorescence spectroscopy obviates any changes in the tertiary structure of the enzyme. By using chemoaffinity-labelling technique, the structural integrity, polarity and the electronic microenvironment changes at the active site of the enzyme in presence of glycine has been investigated. The methyl and ethyl glycine esters had no effect on xylanase activity enhancement. This suggests that the enhancement of xylanase activity at alkaline pH range in the hydrolytic cleavage of the xylan in presence

of glycine is due to the involvement of carboxylate ion of glycine. A possible mechanism for enhancement of xylanase activity in presence of glycine has been proposed.

Chapter-4

Molecular cloning and expression of an aspartic protease inhibitor in *Escherichia coli*

The aspartic protease inhibitor (ATBI) purified from a *Bacillus sp*. is a potent inhibitor of recombinant HIV-1 protease, pepsin, fungal aspartic protease and xylanase. The molecule is of eleven amino acids and is peptidic in nature. The peptide sequence data of the 11-mer was exploited to synthesize the complementary oligonucleotides, which were annealed and subsequently cloned inframe with the gene for GST in to *Escherichia coli (E. coli)* BL21-A1 through the gateway cloning strategy. The expression clone was induced using arabinose which expressed the recombinant peptide as a fusion protein along with GST tag for the ease of purification. The recombinant peptide was purified using reduced glutathione column, and subsequently cleaved with Factor Xa to remove the GST-tag. The resultant product was further purified to homogeneity using *rp-HPLC*. The purified peptide was characterized using mass spectroscopy analysis. The recombinant peptide was found to be active *in vitro* against HIV-1 protease, pepsin, fungal aspartic protease and xylanase.

The cloned cells (*E coli*) expressing recombinant glutathione-S-transferase-peptidic inhibitor (GST-ATBI) gene was used as a model system to demonstrate the importance of intact cell matrix-assisted laser desorption/ionization mass spectrometry (*ICM-MS*) in drug discovery. Using ICM-MS analysis, a 28 kDa peak corresponding to the production of recombinant GST-ATBI under arabinose induced condition has been detected. The regulation of protein expression was studied using glucose as an alternative metabolite. The glucose-mediated regulation of the *ara*-operon was followed using ICM-MS technique. All these results obtained from ICM-MS data were validated using sodium dodecyl sulfate polyacrylamide gel electrophoresis (SDS-PAGE) analysis. The present technique can be extended for *in vivo* screening of drugs and it holds tremendous

potential to discover novel drugs against specific protein expressions in different diseases.

Chapter-5

Development of gold nanoparticle based bioconjugates using fungal aspartic protease

The interactions between artificial nanomaterials and biological systems form an emerging research topic of broad importance. Research efforts in this area are motivated by the hope that bio-nanomaterials will have useful applications in biology and medicine. The research interest of this part of the thesis is to design novel biocatalysts using gold as a template for enzyme immobilization. This chapter is divided into two sections, the first part describes the assembly of the gold nanoparticles on the surface of the amine-functionalized zeolite microspheres for the immobilization of the enzyme fungal protease. The second section deals with the synthesis of a free-standing nanogold membrane which was used as scaffolds for the immobilization of the enzyme fungal protease.

Part-1 Gold nanoparticles assembled on amine-functionalized Na-Y zeolite: A biocompatible surface for enzyme immobilization

Development of simple and reliable protocols for the immobilization of enzymes is an important aspect of biotechnology. Gold nanoparticles are known to bind enzymes, but reuse characteristics of the gold nano-enzyme bioconjugates has hitherto been poor. This chapter discusses the assembly of the gold nanoparticles on the surface of the amine-functionalized zeolite microspheres to form zeolite-gold nanoparticle 'core-shell' structures and thereafter, the use of this structure in the immobilization of the enzyme fungal protease. The assembly of gold nanoparticles on the zeolite surface occurs through the amine groups present in 3-aminopropyltrimethoxysilane (3-APTS). The binding of the enzyme to the gold nanoparticles in turn occurs through the amine groups and the cysteine residue present in the enzyme. The fungal protease bound to the massive 'core-shell' structures were easily separated from the reaction medium by mild centrifugation

and exhibited reuse characteristics. The proteolytic activity of fungal protease in the bioconjugate was marginally enhanced relative to the free enzyme in solution. The bioconjugate also showed significantly enhanced pH and temperature stability and a shift in the optimum temperature of operation.

Part-2 Fabrication, characterization and enzymatic activity of fungal protease-gold nanoparticle membrane bioconjugate

Gold nanoparticles embedded in a polymeric membrane provide a biocompatible surface for the immobilization of the enzymes. This chapter deals with the synthesis of a free-standing gold nanoparticle membrane by the spontaneous reduction of aqueous chloroaurate ions by the diamine molecule DAEE (bis (2-(4-aminophenoxy) ethyl) ether) at a liquid-liquid interface. The presence of gold nanoparticles in the membrane enables facile modification of the surface properties of the membrane and this has been used to immobilize enzymes to the membrane. Fungal protease was used as a model enzyme to immobilize on the gold nanoparticle membrane leading to the formation of a new biocatalyst. A highlight of the new biocatalyst wherein the enzyme is bound to the gold nanoparticle membrane is the ease with which separation from the reaction medium may be achieved by simple filtration. In relation to the free enzyme in solution, the fungal protease in the bioconjugate material exhibited a slightly higher proteolytic activity and significantly enhanced pH and temperature stability. The fungal protease gold nanoparticle membrane bioconjugate material also exhibited proteolytic activity over ten successive reuse cycles.

AWARDS

1. Recipient of "**IUBMB Young Scientist Award**" from International Union of Biochemistry and Molecular Biology (IUBMB) during 20th IUBMB International Congress of Biochemistry and Molecular Biology and 11th FAOBMB Congress, Kyoto, Japan. June-2006.

2. Recipient of "**Department of Science and Technology Award"** for Participation in the 55th Meeting of **Nobel Laureates and Students in Lindau**, Germany from DST, Govt. of India. 26th June to 1st July 2005.

3. **Deutsche Forschungsgemeinschaft** (DFG, Germany) invited to visit various research institutes in Germany working in the area of physics, chemistry and medicine/ biology from 4th July to 9th July 2005.

4. Recipient of **"Keerti Sangoram Endowment Award for the Best Research Scholar"** from National Chemical Laboratory Research Foundation (NCL-RF), February-2004.

5. Recipient of **"Best Poster Award"** in the 2nd National Conference of the Biotechnology Society of India (BSI), 'Biotech 2004 Challenges & Opportunities' held from 13th to 15th October 2004 at India International Center, New Delhi. October-2004.

6. Recipient of "**Best Research Paper Award**", in Biological Sciences from National Chemical Laboratory Research Foundation (NCL-RF), February-2002.

PUBLICATIONS

1. **Vinod, V. P.,** and Rao, M. (2004) Inhibition of 1, 4 -β- D Xylan xylanohydrolase by the specific aspartic protease inhibitor pepstatin: Probing the two-step inhibition mechanism. ***J. Biol. Chem***. 279: 47024-47033.

2. **Vinod, V. P**., Anamika, V., and Rao, M. (2006) Glycine Assisted Enhancement of 1, 4, (- D Xylan Xylanohydrolase Activity at Alkaline pH with a Shift in pH Optimum. ***Biol. Chem***. (*In press*)

3. **Vinod, V. P**., Joshi, H., Phadtare, S., Rao, M., and Sastry, M (2006) Fabrication, Characterization and Biocatalytic activity of Fungal Protease-Nanogold Membrane Bioconjugate. ***J. Nanosci. Nanotech.*** *(In press)*

4. **Vinod, V. P**., Sudheer, S., Vergenia, B., Shukla, P. G., and Rao, M. (2006) Preparation and Characterization of Urea-Formaldehyde-Pepsin Bioconjugate: A new biocatalyst system. ***Biotechnol. Progr***. (*In press*)

5. **Vinod V. P.**, Prem, N. P., and Rao, M. (2005) (β-Secretase: A potential therapeutic target in Alzheimer's disease. ***Adv. Biotech,*** 12-16.

6. **Vinod V. P**., and Rao, M. (2006) Structure Based-Drug Design in Development of HIV-1 Protease Inhibitors. ***Ind. J. Biotech.*** (*In press*).

7. **Vinod, V. P**., Umasankar, P. K., Patole, M., and Rao, M. (2006) Molecular cloning and expression of an aspartic protease inhibitor in *E. coli* : From designed gene to functional recombinant peptide (manuscript under preparation)

8. **Vinod, V. P**., Arabale, G., Vijayamohanan, K., and Rao, M. (2006) Fabrication of Pepsin-SWCNT bioconjugates for biocatalysis (manuscript under preparation).

9. Dash, C., **Vinod V. P.**, George, S. P., and Rao, M. (2002) Slow-tight binding inhibition of Xylanase by an aspartic protease inhibitor: kinetic parameters and conformational changes that determine the affinity and selectivity of the bifunctional nature of the inhibitor. ***J. Biol. Chem.*** 277: 7978-7986.

10. Mahesh. K, **Vinod, V. P.,** Umasankar, P. K., Patole, M., and Rao, M. (2006) Intact cell matrix-assisted laser dissociation/ionization mass spectrometry as a tool to screen drugs *in vivo* for regulation of protein expression ***Rapid Commun. Mass Spectrom.*** 20: 2769-2772.

11. Phadtare, S., **Vinod, V. P.,** Wadgaonkar, P. P., Rao, M., and Sastry, M. (2004). Free standing gold membranes as scaffolds for enzyme immobilization. ***Langmuir.*** 20: 3717-3723.

12. Phadtare, S., **Vinod**, **V. P.**, Mukhopadhyay, K., Kumar, A., Rao, M., Chaudhari, R. V., and Sastry, M. (2004) Immobilization and Biocatalytic Activity of Fungal Protease on Gold Nanoparticle-Loaded Zeolite Microspheres. ***Biotech. Bioeng.*** 85: 629-637.

13. Arabale, G., **Vinod, V. P**., Rao, M., and Vijayamohanan, K (2006) Unique fluorescence of functionalized single walled carbon nanotubes (Communicated to Nature Materials).

14. Kausik, M., Phadtare, S., **Vinod, V. P.**, Kumar, A., Rao, M., Chaudhari, R. V., and Sastry, M. (2003) Gold Nanoparticles Assembled on Amine-Functionalized Na-Y Zeolite: A Biocompatible Surface for Enzyme Immobilization. ***Langmuir*** 19: 3858-3863.

15. Phadtare, S., Kumar, A., **Vinod, V. P.,** Dash, C., Dnyaneshwar, V. P., Rao, M., Shukla, P. G., Sivaram, S., and Sastry, M. (2003) Direct assembly of gold nanoparticle “shells” on polyurethrene microsphere “cores” and their application as enzyme immobilization templates. ***Chem. Mater.*** 15: 1944-1949.

16. Phadtare, S., Dash. C., Gole A., **Vinod, V.P.**, Rao, M., and Sastry, M. (2002) Improved performance of preordered fungal protease stearic acid biocomposites: enhanced catalytic activity, reusability and temporal stability. ***Biotechnol. Progr.*** 18: 700-705.

CHAPTERS IN BOOK

1. **Vinod, V. P** and Rao, M. (2006) "Bionanocomposites for Biocatalysis" In: **Encyclopaedia of Nanoscience and Nanotechnology**, 2nd Edition, Dr. H. S. Nalwa (Editor), American Scientific Publishers, USA. (*Under review*).

2. **Vinod, V. P.**, Phadtare, S., Sastry, M., and Rao, M. (2004) "Nanobiotechnology: New Paradigms and Biological-Oriented Developments" In: **Plant, Microbes and Biotechnology**. Dr. Sampat Nehra (Editor) Pointer Publishers (India), p- 1-13, ISBN 81-7132-398-7.

CONFERENCES / ABSTRACTS / POSTERS

1. **Vinod, V. P**., and Rao, M. Poster presented at the "**Young scientists Program"**, conducted by International Union of Biochemistry and Molecular Biology (IUBMB), at CO-OP Inn Kyoto, Japan. from 16th to 18th June 2006

2. **Vinod, V. P.**, and Rao, M. Poster presented at the 20th IUBMB International Congress of Biochemistry and Molecular Biology and 11th FAOBMB Congress "***Life: Molecular Integration & Biological Diversity"***, at Kyoto International Conference Hall, Japan. 19th to 23rd June-2006

3. Rao, M., Umasankar, P. K., **Vinod, V. P.**, and Patole, M. S. Poster Presented at the 20th IUBMB International Congress of Biochemistry and Molecular Biology and 11th FAOBMB Congress "***Life: Molecular Integration & Biological Diversity"***, at Kyoto International Conference Hall, Japan. 19th to 23rd June-2006

4. **Vinod V. P**., Phadtare, S., Sastry, M., and Rao, M. Poster presented at the International Nano-Bioscience Conference (INBC-2006) organized by Agharkar Research Institute, Pune, from August 6th to 8th 2006.

5. Participated in the **"55th Meeting of Nobel Prize Winners in Lindau, 2nd interdisciplinary meeting"** from 26th June to 1st July 2005 at Lindau, Germany.

6. **Vinod, V. P**., and Rao, M. Poster presented at the 2nd National Conference of the Biotechnology Society of India **(BSI)**, *"**Biotech 2004 Challenges & Opportunities**"* held from 13th to 15th October 2004 at India International Center, New Delhi.

7. Participated in the ***"XXXIII National Seminar on Crystallography"*** held at National Chemical Laboratory, India, from 8th to 10th January 2004.

CHAPTER-1

GENERAL INTRODUCTION

INTRODUCTION

Enzymes are the catalytic cornerstone of metabolic activities of a living thing and most of the reactions in living organisms are catalyzed by these molecules. Hence it can rightly be called the catalytic machinery of living systems. Man has directly / indirectly used enzymes in his daily life almost since the beginning of human history. Enzyme focused research is of favourite not only to biological community, but also with process designers/engineers, chemical engineers, and researchers working in other scientific fields. The most striking characteristics of the enzymes are their catalytic power and specificity. Apart from basic approach, enzymes are widely studied from an industrial point of view. Enzymes have been used since the dawn of mankind in cheese manufacturing and indirectly via yeasts and bacteria in food manufacturing. Isolated enzymes were first used in detergents in the year 1914, their protein nature proven in 1926 and their large-scale microbial production started in 1960s. The past few decades of the twentieth century have witnessed spectacular advances and betterment of living standards due to the beneficial integration of enzyme technology with scientific progress and rapid translation of laboratory findings into practical technologies and commercial-scale manufacturing processes.

The International Union of Biochemistry and Molecular Biology (IUBMB) developed a system of enzyme nomenclature, in which enzymes are divided into six major classes, each with numerous subgroups, based on the nature of the chemical reaction they catalyze.

[1] Oxidoreductases: Catalyze oxidation or reduction of their substrates

[2] Transferases: These enzymes catalyze group transfer of their substrates

[3] Hydrolases: Catalyse bond breakage with the addition of water

[4] Lyases: Lyases remove groups from their substrates

[5] Isomerases: These enzymes catalyze intramolecular rearrangements

[6] Ligases: Catalyze the joining of two molecules at the expense of chemical energy

From an industrial standpoint, only a limited number of all the known enzymes are commercially available and even smaller amount is used in large quantities. More than

75% of industrial enzymes are hydrolases with carbohydrolases being the second largest group. Protein-degrading enzymes constitute about 40% of all enzyme sales. More than fifty commercial industrial enzymes are available and their number increases steadily. Today, the enzymes are commonly used in many industrial applications, and the demand for more stable, highly active and specific enzymes are growing rapidly. Global market for industrial enzymes has been increased from €1 billion in 1995 (Godfrey and West, 1996) to almost €2 billion in 2001 (Godfrey, 2003) and continues to increase as new enzymes and applications are discovered. In the grain-processing enzymes sector alone, which currently accounts for approximately 25–28% of total enzyme sales, an increase in market value from €510 million in 2001 to €760 million in 2010 has been forecasted (Godfrey, 2003). Presently the technical industries, dominated by the detergent, starch, textile and fuel alcohol industries, account for the majority of the total enzymes market, with the feed and food enzymes. Amylases, pectinases, cellulases, lipases, phytases, chitinases, lactase, proteases, and xylanases are some of the major hydrolytic enzymes used in industry.

Amylases are among the most important hydrolytic enzymes for all starch based industries, and the commercialization of amylases is oldest. A US patent has been granted to Caravan Products Company, USA for developing an amylase-supplemented process for making bread in 1970 (Miller, 1970). In 1984, amylase has been used as a pharmaceutical aid for the treatment of digestive disorders. In the present day scenario, amylases find applications in all the industrial processes such as in food, detergents, textiles, and in paper industry, for the hydrolysis of starch. Pectinases are one of the upcoming enzymes of fruit and textile industries (Bajpai, 1999; Bruhlmann et al., 2000). Their commercial application was first observed in 1930s for the preparation of wines and fruit juices. Pectinases are now an integral part of fruit juice and textile industries and have various biotechnological applications. Many patents describe the use of fungal pectinases for fruit processing. Conditioning of the fruit pulp (grapes) to reduce the viscosity and to free more juice by rupture of pulp particles has been described in US patent 3083104 (26th March 1963, R. F. Celmer). The most upcoming application of pectinolytic enzymes is their use in the degumming of plant fibers such as ramie, sunn

hemp, jute, flax and hemp (Cao et al., 1992; Bruhlmann et al., 1994; Henriksson et al., 1997, Henriksson et al., 1999). Pectinase treatment accelerates tea fermentation and also destroys the foam forming property of instant tea powders by destroying the pectins (Carr, 1985). Citrus oils such as lemon oil can be extracted using pectinases, as these enzymes destroy the emulsifying properties of pectin, which interfere with the collection of oils from citrus peel extracts (Scott, 1978).

Cellulases are used in food industry in earlier times. U.S. Patent 3259504 (5th July 1966, P. P Noznick and R. H Bundus) describes the use of cellulase to lower the viscosity of garlic. Another application is in the treatment of mushrooms, US Patent 3150983 (Y. Oshikawa, 29th September 1964, assigned into Japanese Industries). Biotechnology of cellulases began in early 1980s, first in animal feed followed by food applications (Thomke et al., 1980; Voragen et al., 1980, Voragen et al., 1986; Chesson, 1987; Voragen, 1992). Subsequently, it was used in the textile, laundry as well as in the pulp and paper industries (Clarkson et al., 1992; Wong and Saddler, 1992, 1993;Godfrey, 1996; Xia et al., 1996). Cellulases are also used in bioconversion of lingocellulose to soluble sugars (Bhat, 2000). Lipases (triacylglycerol acylhydrolase) are part of the family of hydrolases that act on carboxylic ester bonds. In addition to their natural function of hydrolyzing carboxylic ester bonds, lipases can catalyze esterification, inter-esterification, and trans-esterification reactions in non aqueous media. This versatility makes lipases the enzymes of choice for potential applications in the food, detergent, pharmaceutical, leather, textile, cosmetic, and paper industries. The most significant industrial applications of lipases have been mainly found in the food, detergent, and pharmaceutical sectors. Phytases are *meso*-inositol hexaphosphate phosphohydrolases that catalyze the stepwise phosphate splitting of phytic acid (IP6) or phytate to lower inositol phosphate esters (IP5-IP1) and inorganic phosphate. Phytase are used to improve mineral nutrition of humans, feed supplement in diets largely for swine and poultry. The use of phytase reduces the need to add phosphorus to the feed diet. Apart from that, transgenic mice and pigs have been generated by overexpressing phytase in their salivary glands (Golovan et al. 2001). Chitinases can be employed in human health care, such as making ophthalmic preparations with chitinases and microbiocides. A direct medical use

has been suggested for chitinases in the therapy for fungal diseases in potentiating the activity of antifungal drugs (Oranusi and Trinci 1985). They can also be used as potential additives in antifungal creams and lotions due to their topical applications. The industrial uses of lactases are mainly in milk related industry. Its primary commercial use is to break down lactose in milk to make it suitable for people with lactose intolerance. The hydrolysis of lactate to form glucose and galactose gives more soluble sweeter end products. Lactase provides fermentable sugar and sweetens in milk breads. Hydrolysis of lactose in milk prevents grittiness in ice cream or cheese sweetners. Lactose also crystallises at the low temperatures of ice cream; however, its constituent products stay liquid and contribute to a smoother texture. Lactase is also used in the conversion of whey into syrup.

Proteases

Protein-degrading enzymes or proteases constitute the major part of the industrially used hydrolytic enzymes. Proteases are classified under group 3 [hydrolyses] into 4 subgroups according to the Nomenclature Committee of International Union of Biochemistry and Molecular Biology [IUBMB]; based on three major criteria i) type of reaction ii) chemical nature of the catalytic site and iii) evolutionary relationship with reference to structure. Further, proteases can be grossly divided into two major groups; exopeptidases and endopeptidases, depending on their site of action. Proteases catalyze the addition of water across amide (and ester) bonds to effect cleavage using a reaction involving nucleophilic attack on the carbonyl carbon of the scissile bond. The exact mechanisms of cleavage and the active site substituents vary widely among different protease subtypes. This provides the basis for the classification of proteases into the serine proteases, cysteine proteases, metallo proteases, and aspartic proteases (Barett et al., 1998). There are a few miscellaneous proteases, which do not precisely fit into the standard classification, e.g., ATP-dependent proteases, which require ATP for activity (Menon and Goldberg, 1987). Proteases have found new applications but their use in detergents is the major market.

The serine proteases, comprises two distinct families, the chymotrypsin family, which includes the mammalian enzymes such as chymotrypsin, trypsin, elastase or kallikrein and the subtilisin family including the bacterial enzymes such as subtilisin. The catalytic triad of the serine protease, essential in the catalytic process is His, Asp, and Ser. Chymotrypsin in the pure form has various clinical applications while in crude pancreatin preparation it may be used for the preparation of protein hydrolysates. Trypsin is used in certain industries for the preparation of leather, treatment of raw silk and for the preparation of protein hydrolysates. Subtilisin has many applications in laundering. It is also used in leather tanning, for oral hygiene, production of protein hydrolysates and in brewing. The cysteine proteases include the plant proteases such as papain, actinidin or bromelain, several mammalian lysosomal cathepsins, the cytosolic calpains (calcium-activated) and several parasitic proteases (e.g., *Trypanosoma, Schistosoma*). Papain is the archetype and the best-studied member of the family. Papain is used for tenderizing meat, chill-proofing beer, production of protein hydrolysates, and softening of high gluten flour used in biscuit production. Papain has a marked action on collagen of connective tissue in meat, especially during the early stages of cooking. Bromelain is used in tenderizing meat, chill-proofing beer, in digestive aid preparations and for various clinical uses.

The metallo proteases are one of the older classes of proteases and are found in bacteria, fungi as well as in higher organisms. They differ widely in their sequences and their structures but the great majority of enzymes contain a zinc atom, which is catalytically active. In some cases, zinc may be replaced by cobalt or nickel without loss of the activity. Bacterial thermolysin has been well characterized and its crystallographic structure indicates that two histidines and one glutamic acid bind to zinc. Many enzymes contain the sequence HEXXH, which provides two histidine ligands for the zinc whereas the third ligand is either a glutamic acid (thermolysin, neprilysin, alanyl aminopeptidase) or a histidine (astacin). Metallo proteases are used in many industries including food, textile, leather, and also for the recovery of silver from used photographic films. Aspartic proteases are a group of proteolytic enzymes of the pepsin family that share the same catalytic apparatus and usually function in acidic conditions. This latter aspect limits the function of aspartic proteases to some specific locations in different organisms; thus, the

occurrence of aspartic proteases is less abundant than other groups of proteases, such as serine proteases. However, aspartic proteases have been isolated and studied from a wide range of organisms, varying from vertebrates to plants, fungi, parasites, retroviruses, and very recently bacteria (James, 1998; Hill and Phylip, 1997). Of the five currently documented from the human body, three (pepsin, gastricsin, and renin) are secretory and have well-defined physiological roles. The fourth protease, cathepsin D, is found ubiquitously in the lysosomes of most cells (Saftig et al. 1995), while the fifth, cathepsin E, is neither secretoy nor lysosomal but it is located within the endoplasmic reticulum/trans-Golgi network/endosomal compartments of cells (Kageyama, 1995). The cathepsin E molecule is readily distinguished from the other aspartic proteases not only by this cytomorphological compartmentation but also by its unique molecular architecture (Rao-Naik et al., 1995) and its limited tissue distribution. Aspartic proteases have been extensively studied for their structural and functional relationships and have been the topics of several reviews or monographs (Tang, 1977; Tang, 1979; Kay, 1985; Dunn, 1992; Dunn et al., 1995). Probably the first application of cell free enzymes was the use of rennin isolated from calf or lamb stomach in cheese making. Rennin is an aspartic protease which coagulates milk protein and has been used for hundreds of years by cheese makers and some use in rennet puddings. Aspartic proteases are used commercially for hydrolysis of soyabean proteins to amino acids and in soya sauce manufacturing and exhibit milk clotting activity. They are also used in digestive aids (Kalisz, 1988).

Individually proteases are the most widespread type of enzymes used in detergent and body care products, adding an extra cleaning power particularly for low temperature washes. Enzymes and immobilized enzymes are well known to be used in hair cosmetics that prevent dandruff and head itching, solid soap or bath compositions that easily remove dirt from the surface of skin, and cosmetic compositions that prevent skin staining caused by certain polysaccharides, proteins and lipids (Calvo et al., 1985; Tajima et al., 1985; Yoshizumi et al., 1985; Grollier and Isabelle, 1991; De Salvert et al., 1999). Leather industry uses proteolytic and lipolytic enzymes in leather processing. The use of these enzymes is associated with the structure of animal skin as a raw material. Enzymes

are used to remove unwanted parts. Alkaline proteases are added in the soaking phase. This improves water uptake by the dry skins, removal and degradation of protein, dirt and fats and reduces the processing time. In some cases pancreatic trypsin is also used in this phase. In dehairing and dewooling phases enzymes are used to assist the alkaline chemical process. This results in a more environmentally friendly process and improves the quality of the leather (cleaner and stronger surface, softer leather, less spots). The next phase is bating which aims at deliming and deswelling of collagen. In this phase the protein is partly degraded to make the leather soft and easier to dye. Pancreatic trypsins were originally used but they are being partly replaced by bacterial and fungal enzymes.

Xylanases

Xylanases are glycosidases (*O*-glycoside hydrolases, EC 3.2.1.x) which catalyze the endohydrolysis of 1,4-β- D-xylosidic linkages in xylan. They are a widespread group of enzymes, involved in the production of xylose, a primary carbon source for cell metabolism. First reported in 1955 (Whistler and Masek, 1955), they were originally termed pentosanases, and were recognized by IUBMB in 1961, when they were assigned the enzyme code EC 3.2.1.8. Their official name is endo-1,4-β-xylanase, but commonly used synonymous terms include xylanase, endoxylanase, 1,4-β-D-xylan-xylanohydrolase, endo-1,4-β-D-xylanase, β-1,4-xylanase and β-xylanase. Diverse forms of xylanases exist, displaying varying folds, mechanisms of action, substrate specificities, hydrolytic activities (yields, rates and products) and physico-chemical characteristics.

Research on microorganisms that utilize xylan, and on the enzyme systems involved, is becoming more and more relevant in ecological and economic terms. Xylanolytic enzymes from microorganism have attracted a great deal of attention in the last decade, particularly because of their biotechnological potential in various industrial processes such as food, feed, and pulp and paper industries (Wong and Saddler, 1992; Bajpai, 1999; Niehaus et al., 1999). Xylanases are widely distributed and are produced by prokaryotes and eukaryotes. These enzymes are produced mainly by microorganisms and take part in the breakdown of plant cell walls, along with other enzymes that hydrolyze polysaccharides, and also digest xylan during the germination of some seeds (e.g. in the

malting of barley grain). Xylanases are also reported from marine algae, protozoans, crustaceans, insects, snails and seeds of land plants (Sunna and Antranikian, 1997). Among microbial sources, filamentous fungi are especially interesting as they secrete these enzymes into the medium and their xylanase levels are very much higher than those found in yeasts and bacteria. Most commercial xylanases are mesophilic enzymes produced by the filamentous fungi *Trichoderma reesei* and *Aspergillus niger*. This process reflects well the fact that filamentous fungi are naturally excellent protein secretors and can produce enzymes in industrially feasible amounts. Xylanase genes have been isolated from microorganisms of various genera and expressed in *Escherichia coli* (Honda et al., 1985; Kudo et al., 1985; Sipat et al., 1987; Whitehead and Hespell, 1989; Morosoli et al., 1992; Toshiyoshi et al., 2000). In bacteria xylanases are not only produced at lower activity levels than in fungi, but are also restricted to the intracellular or periplasmic fractions. Amongst prokaryotes, bacteria and cyanobacteria from marine environments produce xylanases. Extra cellular and intracellular xylanases from bacterial and fungal sources have been studied extensively. Intracellular xylanases occur in rumen bacteria and protozoa. They are also found in insects, small crustaceans and germinating seeds of terrestrial plants.

Classifications of xylanases

In addition to the production of a variety of xylanolytic enzymes, many micro-organisms produce multiple xylanases (Gilbert et al., 1988; Yang et al., 1989; Gilbert and Hazlewood, 1993). These may have diverse physico-chemical properties, structures, specific activities and yields, as well as overlapping but dissimilar specificities, thereby increasing the efficiency and extent of hydrolysis, but also the diversity and complexity of the enzymes. The heterogeneity and complexity of xylan has resulted in an abundance of diverse xylanases with varying specificities, primary sequences and folds, and hence has lead to limitations with the classification of these enzymes by substrate specificity alone.

Xylanases have been classified on the basis of their physico-chemical properties by Saddler and coworkers (Wong et al., 1988). They have proposed two groups, one with a

low molecular weight (<30 kDa) and basic *pI*, and the other with a high molecular weight (>30 kDa) and acidic *pI*. Henrissat and Bairoch in 1996 have classified the available sequences of glycosyl hydrolases into 58 families based on HCA (Hydrophobic cluster analysis) and amino acid sequence homology (Henrissat and Bairoch, 1996). Based on HCA, the xylanases are classified into two major families of glycosyl hydrolases i.e., F or 10 and G or 11. Both of these use ion pair catalytic mechanisms and both retain anomeric configuration following hydrolysis (Jeffries, 1996). Family 10 xylanases are larger, more complex and produce smaller oligosaccharides. Family 11 xylanases are more specific for xylan. The relatedness of enzymes within family 10 and 11 can be demonstrated either by pair wise alignments of the protein sequences or by the basic local alignment search tool (BLAST) to discern sequence similarity.

Family 10 xylanases occasionally exhibit endocellulase activity; generally have a higher molecular weight and will occasionally possess a cellulose-binding domain. The catalytic domain of family 10 xylanase is a cylindrical α/β barrel resembling a salad bowl with the catalytic site at the narrower end, near the carboxyl terminus of the β barrel. There are five xylopyranose binding sites. Family 10 xylanases have relatively high molecular weights and they tend to form low degree of polymerization oligosaccharides. The catalytic domains of Family 10 xylanase belong to a superfamily that includes Family 10 cellulases, β-glucosidase, β-galactosidase, β-(1-3)-glucanases, and β- (1-3, 1-4)-glucanases (Jenkins et al., 1995).

Family 11 xylanases are true xylanases. They do have cellulase activity; they consistently exhibit a low molecular weight and can have either a high or low *pI*. Family 11 catalytic domains consist principally of β-pleated sheets formed into a two layered that surrounds the catalytic site. Protruding down into the trough, and located towards one side of the protein is a long loop terminating in an isoleucine. The positions of many amino acids are essentially identical in the family 11 xylanases from bacterial and fungal origins. Thus, there has been a tremendous conservation of the basic structure of the catalytic site of family 11 xylanases during evolution. Generally, there is no significant homology between the xylanases of these two families, including the region around the catalytic residues and they have an altogether different pattern of protein folding.

Production of Xylanases

The basic factors for efficient xylanase production of xylanolytic enzymes are the choice of an appropriate inducing substrate and an optimum medium composition. Xylan has been the most favoured and natural substrate for the production of xylanases (Kelly et al., 1989). A variety of other substrates rich in hemicellulosic content such as wheat bran, rice bran, rice straw, corn cob, corn stalk bagasse, canola meal, sugar beet pulp, aspen wood, saw dust, etc. have been tested as substrates for xylanase production in various microorganisms (Paul and Varma, 1990). Xylanases may be industrially produced in submerged liquid culture or on a solid substrate. In cultures on solid substrate, wheat bran and rice are regarded as inducers. Alternative substrates for enzyme production have also been reported, such as sugarcane, bagasse, rice husks and wood pulp (Kadowaki et al., 1995; Damaso et al., 2000; Medeiros et al., 2000; Pandey et al., 2000; Singh et al., 2000; Anthony et al., 2003). In liquid culture, xylanase is produced in response to xylans from various sources (Gomes et al., 1994; Liu et al., 1999; Rani and Nand, 2000).

The yield of xylanases in a fermentation process is governed by a few key factors in addition to the standard parameters. When xylanase fermentation is carried out on complex heterogeneous substrate, various factors have a combined effect on the level of xylanase expression. They include substrate accessibility, rate and amount of release of the xylooligosaccharides and their chemical nature and quantity of xylose released, which acts as the carbon source and as an inhibitor of xylanase synthesis in most of the cases. Generally, the slow releases of the inducer to its non-metabolizable derivative are believed to boost the level of xylanase activity. The xylanases bind tightly to the substrate. A part of the enzyme produced during the fermentation is often lost and discarded, as bound enzyme, along with the insoluble substrate. The metabolic enzymes of the xylanase producer such as proteases (Penbroke, 1992) and transglycosidases also affect the actual yield of the enzyme (Hrmova, 1991). The addition of glycine, DL - norvaline and D-alanine enhanced production of xylanase in a *Bacillus* strain (Ikura and Horikoshi, 1987). The increased enzyme levels in the presence of glycine and D, L-norvaline were correlated with a concomitant reduction in protease production.

Specific xylanases are synthesized when microorganisms are cultured on xylan, whereas on cellulose the organisms produce cellulases in association with xylanases, perhaps because the cellulose substrate contains traces of hemicelluloses. In the textile and paper industries, it is important to obtain xylanases free of cellulase activity, as it is necessary to extract hemicellulose from the natural fibers, without damaging the cellulose. Other bioprocess parameters that can affect the activity and productivity of xylanase attained in a fermentation process include the pH, temperature and agitation.

Applications of xylanases

In recent years, the biotechnological use of xylans and xylanases has grown remarkably (Aristidou and Pentilla, 2000; Beg et al., 2000; Bhat, 2000; Subramaniyan and Prema, 2000; Beg et al., 2001; Subramaniyan and Prema, 2002; Techapun et al., 2003) in various industrial processes such as food, feed, and pulp and paper industries (Wong and Saddler, 1992; Bajpai, 1999; Niehaus et al., 1999). Xylanases are heavily exploited in paper and pulp industry. In paper production, it is necessary to retain the strength of the cellulase fabrics while removing the lignin from the pulp. It is proposed that the xylanases cleave the hemicellulose chains that are responsible for the close adherence of the lignin to the cellulose chains. The main industrial application of the xylanases is in the bleaching of cellulose pulp. Enzymes began to be used in this sector during the last two decades, ever since peroxidases were applied to the degradation of lignin (Viikari et al., 1991; Wong and Saddler, 1993; Tenkanen et al., 1997; Araujo et al., 1999; Bajpai, 1999, Christov et al., 1999; Christov et al., 2000; Whitmire and Miti, 2002; Sandrim et al., 2005). The efficiency of microbial xylanase in the bleaching process has been studied for *Thermomyces lanuginosus* (Haarhoff et al., 1999), *Trichoderma reesei* (Oksanen et al., 2000), *Streptomyces roseiscleroticus* (Patel et al., 1993), *Streptomyces* sp. (Beg et al., 2000; Georis et al. 2000), *Streptomyces thermoviolaceus* (Garg et al., 1996), *Streptomyces galbus* (Kansoh and Nagieb, 2004), *Bacillus pumilus* (Bim and Franco, 2000; Duarte et al., 2003), *Bacillus circulans* (Dhillon et al., 2000), *Aspergillus kawachii* (Tenkanen et al., 1997), *Aspergillus oryzae* (Christov et al., 1999), *Bacillus sp.* (Kulkarni and Rao, 1996; Shah et al., 1999), *Aspergillus niger* (Zhao et al., 2002), *Aspergillus nidulans* (Taneja et al., 2002), *Aspergillus fumigatus* (Lenartovicz et al., 2002),

Chaetomium cellulolyticum (Baraznenok et al., 1999), *Acrophilophora nainiana* and *Humicola grisea* (Salles et al., 2005).

The xylanase based pre bleach leads to a reduction in organochlorine pollutants such as dioxin from the paper making process. The degree of environmental pollution caused by the large scale discharge of chlorine compounds from pulp and paper industry can potentially be remedied by the application of xylanase. Cellulase-free xylanases are promising agents which might eventually lead to reduced chlorine usage in the bio-bleaching of paper pulps. However, care is needed to prevent the unwanted hydrolysis of cellulose on a large scale. The xylanolytic complex can be used in the textile industry to process plant fibres, such as hessian or linen. For this purpose, the xylanase should be free of cellulolytic enzymes (Prade, 1995).

The use of enzymes in the production of feed is an important sector of agribusiness, with an annual world production exceeding 600 million tons and a turnover of >50 billion dollars (Polizeli et al., 2005). Xylanases are used in animal feed along with glucanases, pectinases, cellulases, proteases, amylases, phytases, galactosidase and lipases. Addition of xylanase stimulates the growth rates of animals by improving digestibility, thereby improving the quality of the animal litter. If xylanase is added to feed containing maize and sorghum, both of which are low viscosity foods, it may improve the digestion of nutrients in the initial part of the digestive tract, resulting in a better use of energy. Treatment of forages with xylanase (along with cellulase) results in better quality silage and improves the subsequent rate of plant cell wall digestion by ruminants (Wong and Sadler, 1992).

Xylanases may be employed in bread-making, together with α-amylase, malting amylase, glucose oxidase and proteases. The xylanases, like the other hemicellulases, break down the hemicellulose in wheat-flour, helping in the redistribution of water and leaving the dough softer and easier to knead. During the bread-baking process, they delay crumb formation, allowing the dough to grow. With the use of xylanases, there has been an increase in bread volumes, greater absorption of water and improved resistance to fermentation (Maat et al., 1992; Harbak and Thygesen, 2002; Camacho and Aguilar,

2003). Xylanases are known to modify wheat flour arabinoxylanas, thus making the bread fluffier and ensures its shelf life by retaining the freshness. As well as crumb softness after storage is also improved (Wong and Saddler, 1992). Xylanase also facilitates the separation of wheat or other cereal gluten from starch (Christophersen et al., 1997). Xylanases, in conjunction with cellulases, amylases and pectinases, lead to an improved yield of juice by means of liquefaction of fruits and vegetables, stabilization of the fruit pulp, increased recovery of aromas, essential oils, vitamins, mineral salts, edible dyes, pigments, etc. Xylanase also reduces the viscosity, hydrolysis of substances that hinder the physical or chemical clearing of the juice, or that may cause cloudiness in the concentrate (Biely, 1985). Xylanases also founds application in bioremediation / bioconversion such as treatment / recycling of agricultural, municipal and food industry wastes and production of renewable fuel (bioethanol) (Prade, 1995).

Xylanases improve degradability of plant waste material (for instance, agricultural wastes) reducing organic waste disposal on landfill sites. Xylanases have applications in laundry industry, which improve the cleaning ability of detergents that are especially effective in cleaning stubborn fruit and vegetable oils and grass stains. In fuel alcohol production xylanases decreases the viscosity of the mash and prevents fouling problems in distilling equipments (McCleary, 1986). Xylanases improves the extraction of oil from oil rich plant material such as corn oil from corn embryos thereby increasing yields. Xylanases have shown an immense potential for increasing the production of several useful products in a most economical way. The end-products of xylan degradation are of considerable importance in commercial applications are furfural and xylitol (Parajo et al., 1998).

Objective of the present study

The present investigation is focused to understand the molecular mechanism of aspartic proteases, xylanases, their interactions with inhibitors and nanoparticles for its possible industrial and biomedical applications. The present work has been organized under the following headings.

1) General introduction

2) Inhibition xylanase by peptidic aspartic protease inhibitors

   i) Structural and mechanistic insights into the inhibition of xylanase by an aspartic protease inhibitor from an extremophilic *Bacillus* sp.

   ii) Slow-tight binding inhibition of xylanase by the specific aspartic protease inhibitor pepstatin

3) Biochemical studies on the enhancement of xylanase activity in presence of glycine.

4) Molecular cloning and expression of an aspartic protease inhibitor in *Escherichia coli*

5) Development of gold nanoparticle based bioconjugates using fungal aspartic protease

   i) Gold nanoparticles assembled on amine-functionalized Na-Y zeolite: A biocompatible surface for enzyme immobilization.

   ii) Fabrication, characterization and enzymatic activity of fungal protease-gold nanoparticle membrane bioconjugate

REFERENCES

Aeaujo, J. H. B., Moraes, F. F., and Zanin, G. M. (1999) *Appl Biochem Biotechnol*. **77–79**, 713–722.

Anthony, T., Raj, K. C., Rajendran, A., and Gunasekaran, P. (2003) *Enzyme Microb. Technol.* **32**, 647–654.

Aristidou, A., and Pentilla, M. (2000) *Curr Opin Biotechnol*. **11,** 187–198

Bajpai, P. (1999) *Biotechnol Prog.* **15**,147–157

Baraznenok, V. A., Becker, E. G., Ankudimova, N. V., and Okunev, N. N (1999) *Enzyme Microb. Technol.* **25**, 651–659

Barett, A. J., Rawlings, N. D., and Woessner, J. F. (1998) *Handbook of Proteolytic Enzymes.* Academic Press Inc., London.

Beg, Q. K., Bhushan, B., Kapoor, M., and Hoondal, G. S. (2000) *Enzyme Microb. Technol.* **27**, 459–466

Beg, Q. K., Kapoor, M., Mahajan, L., and Hoondal, G. S. (2001) *Appl. Microbiol. Biotechnol.* **56**, 326–338.

Bhat, M. K. (2000) *Biotechnol. Adv.* **18,** 355–383.

Biely, P. (1985) *Trends Biotechnol.* **3**, 286-290.

Bim, M. A., and Franco, T. T. (2000) *J Chromatogr*. **43**, 349–356.

Bruhlmann, F., Kim, K. S., Zimmerman, W., and Fiechter, A. (1994) *Appl. Environ. Microbiol.* **60,** 2107–2112.

Bruhlmann, F., Leupin, M., Erismann, K. H., and Fiechter A. (2000) *J Biotechnol*. **76,** 43–50.

Calvo Luis, C., and Bayshore, N. Y., (1985) *Cosmetic compsns for removing sebum - contg. immobilised lipase in cosmetic vehicle* United State Patent, US4556554 to, Germaine Monteil Cosmetiques Corp.

Camacho, N. A., and Aguilar, O. G. (2003) *Appl. Biochem. Biotechnol.* **104**, 159–172

Cao, J., Zheng, L., and Chen, S. (1992) *Enzyme Microb. Technol*. **14**, 1013–1016.

Carr, J. G. (1985) *Tea, coffee and cocoa* In: Microbiology of Fermented Food, Wood, B. J. B. (Eds.) Vol. 2, Elsevier, London, 133-154.

Chesson, A. (1987) *Supplementary enzymes to improve the utilization of pigs and poultry diets.* In: Recent advances in animal nutrition. Haresign, W., Cole, D. J. A. (Eds.) London: Butterworths, 71–89.

Christophersen, C., Andersen, E., Jacobsen, T. S., and Wagner, P. (1997) *Starch/Starke*, **49**, 5–12.

Christov, L. P., Szakacs, G., and Balakrishnan, H. (1999) *Process Biochem.* **34**, 511–517.

Christov, L., Biely, P., Kalogeris, E., Christakopoulos, P., Prior, B. A., and Bhat, M. K. (2000) *J Biotechnol.* **83**, 231–244.

Clarkson, K. A., Weiss, G. L., larenas, E. A., and Shoemaker, S. P. (1992) *Detergent compositions containing cellulase compositions enriched in acidic endoglucanase type components.* PCT Int. Appl. WO 9206210 A1.

Damaso, M. C. T., Andrade, C. M. M. C., and Pereira, N. Jr (2000) *Appl. Biochem. Biotechnol.* **84**, 821–834.

De Salvert, A., Sera, D., Guth, G., Fodor, P., and Maurin, E. (1999) *Product for topical application containing lipase and an active ingredient precursor*, United State Patent, 5932232, to L'Oreal,

Dhillon, A., Gupta, J. K., Jauhari, B. M., and Khanna, S. (2000) *Bioresour. Technol.* **73**, 273–277.

Duarte, M. C. T., Silva, E. C., Gomes, I. M. B., Ponezi, A. N., Portugal, E. P., Vicente, J. R., and Davanzo, E. (2003) *Bioresour. Technol.* **88**, 9–15.

Dunn, B. M. (1992) In *Advances in Detailed Reaction Mechanisms* Coxon, J. (Eds.), JA1 Press, Greenwich, Connecticut, **Vol. 2**, 213-241.

Dunn, B. M., Scarborough, P. E., Lowther, W. T., and Rao-Naik, C. (1995) In *Aspartic Proteinases* Takahashi, K. (Eds.), Plenum Press, pp 1-9.

Garg, A. P., McCarthy, A. J., and Roberts, J. C. (1996) *Enzyme Microb. Technol.* **18**, 261–267.

Georis, J., Giannotta, F., de Buyl, E., Granier, B., and Frere, J. M. (2000) *Enzyme Microb. Technol*. **26,** 178–186.

Gilbert, H. J., and Hazlewood, G. P. (1993) *J. Gen. Microbiol.* **139**, 187–194.

Gilbert, H.J., Sullivan, D.A., Jenkins, G., Kellett, L.E., Minton, N.P., and Hall, J. (1988) *J. Gen. Microbiol.* **134**, 3239–3247.

Godfrey T. (1996) *Textiles*. In: Industrial enzymology, Godfrey, T., West, S. (Eds.), 2nd ed. London: Macmillan Press, 360–71.

Godfrey, T. (2003) The enzymes market for grain processing In: *Recent Advances in Enzymes in Grain Processing.* Courtin, C.M., Veraverbeke, W.S. and Delcour, J.A., (Eds.), Kat. Univ. Leuven, Leuven. 401–406.

Godfrey, T., and West, S. (1996) *Industrial Enzymology*, Second ed. Macmillan Press Ltd., London.

Golovan, S. P., Hayes, M. A., Phillips, J. P., and Forsberg, C. W. (2001) *Nat. Biotechnol.* **19**, 429–433.

Gomes, D. J., Gomes, J., and Steiner, W. (1994) *J. Biotechnol.* **33**, 87–94.

Grollier, J. F., and Isabelle, R. (1991) *Cosmetic or pharmacological composition for treatment of hair and scalp*, Japanese patent, 3014509, to L'Oreal,

Haarhoff, J., Moes, C. J., Cerff, C., van Wyk, W. J., Gerischer, G., Janse, B. J. H. (1999) *Biotechnol. Lett.* **21,** 415–420.

Harbak, L., and Thygesen, H. V. (2002) *Food Chem Toxicol.* **40**, 1–8.

Henriksson, G., Akin, D. E., Hanlin, R. T., Rodriguez, C., Archibald, D., Rigsby, L. L., and Eriksson K. E. L (1997) *Appl. Environ. Microbiol.* **63**, 3950– 3956.

Henriksson, G., Akin, D. E., Slomczynski, D., and Eriksson, K. E. L. (1999) *J Biotechnol.* **68,**115–123.

Henrissat, B., and Bairoch, A. (1996) *Biochem J.* **316,** 695-696.

Hill, J., and Phylip, L. H. (1997) *FEBS Lett.* **409**, 357-360.

Honda, H., Kudo, T., and Horikoshi, K. (1985) *J. Bacteriol.* **161**, 784-785.

Hrmova, M., Petrakova, E., and Biely, P. (1991) *J Gen. Microbiol.* 137, 541–547.

Ikura, Y., and Horikoshi, K. (1987) *Agric. Biol. Chem.* **51**, 3143-3145.

James, M. N. G. (1998) In *"Structure and Function of Aspartic Protease: Retroviral and Cellular Enzymes"* Plenum Press, New York, pp 1-481.

Jeffries, T. W. (1996) *Curr. Opin. Biotechnol.* **7**, 337-342.

Jenkins, J., Leggio, L. L., Harris, G., and Pickersgill, R. (1995) *FEBS Lett.* **362**, 281-285.

Kadowaki, M. K., Pacheco, M. A. C., and Peralta, R. M. (1995) *Rev. Microbiol.* **263**, 219–223.

Kageyama, T. (1995) *Meth. Enzymol.* **248**, 120-136.

Kalisz, H. M. (1988) *Advances in Biochemical Engineering*, Biotechnology, Springer-Verlag: New York, **Vol. 86.**

Kansoh, A. L., and Nagieb, Z. A. (2004) *Antonie van Leeuwenhoek J Microbiol Serol.* 85, 103–114.

Kay, J. (1985) In *Aspartic Proteases and Their Inhibitors.* Kostka, V. (Eds.) Walter de Gruyter, Berlin. 1-17.

Kelly, C. T., O'Mahony, M. R., and Fogarty, W. M. (1989) *Biotech. Lett.* **11**, 885–890.

Kudo, T., Ohkoshi, A., and Horikoshi, K. (1985) *J. Gen. Microbiol.* **131**, 2825-2830.

Kulkarni, N., and Rao, M. (1996) *J Biotechnol.* **51**, 167–173.

Lenartovicz, V., Souza, C. G. M., Moreira, F. G., and Peralta, R. M. (2002) *J Basic Microbiol.* **42**, 388–395.

Liu, W., Lu, Y., and Ma, G (1999) *Process Biochem.* **34**, 67–72.

Maat, J., Roza, M., Verbakel, J., Stam, H., Santos da Silva, M. J., Bosse, M., Egmond, M. R., Hagemans, M. L. D., van Gorcom, R. F. M., Hessing, J. G. M., van den Hondel, C. A. M. J. J., and van Rotterdam, C. (1992) *Xylanases and their applications in bakery.* In: Xylans and xylanases.Visser, J., Beldman, G., Someren Kusters-van, M. A., and Voragem, A. G. J. (Eds) Elsevier, Amsterdam, 349–360.

McCleary, B.V. (1986) *Int J Biol Macromol.* **8**, 349–354.

Medeiros, R. G., Soffner, M. A. P., Tome, J. A., Cacais, A. O. G., Estelles, R. S., Salles, B. C., Ferreira, H. M., Neto SAL, Silva, F. G. Jr., and Filho, E. X. F. (2000) *Biotechnol Prog*. **16**, 522–524.

Menon, A. S., and Goldberg, A. L. (1987) *J. Biol. Chem.* **262**, 14929-14934.

Miller, J. A. (1970) *A simple fast enzyme-supplemented process for making bread United State Patent* , US3494770 to, Caravan Products Company, Incorporated.

Morosoli, R., Durand, S., and Moreau, A. (1992) *Gene*. 117, 145-50.

Oksanen, T., Pere, J., Paavilainen, L., Buchert, J., and Viikari, L. (2000) *J Biotechnol*. **78**, 39–48

Oranusi, N. A., and Trinci, A. P. (1985) *Microbios.* **43**, 17-30.

Pandey, A., Soccol, C. R., Nigam, P., and Soccol, V. T (2000) *Bioresour. Technol.* **74**, 69–80.

Paul, J., and Varma, A. K. (1990) *Biotech. Lett.* **60**, 61-64.

Penbroke, J.T., Sweeny, B., and Whelan, R. A. (1992) *Reduction in xylanase activity in Pseudomonas flavigena extracts is a result of protease activity.* In: xylan and xylanases, Elsvier, Amsterdam, 479-482

Polizeli, M. L. T. M., Rizzatti, A. C. S., Monti, R., Terenzi, H. F., Jorge, J. A., and Amorim, D. S. (2005) *Appl. Microbiol. Biotechnol.* **67,** 577–591.

Prade, R. A. (1995) *Biotechnol Genet Eng Rev* **13**, 101–131

Rani, D. S., and Nand, K. (2000) *Process Biochem.* **36**, 355–362.

Rao-Naik, C., Guruprasad, K., Batley, B., Rapundalo, S., Hill, J., Blundell, T., Kay, J., and Dunn, B. N. (1995) *Proteins Struct. Funct. Genet*. **22**, 168-181.

Rehm, H. J., Reed, G. (Eds) **2nd ed.** Germany: Wiley-VCH, 189-216.

Saftig, P., Hetman, M., Schmahl, W., Weber, K., Heine, L., Mossmann, H., Koster, A., Hess, B., Evers, M., von Figura, K., and Peters, C. (1995) *EMBO J.* **14**, 3599-608.

Salles, B. C., Medeiros, R. G., Bao, S. M., Silva, F. G. Jr., and Filho, E. X. F. (2005) *Process Biochem.* **40***,* 343-349.

Sandrim, V. C., Rizzatti, A. C. S., Terenzi, H. F., Jorge, J. A., Milagres, A. M. F., and Polizeli, M. L. T. M. (2005) *Process Biochem.* **40***,* 1823-1828.

Shah, A. K., Sidid, S. S., Ahmad, A., and Rele. M. V. (1999) *Bioresour. Technol*. **68,**133–140.

Singh, S., Reddy, P., Haarhoff, J., Biely, P., Janse, B., Pillay, B., Pillay, D., and Prior, B. A. (2000) *J. Biotechnol.* **81**, 119–128.

Sipat, A., Taylor, K. A., Lo, R. Y., Forsberg, C. W., and Krell, P. J. (1987) *Appl Environ Microbiol.* **53,** 477–481.

Subramaniyan, S., and Prema, P. (2002) *Crit Rev Biotechnol* **22,** 33–64.

Subramaniyan. S., and Prema, P. (2000) *FEMS Microbiol. Lett.* **183**, 1–7.

Sunna, A., and Antranikian, G. (1997) *Crit. Rev. Biotechnol.* **17**, 39–67.

Tajima, M., Mizushima, M., Tada, T., and Kurokawa, H. (1985) *Hair cosmetics*, Japanese patent, 60126215, to Raion,

Taneja, K., Gupta, S., and Kuhad, R. C. (2002) *Bioresour. Technol.* **85**, 39–42.

Tang, J. (1977) In *Acid Proteases, Structure, Function, and Biology.* New York: Plenum Press.

Tang, J. (1979) *Mol. Cell Biochem.* **26**, 93-109.

Techapun, C., Poosaran, N., Watanabe, M., and Sasaki, K. (2003) *Process Biochem.* **38**, 1327–1340.

Tenkanen, M., Viikari, L., and Buchert, J. (1997) *Biotechnol Tech.* **1112**, 935–938.

Thomke, S., Rundgreen, M., and Hesselman, K. (1980) *The effect of feeding high-viscosity barley to pigs*. In: Proceedings of the 31st meeting of the European Association of Animal Production, Commission on Animal Production, Munich, Germany, 5.

Toshiyoshi, A., Shinnosuke, H., and Tatsuo, M. (2000) *Appl Environ Microbiol.* **66**, 1741–1743.

Viikari, L., Ranua, M., Kantelinen, A., Sundquist, J., and Linko, M. (1986) *Proc. 3rd Int. Conf. Biotechnology Pulp and paper Industry* , Stockholm , 67-69.

Voragen AGJ, Heutink R, Pilnik W. Solubilization of apple cell walls with polysaccharide degrading enzymes (1980) *J. Appl. Biochem.* **2**, 452–68.

Voragen, A. G. J. (1992) *Fruit Process.* **7,** 98–102.

Whistler, R., and Masek, E. (1955) *J. Am. Chem. Soc.* **77**, 1241–1243.

Whitehead, T. R., and Hespell, R. B. (1989) *Appl Environ Microbiol.* **55**, 893-896.

Whitmire, D., and Miti, B. (2002) *Chem. Eng. Commun.* **189**, 608–622.

Windish, W.W., and Mhatre, N. S. (1965) Microbial amylases. In: *Advances in Applied Microbiology* , Wayne WU (Ed) **vol. 7**. New York: Academic Press, 1965, 273-304

Wong, K. K. Y., and Saddler, J. N. (1992) *Trichoderma xylanases, their properties and applications.* In: Progress in Biotechnology, Visser, J., Beldman, G., Kusters-van Someren, M. A., Voragen, A. G. J. (Eds.) **Vol. 7**. Amsterdam: Elsevier, 171–86.

Wong, K. K. Y., and Saddler, J. N. (1993) *Applications of hemicellulases in the food, feed, and pulp and paper industries*. In: Hemicelluloses and hemicellulases. Coughlan MP, Hazlewood GP (eds) Portland Press, London, 127–143.

Wong, K. K. Y., and Saddler, J. N. (1993) *Applications of hemicellulases in the food, feed, and pulp and paper industries.* In: Hemicellulose and hemicellulases. Coughlan, M. P., Hazlewood G. P. (Eds.) London: Portland Press, 127–43.

Wong, K.K.Y., and Saddler, J.N. (1992) Portland press, London 127-143.

Wong, K.K.Y., and Sadler, J.N. (1992) Elsevier, Amsterdam, 171-186.

Wong, K.K.Y., Tan, L.U.L., and Saddler, J.N. (1988) *Microbiol. Rev.* **52**, 305–317.

Xia, Z., Beaudry, A. R., and Bourbonnais, R. (1996) *Prog. Pap. Recycl.* **5**, 46-58.

Yang, R.C., MacKenzie, C.R., Bilous, D., and Narang, S.A. (1989) *Appl. Environ. Microbiol.* **55**, 568–572.

Yoshizumi, H., Amachi, T., Kusumi, T., Tanaka, T., and Ishigooka, H. (1985) *Hair Cosmetics*, Japanese Patent, 60067409, to Suntory.

Zhao, J., Li, X., Qu, Y., and Gao, P. (2002) *Enzyme Microb. Technol.* 30, 734–740

CHAPTER-2

INHIBITION OF XYLANASE BY PEPTIDIC ASPARTIC PROTEASE INHIBITORS

INTRODUCTION

Specific enzyme inhibitors for target enzymes are not only useful probes of the kinetic and chemical mechanisms of enzyme-catalyzed reactions, but their action provides background information for the development of specific bioactive compounds. Of particular importance in these connections are compounds that act as inhibitory analogs of substrates and have high affinities for enzymes. Competitive inhibitors with specificity for a target protein are useful probes of the kinetic mechanisms of enzyme catalyzed reactions and membrane transport processes. The general approach to study such protein-inhibitor interactions involves the analysis of the decrease in reaction velocity that occurs in presence of an inhibitor as compared to inhibitor free control conditions. The demarcation between competitive and non-competitive enzyme inhibition is based on the ability of the inhibitor to dissociate from the enzyme-inhibitor complex. Kinetically competitive/reversible enzyme inhibition can be categorized into four different groups based on the strength of reversibility of the inhibitor as a function of time. Although it has been difficult to draw clear demarcation between the groups, the classification is mainly based on the reversibility, strength, and rates of their interaction with enzyme. Kinetically this classification has been applied to competitive inhibitors whose interactions cannot be explained by classical Michaelis-Menten kinetic parameters. The four categories of reversible inhibitors are classical, tight-binding, slow-binding, and slow, tight-binding inhibitors (Morrison, 1982).

The categories of reversible inhibitors are generally differentiable based on the ratio of total inhibitor (I_t) to total enzyme (E_t) concentration under experimental conditions and the qualitative time required for attainment of the equilibrium between the enzyme, inhibitor, and enzyme-inhibitor complex (Box I) (Morrison, 1982). For classical reversible inhibitors, the affinity for the inhibitor is sufficiently low that $I_t >> E_t$ and the rates at which the inhibitor associate and dissociate from the enzyme are relatively high. Inhibitors inhibiting the enzyme-catalyzed reactions at concentrations comparable to that of the enzyme and under conditions where the equilibria are set up rapidly are referred as tight binding inhibitors. In this case, the affinity of an enzyme for the inhibitor is very high and the experiments are performed in concentration regimes where $I_t \cong E_t$. Under such conditions steady-state treatments are inadequate

and incorrect, even though the net binding and release of inhibitors may be described by fast steps (Williams and Morrison, 1979). There have been some development of the kinetic theory for tight-binding inhibitors, but few studies have been undertaken in sufficient detail to test the theoretical predictions. The future development of inhibitors for chemotherapeutic purpose will undoubtedly depend on application of kinetic techniques that yield quantitative information about the behavior of the inhibitors. When the structure of the inhibitor can be correlated with the dissociation constants for the enzyme-inhibitor complexes, a systematic approach can be made towards the synthesis of more effective inhibitors for a particular enzyme. Delineating the inhibition mechanism and understanding of the binding efficiency will thus provide further insight into their *in vivo* efficacy. While classical and tight-binding inhibitors have been recognized for a very long time, awareness of compounds that cause inhibition of enzymes in a time-dependent manner came into limelight much later (Cha, 1975; Cha, 1976).

Box I

Correlation between the enzyme and inhibitor concentrations in competitive inhibition mechanisms

Inhibition Mechanism	Correlation between the E_t and I_t	Rate of equilibrium between E, I & EI
Classical	$I_t >>> E_t$	Fast
Tight-binding	$I_t \cong E_t$	Fast
Slow-binding	$I_t >>> E_t$	Slow
Slow, tight-binding	$I_t \cong E_t$	Slow

E_t and I_t are the total enzyme and inhibitor concentrations, respectively; E, and I are the free enzyme and inhibitor concentrations, respectively. EI stands for the reversible enzyme-inhibitor complex (adapted from Morrison, J. F. *Trends Biochem. Sci.* 1982)

A number of enzymatic reactions do not respond to the presence of competitive inhibitors instantly, but rather display a slow-onset of the inhibition. In some cases the inhibitor interacts slowly with the enzyme, while in others the formation of the enzyme-inhibitor complex takes place in a very short time. Such inhibition is called slow-binding inhibition and the inhibitor is refereed to as slow-binding inhibitor (Morrison, 1969; Williams and Morrison, 1979; Szedlacsek and Duggleby, 1995). The establishment of the equilibria between enzyme, inhibitor, and enzyme-inhibitor complexes, in slow binding inhibition occurs slowly on the steady-state time scale (Morrison and Walsh, 1988; Sculley et al., 1996), which has been reported for a series of different classes of enzymes (Baici and Gyger-Marazzi, 1982; Turner et al., 1983; Dunlap et al., 1987; Bakker., et al., 1990; Merker et al., 1990; Stover and Schirch, 1991; Hogg et al., 1992; Murphy and Coll, 1992; Gutheil and Bachovchin, 1993; Pegg and Itzstein, 1994; Ando et al., 1995; Garvey et al., 1997; Kati et al., 1998; Yiallouros et al., 1998; Ploux et al., 1999; Bienvenue et al., 2000; Jaffe et al., 2001; Selinsky et al., 2001; Dharmasena et al., 2002). Conditions of slow-binding inhibition where inhibitor concentrations are comparable to that of the enzyme are termed as slow-tight binding inhibition. Table 1 lists the enzymes, which are subjected to slow-binding and / or slow-tight binding inhibitions. As yet, no general concept has emerged for relating inhibitor and/or enzyme structure which allows the predictions to be made about the design of compounds that would give rise to slow-binding inhibition.

Table- 1

Enzymes subject to slow-binding or slow-tight binding inhibition

Enzymes	Inhibitor	Reference
Enoyl-acyl carrier protein reductase	*Triclosan*	Kapoor et al., 2004
Proteinase K	*API(Alkaline Protease Inhibitor)*	Pandhare et al., 2003
Dopamine beta monooxygenase	*3-hydroxy-4-phenylthiazole-2(3H)-thione (3H4PTT)*	Dharmasena et al.,2002
Porphobilinogen synthase (PBGS)	*Pb(II)*	Jaffe et al., 2001
Prostaglandin H(2) synthase	*NSAIDs*	Selinsky et al., 2001
Aminopeptidase	*L-leucinethiol*	Bienvenue et al., 2000
Thrombin	*Anophelin*	Francischetti et al., 1999
Nitric-oxide synthase	*N-(3-(Aminomethyl) benzyl) acetamidine (1400W)*	Garvey et al., 1997
Prostoglandin H synthase 1 and 2	*Indomethacin Flurbiprofen*	Callen et al., 1996
Trehalase	Trehazolin	Ando et al., 1995
Sialidase	*2,3,didehydro-2,4-dideoxy -4-guanidino-N- acetyl –D-Neuraminic acid*	Pegg and Itzstein, 1994
Leucine Aminopeptidase	*Bestatin*	Taylor et al., 1993
Phospholipase A2	*AACOCF3*	Street et al., 1993
Cathepsin B	*PCB1 (Propeptide)*	Fox et al., 1992
Calcium ATPase	*Fluoride*	Murphy and Coll, 1992
Plasmin	*Thrombospondin*	Hogg et al., 1992
Serine hydroxyl	*5-Formyltetrahydrofolate*	Stover and Schirch, 1991

methyl transferase	*polyglutamates*	
Prolyl endopeptidase	*benzyloxycarbonyl-prolyl-prolinal*	Bakker et al., 1990
Leukocyte elastase	*CBz-Ala-Ala-Pro-ambo-Val-CF_3*	Dunlap et al., 1987
Cathepsin B	*Leupeptin*	Baici and Gyger-Marazzi, 1982
Ribulose bisphospate carboxylase	*2-Carboxyarabinitol 1,5-bisphospate*	Pierce et al., 1980
Pepsin	*Pepstatin*	Rich and Sun, 1980
Hexokinase	*M (III) ATP complexes*	Viola et al., 1980
Aconitase	*Nitroisocitrate*	Schloss et al., 1980
Dihydrofolate reductase	*Methotexate*	Williams et al., 1979
	1-Deazamethotexate	Williams et al., 1980
Glutamine synthetase	*3-(Phosphonoacetylamido) -L-alanine*	Wedler and Horn, 1976
	4-(Phosphonocetyl)-L-α-aminobutyrate	Wedler and Horn, 1980
ATPase	*Vanadate*	Goodno, 1979
β-Lactamase	*Clavulanate*	Fisher et al., 1978
Adenosine deaminase	*9-(2-hydroxy-3-nonyl) adenine, coformycine*	Agarwal et al., 1977
Cytidine deaminase	*Tetrahydrouridine*	Wentworth and Wolfenden, 1975
Lactate oxidase	*Oxalate*	Ghisla and Massey, 1975
Xanthine oxidase	*Allopurinol*	Cha et al.,1975
Isocitrate lyase	*Itaconate*	Rittenhouse and McFadden, 1974
Enolase	*3-Aminoenolpyruvate*	Spring and Wold, 1971
Acetoacetate deacroboxylasse	*Acetylacetone*	Fridovich, 1968

From the kinetic point of view, the possible mechanisms for the slow-binding inhibition phenomena are described in Scheme I (Box II). When an inhibitor has a low K_i value and the concentration of I varies in the region of K_i, both k_3I and k_4 values would be low (Wolfenden, 1976; Cleland, 1979; Morrison and Stone, 1985; Bieth, 1995). Thus, a simple second-order interaction between enzyme and inhibitor, and low rates of association and dissociation would lead to slow-binding inhibition (Scheme Ia). In this case, the formation of an EI complex is a single slow step and the magnitude of k_3I is quite small relative to the rate constants for the conversion of substrate to product. However, scheme I b demonstrates the two-step slow-binding inhibition, where the first step involves the rapid formation of a reversible EI complex, which in the second step undergoes slow isomerization to a stable, tightly bound slow dissociating complex, EI* (Scheme Ib). The two-step mechanism of inhibition can be considered as the prototype of slow-binding inhibition on a steady-state time scale. The ratio between the kinetic constants of k_5/k_6 can be taken as an index of the accumulation of EI* and the energetic of its formation. The higher the values of k_5/k_6 ratio, the longer-lived is the EI* and the more likely the inhibitor is to have a useful *in vivo* lifetime. Slow binding inhibition can also arise due to an initial slow inter conversion of the enzyme E, to a conformationally-altered transition-state configuration E*, which binds to the inhibitor by a fast step (Scheme Ic). Kinetically, these mechanisms can be differentiated by investigating the behavior of the enzyme-inhibitor system at various concentrations of the inhibitor. Scheme Ia would predict that in the presence of substrate the initial rate of substrate hydrolysis will be independent of inhibitor concentrations since the concentration of EI would be significantly low. However, in Scheme Ib (slow-tight binding inhibition), the inhibitor will inhibit the enzyme competitively at the onset of the reaction, and at increasing concentration of inhibitor, the initial rate of substrate hydrolysis will decrease hyperbolically as a function of time. In tight binding inhibition, corrections have to be made for the reduction in the inhibitor concentration that occurs on formation of the EI complex, since the concentration of EI is not negligible in comparison to the inhibitor concentration and the free inhibitor concentration is not equal to the added concentration of the inhibitor. An understanding of the basis of the isomerization of EI complex to EI* complex could lead to the design of structures that allow titration of the lifetime of an EI* complex. The future development of slow-tight binding

inhibitors will undoubtedly depend on application of kinetic techniques that yield quantitative information about the properties of the inhibitor.

Box II

Scheme I

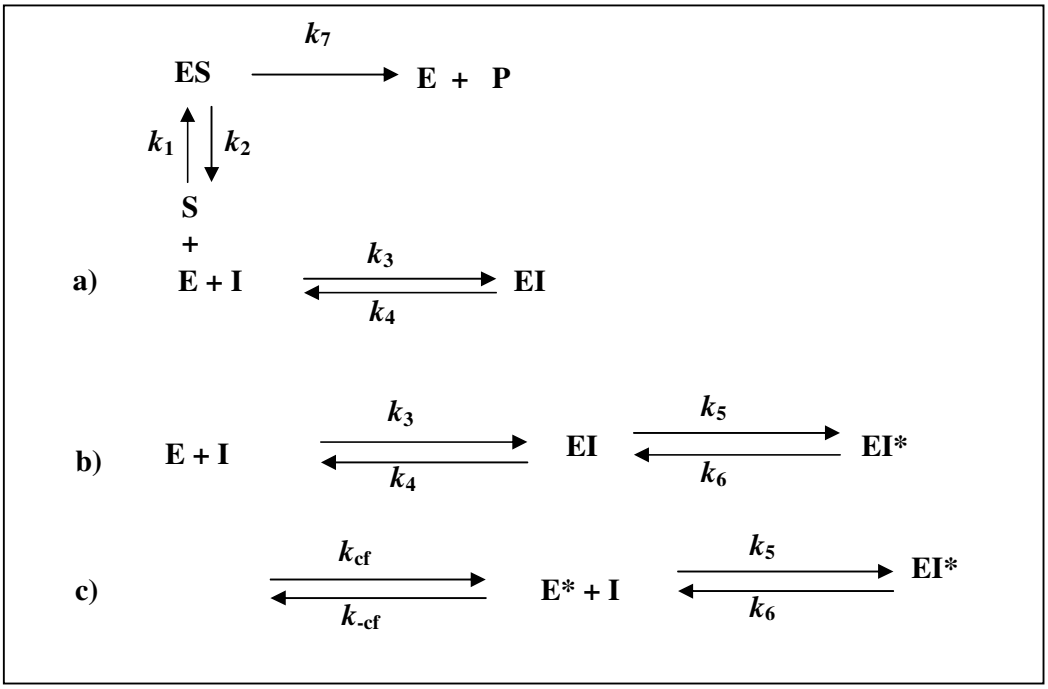

Kinetic schemes for slow-tight binding inhibition mechanism. E stands for free enzyme, I is free inhibitor, S is free substrate. ES and EI are the rapidly forming pre-equilibrium complex between enzyme-substrate and enzyme-inhibitor, respectively. EI* is the enzyme inhibitor complex which is the consequence of inhibitor induced conformational changes in EI. E* is the conformationally altered E, and k_{cf} and k_{-cf} are the rate constants for forward and backward reactions, respectively, associated with the conformational changes of the enzyme for. K_i is the ratio of k_4/k_3, the rate constants for the formation and dissociation of EI, respectively. K_i*, the overall inhibition constant for slow-tight binding inhibition, is a function of (k_6/k_5+ k_6) and is equal to the product of K_i and this function. k_5 and k_6 are the rate constants for the conversion of the first enzyme-inhibitor complex to the slowly dissociable EI* complex. k_1, k_2, are the rate constants associated with the formation and dissociation of ES, respectively, whereas, k_7 is the rate constant for product formation.

As in most ground-state inhibitors, formation of *EI* complex is too rapid to be measured at steady-state kinetics and was likely to be near diffusion control in slow-tight binding inhibition. However, the isomerization of EI to the second tightly bound enzyme-inhibitor complex EI* is too slow and relatively independent of the stability of the EI. Further the EI* complex is highly stable, and dissociates very slowly, therefore for slow-tight binding inhibition one of the major variable is k_6, the first-order rate constant associated with the conversion of *EI** to *EI*. The second major

variable is the apparent inhibitor constant K_i* which depends on the ability of the inhibitor to stabilize the EI*. The half-life of the *EI** depends on the k_6 value and longer the half-life of *EI** is an essential parameter for an inhibitor to have biomedical applications as drugs.

The onset of slow-tight binding inhibition is caused by a normal conformational mode of the enzyme-inhibitor complex that attains the stable configuration. The slow binding inhibitors bind at the active site of the target enzyme and then induce conformational changes that cause the enzyme to clamp down onto the inhibitor resulting in the formation of a more stable enzyme-inhibitor complex. The mechanism of conformational changes depends on the localization of the amino acids comprising the active center and the neighboring residues which actively interact with the inhibitor molecule. The conformational changes associated with the clamping down onto the inhibitor can be attributed to the network of molecular interactions, which includes hydrogen bonding, non-ionic and other weak interactions such as hydrophobic, Van der Waal's, ionic, etc, between the active site residues of the enzyme and reactive site residues of the inhibitor. As a function of time these network of interactions contribute to the stability and slow dissociative nature of the *EI** complex. These conformational changes in the enzyme-inhibitor complex are inhibitor induced and specifically different from gross three-dimensional conformational changes.

This chapter discusses the inhibition mechanisms and also evaluates the kinetic parameters associated with the interactions of xylanase, as a model system for hydrolytic enzymes, by aspartic protease inhibitors. Xylanases are carbohydrolases which catalyze the hydrolytic cleavage of β-1, 4 linked polymers of D-xylose. In recent years, considerable research efforts have been expended in the design and synthesis of glycosidase inhibitors, not only to understand about the active site structures and mechanisms of these interesting enzymes but also in generating new therapeutic agents. This chapter is divided into two sections; the first part describes the inhibition of xylanase by a peptidic aspartic protease inhibitor ATBI, isolated from an extremophilic *Bacillus* sp. and the second part discusses the mechanism of xylanase inhibition by specific aspartic protease inhibitor pepstatin obtained from commercial source.

PART - 1

STRUCTURAL AND MECHANISTIC INSIGHTS INTO THE INHIBITION OF XYLANASE BY AN ASPARTIC PROTEASE INHIBITOR FROM AN EXTREMOPHILIC *BACILLUS* SP.

SUMMARY

This section of the chapter describes the evaluation of the kinetic parameters of the slow-tight binding inhibition of xylanase by a peptidic inhibitor, *Alkalo Thermophilic Bacillus Inhibitor* (ATBI), from an extremophilic *Bacillus* sp. The steady-state kinetics revealed time-dependent competitive inhibition of xylanase by ATBI, consistent with two-step inhibition mechanism. The inhibition followed a rapid equilibrium step to form a reversible enzyme-inhibitor complex (*EI*), which isomerizes to the second enzyme-inhibitor complex (*EI**), which dissociated at a very slow rate. The rate constants determined for the isomerization of *EI* to *EI**, and the dissociation of *EI** were 13 ± 1 x 10^{-6} s^{-1} and 5 ± 0.5 x 10^{-8} s^{-1}, respectively. The K_i value for the formation of *EI* complex was 2.5 ± 0.5 μM, whereas the overall inhibition constant K_i* was 7 ± 1 nM. The conformational changes induced in xylanase by ATBI were monitored by fluorescence spectroscopy and the rate constants derived were in agreement with the kinetic data. Thus, the conformational alterations were correlated to the isomerization of *EI* to *EI**. ATBI binds to the active site of the enzyme and disturbs the native interaction between the histidine and lysine, as demonstrated by the abolished isoindole fluorescence of o-phthalaldehyde-labeled xylanase. The experimental results revealed that the inactivation of xylanase is due to the disruption of the hydrogen-bonding network between the essential histidine and other residues involved in catalysis and a model depicting the probable interaction between ATBI or OPTA with xylanase has been proposed.

INTRODUCTION

Specific inhibitors of glycosidases have proved valuable in a number of applications ranging from mechanistic studies (Legler, 1990; Sinnot, 1990) to possible therapeutic uses such as viral infectivity through interference with normal glycosylation of coat proteins (Elbein et al., 1984), against cancer, bacterial infections, and as insecticides (Leroy and Reymond, 1999). Modifying or blocking biological processes by specific glycosidase inhibitors have revealed the vital functions of the glycosidases in living systems. Since enzyme-catalyzed carbohydrate hydrolysis is a biologically widespread process, glycosidase inhibitors have many potential applications as agrochemicals and therapeutic agents. Glycosidases are involved in the biosynthesis of the oligosaccharide chains and quality control mechanisms in the endoplasmic reticulum of the N-linked glycoproteins. Inhibition of these glycosidase will have profound effects on quality control, maturation, transport, and secretion of glycoproteins, and can alter cell-cell or cell-virus recognition processes. This principle is the basis for the potential use of glycosidase inhibitors in viral infection, cancer and genetic disorders.

Glycosidase inhibitors as therapeutics have been highlighted in recent years with the successful marketing of the α-amylase inhibitor acarbose for the control of blood glucose levels and of the sialidase inhibitor relenza as a treatment for influenza. Acarbose is one of the new classes of oral α-glucosidase inhibitors used in the treatment of type-II diabetes. It is a linear tetrasaccharide of α - D-glucose residues modified at the non-reducing end. The non-reducing end group saccharide residue has a nitrogen replacing the interglycosidic oxygen atom and a double bond between C-4 and C-5 positions (Truscheit et al., 1981). Glyset or Miglitol (N-hydroxyethyldeoxynojirimycine), targeting the intestinal disaccharidases (Mitrakou et al., 1998) has been commercially available since 1996 for the treatment of type II diabetes (Sels et al., 1999; Scott and Spencer, 2000) Relenza (4-guanidino-2,4-dideoxy-2,3-dehydro-N-acetylneuraminic acid; Zanamivir; GG167) is a potent and highly specific sialidase inhibitor with inhibitory activity *in vivo* against both influenza A and B viruses (Fenton et al., 1999). This compound has been extensively tested in both mouse and ferret models of influenza and has recently been approved for the treatment of influenza. The compound markedly reduces the clinical course of

disease in humans when given therapeutically by inhalation directly into the respiratory tract (Fenton et al., 1999). Relenza belongs to a group of compounds called neuraminidase inhibitors. Neuraminidase is an enzyme, which breaks the bond holding new virus particles to the infected cell. Once broken, the new viruses are free to infect other cells, spreading the infection. Relenza is thought to work by inhibiting breakage of the bond and preventing release of the new viruses, therefore interrupting the spread of infection within the respiratory tract. Tamiflu or oseltamivir phosphate is a neuraminidase inhibitor also used to treat the infection of influenza virus (Lew et al., 2000).

A number of naturally occurring reversible glycosidase inhibitors such as nojirimycin, castanospermine and swainsonine have been reported (Legler, 1990). Nojirimycin and castanospermine are naturally occurring polyhydroxylated alkaloids known as aza-sugars. Nojirimycin is produced by *Bacilli* and *Streptomyces* sp. and shows inhibitory activity against plant and fungal glucosidases (Murao and Miyata, 1980). Castanospermine was isolated from the seeds of *Castanospermum australe* (Hohenschutz et al., 1981) and was found to be a powerful inhibitor of α and β glucosidases (Pan et al., 1983). Swainsonine, which is an indolizidine alkaloid, was isolated from the plant *Swainsona canescens*. Swainsonine is a specific and potent inhibitor of α-mannosidase (Dorling et al., 1980). Another class of inhibitors is the covalent, irreversible type, typically affinity labels. These are generally synthetic analogues of sugars containing reactive groups such as epoxides, isothiocyanates, and α-halocarbonyls (Legler, 1990; Withers and Aerbersold, 1995). There are reports of mechanism-based inhibitors such as conduritol epoxides (Legler, 1968), the quinone methide-generating glycosides (Halazy et al., 1990), and the glycosylmethyl triazenes (Marshall et al., 1980). These are more selective inhibitors whose efficacy depends upon binding and subsequent enzymatic action to generate a reactive species.

Glycosidases have also been studied with a clinical perspective of locating enzyme-allergens (Tarvainen and Keskinen, 1991). Some of these enzymes including xylanases and cellulases have been found to cause occupational and non-occupational allergies, such as respiratory and irritant contact dermatitis. Therefore, from the biomedical point of view inhibitors of this class of enzymes will have tremendous importance in near future. In addition, inhibition of cellulolytic and hemicellulolytic

enzymes have potential applications to prevent the degradation of wood and cloth by the action of the hydrolytic enzymes present in the gut of the termites. Xylanases (1, 4-β-D-xylan xylanohydrolase) are glycosidases that catalyze the hydrolytic cleavage of β-1, 4 linked polymers of D-xylose (Biely, 1985). The three dimensional structures of family 10 xylanases (Harris et al., 1994; White et al., 1994) have revealed the extended substrate binding cleft in which the surface residues are linked by an extensive hydrogen bond network. The cleft form deep grooves, consistent with their endo-mode action, and comprises a series of subsites, each one capable of binding a xylose moiety (Davies et al., 1997). The active site of xylanase contains two essential catalytic groups, one playing the role of acid/base and the other functioning as a nucleophile (Royers and Nakas, 1989). These two groups have been identified as carboxyl groups and a covalent intermediate is formed, which undergoes hydrolysis to afford hemiacetal with net retention of anomeric stereochemistry (Ly and Withers, 1999). The transition states leading to and from the covalent intermediate have substantial oxacarbonium ion character, as indicated by kinetic isotope effects and by the effects of electron-withdrawing substituents on the sugar ring upon reaction rate (Sinnot, 1990; Ly and Withers, 1999). Analysis of active site amino acids that plays an important role in substrate binding and in catalysis has been greatly facilitated by solving the crystal structure of family 10 xylanases covalently linked to mechanism-based cellobiosyl (2-deoxy-2-fluorocellobiosyl) and xylobiosyl (2-deoxy-2-fluoroxylobiosyl) inhibitors (White et al., 1996). To gain further insight into the details of the hydrolytic mechanism of glycosidases, specific inhibitors are necessary, which can act as mechanistic and structural probes. A diverse array of extremely potent, basic, nitrogen containing inhibitors has been developed over the years, and they have been found to be of great utility in the study of the glycosidase mechanism (Legler, 1990; Stutz, 1999).

Proteinaceous inhibitors of xylanase from plant sources

Plants produce proteinaceous inhibitors that target a range of glycosidases of plant, insect and fungal origin. Inhibitors for xylanase, polygalacturonases (Hoffman and Turner, 1984; Lafitte et al., 1984; Johnston et al., 1993), pectin methyl esterases (Marquis and Bucheli, 1994; Giovane et al., 1995), invertases (Jaynes, 1971; Bracho and Whitaker, 1990; Pressey, 1994) and α-amylases (Mundy et al., 1983; Weselake et al., 1983; Wilcox and Whitaker, 1984) have been isolated from a number of plant

species. The first evidence of a xylanase inhibitor protein was reported in 1997 by Debyser et al. (Debyser et al., 1997). The overall inhibition of xylanase activity in cereals can be attributed to the existence of two distinct classes of endoxylanase inhibitors, i.e. TAXI-type (*Triticum aestivum* xylanase inhibitor) and XIP (Xylanase Inhibitor Protein) type inhibitors, which can be further subdivided into families (Juge et al., 2004; Goesaert et al., 2004). Both inhibitor classes occur in monocots as multi-isoform families. TAXI -type are approximately 40-kDa proteins, which occur in a nonprocessed and a processed form (Debyser et al., 1999; Gebruers et al., 2001; Goesaert et al., 2001; Gebruers et al., 2002; Goesaert et al.,2002). TAXI-type proteins have been purified from different cereal sources, i.e., bread wheat (*T. aestivum*) (Debyser et al., 1999; Gebruers, 2001; Gebruers, 2002), rye (*Secale cereale*) (Goesaert et al., 2002), durum wheat (*Triticum durum*) (Goesaert, 2002) and barley (*Hordeum vulgare*) (Goesaert et al., 2001; Goesaert, 2002) , but have not been detected in corn (*Zea mays*), rice (*Oryza sativa*), oats (*Avena sativa*) and buckwheat (*Fagopyrum esculentum*) (Goesaert, 2002). Multiple isoinhibitors were obtained from *T. aestivum* (Gebruers et al., 2001; Gebruers et al., 2002) and *S. cereale* (Goesaert, 2002; Goesaert et al, 2002), while *T. durum* and *H. vulgare* contained two and one predominant TAXI-like inhibitors, respectively (Goesaert, 2002). The first two cereals contained much higher inhibitor levels than the latter two. After wheat milling, TAXI-related inhibition activity can be detected. The highest activity, however, occurs in the shorts, followed by the bran and flour, suggesting that most of the TAXI-related activity occurs in the outer wheat kernel tissues (Gebruers et al., 2002). Most of the TAXI-type inhibitors present in wheat grains are synthesized during the first 35 days after anthesis. They are possibly synthesized as precursor proteins with a signal sequence for secretion outside the plant cell. The TAXI-type xylanase inhibitors inhibit family 11 xylanases of bacterial and fungal origin, but have no activity towards family 10 xylanases (Gebruers, 2002).

XIP-I was first purified from wheat flour (*T. aestivum*) as a monomeric, glycosylated protein with a molecular mass of 29 kDa and a *pI* of 8.7–8.9 (McLauchlan et al., 1999). XIP-type proteins have since been detected in *S. cereale*, *H. vulgare*, *Z. mays*, *T. durum*, and other varieties of wheat, but not in *O. sativa* (Juge et al., 2004; Goeasert et al., 2004). The XIP-type inhibitors are specific for fungal endoxylanases of family 10 and family 11 but cannot inhibit bacterial xylanases (Flatman et al.,

2002). XIP-I shows the ability to inhibit barley α-amylases of glycoside hydrolase families 10 and 11 (Juge et al., 2004). There have been very few reports of naturally occurring inhibitors of xylanases and in literature there are no reports on low molecular weight peptidic inhibitors of this class of enzyme from extremophilic organisms. Low-molecular weight inhibitors released from microbial cells are different from macromolecular endogenous inhibitors. The low molecular weight inhibitors usually do not have functional roles in its cell, whereas the macromolecular endogenous inhibitors exhibit some functions in the cells.

The present chapter describes the interaction of ATBI, a peptidic inhibitor, with xylanase (Xyl I) from a *Thermomonospora* sp. The aspartic protease inhibitor (ATBI) was produced extracellularly by an extremophilic *Bacillus* sp. and was characterized for its inhibitory activity towards HIV-1 protease, pepsin, and the protease from *Aspergillus saitoi* (Dash and Rao, 2001; Dash et al., 2001a; Dash et al., 2001b). In this study, the kinetic parameters associated with the slow-tight binding inhibition of xylanase by the inhibitor have been evaluated. The steady state kinetics revealed a two-step inhibition mechanism and the conformational modes observed during the binding of inhibitor to the enzyme were conveniently monitored by fluorescence analysis. The mechanism of inactivation of Xyl I by ATBI was delineated by monitoring the isoindole fluorescence of the o-phthalaldehyde (OPTA) labeled enzyme.

MATERIALS AND METHODS

Chemicals

Oat spelt xylan, Dinitrosalicylic acid (DNSA), and o-phthalaldehyde (OPTA) were obtained from Sigma Chemical Co., U.S.A. Sephadex A-50 and Sephacryl S-200 were obtained from Amersham Biosciences, Sweden. All other chemicals used were of analytical grade.

Microorganisms and growth conditions

Thermomonospora sp. producing Xyl I is an alkalothermophilic actinomycete having optimum growth at pH 9 and 50°C. It was isolated from self-heating compost from the Barabanki district of Uttar Pradesh, India (George et al., 2001a). The ATBI producing extremophilic *Bacillus* sp. was isolated in this laboratory from the soil sample of a hot spring at Vajreswari, Maharashtra, India (Dey et al., 1991). The optimal growth condition of the *Bacillus* sp. is pH 10 and 50°C. For the production of the inhibitor, the *Bacillus* sp. was grown in a liquid medium containing soyameal and other nutrients (Table-2).

Table-2

(A). Media constituents used for *Bacillus* sp.

Constituents	Concentration (%)
Glucose	1.00
Peptone	0.75
Beef Extract	0.75
Sodium Chloride	0.30
Magnesium sulfate	0.10
Dipotassium hydrogen phosphate	0.10
Soyameal	2.00

The pH of the autoclaved medium was adjusted to 10 by the addition of sterile 10% sodium carbonate separately. Production of inhibitor was carried out by inoculating a loop full of freshly grown culture into the inoculum flask containing the liquid medium with the above composition at 50°C. The inoculum was kept for 24 hours in

the inoculum flasks at 50°C. 10 mL of inoculum was transferred into 500 mL Erlenmeyer flasks containing 100 mL of the above medium and was incubated under shaking conditions (250 rpm) at 50°C for 48 hours for the production of inhibitor.

Purification of ATBI

The cells and the residual soyameal from the extracellular culture broth of the extremophilic *Bacillus* sp. were separated by centrifugation at 6000 rpm, at 4°C, for 20 min in a Sorvall RC 5C super speed cooling centrifuge. The resulting extracellular culture filtrate (1000 mL) was treated with 65 gm of activated charcoal and incubated at 4°C overnight. The charcoal was removed by filtration through Whatman No. 3 filter paper. The colorless filtrate thus obtained was subjected to membrane filtration through Amicon UM10 (Mr cut off 10,000) and subsequently through amicon-UM2 (Mr cut off 2000). The resulting clear filtrate was concentrated by lyophilisation to 50 mL. The residual concentrated inhibitor was further purified by reverse phase high performance liquid chromatography (*rp-HPLC*). The concentrated inhibitor sample (100 µL) was loaded onto a prepacked Ultopac Lichrosorb RP-18 (LKB) column which was pre-equilibrated with 10 % acetonitrile (CH_3CN) and 0.1% trifluroacetate (TFA). The fractions detected at 210 nm were eluted on a linear gradient of 0-50% acetonitrile and water containing 0.1 % TFA. The fractions detected were collected manually and checked for its inhibitory activity against xylanase. The fractions showing the inhibitory activity were pooled and lyophilized for further studies.

Purification of Xyl I

Thermomonospora sp. is an alkalophilic actinomycete having optimum growth at pH 9 and 50°C. It was isolated from self –heating compost (George et al., 2001a). The cultivation medium used for xylanase production was modified Reses media.

Reses media (100mL) consists of the following components in the specified concentration (Table 3)

Table-3

(B). Reses media constituents used for *Thermomonospora sp.*

Constituents	Concentration
Tween 80	0.10%
K_2HPO_4	0.20%
$(NH_4)_2SO_4$	0.70%
Urea	0.15%
$MgSO_4$. $7H_2O$	0.03%
Peptone	0.125%
Yeast Extract	1.00%
$FeSO_4.7H_2O$ (1%)	50.0 µL
$MnSO_4.H_2O$ (1%)	15.6 µL
$ZnSO_4.7H_2O$ (1%)	14.0 µL
$CoCl_2$ (1%)	20.0µL

The microorganism was maintained in L.B plates. The inoculam was consisting of Reses medium with 2 % wheat bran and for the production of xylanase, 4 % of cellulose paper powder was used along with Reses medium. Always the medium was adjusted to pH 9 by using sterile 10 % Na_2CO_3. The fermentation was carried out at 50°C in a rotary shaker at 200 revolutions per minute for 96 hours. At the end of 96 hours, the fermentation broth was centrifuged at 10,000 r.p.m. at 4°C for 20 min. The supernatant was used as the source of enzyme. The culture filtrate (200 mL) was subjected to fractional ammonium sulphate precipitation (35-55%). The culture filtrate was initially saturated to 35 % by the slow addition of 38.8 g of ammonium sulphate. The solution was allowed to stand at 4°C. The precipitated solution was centrifuged at 10,000 rpm for 10 min at 4°C and the pellet was discarded while the supernatant was subjected to 55% saturation by the addition of 23.6 g of ammonium sulphate. The precipitate was recovered by centrifuging at 10,000 rpm for 10 min at 4°C. The pellet was dissolved in minimum amount of 0.05 M sodium phosphate buffer at pH 6 and dialyzed against 100 volumes of same buffer with several changes for 24 hours. The dialyzed fraction was applied to DEAE sephadex A-50 column, previously equilibrated with 0.05 M sodium phosphate buffer at pH 6. The sample

was loaded at a rate of 12 mL/ hour. The column was initially washed with 0.05 M sodium-phosphate buffer pH 6 at a rate of 16 mL / hour to remove the unadhered and loosely adhered proteins. It was observed that xylanase does not elute out until a salt concentration of 0.35 M, therefore the column first washed with two column volumes of 0.3 M sodium chloride in 0.05M sodium phosphate buffer, pH 6. The elution of the adhered proteins was carried out by a linear gradient of sodium chloride 0.3- 0.5 M in 0.05 M sodium phosphate buffer pH 6. Fractions of 8 mL each were collected and the fractions having maximum specific activity were pooled and concentrated by lyophilization. The concentrated sample was then loaded onto a sephacryl S-200 column, which was equilibrated with 0.05 M sodium phosphate buffer pH 6. Elution was carried out by using the same eluant at a flow rate of 10 ml per hour and 2 ml fractions were collected (George et al., 2001b).

Xylanase assay and inhibition kinetics

Xylanase assay was carried out in phosphate buffer, 0.05 M, pH 6.0, by mixing a specified concentration of the enzyme with 0.5 ml of oat spelt xylan (10 mg/ml) in a reaction mixture of 1 mL and incubating at 50°C for 30 min. The reducing sugar released was determined by the dinitrosalicylic acid method (Miller, 1959). One unit of xylanase activity was defined as the amount of enzyme that produced 1 µmol of xylose equivalent per min using oat spelt xylan as the substrate under assay conditions. Protein concentration was determined according to the method of Bradford (Bradford, 1976) using bovine serum albumin as the standard.

For initial kinetic analysis, the kinetic parameters for the substrate hydrolysis were determined by measuring the initial rate of enzymatic activity. The inhibition constant (K_i) was determined by the Lineweaver-Burk's equation. The K_m value was also calculated from the double-reciprocal equation by fitting the data into the computer software Microcal Origin. For the Lineweaver-Burk's analysis Xyl I (2 µM) was incubated with ATBI at (1 µM) and (2.5 µM) and assayed at increased concentration of xylan (1-10 mg/mL) at 50°C for 30 min. The reciprocals of substrate hydrolysis (1/v) for each inhibitor concentration were plotted against the reciprocals of the substrate concentrations and the K_i was determined by fitting the resulting data.

For the progress curve analysis, assays were carried out in a reaction mixture of 1 mL containing enzyme, substrate, and inhibitor at various concentrations. The reaction mixture contained Xyl I (50 nM) in sodium-phosphate buffer, 0.05 M, pH 6.0, and varying concentrations of ATBI (0.5-3 μM) and xylan (10 mg/mL). Reaction was initiated by the addition of Xyl I at 50°C and the release of products were monitored at different time intervals by estimating the reducing sugar at 540 nm. In each slow-binding inhibition experiment, five to six assays were performed with appropriate blanks. For the kinetic analysis and rate constant determinations, the assays were carried out in triplicates and the average value was considered throughout.

Evaluation of kinetic parameters

Initial rate studies for reversible, competitive inhibition were analyzed according to Equation 1.

$$v = \frac{V_{\max} S}{K_m (1 + I/K_i) + S} \qquad \text{(Eq. 1)}$$

Where K_m is the Michaelis constant, V_{max} is the maximal catalytic rate at saturating substrate concentration [S], $K_i = (k_4/k_3)$ is the dissociation constant for the first reversible enzyme-inhibitor complex, and I is the inhibitor concentration (Cleland, 1979). The progress curves for the interactions between ATBI and Xyl I were analyzed using Equation 2 (Beith, 1995; Morrison and Stone, 1985).

$$[P] = v_s t + \frac{v_0 - v_s}{k} (1 - e^{-kt}) \qquad \text{(Eq. 2)}$$

Where [*P*] is the product concentration at any time t, v_0 and v_s are the initial and final steady-state rates, respectively, and *k* is the apparent first-order rate constant for the establishment of the final steady-state equilibrium. As a prerequisite for tight-binding inhibitors, corrections have been made for the reduction in the inhibitor concentration that occurs on formation of the enzyme inhibitor (*EI*) complex. This is because in case of tight binding inhibition, the concentration of *EI* is not negligible in comparison to the inhibitor concentration and the free inhibitor concentration is not equal to the added concentration of the inhibitor [*I*]. The corrections of the variation of the steady-

state velocity with the inhibitor concentrations were made according to Equation 3 and 4 as described by Morrison and Walsh (Morrison and Walsh, 1988).

$$v_s = \frac{k_7 SQ}{2(K_m + S)} \qquad \text{(Eq. 3)}$$

$$Q = [(K_i' + I_t - E_t) + 4K_i' E_t]^{1/2} - (K_i' + I_t - E_t) \qquad \text{(Eq. 4)}$$

Where $K_i' = K_i^* (1 + S/K_m)$, k_7 rate constant for the product formation, I_t and E_t stands for total inhibitor and enzyme concentration, respectively.

The relationship between the rate constant of enzymatic reaction k, and the kinetic constants for the association and dissociation of the enzyme and inhibitor was determined as per Equation 5.

$$k = k_6 + k_5 \left[\frac{I / K_i}{1 + (S / K_m) + (I / K_i)} \right] \qquad \text{(Eq. 5)}$$

The progress curves were analyzed by equations 2 and 5 using non-linear least-square parameter minimization to determine the best-fit values with the corrections for the tight binding inhibition. The overall inhibition constant is determined as given by Equation 6.

$$K_i^* = \frac{[E][I]}{[EI] + [EI^*]} = K_i \left[\frac{k_6}{k_5 + k_6} \right] \qquad \text{(Eq. 6)}$$

The rate constant k_6, for the dissociation of the second enzyme-inhibitor complex was measured directly from the time-dependent inhibition. Concentrated Xyl I and ATBI were incubated in a reaction mixture to reach equilibrium, followed by large dilutions in assay mixtures containing near-saturating substrate. Xyl I (2 mM) was pre-incubated with equimolar concentrations of ATBI for 120 min in sodium-phosphate buffer, 0.05 M, pH 6.0. From the pre-incubated sample, 5 µl was removed and diluted 5000-fold in the same buffer and assayed at 50°C using xylan at (150 mg/ml) at different time intervals.

Fluorescence analysis

Fluorescence measurements were performed on a Perkin-Elmer LS50 Luminescence spectrometer connected to a Julabo F20 water bath. Protein fluorescence was excited at 295 nm and the emission was recorded from 300-500 nm at 25°C. The slit widths on both the excitation and emission were set at 5 nm and the spectra were obtained at 100 nm/min. For inhibitor binding studies, Xyl I (2 μM) was dissolved in sodium phosphate buffer, 0.05 M, pH 6.0. Titration of the enzyme with ATBI was performed by the addition of different concentrations of the inhibitor to a fixed concentration of enzyme solution. For each inhibitor concentration on the titration curve a new enzyme solution was used. All the data on the titration curve were corrected for dilutions and the graphs were smoothened. The magnitude of the rapid fluorescence decrease ($F_0 - F$) occurring at each ATBI concentration was computer fitted to the Equation 7, to determine the calculated value of K_i and ΔF_{max} (Houtzager, 1996).

$$(F_0 - F) = \Delta F_{max}/\{1 + (K_i/[I])\} \qquad \text{(Eq. 7)}$$

The first order rate constants for the slow loss of fluorescence k_{obs}, at each inhibitor concentration [I] were computer fitted to the Equation 8 (Houtzager, 1996), for the determination of k_5 under the assumption that for a tight binding inhibitor, k_6 can be considered negligible at the onset of the slow loss of fluorescence.

$$k_{obs} = k_5[I]/\{K_i + [I]\} \qquad \text{(Eq. 8)}$$

Time course of the protein fluorescence following the addition of inhibitor were measured for 10 min with excitation and emission wavelengths fixed at 295 and 340 nm, respectively, with data acquisition at 0.1 s intervals. Corrections for the inner filter effect were performed as described by Equation 9 (Lakowicz, 1983).

$$F_c = F \text{ antilog } [(A_{ex} + A_{em})/2] \qquad \text{(Eq.9)}$$

Where F_c and F stand for the corrected and measured fluorescence intensities, respectively, and A_{ex} and A_{em} are the absorbances of the solution at the excitation and emission wavelengths, respectively. Background buffer spectra were subtracted to remove the contribution from Raman scattering.

Effect of ATBI on the isoindole fluorescence of OPTA labeled Xyl I

Fresh OPTA solution was prepared in methanol for each experiment. The modification was carried out by incubating Xyl I (2 μM) in 1 mL 0.05 M sodium phosphate buffer, pH 6, with 50 μM of OPTA at 25°C. Methanol had no effect on the activity of the enzyme and was always less than 2 % (v/v). The formation of Xyl I-isoindole derivative was followed spectrofluorometrically by monitoring the increase in fluorescence with the excitation wavelength fixed at 338 nm. To monitor the effect of ATBI on the isoindole fluorescence of Xyl I, the enzyme was preincubated with ATBI (1 μM) for 15 min and then OPTA was added and the formation of isoindole derivative was monitored as described above.

RESULTS

Since the discovery of the potent inhibitory effects of deoxynojirimycin towards glycosidases in the early 1970s, this class of compound has engaged a vast amount of ongoing research interest concerning synthesis and the evaluation of their biological properties (Harris et al., 1994). Although a plethora of synthetic inhibitors have been reported, there is a lacuna of peptidic inhibitors of glycosidases from extremophilic microorganisms. It is noteworthy to point out that several extremophiles are known to produce highly thermostable xylanases and cellulases, however these organisms have not been studied extensively, for their potential exploitation towards isolation of inhibitors of important enzymes. This chapter deals with a bifunctional peptidic inhibitor ATBI, from an extremophilic *Bacillus* sp., exhibiting slow-tight binding inhibition against xylanase.

Kinetic analysis of the inhibition of Xyl I

The aspartic protease inhibitor (ATBI) was produced extracellularly by an extremophilic *Bacillus* sp. and was characterized for its inhibitory activity towards several aspartic proteases (Dash and Rao, 2001; Dash et al., 2001a; Dash et al., 2001b). The bifunctional nature of ATBI was established by its potency towards Xyl I, the xylanase purified from the *Thermomonospora* sp. Xyl I, a member of family 10 xylanase is highly thermostable with half-lives of 86, 30, and 15 min at 80, 90, and 100°C, respectively, and is stable in an expansive pH range of 5-10 with more than 75 % residual activity. Initial kinetic assessments revealed that ATBI is a competitive inhibitor of Xyl I with an IC_{50} value of 6.5 ± 0.5 μM (Figure 1). In the absence of ATBI, the steady-state rate of xylanolytic activity of Xyl I reached rapidly whereas, in its presence a time-dependent decrease in the rate as a function of the inhibitor concentration was observed. Examination of the progress curves revealed a time range where the initial rate of reaction did not deviate from linearity (Figure 2), and the conversion of *EI* to *EI** was minimal. For a low concentration of ATBI this time range was 8 min, within which classical competitive inhibition experiments was used to determine the K_i values (Equation 5). The value of the inhibition rate constant K_i, associated with the formation of the reversible enzyme inhibitor complex (*EI*) determined from the fits of data to the reciprocal equation was 2.5±0.5 μM (Figure 3).

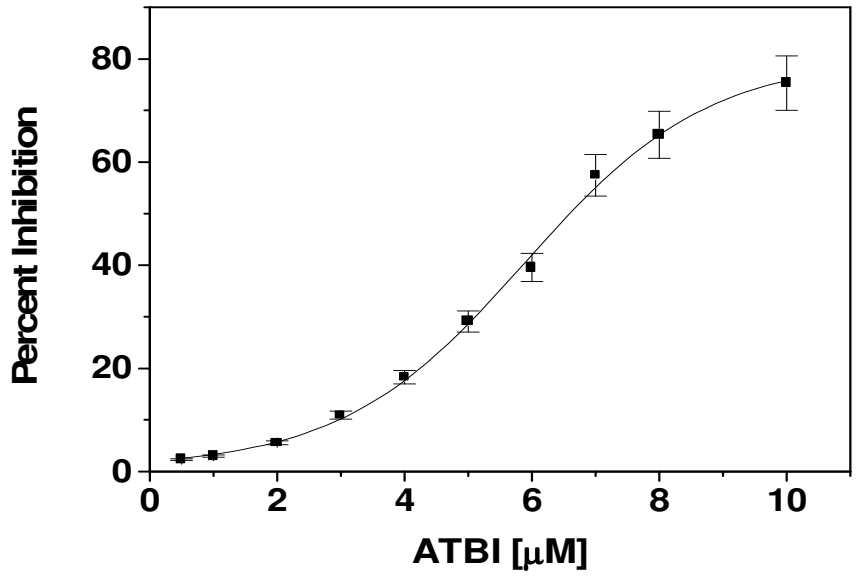

Figure 1. Inhibition of Xyl I by ATBI. The xylanolytic activity of the purified Xyl I (2 μM) was determined in the presence of increasing concentrations of ATBI. The percent inhibition of the xylanase activity was calculated from the residual enzymatic activity. The sigmoidal curve indicates the best fit for the percent inhibition data (average of triplicates) obtained and the IC_{50} value was calculated from the graph.

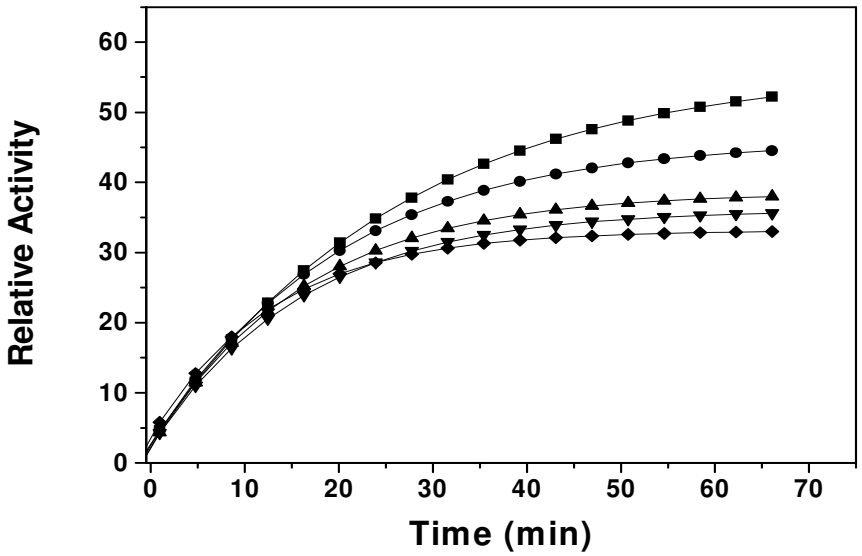

Figure 2. Time course of inhibition of Xyl I by ATBI The reaction mixture contained Xyl I (50 nM) in sodium-phosphate buffer, 0.05 M, pH 6.0, and varying concentrations of ATBI and xylan (10 mg/ml). Reaction was initiated by the addition of Xyl I at 50°C. The points represent the hydrolysis of substrate as a function of time and the lines indicate are the best fits of data obtained from eq 2 and 5, with the corrections made as per the eq 3 and 4. Concentrations of ATBI were 0.465 μM (■), 0.62 μM (♦), 0.95 μM (▲), 1.55 μM (▼), and 3 μM (♦)

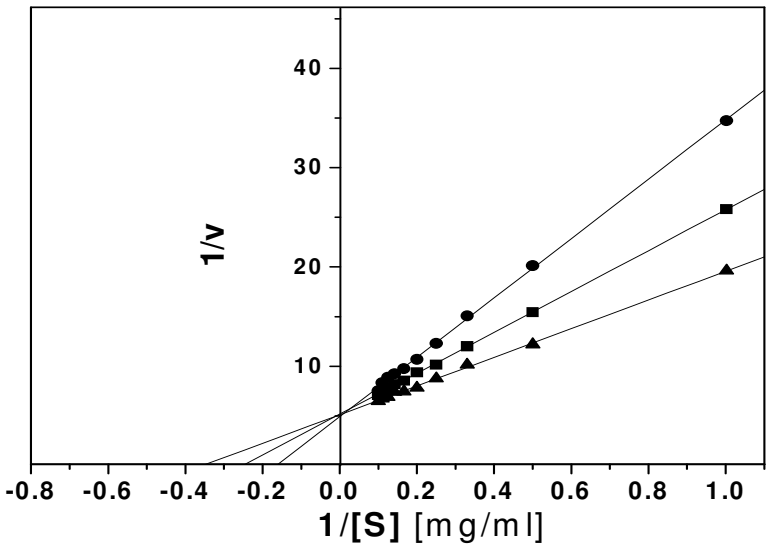

Figure 3. Initial rate of enzymatic reaction of Xyl I in the presence of ATBI Enzymatic activity of Xyl I was estimated using oat spelt xylan in sodium-phosphate buffer, 0.05 M, pH 6.0 and the xylose equivalent was determined at 540 nm. Xyl I (2 µM) was incubated without (▲) or with the inhibitor at 1 µM (■) and 2.5 µM (●) and assayed at increased concentration of xylan (1-10 mg/ml) at 50°C for 30 min. The reciprocal of substrate hydrolysis (1/v) for each inhibitor concentration were plotted against the reciprocal of the substrate concentration. The straight lines indicated the best fits for the data obtained by non-linear regression analysis and analyzed by Lineweaver-Burk's reciprocal equation.

The apparent rate constant *k*, derived from the progress curves when plotted *versus* the inhibitor concentration followed a hyperbolic function (Figure 4), revealing a fast equilibrium precedes the formation of the final slow dissociating enzyme-inhibitor complex (*EI**), indicating two-step, slow-tight inhibition mechanism (Scheme I, Page 30). Indeed, the data could be fitted to Equation 5 by non-linear regression analysis, which yielded the best estimate of the overall inhibition constant K_i* of 7± 1 nM.

In an alternative method, the rate constant k_6, for the conversion of *EI** to *EI*, was determined by pre-incubating high concentrations of enzyme and inhibitor for sufficient time to allow the system to reach equilibrium. Dilution of the enzyme-inhibitor complex into a relatively large volume of assay mixture containing saturating substrate concentration causes dissociation of the enzyme-inhibitor complex and thus regeneration of enzymatic activity. Under these conditions, v_0 and the effective inhibitor concentration can be considered approximately equal to zero and the rate of activity regeneration will provide the k_6 value. After pre-incubating

Xyl I with ATBI, the enzyme inhibitor mixture was diluted 5,000-fold into the assay mixture containing the substrate at 50 K_m. By least-squares minimization of equation 2 to the data for recovery of enzymatic activity, the determined k_6 value was 5±0.5 x 10^{-8} s^{-1} (Figure 5), which clearly indicated a very slow dissociation of *EI**. The final steady-state rate v_s, was determined from the control that was pre-incubated without the inhibitor. The value of the rate constant k_5, associated with the isomerization of *EI* to *EI**, was 13 ±1 x 10^{-6} s^{-1} as obtained from fits of equation 5 to the onset of inhibition data using the experimentally determined values of K_i and k_6 (Table-4). The overall inhibition constant K_i* is a function of $k_6/(k_5 + k_6)$ and is equal to the product of K_i and this function. The k_6 value indicated a slower rate of dissociation of *EI** complex and the half-life $t_{1/2}$, for the reactivation of *EI** as determined from k_6 value was 38.5 ± 4 x 10^2 hours, suggesting higher binding affinity of ATBI towards Xyl I.

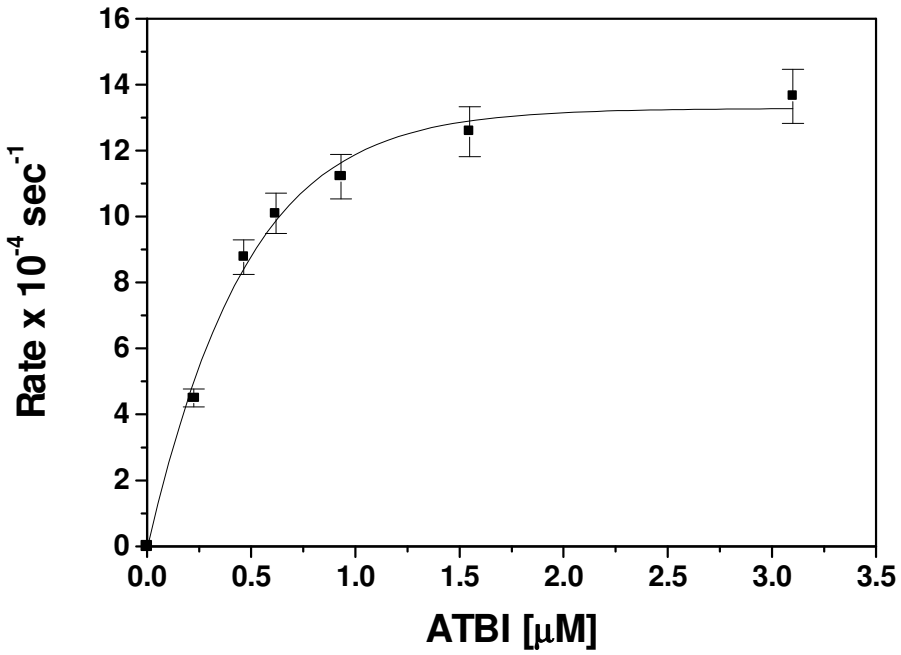

Figure 4. Dependence of Xyl I inhibition on ATBI concentration The rate constants *k*, were calculated from the progress curves recorded following the addition of Xyl I to the reaction mixture containing xylan and ATBI. The solid line indicates the best fit of the data obtained.

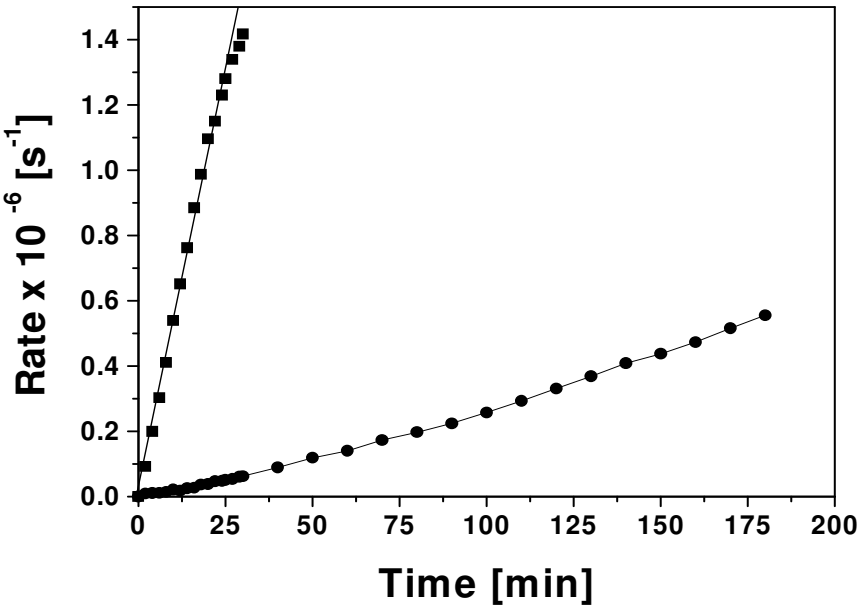

Figure 5. Dissociation rate constant (k_6) for Xyl I-ATBI complex Xyl I (2 mM) was pre-incubated without (■) or with (●) equimolar concentrations of ATBI for 120 min in sodium-phosphate buffer, 0.05 M, pH 6.0, at 50°C. The rate constant associated with the regeneration of activity (k_6) was determined by estimating the reducing sugar.

Table-4

Inhibition constants of ATBI against Xyl I

Inhibition Constants	Values
IC_{50}	6.5 x 10^{-6} M
K_i	2.5±0.5 x 10^{-6} M
K_i*	7.0±1 x 10^{-9} M
k_5	13.0±1 x 10^{-6} s^{-1}
k_6	5.0±0.5 x 10^{-8} s^{-1}
k_5/k_6	2.60 ±3 x 10^2
$t_{1/2}$	38.5 x 10^2 h

Values of rate constants for Xyl I inhibition by ATBI were calculated from Scheme I (Page 30) at 50°C in sodium-phosphate buffer, 0.05 M, pH 6.0 using oat spelt xylan as the substrate. IC_{50} is from the inhibition profile; K_i was determined from the steady-state time range for the competitive inhibition. k_6 is calculated from the regeneration assay, K_i* and k_5 were determined from the equations as described in the materials and methods.

There are two alternative models for the time-depended inhibition by Scheme I (Page 30) (Beith, 1995; Erison and Walsh, 1987). The mechanism in scheme Ia, where the binding of the inhibitor to the enzyme is slow and tight, but occurs in a single step, is eliminated based on the data of Table-4, because the inhibitor has measurable effect on the initial rates before the onset of slow-tight binding inhibition. Scheme Ic represents the inhibition model where the inhibitor binds only to the free enzyme that has slowly adopted the transition-state configuration can also be eliminated by the observed rates of onset of inhibition. From the observed results, it is concluded that the inactivation of Xyl I followed slow-tight binding mechanism as described in Scheme Ib.

Effect of inhibitor binding on the fluorescence of Xyl I

The kinetic analysis revealed a two-step inhibition mechanism, where the *EI* complex isomerizes to a tightly bound, slow dissociating *EI** complex. This isomerization is characterized by the induction of conformational changes in the enzyme due to the binding of ATBI. To delineate the conformational changes induced in the aspartic protease due to the binding of ATBI, the fluorescence of the enzyme-inhibitor complexes were monitored. The conformational changes induced in Xyl I upon binding of ATBI were monitored by exploiting the intrinsic fluorescence by excitation of the π - π^* transitions in Trp residues. The tryptophanyl fluorescence of Xyl I exhibited an emission maxima (λ_{max}) at ~339 nm, as a result of the radiative decay of the π - π^* transition from the Trp residues (Figure 6).

The binding of ATBI resulted in a concentration dependent quenching of the fluorescence with saturation reaching at/above 6 μM of ATBI (Inset of Figure 6). The absence of blue or red shift in λ_{max} negated any drastic gross conformational changes in the three-dimension structure of the enzyme due to inhibitor binding. The subtle conformational changes induced during the isomerization of *EI* to *EI** was monitored by analyzing the tryptophanyl fluorescence of the complexes as a function of time. Binding of ATBI resulted an exponential decay of the fluorescence intensity as indicated by a sharp decrease in the quantum yield of fluorescence followed by a slower decline to a stable value (Figure 7). Furthermore, titration of ATBI against Xyl I revealed that the magnitude of the initial rapid fluorescence loss ($F_0 - F$) increased in a saturation-type manner (Figure 8), which corroborated the two-step slow tight

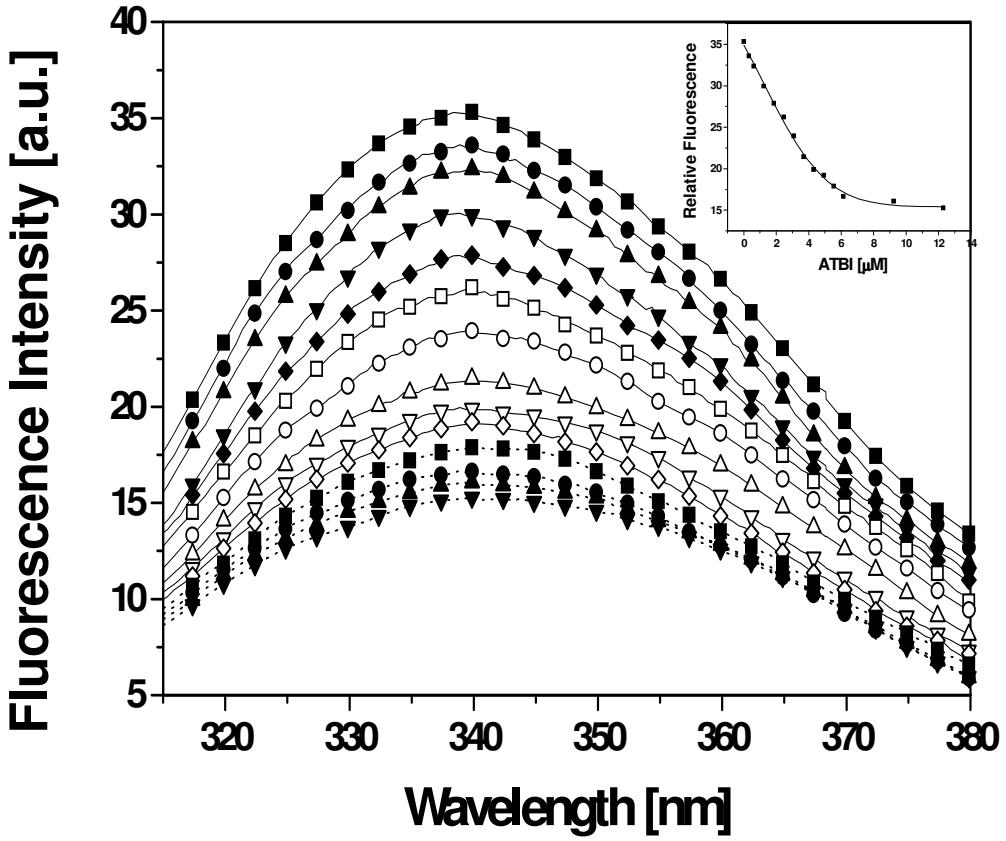

Figure 6. Steady state fluorescence emission spectra of Xyl I as a function of ATBI Protein fluorescence was excited at 295 nm and emission was monitored from 300-400 nm at 25°C. Titration was performed by the addition of different concentrations of the inhibitor to a fixed concentration of enzyme. Xyl I was dissolved in sodium-phosphate buffer, 0.05 M, pH 6.0, and the concentrations of ATBI used were 0 μM (■), 0.31 μM (●), 0.62 μM (▲), 1.24 μM (▼), 1.86 μM (♦), 2.48 μM (o), 3.1 μM (o), 3.72 μM (Δ), 4.34 μM (∇), 4.96 μM (◊), 5.58 μM (- -■- -), 6.2 μM (- -●- -), 9.3 μM (- -▲- -), and 12.4 μM (- -▼- -). The curve in the inset represents the best fit of the fluorescence quenching data of Xyl I at 339 nm (λ_{max}) as a function of ATBI concentration

binding inhibition of Xyl I by ATBI. From the data in figure 8, the magnitude of the rapid fluorescence decrease at a specific ATBI concentration was found to be close to the total fluorescence quenching observed figure 6, indicating that the *EI* and *EI** complexes have the same intrinsic fluorescence. The value of K_i determined by fitting the data for the magnitude of the rapid fluorescence decrease ($F_0 - F$) was 2.6±0.5 μM and the k_5 value determined from the data derived from the slow decrease in fluorescence was 13.5±0.5 x 10^{-6} s^{-1}. These rate constants are in good agreement with that obtained from the kinetic analysis, therefore, the initial rapid fluorescence decrease can be correlated to the formation of the reversible complex *EI*, while the

slow, time dependent decrease reflected the accumulation of the tight bound slow dissociating complex *EI**.

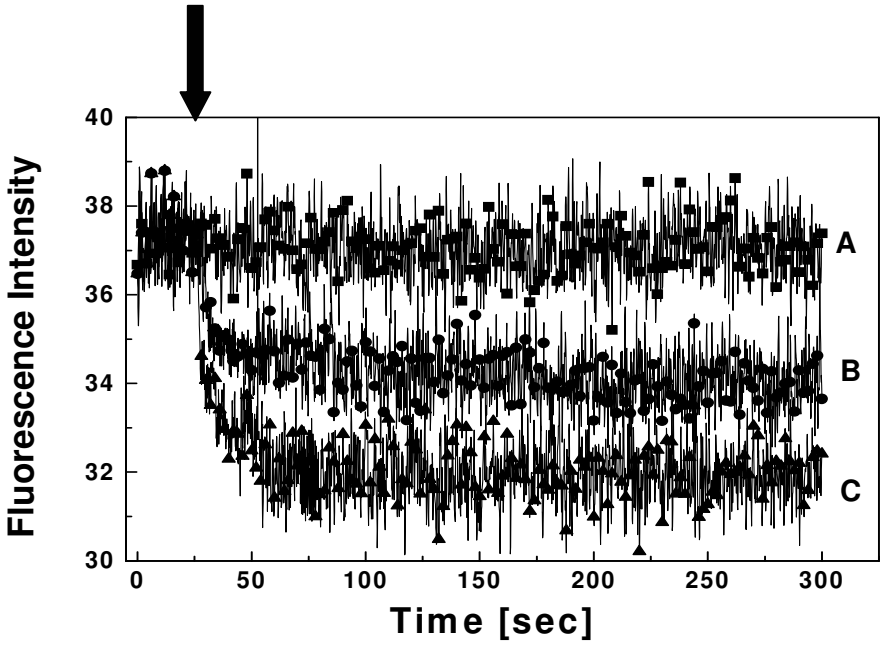

Figure 7. Time dependent Effect of ATBI on the fluorescence quenching of Xyl I The concentrations of ATBI used were 0 μM (A), 0.62 μM (B), and 1.24 μM (C)

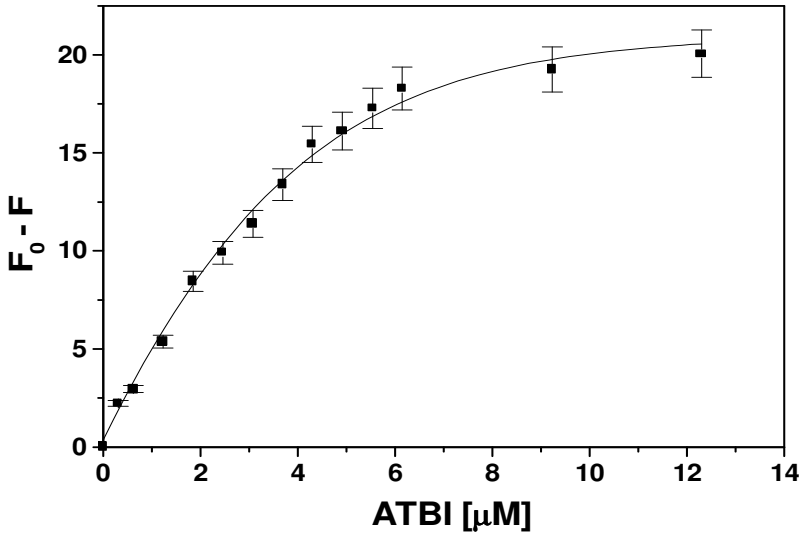

Figure 8. Effect of ATBI concentration on the tryptophan fluorescence of Xyl I. The fluorescence changes ($F-F_0$) were plotted against the inhibitor concentrations. The resulting hyperbola indicates the best fit of the data obtained.

Effect of ATBI on the isoindole fluorescence of Xyl I by OPTA

In our laboratory, we have investigated the role of essential histidine and lysine residues in the active site of the Xyl I and showed that binding of the chemoaffinity label OPTA to these residues of the active site resulted in the formation of an isoindole derivative (George and Rao, 2001). The active site of Xyl I constitute of the catalytic carboxylic groups and the histidine residue, which play crucial role in catalysis. In order to investigate the binding of ATBI to the active site and changes in the native intermolecular interactions, the interaction of the lysine and histidine due to ATBI binding and their influence on the isoindole fluorescence of Xyl I have been monitored using fluorescence spectroscopy (Figure 9). The unbound enzyme did not show fluorescence when excited at 338 nm, however incubation of OPTA with Xyl I resulted in an increase in the fluorescence with a λ_{max} at 417 nm due to the formation of the isoindole derivative. The ATBI pre-incubated Xyl I failed to react with OPTA as revealed by the total loss of isoindole fluorescence, which not only confirmed the binding of ATBI to the active site of Xyl I but also further revealed that the binding of ATBI resulted in the formation of a new set of hydrogen bonding and other nonionic interactions. These altered weak interactions cause disruption of the native hydrogen-bonding network of the histidine and lysine residues, which are essential for the formation of isoindole derivative.

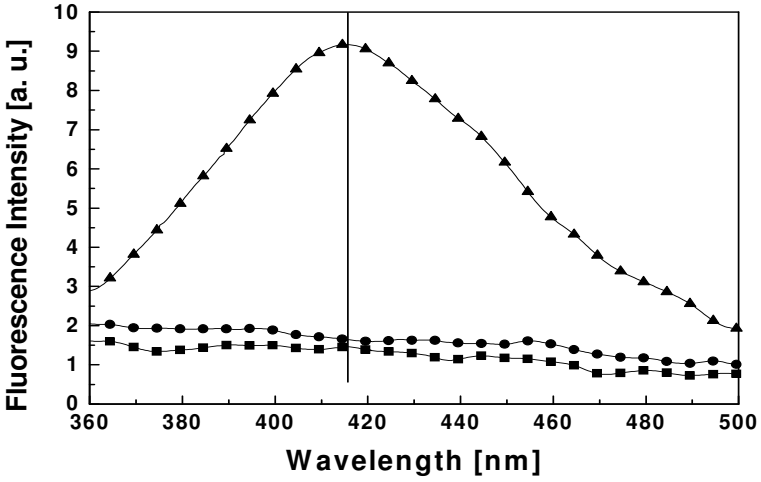

Figure 9. Isoindole fluorescence of Xyl I on reaction with OPTA. Xyl I (2 μM) was treated without or with ATBI (1 μM) and was incubated at 25°C for 20 min and then further incubated with a fresh solution of OPTA (50 μM). The isoindole fluorescence of the Xyl I bound OPTA was measured with excitation at 330 nm. The lines represent the isoindole fluorescence of Xyl I (■), Xyl I + OPTA (▲), and Xyl I + ATBI (preincubated) and OPTA (♦) and are the average of six scans with corrections from buffer and respective controls.

DISCUSSION

A bifunctional peptidic inhibitor ATBI, from an extremophilic *Bacillus* sp., exhibiting slow-tight binding inhibition against xylanase is described in this chapter. The inhibitor showed exceptionally high potency against Xyl I, the thermostable xylanase from a *Thermomonospora* sp., and its 1:1 molar ratio of interaction with the enzyme indicated its "tight-binding" nature. The two-step inhibition mechanism was corroborated by the equilibrium binding studies of the enzyme and inhibitor, and the correlation of the kinetic data with the conformational changes induced in the enzyme-inhibitor complexes.

In the presence of competitive inhibitors, a number of enzymatic reactions do not respond immediately, but display a slow-onset of inhibition, which is referred as slow-binding inhibition (Williams and Morrison, 1979; Wolfenden, 1976; Szedlacsek and Duggleby, 1995; Sculley et al., 1996). The establishment of the equilibria between enzyme, inhibitor, and enzyme-inhibitor complexes, in slow binding inhibition occurs slowly on the steady-state time scale (Morrison, 1982; Yiallouros et al., 1998; Ploux et al., 1999; Pegg and Itzstein, 1994; Kati et al., 1998). Enzyme-catalyzed reactions, where the concentrations of the enzyme and inhibitor are comparable, and the equilibria are set up rapidly are referred as tight binding inhibition. Kinetically the slow-binding inhibition can be illustrated by three mechanisms (Scheme I; Page 30). When an inhibitor has a low K_i value and the concentration of I varies in the region of K_i, *both* k_3I and k_4 values would be low. Thus, a simple second-order interaction between enzyme and inhibitor, and low rates of association and dissociation would lead to slow-binding inhibition. Alternatively, a two-step model depicts the rapid formation of an initial collisional complex *EI*, which slowly isomerizes to form a tightly bound slow dissociating complex *EI**. Slow binding inhibition can also arise due to an initial slow inter conversion of the enzyme *E*, into another form *E**, which binds to the inhibitor by a fast step. Understanding the basis of the isomerization of *EI* to *EI** could lead to design of inhibitors that allow titration of the lifetime of the *EI**. In case of slow-tight binding inhibition, the inhibitor will inhibit the enzyme competitively at the onset of the reaction, however at increasing concentration of inhibitor, the rate of substrate hydrolysis will decrease hyperbolically as a function of time. In tight binding inhibition corrections have to be made for the reduction in the inhibitor concentration that occurs on formation of the

EI complex, since the concentration of *EI* is not negligible in comparison to the inhibitor concentration and the free inhibitor concentration is not equal to the added concentration of the inhibitor. The formation of *EI* complex between Xyl I and ATBI was too rapid to be measured at steady-state kinetics and was likely to be near diffusion control. However, the isomerization of *EI* to the second tightly bound enzyme inhibitor complex *EI**, was too slow and relatively independent of the stability of the *EI* or the ability of the inhibitor to stabilize the *EI**. The k_6 values revealed very slow dissociation of the inhibitor from the *EI** indicating a highly stable, non-dissociative nature of the second complex. Therefore for slow-tight binding inhibition the major variable is k_6, the first-order rate constant associated with the conversion of *EI** to *EI*, and the apparent inhibitor constant K_i* depends on the ability of the inhibitor to stabilize the *EI**. The half-life as derived from the k_6 value indicated a longer half-life of the *EI**, which is an essential parameter for an inhibitor to have biomedical applications.

The characteristic feature of slow binding inhibition is the induction of conformational changes in the enzyme-inhibitor complex, resulting in the clamping down of the enzyme to the inhibitor, thus the formation of a stable enzyme-inhibitor complex. The two-step inhibition mechanism of Xyl I by ATBI was reflected in the quenching pattern of the fluorescence of the enzyme-inhibitor complexes. The rate constants derived from the fluorescence analysis of the complexes corroborated the values derived from the kinetic analysis. Therefore, it is proposed that the initial rapid fluorescence loss reflected the formation of the reversible complex *EI*, whereas the subsequent slower decrease was correlated to the accumulation of the tightly bound complex *EI**. Any major alteration in the three-dimensional structure of Xyl I due to the binding of ATBI can be ruled out, since there was no shift in the tryptophanyl fluorescence of the complexes. Any disturbance in the environment of tryptophan residues may reflect in an alternation in emission wavelength, quantum yield, and susceptibility to quenching (Pawagi and Deber, 1990). Energy transfer to an acceptor molecule having an overlapping absorption spectrum can also contribute to fluorescence quenching (Cheung, 1991). However, as the inhibitor has no absorption in the region of 290-450 nm, the fluorescence quenching due to the energy transfer between the inhibitor and the tryptophan residues of Xyl I have been neglected. The other possibility is the presence of multiple sites, where binding at one induced rapid

fluorescence change and at a second site caused the slow fluorescence decrease. This was verified by titrating a fixed concentration of Xyl I with increasing concentrations of ATBI. The xylanolytic activity decreased linearly with increasing concentrations of ATBI yielding a stoichiometry close to 1:1 (also revealed by fluorescence) expected for the slow-tight binding inhibition, therefore inconsistent with the presence of multiple high-affinity sites. From the physical explanation for the quenching process, it was apparent that the inhibitor induced fluorescence quenching followed the formation of both the complexes. The agreement of the rate constants concomitant with the fluorescence changes observed during the time-dependent inhibition, correlates well with the localized conformational changes in the enzyme-inhibitor complex to the isomerization of the *EI* to *EI**.

Conformational integrity of the active site of an enzyme is essential for its catalysis and investigations on the molecular orientation of the functional groups of active site as well as their microenvironment are the areas of growing scientific interest. Chemo-affinity labeling is a powerful technique to assign the binding sites of ligand-macromolecule complexes, which combines some of the advantages of both the photo activated and electrophilic affinity labeling (Simons et al., 1979). OPTA is a bifunctional, fluorescent chemoaffinity label, which until recently was known to have absolute specificity for amino and thiol groups (Palczewski et al., 1983) for the formation of an isoindole derivative. However, application of OPTA as a probe to ascertain the conformational flexibility and polarity of the active site of Xyl I by the formation of a fluorescent isoindole derivative with the lysine and histidine residue have been reported in our laboratory (George and Rao, 2001). OPTA contains two aldehyde groups; one of which reacts with the primary amine of lysine, while the second group reacts with the secondary amine of the imidazole ring of histidine, resulting in the formation of the isoindole derivative. A schematic model depicting the interaction of the aldehyde groups of OPTA with the secondary amine of His and the primary amine of Lys residue of the Xyl I has been proposed (Figure 10A). The present results revealed that, when Xyl I was preincubated with ATBI, OPTA failed to form the isoindole derivative as reflected by the loss of fluorescence. The inability of OPTA to form the isoindole derivative with the ATBI bound Xyl I could be attributed to the interaction of ATBI with either lysine or histidine or both the residues, thereby changing the native molecular interactions of these residues. The

amino acid sequence of ATBI (Ala-Gly-Lys-Lys-Asp-Asp-Asp-Asp-Pro-Pro-Glu) revealed the presence of amino acid residues such as Asp, Lys, and Glu with charged side chains. It is proposed that, the carboxyl group of the Asp residues of ATBI (Figure 10B) can form hydrogen bonding with the amines of His and Lys residues of Xyl I, thereby preventing the binding of OPTA. This, however, does not exclude the possible role of steric hinderance exerted by the bound ATBI in preventing the binding of OPTA to the active site. The catalytic site of xylanases consists of two carboxyl groups and an essential lytic water molecule and follows a general acid-base catalytic mechanism (Rao et al., 1998). Based on the existing experimental evidences, it is further proposed that the charged side chains of the amino acids, the amide nitrogens, and the carbonoyl oxygen groups of ATBI could form many intermolecular hydrogen bonds and other weak interactions (van der Waal's, ionic, etc.) with the residues in or near the active site of Xyl I. The tight-binding nature of ATBI in conjunction with the multiple nonbonded interactions may be sufficient to interfere in the native weak interactions between the carboxyl groups, the lytic water molecule and the essential histidine residue of the active site, leading towards the inactivation of Xyl I.

In figure 10, the active site of the Xyl I has been modeled based on the X-ray crystallographic structure of a similar thermostable family 10 xylanase from *Thermoascus aurantiacus* (Natesh et al., 1999) (PDB ID 1TUX) using the software Quanta/SYBYL, MSI. The active site of Xyl I includes the essential Glu, His, and Lys residues. Figure 10 A, the chemoaffinity label OPTA (shown in *purple color*) contains two aldehyde groups, one of which binds to the primary amine of the Lys and the other group reacts with the secondary amine of the imidazole ring of His of Xyl I resulting in the release of two water molecule (not shown). These chemical reactions result in the formation of a fluorescent isoindole derivative. In figure 10 B., preincubation of ATBI with Xyl I resulted in the binding of the inhibitor in the active site of the enzyme. Based on the obtained results, it is proposed that, the Asp residues in the ATBI (shown in *purple color*) form hydrogen bonds (*solid dashed lines*) with the free amine group of the Lys and the secondary amine of the His of Xyl I. The other charged residues (not shown) can form many non-bonded interactions with the active site residues of Xyl I. These interactions in conjunction with the tight binding

nature of ATBI probably prevent the binding of OPTA to the His and Lys residues, thus an isoindole derivative failed to be formed with the ATBI-preincubated Xyl I.

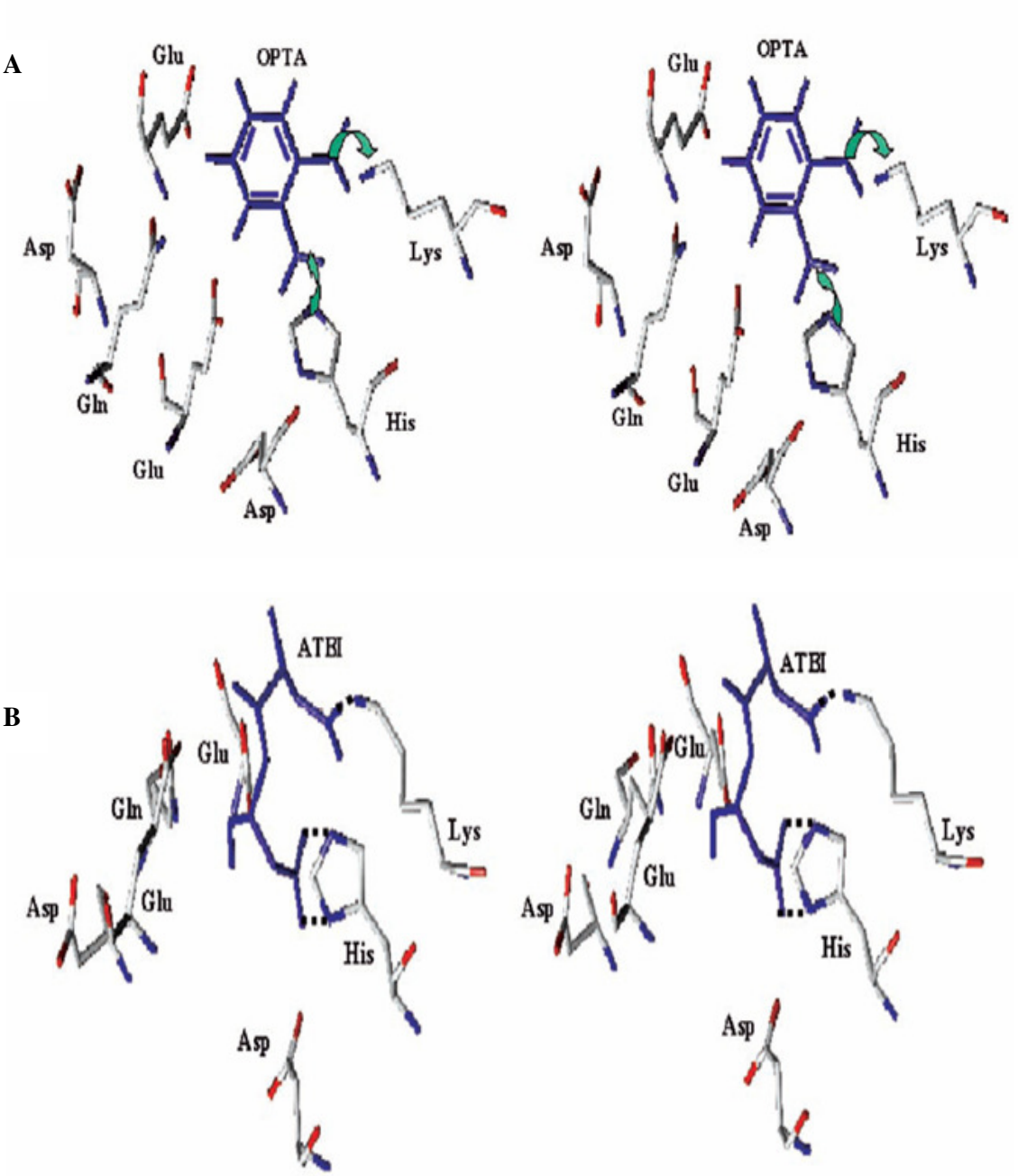

Figure. 10. Schematic representation of the stereo view model depicting the probable mechanism of OPTA and ATBI binding to the active site of Xyl I.

CONCLUSION

The kinetic analysis demonstrated that the inhibition of Xyl I by ATBI, followed slow-tight binding inhibition mechanism and the induced conformational changes are conveniently monitored by fluorescence spectroscopy. ATBI binds to the active site of the enzyme and disturbs the native interaction between the histidine and lysine, as demonstrated by the abolished isoindole fluorescence of o-phthalaldehyde-labeled xylanase. The experimental results revealed that the inactivation of xylanase is due to the disruption of the hydrogen-bonding network between the essential histidine and other residues involved in catalysis. A model depicting the probable interaction between ATBI or OPTA with xylanase has been proposed.

PART - 2

SLOW-TIGHT BINDING INHIBITION OF XYLANASE BY THE SPECIFIC ASPARTIC PROTEASE INHIBITOR PEPSTATIN

SUMMARY

This section of the chapter describes the inhibition mechanism of xylanase by pepstatin, a specific inhibitor towards aspartic proteases. The kinetic analysis revealed competitive inhibition of xylanase by pepstatin with an IC_{50} value 3.6 ± 0.5 μM. The progress curves were time depended, consistent with a two-step slow tight binding inhibition. The inhibition followed a rapid equilibrium step to form a reversible enzyme-inhibitor complex (*EI*), which isomerizes to the second enzyme-inhibitor complex (*EI**), which dissociated at a very slow rate. The rate constants determined for the isomerization of *EI* to *EI**, and the dissociation of *EI** were 15 ± 1 x 10^{-5} s^{-1} and 3.0 ± 1 x 10^{-8} s^{-1}, respectively. The K_i value for the formation of *EI* complex was 1.5 ± 0.5 μM, whereas the overall inhibition constant K_i* was 28.0 ± 1 nM. Pepstatin binds to the active site of the enzyme and disturbs the native interaction between the histidine and lysine, as demonstrated by the abolished isoindole fluorescence of o-phthalaldehyde-labeled xylanase. The experimental results revealed that the inactivation of xylanase is due to the interference in the electronic microenvironment and disruption of the hydrogen-bonding network between the essential histidine and other residues involved in catalysis and a model depicting the probable interaction between pepstatin with xylanase has been proposed.

INTRODUCTION

Pepstatin is a naturally occurring low molecular weight potent inhibitor of microbial origin specific for aspartic proteases (Umezawa, et al., 1970). The chemical structure of pepstatin is determined by Umezawa and co-workers in 1970 (Morishima, 1970) and it is a hexapeptide, which contains two residues of an unusual amino acid, 4-amino-3-hydroxy-6-methylheptanoic acid (statin). The complete structure of pepstatin is iso-valeryl-L-valyl-L-valyl-statyl-L-alanyl-statine (Chart-1). Statine, an amino acid not found in protein, is a key constituent of naturally occurring aspartic protease inhibitors and was first identified by Umezawa and coworkers in pepstatin (Umezawa, et al., 1970). Studies with pepstatin analogs have shown that statine is the major structural component responsible for pepstatin inhibition and it is an analog of the transition state of peptic catalysis (Marciniszyn et al., 1976). Statine mimics the putative tetrahedral transition state intermediate formed during the cleavage of the peptide bond by aspartic proteases and its hydroxylethylene unit occupies the scissile dipeptide binding site with the (S)-hydroxy group oriented between the two catalytic Asp carboxyl residues of the aspartic proteases. This prevents the binding of the solvent molecule necessary for cleavage of the peptide bond.

Chart-1

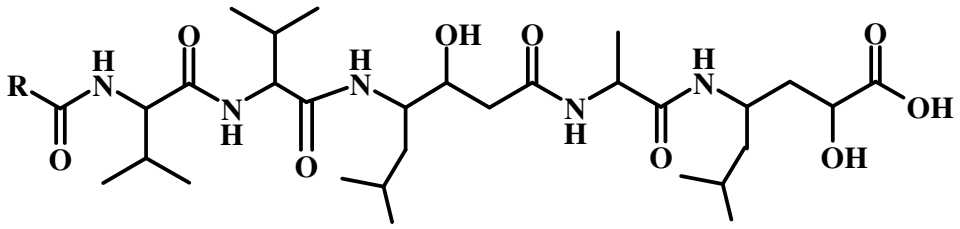

Pepstatin A, R= Methyl
Acetyl pepstatin, R= Iso-propyl

A pepstatin producing strain, classified as *Streptomyces testaceus,* produced various pepstatins that different from one another in the fatty acid moiety (C_2-C_{20}) (Aoyagi et al., 1973). A pepstatin containing an isovaleryl group has been most widely used for biological and biochemical studies (Umezawa, 1982). Moreover, as minor components, pepstanone (Miyano et al., 1972), containing (S)-3-amino-5-methylhexane-2-one instead of the C-terminal (3S, 4S)-4-amino-3-hydroxy-6-methylheptanoic acid (AHMHA), and hydroxylpepstatin (Umezawa et al., 1973),

containing L-serine instead of L-alanine, were isolated. Pepstatin containing an acetyl, propionyl or isobutyryl groups were also isolated from *Streptomyces naniwaensis* (Murao and Satoi, 1970) and from *Streptomyces* No. 2907 (Kakinuma and Kanamaru, 1976). Pepstatins, pepstanones, and hydroxyl pepstatins have almost identical activity against pepsin and cathepsin D (Umezawa, 1982). Esters of pepstatin, pepstatinal and pepstatinol, possess anti-pepsin activity similar to pepstatins. Several pepstatin analogs have also been synthesized to date. AHMHA and its N-acyl derivative exhibit no potency towards pepsin, however, N-acetyl-valyl-AHMHA is active, and the addition of another valine between the acetyl and valyl groups does not increase their activity. Addition of L-alanine to the C-terminal group increases the activity about 100 times. This suggests that the acetyl-valyl-AHMHA-L-alanine is the smallest molecular structure that exhibits inhibition against pepsin and cathepsin D similar to pepstatin (Aoyagi et al., 1972). Acetyl-L-valyl-L-valyl-[(3S, 4R)-4-amino-3-hydroxy-6-methyl] heptanoic acid prepared by chemical synthesis shows absence of activity (Kinoshita et al., 1973) suggesting that the 4S-configuration of AHMHA is essential for activity.

The unusual potency of pepstatin towards aspartic proteases has been widely exploited as a research tool for unraveling the mechanism of this group of enzymes (Sachdev, et al., 1973), its biological functions (Barrett and Dingle, 1972), and in affinity chromatography (Carvol, et al., 1973; Murakami, et al., 1973). For instance, renin was first purified by affinity chromatography with pepstatin as the functional group (Murakami, et al., 1973). Pepstatin has been tested as a therapeutic agent for experimental control of gastric ulcer (Umezawa, et al., 1970; Umezawa, 1972), carrageenin edema (Umezawa, et al., 1970), hypertension (Lazar, et al., 1972; Miller, et al., 1972) and infectious diseases like AIDS (Von der Helm, et al., 1989). Pepstatin suppresses the generation of Shay rat ulcer as well as therapeutic effects on stomach ulcers in man have also been observed (Umezawa, et al., 1970; Umezawa, 1972; Umezawa, 1982). Pepstatin has been reported effective against experimental muscle dystrophy and enhances the effect of leupeptin (Chelmicka-Schorr et al., 1978; McGowan et al., 1976). Pepstatin also inhibits leukokinin formation and ascites accumulation in ascites carcinoma of mice (Greenbaum et al., 1975). Pepstatin inhibits the growth of *Plasmodium beghei* (Levy and Chow, 1974; Levy and Chow,

1975) and also reported to inhibit focus formation by murine sarcoma virus (Yuasa et al., 1975).

Mothes et al demonstrated the polymerization of pepstatin A into filaments at low ionic strength and neutral pH in a concentration depended manner (Mothes et al., 1994). Pepstatin shown the ability to self-associate / polymerize into filaments which may extend over several micrometers and it is a more rare event for such small peptides. These filaments revealed a helical substructure with characteristics diameters ranging from 6-12 nm and suggested the filaments are composed of two intertwined 6 nm strands. In physiological salt solution or at higher concentration of pepstatin A, a variety of higher order structures were shown, including ribbons, sheets and cylinders with both regular and twisted or irregular geometries (Mothes et al., 1990). These polymerized higher order structures of pepstatin failed to inhibit the aspartic protease of the human immunodeficiency virus type I (Mothes et al., 1990; Mothes et al., 1994).

Yoshida and co-workers very recently reported the pharmacological action of pepstatin on osteoclast differentiation apart from its role as a protease inhibitor (Yoshida et al., 2006). They demonstrated a dose depended suppression of osteoclast differentiation by pepstatin in cell lines. Cell signaling analysis indicated that the phosphorylation of ERK was inhibited in pepstatin A treated cells (Yoshida et al., 2006). Pepstatin A is also known to attenuate the inhibitory effect of N-acetyl-L-cystein on proliferation of hepatic myofibroblasts (stellate cells) (Takashima et al., 2002). Pepstatin A restored DNA synthesis of stellate cells stimulated by either platelet-derived growth factor-BB (PDGF-BB) or insulin-like growth factor-I (IGT-I), an effect that was attenuated by N-acetyl-L-cystein (Takashima et al., 2002). Pepstatin A is also reported for inducing contractile effects on isolated rat aorta rings (Petrescu et al., 2002). The extrusion of protons is considered a very general parameter of the activation of many kinds of membrane or intracellular molecules, such as receptors, ion channels, and enzymes. Okada and co-workers demonstrated a concentration-related increase in the extra cellular acidification rate specifically in microglial cell lines by pepstatin A, distinct from aspartic protease inhibition (Okada et al., 2003). Pepstatin is also documented to be chemotactic for human neutrophils (Spilberg et al., 1984). Pepstatin induced superoxide radical generation, release of lysosomal

enzymes, and transient increases in intracellular adenosine-3'-5'-cyclic monophosphate (cAMP) levels in a dose-dependent manner (Spilberg et al., 1984).

Apart from protease inhibition, Kuwabara and his group demonstrated the inhibition of a redox enzyme violaxanthin de-epoxidase (VDE) by pepstatin. VDE is an enzyme involved in xanthophyll cycle and which plays an important role in protection of plants against excess light (Demming-Adams and Adams, 1992). VDE catalyzes the de-epoxidation of violaxanthin to zeaxanthin though the intermediate antheraxanthin. Pepstatin inhibition on VDE was similar to that of aspartic protease in that it was reversible and accompanied by the protonation of the enzyme. Their results suggested that the reaction centers of VDE and aspartic proteases have a common structural feature (Kawano and Kuwabara, 2000).

In the previous part of this chapter, the slow-tight binding inhibition of the thermostable Xyl I by a peptidic aspartic protease inhibitor (ATBI) has been described. In this section, the inhibition of Xyl I by specific aspartic protease inhibitor, pepstatin A is demonstrated. The kinetic analysis revealed competitive inhibition of xylanase by pepstatin. The time-depended inhibition displays the progressive tightening of enzyme inhibitor complex from a low micromolar K_i to nanomolar K_i* value. The mechanism of inactivation of xylanase by Pepstatin A was delineated by monitoring the isoindole fluorescence of the *o*-phthalaldehyde (OPTA) labeled enzyme and a model for the probable interactions has been proposed.

MATERIALS AND METHODS

Materials

Pepstatin A was purchased from Sigma Chemical Co., U.S.A. All other chemicals used are described in the earlier section.

Microorganisms growth condition and purification of Xyl I

Thermomonospora sp. producing Xyl I is an alkalothermophilic actinomycete having optimum growth at pH 9 and 50°C. It was isolated from self-heating compost from the Barabanki district of Uttar Pradesh, India (George, et al., 2001a). The enzyme was purified as described in section I of this chapter. To recollect, *Thermomonospora* sp. was grown at 50°C for 96 h for the production of Xyl I. The enzyme was purified to homogeneity from the extracellular culture filtrate by fractional ammonium sulfate precipitation (35-55%), DEAE-Sephadex ion exchange chromatography and Sephacryl S-200 gel filtration chromatography (George, et al., 2001b).

Xylanase assay and inhibition kinetics

Xylanase assay was carried out as described in the earlier section of this chapter. The reducing sugar released was determined by the dinitrosalicylic acid method (Miller, 1959). One unit of xylanase activity was defined as the amount of enzyme that produced 1 μmol of xylose equivalent per min using oat spelt xylan as the substrate under assay conditions.

For initial kinetic analysis, the kinetic parameters for the substrate hydrolysis were determined by measuring the initial rate of enzymatic activity. The inhibition constant (K_i) was determined by Dixon method (Dixon, 1953) and also by the Lineweaver-Burk's equation. The K_m value was also calculated from the double-reciprocal equation by fitting the data into the computer software Microcal Origin. For the Lineweaver-Burk's analysis Xyl I (2 μM) was incubated with pepstatin at (1μM) and (2 μM) and assayed at increased concentration of xylan (1-10 mg/mL) at 50°C for 30 min. The reciprocals of substrate hydrolysis (*1/v*) for each inhibitor concentration were plotted against the reciprocals of the substrate concentrations and the K_i was determined by fitting the resulting data. In Dixon's method, xylanolytic activity of Xyl I (2 μM) was measured in the presence of (5 mg/mL) and (10 mg/mL) of xylan,

at concentrations of pepstatin ranging from 0-7 μM at 50°C for 30 min. The reciprocals of substrate hydrolysis (1/v) were plotted against the inhibitor concentration using Microcal Origin.

For the progress curve analysis, assays were carried out in a reaction mixture of 1 ml containing enzyme, substrate, and inhibitor at various concentrations. The reaction mixture contained Xyl I (50 nM) in sodium-phosphate buffer, 0.05 M, pH 6.0, and varying concentrations of pepstatin (0.3-3 μM) and xylan (10 mg/mL). Reaction was initiated by the addition of Xyl I at 50°C and the release of products were monitored at different time intervals by estimating the reducing sugar at 540 nm. In each slow-binding inhibition experiment, five to six assays were performed with appropriate blanks. For the kinetic analysis and rate constant determinations, the assays were carried out in triplicates and the average value was considered throughout.

Evaluation of kinetic parameters

The kinetic parameters associated with the interaction of pepstatin with Xyl I was evaluated as per the equations described in the previous section of the chapter (equation 1 to 6). Apart from LB analysis, values for K_i were obtained from Dixon analysis at a constant substrate concentration as described in Equation 10.

$$\frac{1}{v} = \frac{1}{V_{max}} + \frac{K_m}{V_{max}S}(1 + I / K_i) \qquad \text{(Eq. 10)}$$

The rate constant k_6, for the dissociation of the second enzyme-inhibitor complex was measured directly from the time-dependent inhibition. Concentrated Xyl I and pepstatin were incubated in a reaction mixture to reach equilibrium, followed by large dilutions in assay mixtures containing near-saturating substrate. Xyl I (2 mM) was pre-incubated with equimolar concentrations of Pepstatin for 120 min in sodium-phosphate buffer, 0.05 M, pH 6.0. 5 μL of the pre-incubated sample was removed and diluted 5000-fold in the same buffer and assayed at 50°C using xylan at (150 mg/mL) at different time intervals.

Effect of pepstatin on the isoindole fluorescence of OPTA labeled Xyl I

Fresh OPTA solution was prepared in methanol for each experiment. The modification was carried out by incubating Xyl I (2 μM) in 1 mL 0.05 M sodium phosphate buffer, pH 6, with 50 μM of OPTA at 25°C. The formation of Xyl I-isoindole derivative was followed spectrofluorometrically by monitoring the increase in fluorescence with the excitation wavelength fixed at 330 nm. To monitor the effect of pepstatin on the isoindole fluorescence of Xyl I, the enzyme was preincubated with pepstatin (2 μM) for 20 min and then OPTA was added and the formation of isoindole derivative was monitored as described above.

RESULTS

Kinetic analysis of the inhibition of Xyl I

The aspartic protease inhibitor (pepstatin) is well documented for its inhibitory activity towards pepsin, renin, cathepsin-D and HIV-1 protease (McKown, et al., 1974; Marciniszyn, et al., 1976; Knight and Barrett, 1976; Von der Helm, et al., 1989). The bifunctional nature of pepstatin was established by its potency towards the xylanase purified from the *Thermomonospora* sp. Initial kinetic assessments revealed that pepstatin is a competitive inhibitor of Xyl I with an IC_{50} value of 3.6 ± 0.5 μM (Figure 1). In the absence of pepstatin, the steady-state rate of xylanolytic activity of Xyl I reached rapidly whereas, in its presence a time-dependent decrease in the rate as a function of the inhibitor concentration was observed. Examination of the progress curves revealed a time range where the initial rate of reaction did not deviate from linearity (Figure 2), and the conversion of *EI* to *EI** was minimal.

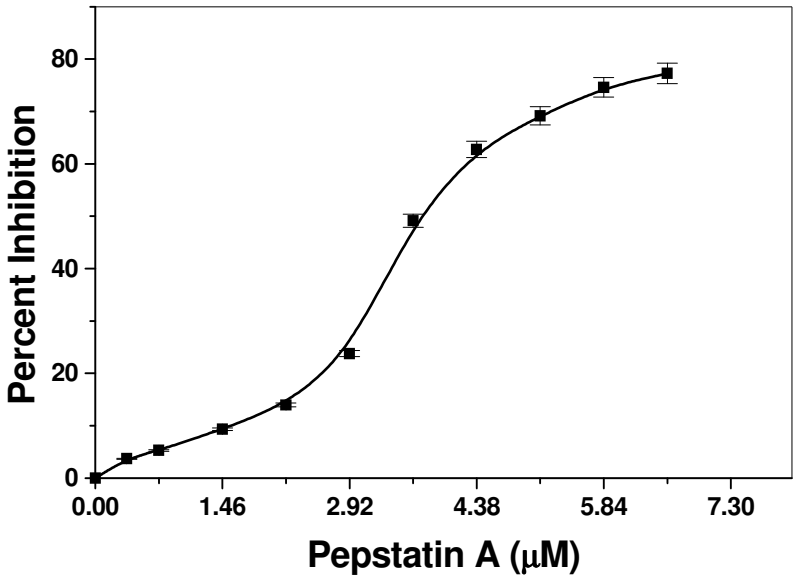

Figure 1. Inhibition of Xyl I by Pepstatin. The xylanolytic activity of the purified Xyl I (2 μM) was determined in the presence of increasing concentrations of Pepstatin A. The percent inhibition of the xylanase activity was calculated from the residual enzymatic activity. The sigmoidal curve indicates the best fit for the percent inhibition data (average of triplicates) obtained and the IC_{50} value was calculated from the graph.

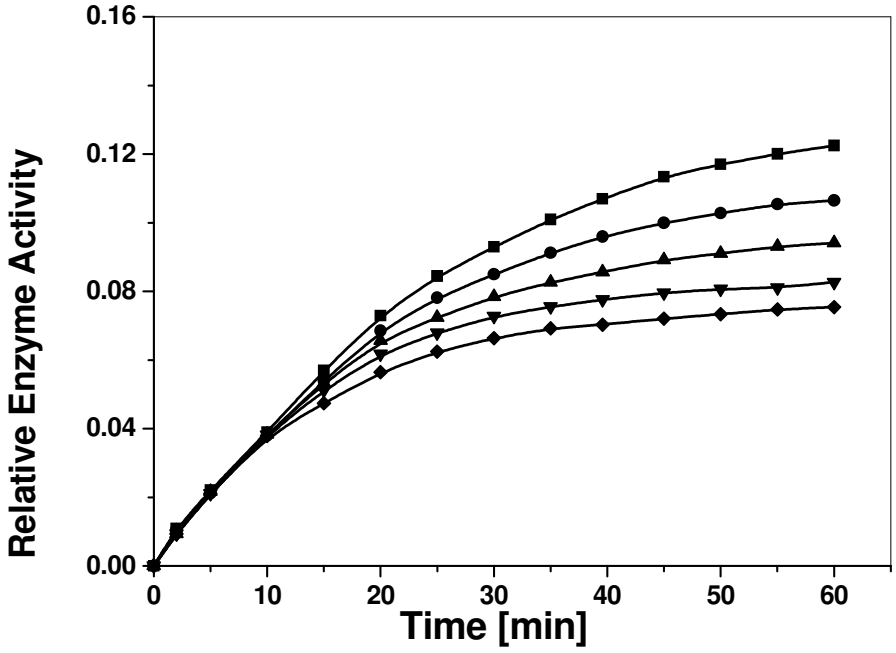

Figure 2. Time course of inhibition of Xyl I by Pepstatin A. The reaction mixture contained Xyl I (50 nM) in sodium-phosphate buffer, 0.05 M, pH 6.0, and varying concentrations of Pepstatin A and xylan (10 mg/mL). Reaction was initiated by the addition of Xyl I at 50°C. The points represent the hydrolysis of substrate as a function of time and the lines indicate are the best fits of data obtained from equations 2 and 5, with the corrections made as per the eq 3 and 4. Concentrations of Pepstatin A were 0.365 µM (■), 0.73 µM (●), 1.1 µM (▲), 1.5 µM (▼), and 3 µM (♦)

For a low concentration of pepstatin this time range was 10 min, within which classical competitive inhibition experiments was used to determine the K_i value (equation 5). The value of the inhibition rate constant K_i, associated with the formation of the reversible enzyme inhibitor complex (EI) determined from the fits of data to the reciprocal equation was 1.5 ± 0.5 µM (Figure 3.A), which was corroborated by the Dixon method (Figure 3.B).

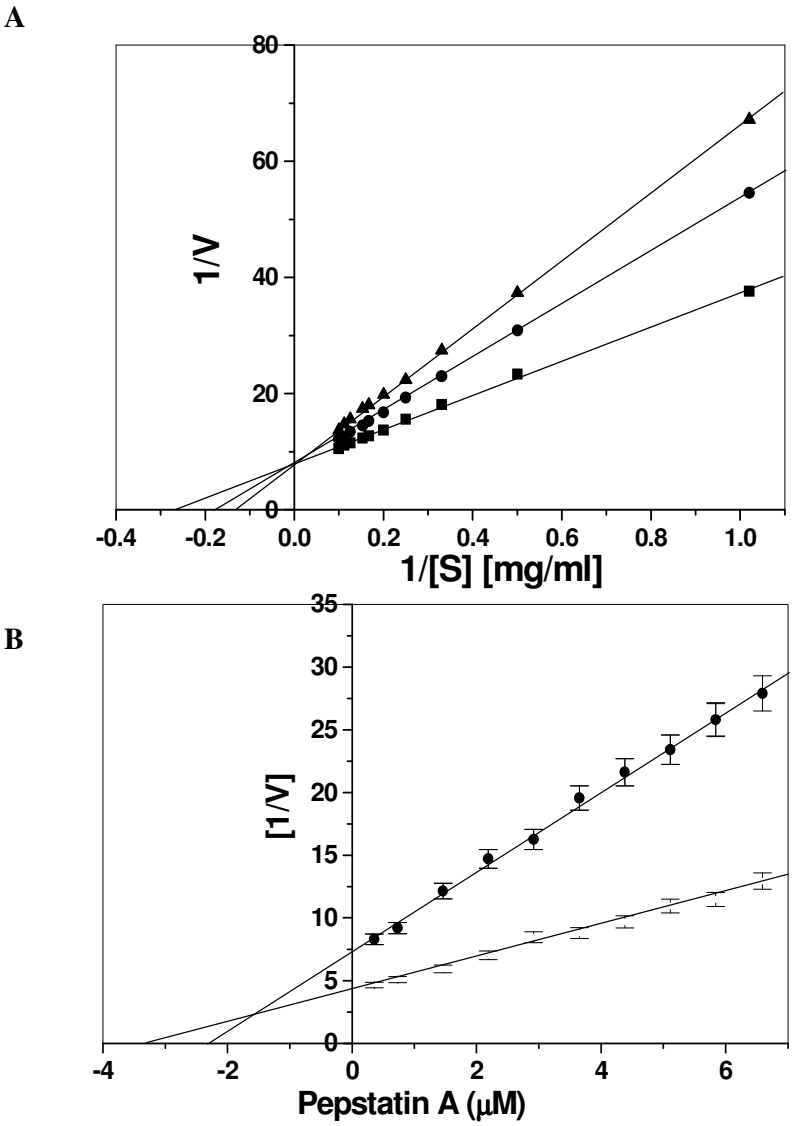

Figure 3. Initial rate of enzymatic reaction of Xyl I in the presence of Pepstatin A. A. Enzymatic activity of Xyl I was estimated using oat spelt xylan in sodium-phosphate buffer, 0.05 M, pH 6.0 and the xylose equivalent was determined at 540 nm. Xyl I (2 μM) was incubated without (■) or with the inhibitor at 1 μM (●) and 2 μM (▲) and assayed at increased concentration of xylan (1-10 mg/ml) at 50°C for 30 min. The reciprocal of substrate hydrolysis (1/v) for each inhibitor concentration were plotted against the reciprocal of the substrate concentration. **B.** Xylanase (2 μM) was assayed using xylan at (●) 5 mg/ml and (■) 10 mg/mL with increasing concentration of Pepstatin A at 50°C for 30 min. The reciprocal of substrate hydrolysis (1/v) were plotted against inhibitor concentration. The straight lines indicated the best fits for the data obtained by non-linear regression analysis and analyzed by Lineweaver-Burk's reciprocal equation (A) and Dixon method (B), respectively.

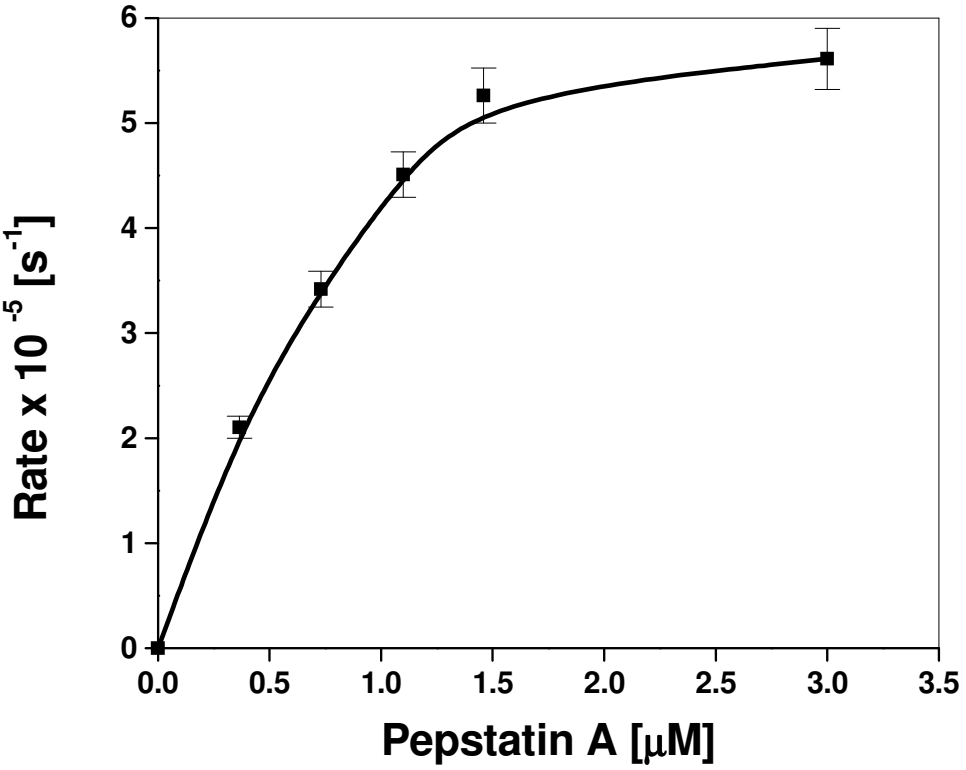

Figure 4. Dependence of Xyl I inhibition on Pepstatin A concentration. The rate constants k, were calculated from the progress curves recorded following the addition of Xyl I to the reaction mixture containing xylan and Pepstatin A. The solid line indicates the best fit of the data obtained.

The apparent rate constant k, derived from the progress curves when plotted versus the inhibitor concentration followed a hyperbolic function (Figure 4), revealing a fast equilibrium precedes the formation of the final slow dissociating enzyme-inhibitor complex (*EI**), indicating two-step, slow-tight inhibition mechanism (Scheme I, Page 30). Indeed, the data could be fitted to equation 5 by non-linear regression analysis, which yielded the best estimate of the overall inhibition constant K_i* of 28.0 ± 1 nM.

In an alternative method, the rate constant k_6, for the conversion of *EI** to *EI*, was determined by pre-incubating high concentrations of enzyme and inhibitor for sufficient time to allow the system to reach equilibrium. Dilution of the enzyme-inhibitor complex into a relatively large volume of assay mixture containing saturating substrate concentration causes dissociation of the enzyme-inhibitor complex and thus regeneration of enzymatic activity. Under these conditions, v_0 and the effective inhibitor concentration can be considered approximately equal to zero and the rate of activity regeneration will provide the k_6 value. After pre-incubating

Xyl I with Pepstatin A, the enzyme inhibitor mixture was diluted 5,000-fold into the assay mixture containing the substrate at 50 *Km*. By least-squares minimization of equation 2 to the data for recovery of enzymatic activity, the determined k_6 value was $3.0 \pm 1 \times 10^{-8}$ s^{-1}, (Figure 5), which clearly indicated a very slow dissociation of *EI**. The final steady-state rate v_s, was determined from the control that was pre-incubated without the inhibitor. The value of the rate constant k_5, associated with the isomerization of *EI* to *EI**, was $15 \pm 1 \times 10^{-5}$ s^{-1} as obtained from fits of equation 5 to the onset of inhibition data using the experimentally determined values of K_i and k_6 (Table-5). The overall inhibition constant K_i^* is a function of $k_6/ (k_5 + k_6)$ and is equal to the product of K_i and this function. The k_6 value indicated a slower rate of dissociation of *EI** complex and the half-life $t_{1/2}$, for the reactivation of *EI** as determined from k_6 values was $64 \pm 2 \times 10^2$ h, suggesting higher binding affinity of pepstatin towards Xyl I.

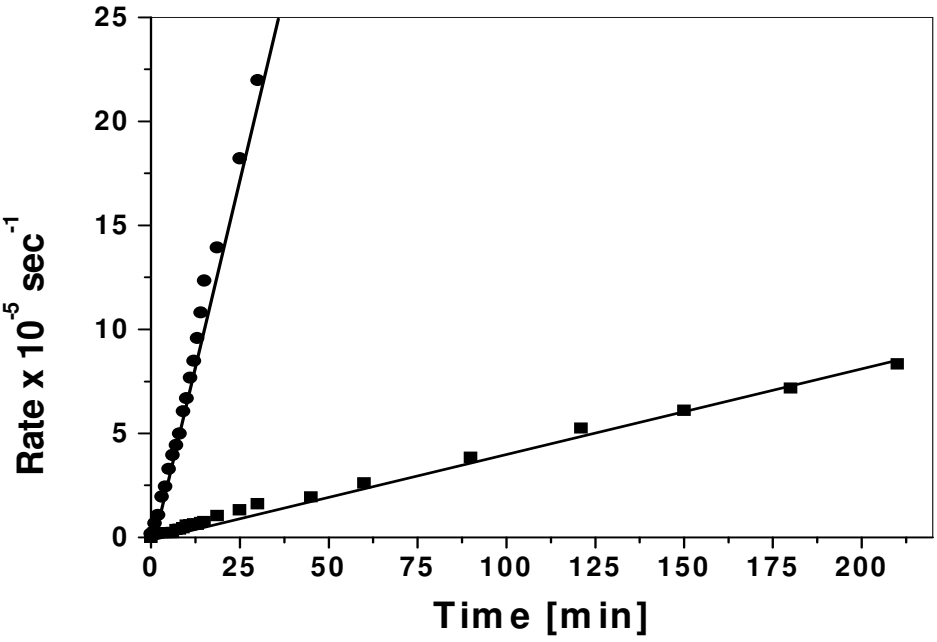

Figure 5. Dissociation rate constant (k_6) for Xyl I-Pepstatin A complex. Xyl I (2 mM) was pre-incubated without (●) or with (■) equimolar concentrations of Pepstatin A for 120 min in sodium-phosphate buffer, 0.05 M, pH 6.0. At the specified times indicated by the points, 5 µl of the pre-incubated sample was removed, diluted 5000-fold in the same buffer, and was assayed for the xylanolytic activity using xylan (150 mg/ml).

Table-5

Inhibition constants of pepstatin against Xyl I

Inhibition Constants	Values
IC_{50}	$3.6 \pm 0.5 \times 10^{-6}$ M
K_i	$1.5 \pm 0.5 \times 10^{-6}$ M
K_i*	$28.0 \pm 1 \times 10^{-9}$ M
k_5	$15.0 \pm 1 \times 10^{-5}$ s^{-1}
k_6	$3.00 \pm 1 \times 10^{-8}$ s^{-1}
$t_{1/2}$	$64.0 \pm 2 \times 10^{2}$ h

Values of rate constants for Xyl I inhibition by Pepstatin were calculated from Scheme I at 50°C in sodium-phosphate buffer, 0.05M, pH 6.0 using oat spelt xylan as the substrate. IC_{50} is from the inhibition profile; K_i was determined from the steady-state time range for the competitive inhibition. k_6 is calculated from the regeneration assay, K_i* and k_5 were determined from the equations as described in the materials and methods.

Effect of pepstatin on the isoindole fluorescence of Xyl I by OPTA

The active site of Xyl I constitute of the catalytic carboxylic groups and the histidine residue, which play crucial role in catalysis. In order to investigate the binding of Pepstatin A to the active site and changes in the native intermolecular interactions, the interaction of the lysine and histidine due to Pepstatin A binding and their influence on the isoindole fluorescence of Xyl I have been monitored (Figure 6). The unbound enzyme did not show fluorescence when excited at 338 nm, however incubation of OPTA with Xyl I resulted in an increase in the fluorescence with a λ_{max} at 417 nm due to the formation of the isoindole derivative. The Pepstatin A pre-incubated Xyl I failed to react with OPTA as revealed by the total loss of isoindole fluorescence, which confirmed the binding of Pepstatin A to the active site of Xyl I. This may

resulted in the formation of a new set of hydrogen bonding and other nonionic interactions. These altered weak interactions cause disruption of the native hydrogen-bonding network of the histidine and lysine residues, which are essential for the formation of isoindole derivative.

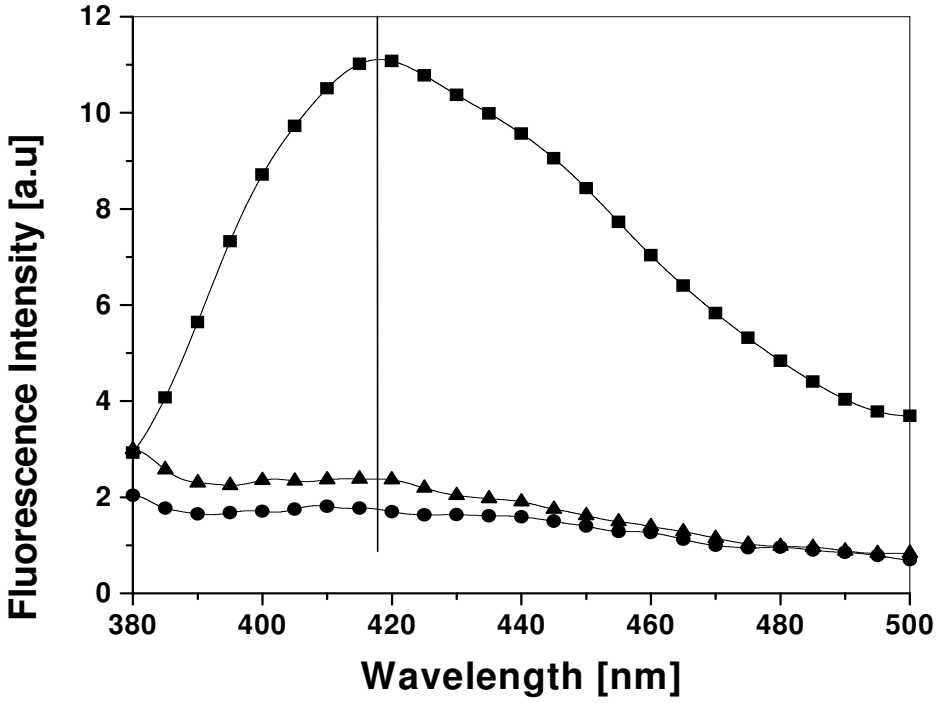

Figure 6. Isoindole fluorescence of Xyl I on reaction with OPTA Xyl I (2 μM) was treated without or with Pepstatin A (2 μM) and was incubated at 25°C for 20 min and then further incubated with a fresh solution of OPTA (50 μM). The isoindole fluorescence of the Xyl I bound OPTA was measured with excitation at 330 nm. The lines represent the isoindole fluorescence of Xyl I (♦), Xyl I + OPTA (■), and Xyl I + Pepstatin A (preincubated) and OPTA (▲) and are the average of six scans with corrections from buffer and respective controls

DISCUSSION

There are several reports on the inhibition of Pepstatin against various aspartic proteases (Umezawa et al., 1970; Marciniszyn et al., 1976; McKown et al., 1974; Knight and Barrett, 1976; Von der Helm et al., 1989). The present study explored the inhibition mechanism of specific aspartic protease inhibitor against a thermostable xylanase from a *Thermomonospora* sp. Pepstatin forms a 1:1 complex with proteases such as pepsin (Umezawa, 1976; Marciniszyn et al., 1977), renin (Umezawa, 1976; Marciniszyn et al., 1977), cathepsin D (Umezawa, 1976; Marciniszyn et al., 1977), bovine chymosin (Marciniszyn et al., 1977), and protease B from *Aspergillus niger* (Takahashi and Chang, 1976). The inhibitor does not inhibit thiol proteases, neutral proteases and serine proteases (Dunn, 1989). Solubilized γ-secretase (Li et al., 2000) and retroviral protease (Katoh et al., 1987) are also inhibited by pepstatin. It has been also used to characterize proteases from several sources (Arima et al., 2000; Farias and Manca de Nadra, 2000). Pepstatin inhibits pepsin with a K_i value of 10^{-10} M (Marciniszyn et al., 1976). Pepsin is a monomeric, two domain, mainly β–protein, with a high percentage of acidic residues. The catalytic site is formed by two aspartate residues, Asp32 and Asp215, one of which has to be protonated, and the other deprotonated, for the protein to be active (Antonov et al., 1978). Pepstatin is an analog of the transition state of peptic catalysis and which tightly binds to active site of the enzyme (Marciniszyn, et al., 1976). Pepsin and Xyl 1 catalyze hydrolytic cleavage of two different substrates made of peptide bond and glycosidic bond respectively. Pepsin, a model enzyme for aspartic protease, was not showing any activity towards xylan, a sugar polymer made of glycosidic bond. The Xyl I did not show any activity against protein substrates, such as hemoglobin and casein, made of peptide bonds, indicating these enzymes are absolutely specific towards their natural substrates. Whereas, the pepsin inhibitor showed exceptionally high potency against Xyl I hence established the bifunctional nature of the inhibitor. The 1:1 molar ratio of interaction of the inhibitor with the enzyme indicated its “tight-binding” nature. The two-step inhibition mechanism was corroborated by the equilibrium binding studies of the enzyme and inhibitor.

The amino acids comprising the active center and the interactions between these residues with the inhibitor are essential to understand the mechanism of enzyme inactivation by the inhibitor. OPTA has been used as a probe to ascertain the

conformational flexibility and polarity of the active site of Xyl I by the formation of a fluorescent isoindole derivative with the lysine and histidine residue present in the active site of Xyl I (George and Rao, 2001). OPTA contains two aldehyde groups; one of which reacts with the primary amine of lysine, while the second group reacts with the secondary amine of the imidazole ring of histidine, resulting in the formation of the isoindole derivative. The present results revealed that, when Xyl I was preincubated with Pepstatin A, OPTA failed to form the isoindole derivative as reflected by the loss of fluorescence. The inability of OPTA to form the isoindole derivative with the Pepstatin A bound Xyl I could be attributed to the interaction of the inhibitor with either lysine or histidine or both the residues, thereby changing the native molecular interactions of these residues. The chemical structure of pepstatin is isovaleryl-L-valyl-L-valyl-statyl-L-alanyl-statine, which contains two residues of unusual amino acid statine ((3S, 4S)-4-amino-3-hydroxy-6-methyl-heptanoic acid). The statine is the major structural component responsible for the pepstatin inhibition against the aspartic protease. Aspartic proteases consist of two carboxyl groups at the active site one of which has to be protonated, and the other deprotonated, for the enzyme to be active. Aspartic protease undergoes a general acid-base catalysis, which may be called a "push-pull" mechanism. The nucleophilic attack is achieved by two simultaneous proton transfers, one from a water molecule to the diad of the two-carboxyl groups and a second one from the diad to the carbonyl oxygen of the substrate with the concurrent CO-NH bond cleavage. Pepstatin is an analog of the transition state of peptic catalysis and which tightly binds to active site of the enzyme (Marciniszyn, et al., 1976). In case of xylanase, the catalytic site consists of two carboxyl groups and an essential lytic water molecule and follows a general acid-base catalytic mechanism (Rao, et al., 1998). Based on the experimental results, it is proposed that pepstatin makes several interactions with the active site residues of Xyl I both through hydrogen bonds and non-bonded interactions (Figure 7)

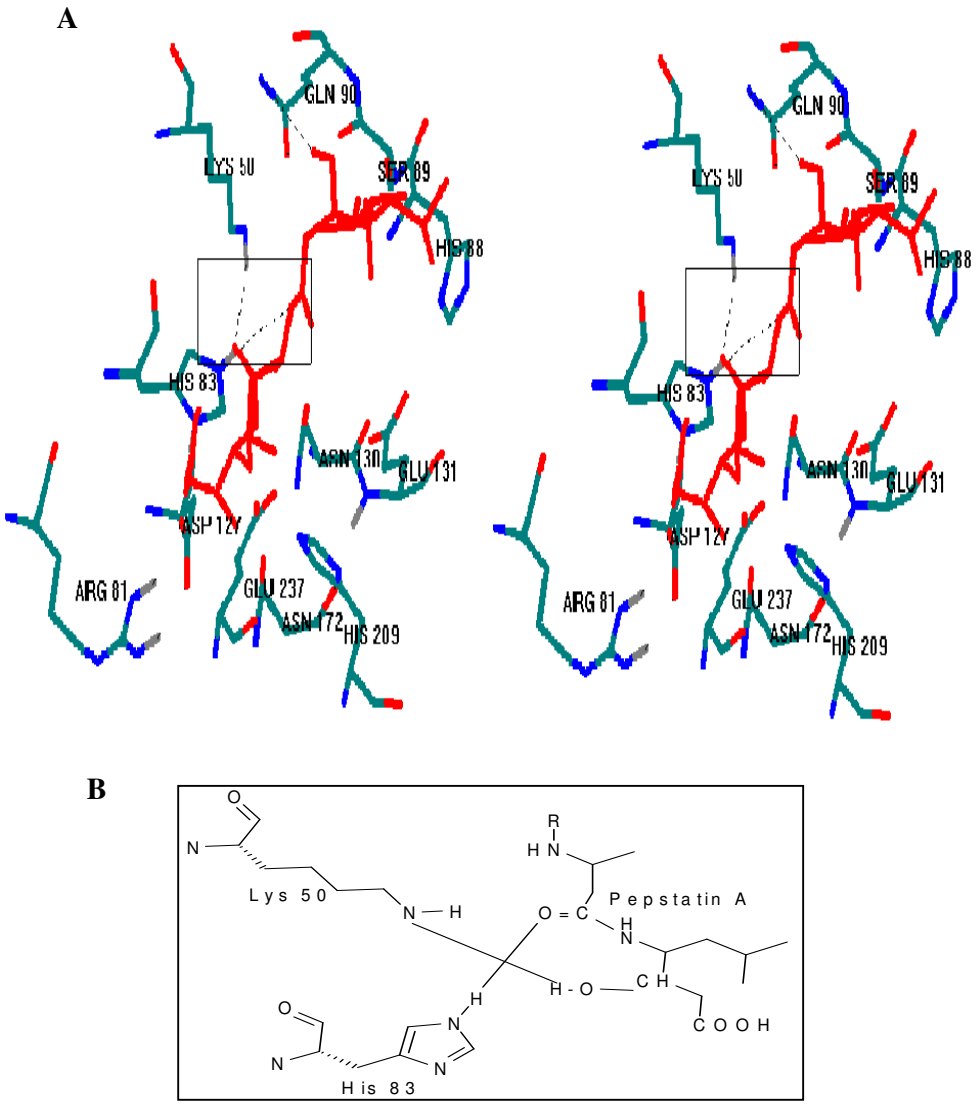

Figure 7. Schematic representation of the model depicting the probable mechanism of Pepstatin A binding to the active site of the Xyl I

In figure 7 A, the active site of the Xyl I has been modeled based on the X-ray crystallographic structure of a similar thermostable family 10 xylanase from *Thermoascus aurantiacus* (Natesh et al., 1999) (PDB ID 1 TUX) and the Pepstatin structure was obtained from the PDB ID 1 PSO (Fujinaga et al., 1995). The interactions were modeled by using the software MOLMOL. The active site of Xyl I include the essential Glu, His, Gln and Lys residues. The dotted lines indicates the hydrogen bonding between the inhibitor and the catalytic amino acid residues of Xyl I. Based on the experimental results, it is proposed that the hydoxyl group of statin

residues of the inhibitor form hydrogen bonding with the free amine groups of the Lys and Gln. The model also depicts the hydrogen bonding between carbonyl oxygen of Ala of the inhibitor with the secondary amine of the His of Xyl I. The other residues of the inhibitor can also form many non-bonded interactions with the active site residues of Xyl I. Figure 7.B demonstrating the probable interactions of the amine groups of essential His and Lys residues of Xyl I with the hydroxyl and carbonyl groups present in the inhibitor. Based on the existing experimental evidences, it is further proposed that the other residues of the inhibitor could form many intermolecular hydrogen bonds and other weak interactions with the residues in or near the active site of Xyl I. The tight-binding nature of Pepstatin A in conjunction with the multiple nonbonded interactions may be sufficient to interfere in the native weak interactions between the carboxyl groups, the lytic water molecule and the essential histidine residue of the active site, leading towards the inactivation of Xyl I.

CONCLUSION

The inhibition of Xyl I by pepstatin, an aspartic protease inhibitor, has been demonstrated. The kinetic analysis revealed competitive inhibition of Xyl I by pepstatin and followed slow-tight binding inhibition mechanism. The time-depended inhibition displays the progressive tightening of enzyme inhibitor complex from a low micromolar K_i to nanomolar K_i* value. Chemo-affinity labeling of the enzyme active site has been demonstrated that the inactivation of xylanase is due to the interference in the electronic microenvironment and disruption of the hydrogen-bonding network between the essential histidine and other residues involved in catalysis. A possible model for enzyme inhibitor interaction has been proposed. However, the crystal structure of the enzyme-inhibitor complex will aid to understand the mechanism of inactivation of Xyl I in depth and will further shed light on the molecular interactions between the enzyme and inhibitor.

REFERENCES

Agarwal, R. P., Spector, T., and Parks, R. E (1977) *Biochem. Pharmacol.* **26**, 359-367.

Ando, O., Nakajima, M., Kifune, M., Fang, H., and Tanzawa, K. (1995) *Biochim Biophys Acta.* **1244**, 295-302.

Antonov, V. K., Ginodman, L. M., Kapitannikov, Y. V., Barshevskaya, T .N., Gurova, A. G., and Rumsh, L. D. (1978) *FEBS Lett.* **88**, 87-90.

Aoyagi, T., Kunimoto, S., Morishima, H., Takeuchi, T., and Umezawa, H. (1971) *J. Antibiot.* **24**, 687-694.

Aoyagi, T., Yagisawa, Y., Kumagai, M., Hamada, M., Morishima, H., Takeuchi, T., and Umezawa, H. (1973) *J. Antibiot*. **26**, 539-541.

Arima, K., Uchikoba, T., Yonezawa, H., Shimada, M., and Kaneda, M. (2000) *Phytochemistry* **54**, 559-565.

Baici, A., and Gyger-Marazzi, M. (1982) *Eur. J. Biochem.* **129**, 33-41.

Bakker, A. V., Jung, S., Spencer, R. W., Vinick, F. J., and Faraci, W. S. (1990) *Biochem. J*. **271**, 559-562.

Barrett, A. J., and Dingle, J. T. (1972) *Biochem. J.* **127**, 439-441.

Beith, J. G. (1995) *Methods Enzymol.* **248**, 59-84.

Biely, P. (1985) *Trends Biotechnol.* **3**, 286-290.

Bienvenue, D. L., Bennett, B., and Holz, R. C. (2000) *J. Inorg. Biochem.* **78**, 43-54.

Bracho, G. E., and Whitaker, J. R. (1990) *Plant Physiol*. **92**, 386– 394.

Bradford, M. M. (1976) *Anal. Biochem*. **72**, 248-254.

Callen, O. H., So, O-Y., and Swinney, D. C. (1996) *J. Biol. Chem.* **271**, 3548-3554.

Carvol, P., Devaux, C., and Menard, J. (1973) *FEBS Lett.* **34**, 189-192.

Cha, S. (1975) *Biochem. Pharmacol.* **24**, 2177-2185.

Cha, S. (1976) *Biochem Pharmacol.* **25**, 2695-2702.

Cha, S., Agarwal, R. P., and Parks, R. E. (1975) *Biochem. Pharmacol.* **24**, 2187-2197.

Chelmicka-Schorr, E. E., Arnason, B. G. W., Astrom, K. E., and Darzynkiewicz, Z. (1978) *J. Neuropathol. Exp. Neurol*. **37**, 263-268.

Cheung, H. C. (1991) in *Topics in Fluorescence Spectroscopy, **Vol. 2*** (Lakowicz, J. R., Ed.) pp127-176, Plenum Press, New York.

Cleland, W. W. (1979) *Methods Enzymol.* **63**, 103-138.

Dash C., Ahmad, A., Nath, D., and Rao, M. (2001a) *Antimicrob. Agents Chemother.* **45**, 2008-20117.

Dash, C., and Rao, M. (2001) *J. Biol. Chem.* **276**, 2487-2493.

Dash, C., Phadtare, S. U., Ahmed, A., Deshpande, V. V., and Rao, M. B. (1998). *Indian Patent* **3560-DEL-98**.

Dash, C., Phadtare, S., Deshpande, V., and Rao, M. (2001b) *Biochemistry* **40**, 11525-11532.

Davies, G. J., Wilson, K., and Henrissat, B. (1997) *Biochem. J.* **321**, 557-559.

Debyser, W., Derdelinckx, G., and Delcour, J. A (1997) *J. Am. Soc. Brew. Chem.* **55**, 153–157.

Debyser, W., Peumans, W. J., Van Damme, E. J. M., and Delcour, J. A (1999) *J. Cereal Sci*. **30**, 39–43.

Demming-Adams, B., and Adams III, W. W. (1992) *Annu. Rev. Plant Physiol. Plant Mol. Biol*. **43**, 599-626.

Dey, D., Hinge, J., Shendye, A., and Rao. M. (1991) *Can. J. Microbiol.* **38**, 436-442.

Dharmasena, S. P., Wimalasena, D. S., and Wimalasena, K. (2002) *Biochemistry* **41**, 12414-12420.

Dixon, M. (1953) *Biochem. J*. **55**, 170-171.

Dorling, P. R., Huxtable, C. R., and Colegate, S. M. (1980) *Biochem. J.*, **191**,649-651.

Dunlap, R.P., Stone, P. J., and Abeles, R. H. (1987) *Biochem Biophys Res Commun.* **145**, 509-513.

Dunn, B. M. (1989) *in Proteolytic Enzymes: A Practical Approach,* Beynon, R. J., and Bond, J. S., eds. (IRL Press), p.63-73.

Elbein, A. D., Legler, G., Trusty, A., McDowell, W., and Schwarz, R. (1984) *Arch. Biochem. Biophys*. **235**, 579-588.

Farias, M. E., and Manca de Nadra, M. C. (2000) *FEMS Microbiol. Lett.* **185**, 263-266.

Fenton, R. J., Morley, P. J., Owens, I. J., Gower, D., Parry, S., Crossman, L.,and Wong, T. (1999) *Antimicrob. Agents Chemother.* **43**, 2642-2647.

Fisher, J., Charnas, R. L., and Knowles, J. R. (1978) *Biochemistry* **17**, 2180-2184.

Flatman, R., McLauchlan, W. R., Juge, N., Furniss, C. S., Berrin, J. G., Hughes, R. K., Manzanares, P., Ladbury, J. E., O'Brien, R., and Williamson, G. (2002) *Biochem. J.* **365**, 773-781

Fox, T., de Miguel, E., Mort, J. S., and Storer, A. C. (1992) *Biochemistry* **31**, 12571-12576.

Francischetti, I. M. B., Valenzuela, J. G., and Ribeiro, J. M. C (1999) *Biochemistry* **38**, 16678 -16685.

Fridovich, I. (1968) *J. Biol. Chem.* **243**, 1043-1051.

Fujinaga, M., Chernaia, M. M., Tarasova, N. I., Mosinann, S. C., and James, M. N.G. (1995) *Protein Sci*. **4**, 960-972.

Garvey, E. P., Oplinger, J. A., Furfine, E. S., Kiff, R. J., Laszlo, F., Whittle, B. J., and Knowles, R. G. (1997) *J. Biol. Chem.* **272**, 4959-4963.

Gebruers, K. K.U. Leuven, Thesis/Dissertation, 2002.

Gebruers, K., Courtin, C. M., Goesaert, H., van Campenhout, S., and Delcour, J. A (2002) *Cereal Chem*. **79**, 613– 616.

Gebruers, K., Debyser, W., Goesaert, H., Proost, P., van Damme, J., and Delcour, J. A. (2001) *Biochem. J*. **353**, 239– 244.

Gebruers, K., Goesaert, H., Brijs, K., Courtin, C. M and Delcour, J. A (2002) *J. Enzyme Inhib. Med. Chem.* **17**, 61– 68.

George, S. P., Ahmad, A., and Rao, M. (2001b) *Biochem. Biophys. Res. Commun.* **282**, 48-54.

George, S. P., and Rao, M. (2001) *Eur. J. Biochem.* **268**, 2881-2888.

George, S.P., Ahmad, A., and Rao, M. (2001a) *Bioresour. Technol.* **77**, 171-175.

Ghisla, S., and Massey, V. (1975) *J. Biol. Chem.* **250**, 577-584.

Giovane, A., Balestrieri, C., Quagliuolo, L., Castaldo, D., and Servillo, L. (1995) *Eur. J. Biochem*. **233**, 926– 929.

Goesaert, G. K.U. Leuven, Thesis/Dissertation, 2002.

Goesaert, H., Debyser, W., Gebruers, K., Proost, P., van Damme, J and Delcour, J. A. (2001) *Cereal Chem.* **78**, 453– 457.

Goesaert, H., Elliott, G., Kroon, P. A., Gebruers, K., Courtin, C. M., Robben, J., Delcour, J. A., and Juge, N. (2004) *Biochim. Biophys. Acta* **1696**, 193-202

Goesaert, H., Gebruers, K., Courtin, C. M., Proost, P., van Damme, J and Delcour, J. A. (2002) *J. Cereal Sci.* **36**, 177– 185.

Goodno, C. C. (1979) *Proc. Natl. Acad. Sci.* **76**, 2620-2624.

Greenbaum, L. M., Grebow, P., Johnston, M., Prekash, A., and Semente, G. (1975) *Cancer. Res.* **35**, 706-710.

Gutheil, W.G. and Bachovchin, W.W. (1993) *Biochemistry* **32**, 8723-8731.

Halazy, S., Berges, V., Ehrhard, E., and Danzin, C. (1990) *Bioorg. Chem.* **18**, 330-334.

Harris, G. W., Jenkins, N. A., Connerton, I., Cummings, N., Lo Leggio, L., Scott, M., Hazlewood, G. P., Laurie, J. I., Gilbert, H. J., and Pickersgill, R. W. (1994) *Structure* **2**, 1107-1116.

Hoffman, R. M., and Turner, J. G (1984) *Physiol. Plant Pathol.* **24**, 49–59.

Hogg, P. J., Stenflo, J., and Mosher, D. F. (1992) *Biochemistry* **31**, 265-269.

Hohenschutz, L. D., Bell, E. A., Jewess, P. J., Leworthy, D. P., Pryce, R. J., Arnold, E., and Clardy, J. (1981) *Phytochemistry*, **20**,811–814.

Houtzager, V., Oullet, M., Falgueyret, J.-P., Passmore, L. A., Bayly, C., and Percival, M. D. (1996) *Biochemistry* **35**, 10974-10984.

Jaffe, E. K., Martins, J., Li, J. , Kervinen, J., and Dunbrack RL, Jr. (2001) *J. Biol. Chem.* **276**, 1531-1537.

Jaynes, T. A., and Nelson, O. E (1971) *Plant Physiol*. **47**, 629–634.

Johnston, D. J., Ramanathan, V., and Williamson, B. (1993) *J. Exp. Bot*. **44**, 971–976.

Juge, N., Payan, F., and Williamson, G. (2004) *Biochim. Biophys. Acta* **1696**, 203-211.

Kakinuma, A., and Kanamaru, T. (1976) *J. Takeda Res. Lab*. **35**, 123-127.

Kapoor, M., Reddy, C. C., Krishnasastry, M. V., Surolia, N., and Surolia, A. (2004) *Biochem. J.* **381**, 719-724.

Kati, W. M., Saldivar, A. S., Mohamadi, F., Sham, H. L., Laver, W. G., and Kohlbrenner, W. E. (1998) *Biochem. Biophys. Res. Com.* **244**, 408-413.

Katoh, I., Yasunaga, T., Ikawa, Y., and Yoshinaka, Y. (1987) *Nature* **329**, 654-656.

Kawano, M., and Kuwabara, T. (2000) *FEBS Lett.* **481**, 101-104.

Kinoshita, M., Aburaki, S., Hagiwara, A., and Imai, J. (1973) *J. Antibiot.* **26**, 249-251.

Knight, C. G., and Barrett, A. J. (1976), *Biochem. J.* **155**, 117-125.

Kulkarni, N., Shendye, A., and Rao, M. (1999) *FEMS Microbiol. Rev*. **23**, 411-456.

Lafitte, C., Barthe, J. P., Montillet, J. L., and Touze, A. (1984) *Physiol. Plant Pathol.* **25**, 39– 53.

Lakowicz, J. R. (1983) *Principles of Fluorescence Spectroscopy*, Plenum Press, New York.

Lazar, J., Orth, H., Mochring, J., and Gross, F. (1972) *Arch. Pharmacol.* **275**, 114-118.

Leger, G. (1968) *Hoppe-Syler's Z. Physiol. Chem.* **349**, 767-774.

Legler, G. (1990) *Adv. Carb. Chem. Biochem.* **48**, 319-385.

Leroy, E., and Reymond, J.-L. (1999) *Org. Lett*. **1**, 775-777.

Levy, M. R., and Chow, S. C. (1974) *Biochim. Biophys. Acta*. **334**, 423-430.

Levy, M. R., and Chow, S. C. (1975) *Experientia.* **31**, 52-54

Lew, w., Chen, X., and Kim, C. U (2000) *Curr. Med. Chem*. **7**, 663-672.

Li, Y. –M., Lai, M. T., Xu, M., Huang, Q., Dimuzio-Mower, T., Sardana, M. K., Shi, X. P., Yin, K. C., Shafer, J. A., and Gardell, S. J. (2000) *Proc. Natl. Acad. Sci. USA.* **97**, 6138-6143.

Ly, H. D., and Withers, S. G. (1999) *Annu. Rev. Biochem.* **316**, 695-696.

Marciniszyn, J. JR., Hartsuck, J. A., and Tang, J. (1976) *J. Biol. Chem.*, **251**, 7088-7094.

Marciniszyn, J., Jr. Hartsuck, J. A., and Tang, J. (1977) *Adv. Exp. Med. Biol.* **95,** 199-210.

Marquis, H., and Bucheli, P. (1994) *Int. J. Food Sci. Technol.* **29**, 121–128.

Marshall, P. J., Sinnott, M. L., Smith, P. J., and Widdows, D. (1980) *J. Chem. Soc. Perkin I*, 366-376.

McGowan, E. B., Shafiq, S. A., and Stracher, A. (1976) *Exp. Neurol*. **50**, 649-657.

McKown, M. M., Wrokman, R, J., and Gregerman, R.I. (1974) *J. Biol. Chem.* **249**, 7770-7774.

Merker, D. J., Brenowitz, M., and Schramm, V. L. (1990) *Biochemistry* **29,** 8358-8364.

Miller, G. L. (1959) *Anal. Chem*. **31**, 426-428.

Miller, R. P., Poper, C. J., Wilson, C. W., and De Vito, E. (1972) *Biochem. Pharmacol.* **21**, 2941-2944.

Mitrakou, A., Tountas, N., Raptis, A. E., Bauer, R. J., Schulz, H., and Raptis, S. A (1998) *Diabet. Med*. **15**, 663-672

Miyano, T., Tomiyasu, M., Iizuka, H., Tomisaka, S., Takita, T., Aoyagi,T., and Umezawa, H. (1972) *J. Antibiot.* **25**, 489-491.

Morishima, H., Takita, T., Aoyagi, T., takeuchi, T., and Umezawa, H. (1970) *J. Antibiot.* **23**, 263-265.

Morrison, J. F. (1969) *Biochim. Biophys. Acta*, **185**, 269-286.

Morrison, J. F. (1982) *Trends Biochem. Sci.* **7**, 102-105.

Morrison, J. F. and Stone, S.R. (1985) *Comments Mol. Cell. Biophys.* **2**, 347-368.

Morrison, J. F., and Stone, S. R. (1985) *Comments Mol. Cell. Biophys.* **2**, 347-368.

Morrison, J. F., and Walsh, C. T. (1988) *Adv. Enzymol.* **62**, 201-302.

Mothes, E., Shoeman, R. L., and Traub, P. (1994) *Micron* **25**, 189-217.

Mothes, E., Shoeman, R. L., Schroder, R. R., and Traub, P. (1990) *J. Struct. Biol.* **105**, 80-91.

Mundy, J., Svendsen, I. B., and Hejgaard, J. (1983) *Carlsberg Res. Commun*. **48**, 81–90.

Murakami, K., Inagami, T., Michelakis, A. M., and Cohen, S. (1973) *Biochem. Biophys. Res. Commun.* **54**, 482-487.

Murao, S., and Miyata, S. (1980) *Agric. Biol. Chem.* **44**, 219-221.

Murao, S., and Satoi, S. (1970) *Agri. Biol. Chem.* **34**, 1265-1267.

Murphy, A. J., and Coll, R. J. (1992) *J. Biol. Chem.* **267**, 5229-5235.

Natesh, R., Bhanumoorthy, P., Vithayathil, P. J., Sekar, K., Ramakumar, S., and Viswamitra, M. A. (1999) *J. Mol. Biol.* **288**, 999-1012.

Okada, M., Irie, S., Sawada, M., Urae, R., Urae, A., Iwata, N., Ozaki, N., Akazawa, K., and Nakanishi, H. (2003) *Glia.* **43**, 167-174.

Palczewski, K., Hargrave, P.A., and Kochman, M. (1983) *Eur. J. Biochem.* **137**, 429-435.

Pan, Y. T., Hori, H., Saul, R., Sanford, B. A., Molyneux, R. J., and Elbein, A. D. (1983) *Biochemistry*, **22**, 3975–3984.

Pawagi, A. B., and Deber, C. M. (1990) *Biochemistry* **20**, 950-955.

Pegg, M. S., and Itzstein, M. von (1994) *Biochem. Mol. Biol. Int.* **32**, 851-858.

Petrescu, G., Costuleanu, M., Slatineanu, S. M., Costuleanu, N., and Cernucan, D. L. (2002) *Rev. Med. Chir. Soc. Med. Nat. Iasi.* **106**, 741-745.

Phadhare, J., Dash, C., Rao, M., and Deshpande, V. V. (2003) *J. Biol. Chem.* **278**, 48735-48744.

Pierce, J., Tolbert, N. E., and Barker, R. (1980) *Biochemistry* **19**, 934-942.

Ploux, O., Breyne, O., Carillon, S., and Margnet, A. (1999) *Eur. J. Biochem.* **259**, 63-70.

Pressey, R. (1994) *Phytochemistry* **36**, 543– 546.

Rao, M. B., Tanksale, A. M., Ghatge, M. S., and Deshpande, V. V. (1998) *Microbiol. Mol. Biol. Rev.* **62**, 597-635.

Rich, D. H., and Sun, E. T. O. (1980) *Biochem. Pharmacol.* **29**, 2205-2212.

Rittenhouse, J. W., and McFadden, B. A. (1974) *Arch. Biochem. Biophys.* **163**, 79-86.

Royers, J. C., and Nakas, J. P. (1989) *Enz. Microbiol. Technol.* **11**, 405-410.

Sachdev, G. P., Brownstein, A. D., and Fruton, J. S. (1973) *J. Biol. Chem.* **248**, 6292-6299.

Schloss, J. V., Porter, D. J. T., Bright, H. J., and Cleland, W. W. (1980) *Biochemistry* **19**, 2358-2362.

Sculley, M. J., Morrison, J. F., and Cleland, W. W. (1996) *Biochim. Biophys. Acta.* **1298**, 78-86.

Selinsky, B. S., Gupta, K., Sharkey, C. T., and Loll, P. J. (2001) *Biochemistry* **40**, 5172-5180.

Sels, J. P., Huijberts, M. S., and Wolffenbuttel, B. H. (1999) *Expert Opin. Pharmacother.* **1**, 149-156.

Simons, S. S. Jr., Thompson, E. B., and Johnson, D. F. (1979) *Biochemistry*, **18**, 4915-4922.

Sinnot, M. L. (1990) *Chem. Rev*. **90**, 1171-1202.

Spilberg, I., Mehta, J., Muniain, M. A., Simchowitz, L., and Atkinson, J. (1984) *Inflammation* **8**, 73-86.

Spring, T. G., and Wold, F. (1971) *Biochemistry* **10**, 4655-4660.

Stover, P. and Schirch, V. (1991) *J. Biol. Chem.* **266**, 1543-1550.

Street, I. P., Lin, H-K., Lalibert, F., Ghomashchi, F., Wang, Z., Perrier, H., Tremblay, N. M., Huang,Z., Weech, P. K., and Gelb, M. H. (1993) *Biochemistry* **32**, 5935-5940.

Stutz, A. E. (1999) *Immunosugars as glycosidase inhibitors: nojirimycin and beyond*; Wiley-VCH, Weinheim.

Szedlacsek, S., and Duggleby, R. G. (1995) *Methods Enzymol.* **249**, 144-180.

Takahashi, K., and Chang, W. J. (1976) *J. Biochem. (Tokyo)* **80**, 497-506.

Takashima, T., Kawada, N., Maeda, N., Okuyama, H., Uyama, N., Seki, S., and Arakawa, T. (2002) *Eur. J. Pharmacol.* **451**, 265-270.

Tarvainen, K., and Keskinen, H. (1991) *Clin. Exp. Allergy* **21**, 609-615.

Taylor, A., Peltier, C. Z., Torre, F. J., and Hakamiant, N. (1993) *Biochemistry* **32**, 784-790.

Truscheit, E., Frommer, W., Junge, B., Muller, L., Schimdt, D. D., and Wingender, W. (1981) *Angew. Chem. Int. Ed. Engl.* **20**, 744-761.

Turner, P. M., Lerea, K. M., and Kull, F. J. (1983) *Biochem Biophys Res Commun.* **114**, 1154-1160.

Umezawa, H. (1972) *Enzyme Inhibitors of Microbial Origin*, p. 31, University Park Press, Baltimore.

Umezawa, H. (1982) *Ann. Rev. Microbiol.* **36**, 75-99.

Umezawa, H., (1976) *Methods Enzymol.* **45**, 689-695

Umezawa, H., Aoyagi, T., Morishima, H., Hamed, M., and Takeuchi, T. (1970) *J. Antibiot.* **23**, 259-253.

Umezawa, H., Miyano, T., Murakami, T., Takita, T., Aoyagi, T., Takeuchi, T., Naganawa, H., and Morishia, H. (1973) *J. Antibiot.* **27**, 615-617.

Viola, R. E., Morrison, J. F., and Cleland, W. W. (1980) *Biochemistry* **19**, 3131-3137.

Von der Helm, K., Gurtler, L., Eberle, J., and Deinhardt, F. (1989) *FEBS. Lett.* **247**, 349-352.

Wedler, F. C., and Horn, B. R. (1976) *J. Biol. Chem.* **251**, 7530-7538.

Wedler, F. C., Horn, B. R., and Roby, W. G. (1980) *Arch. Biochem. Biophys.* **202**, 482-490.

Wentworth, D. F., and Wolfenden, R. (1975) *Biochemistry* **14**, 5099-5105.

Weselake, R. J., MacGregor, A.W., and Hill, R. D. (1983) *Plant Physiol.* **72**, 809–812.

White, A., Tull, D., Johns, K., Withers, S. G., and Rose, D. R. (1996) *Nature Struct. Biol.* **3**, 149-154.

White, A., Withers, S. G., Gilkes, N. R., and Rose, N. R. (1994) *Biochemistry* **33**, 12546-12552.

Wilcox, E. R., and Whitaker, j. R. (1984) *Biochemistry* **23**, 1783–1791.

Williams, J. W., and Morrison, J. F. (1979) *Methods Enzymol.* **63**, 437-467.

Williams, J. W., Duggleby, R. G., Cutler, R., and Morrison, J. F. (1980) *Biochem. Pharmacol.* **29**, 589-595.

Williams, J. W., Morrison, J. F., and Duggleby, R. G. (1979) *Biochemistry* **18**, 2567-2573.

Withers, S. G., and Aerbersold, R. (1995) *Protein Sci*. **4**, 361-372.

Wolfenden, R. (1976) *Annu. Rev. Biophys. Bioeng*. **5**, 271-306.

Yiallouros, I., Vassiliou, S., Yiotakis, A., Zwilling, R., Stocker, W., and Dive, V. (1998) *Biochem. J.* **331**, 375-379.

Yoshida, H., Okamoto, K., Iwamoto, T., Sakai, E., Kanaoka, K., Hu, J-P., Shibata, M., Hotokezaka, H., Nishishita, K., Mizuno, A., and Kato, Y. (2006) *J. Biochem.* **139**, 583-590.

Yuasa, Y., Shimijo, H., Aoyagi, T., and Umezawa, H. (1975) *J. Natl. Cancer. Inst.* **54**, 1255-1256.

CHAPTER-3

BIOCHEMICAL STUDIES ON THE ENHANCEMENT OF XYLANASE ACTIVITY IN PRESENCE OF AMINO ACIDS

SUMMARY

This chapter describes the enhancement of xylanase activity from an alkalothermophilic *Thermomonospora* sp. by amino acids. The xylanase activity increased seven-fold at alkaline pH in presence of glycine and its pH optimum shifted from 7 to 8 without using any protein engineering techniques. The steady state kinetics revealed that glycine in the reaction mixture increased the K_m and K_{cat} values of the enzyme from 3.6 to 8.2 mg / ml and 7.8×10^4 to 1.08×10^5 min^{-1} respectively. Analysis of the enzyme conformation in presence of glycine using fluorescence spectroscopy obviates any changes in the tertiary structure of the enzyme. By using chemoaffinity-labeling technique, the structural integrity, polarity and the electronic microenvironment changes at the active site of the enzyme in presence of glycine has been investigated. The methyl and ethyl glycine esters had no effect on xylanase activity enhancement. This suggests that the enhancement of xylanase activity at alkaline pH range in the hydrolytic cleavage of the xylan in presence of glycine is due to the involvement of carboxylate ion of glycine. A possible mechanism for enhancement of xylanase activity in presence of glycine has been proposed.

INTRODUCTION

An effervescence of research efforts has been expended to understand and to explore the basic principles which govern enzyme catalysis. In 1946, before structural information was available, Linus Pauling proposed that enzyme can accelerate rates because they bind the transition state better than the substrate (Pauling, 1946). This key concept in enzyme catalysis can now be augmented by a detailed description of the sources of enzyme rate enhancements based on developments in transition state theory. In an insightful paper published in 1978, which is as valid today as it was then, Schowen wrote, in accord with Pauling's original insight "*the entire and sole source of catalytic power of enzyme is the stabilization of the transition state*" (Schowen, 1978). Enzymatic reactions are characterized by two principle properties such as high catalytic efficiency and selectivity. Both properties ultimately derive from the binding of the substrate molecule at the active site and the subsequent stabilization of the transition state. As enzyme reaction approach limiting rates as substrate concentration increase, early attention was focused on the binding of the substrate as a part of the catalytic process. More recent studies demonstrate that the enhancement of reaction rates is not achieved through the ability of enzyme to bind their substrate tightly. Instead, catalysis depends on the ability of the enzymes to bind and stabilize altered forms of the substrate that occur in the transition states of their chemical transformation.

Knowledge of the identities of catalytically important active site residues is essential for understanding the catalytic mechanism, for enzyme classification, and for targeted bioengineering of enzymes with desired characteristics. Glycosidases are hydrolytic enzymes involved in the degradation of carbohydrates, and the processing of glycoproteins and glycolipids in both prokaryotic and eukaryotic cells. These group of enzymes are more rigorously classified based on the stereochemistry of the anomeric glycosidic bond that they cleave. Enzymes catalyzing the cleavage of a α-glycosidic bond are termed as α-glycosidases, while those cleaving a β-glycosidic bond are termed as β-glycosidases. Typical glycosidase reaction mechanism is depicted below (Box I). α-Glycosidases are generally believed to act through an E2 type elimination mechanism during which a positively charged aglycon (the leaving group) and the lone pair of the ring oxygen are positioned antiperiplanar, cooperatively facilitating

the glycosidic bond cleavage reaction. In the case of the β-glycosidase reaction, if the enzyme proceeds via an E2 type mechanism, similar to that of the α-glycosidases, the protonated substrate **A** has to go through a highly strained intermediate **B** that may not favor further reaction. Therefore, in the case of a β-glycosidase reaction, the positively charged aglycon leaves via an E1 like mechanism involving the glycosyl cation **C** that is further stabilized by the lone pair of electrons on the ring oxygen to give **D**. Although the final reaction intermediate in both the reaction mechanisms is the same flattened, half chair oxocarbonium ion **D**; the first intermediate in the case of β-glycosidase reaction differs with respect to the position of charge development. Glycosidases are also classified on the basis of the stereochemical outcome of the newly formed anomeric bond. The enzymatic cleavage of the glycosidic bond liberates a sugar hemiacetal with either the same configuration as the substrate (retention) or less commonly, the opposite configuration (inversion) and based on this criterion glycosidases are classified as retaining or inverting glycosidases.

Box I

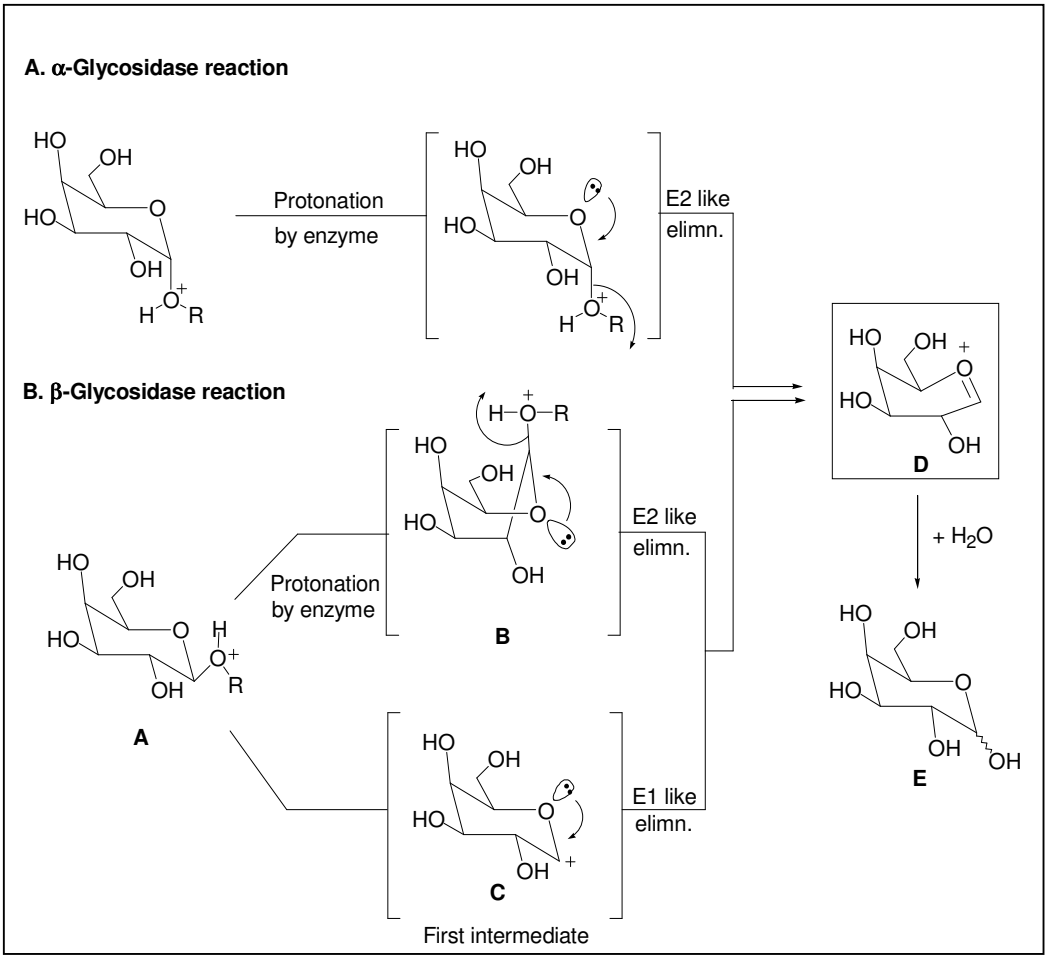

The commercial use of glycosidases in the biotechnology industry has also dramatically increased in recent years (Vilkari, 1994; Kulkarni et al., 1999). Xylanases (1, 4 -β- D-xylan xylanohydrolase) are glycosidases that catalyze the hydrolytic cleavage of β-1, 4 linked polymers of D-xylose (Biely, 1985). They have raised enormous interest in the past decade in view of their application in clarification of juices and wines, conversion of renewable biomass into liquid fuels, in development of environmentally sound pre-bleaching processes in the paper and pulp industry and biofinishing in textile industry (Kulkarni et al., 1999; Collins et al., 2005). The elucidation of enzyme-substrate and enzyme-inhibitor interactions is a crucial issue in fully exploiting the potential of biocatalysts for a variety of purposes. The potential uses of xylanases in biotechnological applications generated an intensive academic and industrial activity to hunt xylanases with desired properties from all kinds of natural sources. Widely used commercial enzymes for biomass modification in animal feeding, bakery and pulp bleaching have come from mesophilic filamentous fungi *Trichoderma reesei* and *Aspergillus niger* (Vilkari, 1994; Prade, 1996). The mesophilic xylanases are useful but not optimal in all industrial applications. These enzymes are easily inactivated in the preparation of animal feed as well as they are not very active in hot alkaline conditions of pulp bleaching.

Considering the future prospects of xylanase for biotechnological exploitations, especially in the field of biopulping and bleaching, it is very essential to analyze the properties of xylanase with respect to mechanism of action. Commercial applications of xylanases demand identification of highly stable enzymes active under routine handling conditions. The use of biocatalysts has been constrained due to their labile nature under extreme temperature and pH conditions. Therefore, attention is focused on the discovery of new xylanases or improvement of existing ones in order to meet the requirements of industry such as stability and activity at high temperature and pH. Although extensive studies have been carried out on the industrial applications of xylanases, there is a paucity of reports on their molecular enzymology. The study of molecular enzymology of xylanase can extend the present understandings of enzyme chemistry in addition to expanding the potential application of biocatalysts.

In the earlier chapter, the interactions of xylanase (Xyl I) with peptidic inhibitors have been discussed. This chapter describes the enhanced activity at higher pH and an optimum pH shift of the thermostable Xyl I by using the amino acid glycine. The Xyl I, a member of family 10 xylanase, is highly thermostable with half-lives of 86, 30, and 15 min at 80, 90, and 100 °C, respectively with an optimum pH at 7. The effects of glycine on thermal stabilization of proteins and enzymes are well documented (Goller and Galinski, 1999; Santoro et al., 1992; Gupta, 1991; Nath and Rao, 1995). However there are no reports of glycine resulted enhancement of enzyme activity at higher pH. The steady state kinetics revealed an increase in both K_m and K_{cat} values of the enzyme in presence of glycine. The mechanism of enhancement of Xyl I activity by glycine was deciphered by monitoring the isoindole fluorescence of the o-phthalaldehyde (OPTA) labeled enzyme and a possible mechanism has been proposed.

MATERIALS AND METHODS

Chemicals

All amino acids were obtained from Sigma Chemical Co., U.S.A. All other chemicals used are mentioned in the earlier chapter.

Microorganisms and growth conditions

Thermomonospora sp. producing Xyl I is an alkalothermophilic actinomycete (George et al., 2001). The growth condition of the organism and enzyme purification steps are same as described in the earlier chapter.

Xylanase assay

Xylanase assay was carried out in phosphate buffer, 0.05 M, pH 7.0, by mixing a specified concentration of the enzyme with 0.5 ml of oat spelt xylan (10 mg/ml) in a reaction mixture of 1 ml and incubating at 50°C for 30 min. The reducing sugar released was determined by the dinitrosalicylic acid method (Miller, 1959). One unit of xylanase activity was defined as described in the earlier chapter.

Effect of glycine, representative amino acids and glycine derivatives on Xyl I activity

The concentration depended glycine effect on xylanase was monitored by adding different concentration of glycine (0- 0.3 M) to the reaction mixture. The effect of glycine on Xyl I activity was also investigated in a wide pH range, pH 5- 10 (pH 5 Acetate buffer 0.05 M; pH 6 and 7 Phosphate buffer 0.05 M; pH 8 and 9 Tris (hydroxymethyl)aminomethane buffer 0.05 M; pH 10 Carbonate-bicarbonate buffer 0.05 M) using 0 - 0.3 M final concentration of glycine. The pH of the reaction mixture was adjusted accordingly before the assay. In order to determine the confidence limits of the biocatalytic activity measurements, all the assays were carried out in triplicates.

Aspartic acid (Acidic Polar; Monoamino, Dicarboxylic), Lysine (Basic Polar; Diamino, Monocarboxylic), Alanine (Neutral), and Phenylalanine (Heterocyclic Nonpolar) were evaluated for their influence on Xyl I activity. The assay was carried out in phosphate buffer, 0.05 M, pH 7.0, containing 0.2 M of Asp or Lys or Ala or Phe or methyl or ethyl glycine ester and incubating at 50°C for 30 min. The pH was

adjusted to 7 before adding the enzyme into the reaction mixture. All the assays were carried out in triplicates.

Evaluation of kinetic parameters

The *Km* value was calculated from the double-reciprocal equation by fitting the data into the computer software Microcal Origin (Eq. 1). For the Lineweaver-Burk's analysis Xyl I (2 μM) assayed at increased concentration of xylan (1-10 mg/ml) at 50°C for 30 min without and with glycine (0.2 M). The reciprocals of substrate hydrolysis (1/v) were plotted against the reciprocals of the substrate concentrations.

$$\frac{1}{V} = \frac{1}{V_{max}} + \frac{K_m}{V_{max}} \cdot \frac{1}{[S]} \qquad \text{Eq. 1}$$

Fluorescence Analysis

Fluorescence measurements were performed on a Perkin-Elmer LS50 Luminescence spectrometer connected to a Julabo F20 water bath. Protein fluorescence was excited at 295 nm and the emission was recorded from 300-400 nm at 25°C. The slit widths on both the excitation and emission were set at 5 nm and the spectra were obtained at 100 nm/min. Titration of the enzyme with glycine was performed by the addition of different concentrations of the glycine to a fixed concentration of enzyme solution. For each glycine concentration for the titration a new enzyme solution was used.

Isoindole Fluorescence of OPTA Labeled Xyl I

Fresh OPTA solution was prepared in methanol for each experiment. The modification was carried out by incubating Xyl I (2 μM) in 1 ml 0.05 M sodium phosphate buffer, pH 7, with 50 μM of OPTA at 25°C as described in chapter 1. The formation of Xyl I-isoindole derivative was followed spectrofluorometrically by monitoring the increase in fluorescence with the excitation wavelength fixed at 330 nm. To monitor the effect of glycine on the isoindole fluorescence of Xyl I, the enzyme was preincubated with glycine (0.2 M) for 10 min and then OPTA was added and the formation of isoindole derivative was monitored as described above.

RESULTS

Effect of different concentration of glycine on Xyl I activity

The concentration dependent glycine effect on Xyl I activity was monitored using varying concentration of glycine (Figure 1). The effective concentration of glycine for the enzyme maximal activity was found to be 0.2 M. The stimulatory effect of glycine on Xyl I activity was decreased when the concentration was at or above 0.25 M. Hence 0.2 M concentration of glycine was used for further studies. The presence of glycine in the reaction mixture resulted in a three-fold increase in Xyl I activity at pH 7 (Table 1).

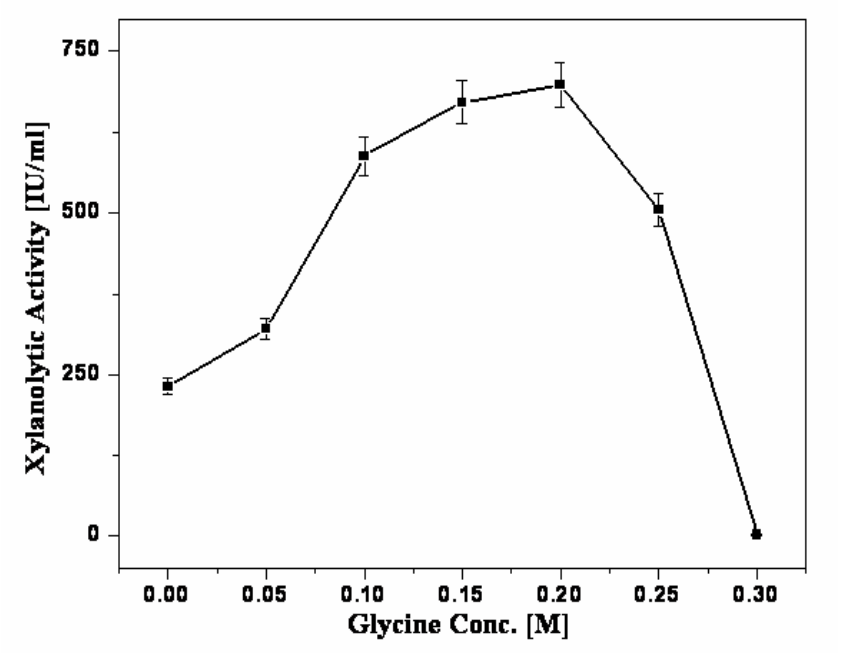

Figure 1. Effect of glycine concentration on Xyl I activity. The xylanolytic activity of the purified Xyl I (2 μM) was determined in the presence of increasing concentrations of glycine

Table-1

Activity of Xyl I in presence of glycine

	Xylanase activity (IU/ mL)*	
pH	**---**	**Glycine (0.2 M)**
7	232	705
8	109	758
9	107	610
10	65	405

[#] One unit of xylanase activity was defined as the amount of enzyme that produced 1 μmol of xylose equivalent per min using oat spelt xylan as the substrate under assay conditions.

Interestingly, at pH 8 the Xyl I activity was increased by approximately seven fold in presence of 0.2 M glycine. At pH 9 the Xyl I activity was increased 5.7 folds in compared with the control. The most significant aspect of this study is even at pH 10 the Xyl I shows significant activity in presence of glycine. At pH 10 Xyl I with glycine was showing almost 6.2 folds increase in activity in compared with control and was retaining 58 % of the initial activity, but the control was showing only 28 % of the initial catalytic activity.

Table 2 lists the effect of aspartic acid, lysine, alanine and phenylalanine on Xyl I activity. These amino acids had no effects on the enhancement of Xyl I activity at 0.2 M final concentration in the reaction mixture, where as at the same concentration glycine was showing remarkably significant activity indicating the unique glycine effect on Xyl I activity.

Table-2

Activity of Xyl I in presence of different amino acids

Amino acids (0.2 M)	Xylanase activity (IU/mL)
----	235
Glycine	710
Alanine	230
Aspartic acid	215
Lysine	238
Phenylalanine	206

Effect of glycine on pH optimum of Xyl I

The enzyme activity of Xyl I exhibited maximum at pH 7 and decreased either side of the optimum. Glycine in the reaction mixture showed an increase in Xyl I activity at alkaline region as well as the pH optimum of the enzyme shifted from pH 7 to 8 (Figure 2).

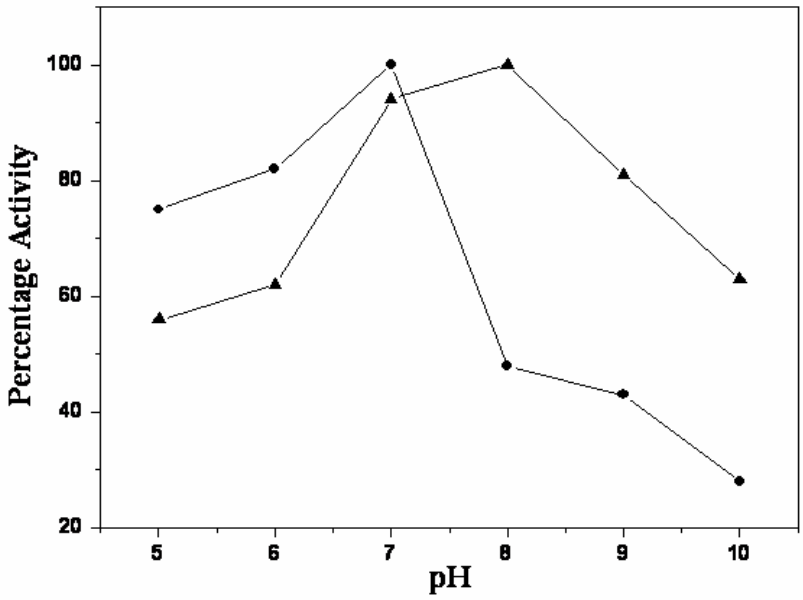

Figure 2. Effect of Glycine on pH optima of Xyl I. The xylanolytic activity was determined in the absence (●) and presence of 0.2 M glycine (▲)

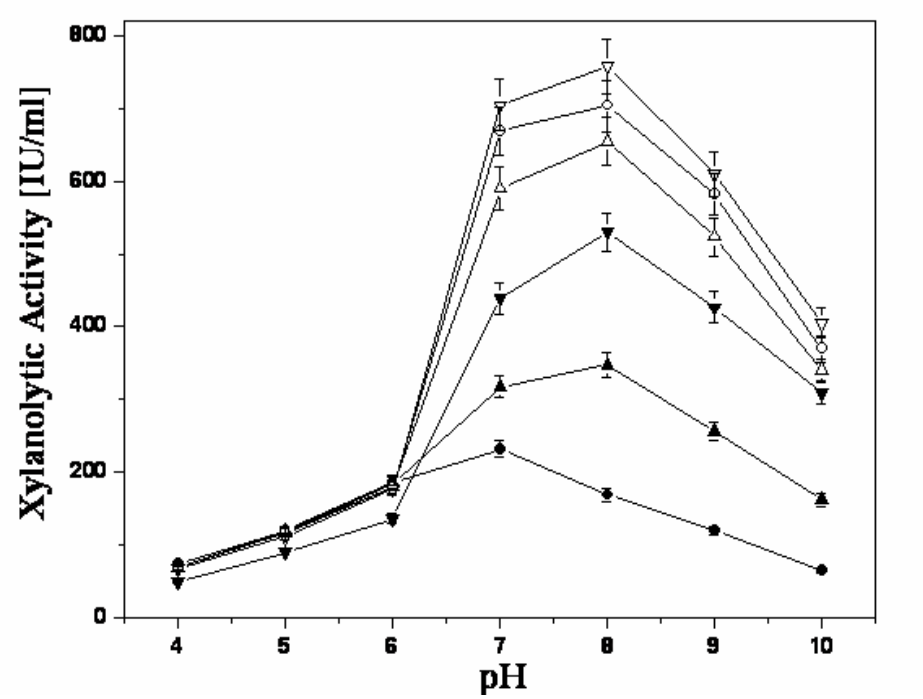

Figure 3. pH dependent activity profile of Xyl I in the presence of 0 (●), 0.05 (▲), 0.1 (Δ), 0.15 (○), 0.20 (∇) and 0.25 M (▼) of glycine

Effect of different concentration of glycine on pH profile of Xyl I

The presence of glycine resulted in a significant effect on the pH dependent activity of Xyl I. Figure 3. shows the effect of glycine at different concentrations on Xyl I, which clearly underlines the concentration depended effect of glycine on Xyl I activity at the alkaline region. Table-1 lists the Xyl I activity at different pH without and with glycine (0.2 M). Glycine had no effect on Xyl I activity from pH 4 to 6 (Figure 3).

Effect of glycine derivatives on Xyl I activity

Methyl glycine ester and ethyl glycine esters were evaluated for its stimulatory effect on Xyl I (Box II). Table 3 lists the effect of these compounds on Xyl I activity. The methyl and glycine esters fail to give any increase in Xyl I activity at 0.2 M concentration. While at the same concentration, glycine exhibited significant increase in Xyl I activity. This clearly underlines the involvement of carboxyl group of glycine in the enhancement of Xyl I activity.

Box II

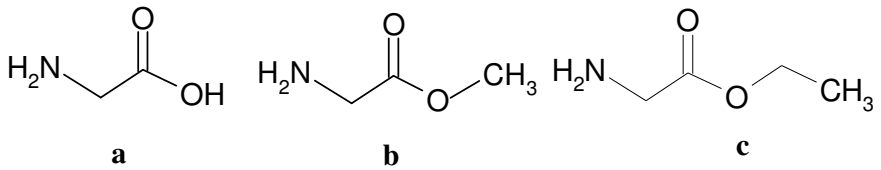

a **b** **c**

a— Glycine
b— Methyl glycine ester
c— Ethyl glycine ester

Table-3

Activity of Xyl I in presence of glycine esters

Concentration (0.2 M)	**Xyl I activity [IU/ mL]**
--	232
Glycine	705
Methyl glycine ester	228
Ethyl glycine ester	222

Evaluation of kinetic parameters

The steady-state kinetic parameters were determined by measuring the initial velocities of the reaction as a function of varying oat-spelt xylan concentrations (1-10 mg/ml) at 50°C for 30 min without and with glycine (0.2 M). *Km* was obtained from the double reciprocal plot of Xyl I reaction velocity versus oat-spelt xylan concentrations at 0 and 0.2 M glycine (Figure 4). The presence of glycine in the reaction mixture resulted in an increase in K_m and K_{cat} values for the substrate from 3.6 to 8.2 mg / ml and 7.8×10^4 to 1.08×10^5 min^{-1} respectively. The K_{cat} / K_m ratio of enzyme was 21666 and with glycine the ratio decreased to 13170. K_{cat} describes how rapidly the bound states can produce free product and regenerate free enzyme whereas the K_{cat} / K_m ratio describes how well the enzyme operates at low concentration at which the reaction is also limited by the rate of substrate binding. The observed results clearly shows that glycine reduced the substrate binding to the active site of Xyl I but promoted catalysis process accelerating final product formation (Scheme-I).

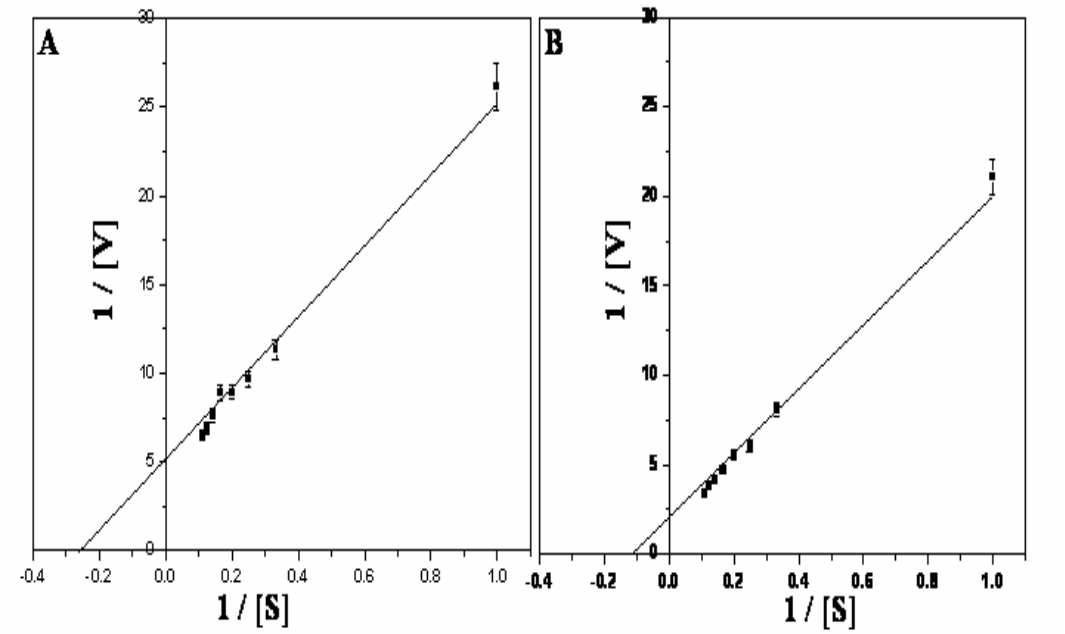

Figure 4. Initial rate of enzymatic reaction of Xyl I in the presence of glycine. Xyl I (2 μM) was incubated without (A) and with the 0.2 M glycine (B) and assayed at increased concentration of xylan (1-10 mg/ml) at 50°C for 30 min. The reciprocal of substrate hydrolysis (1/ [V]) were plotted against the reciprocal of the substrate concentration (1/ [S]). The straight lines indicated the best fits for the data and analyzed by Lineweaver-Burk's reciprocal equation

Effect of glycine on the fluorescence of Xyl I

The tryptophanyl fluorescence of Xyl I exhibited an emission maxima (λmax) at ~340 nm, as a result of the radiative decay of the π - π* transition from the Trp residues. This fluorescent signature is very sensitive to the conformational changes of Xyl I. The titration of the enzyme with glycine was performed by the addition of different concentrations of the glycine at pH 7 to a fixed concentration of enzyme solution. The absence of any changes in florescence signature and blue or red shift in λmax negated any conformational changes in the tertiary structure of the enzyme in presence of glycine (Figure 5).

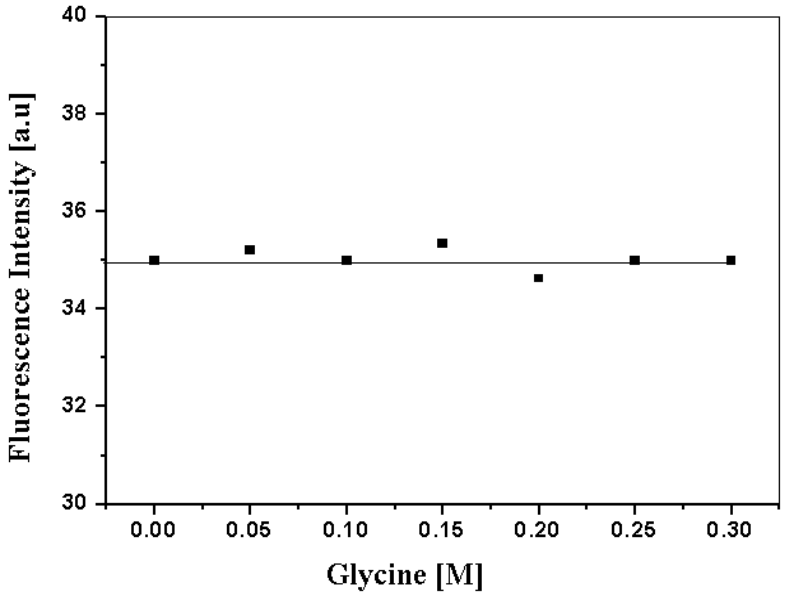

Figure 5. The tryptophanyl fluorescence of Xyl I. Protein fluorescence was excited at 295 nm and the emission was recorded from 300-400 nm at 25°C. The slit widths on both the excitation and emission were set at 5 nm and the spectra were obtained at 100 nm/min. The lines represent the tryptophanyl fluorescence of Xyl I at 340 nm (λmax) as function of glycine concentration.

Effect of glycine on the isoindole fluorescence of Xyl I by OPTA

In earlier studies from our laboratory, the role of essential histidine and lysine residues in the active site of the Xyl I have been investigated and showed that binding of the chemoaffinity label OPTA to these residues of the active site resulted in the formation of an isoindole derivative (Sudeep and Rao, 2001). The active site of Xyl I constitute of the catalytic carboxylic groups and the histidine residue, which play crucial role in catalysis. In order to investigate the role of glycine in the active site and changes in the electronic microenvironment, the isoindole fluorescence of Xyl I has been monitored. The enzyme did not show fluorescence when excited at 338 nm, however incubation of OPTA with Xyl I resulted in an increase in the fluorescence with a λmax at 417 nm due to the formation of the isoindole derivative (Figure 6). The present results revealed that, when Xyl I was preincubated with glycine, OPTA failed to form the isoindole derivative as reflected by the total loss of isoindole fluorescence, which not only confirmed the presence of glycine in the active site of Xyl I but also further revealed the secondary interactions of glycine with the catalytic

amino acid residues. The active site of Xyl I constitute of the catalytic carboxylic groups and the histidine residue, which play crucial role in catalysis. The secondary interaction of the amino groups of glycine with the carboxylic catalytic residue (Scheme I) may also lead to the changes in the conformational flexibility of the catalytic site and hinders the OPTA interaction. These altered polarity and the electronic microenvironment changes of the Xyl I active site cause disruption of the native hydrogen-bonding network of the histidine and lysine residues, which are essential for the formation of isoindole derivative.

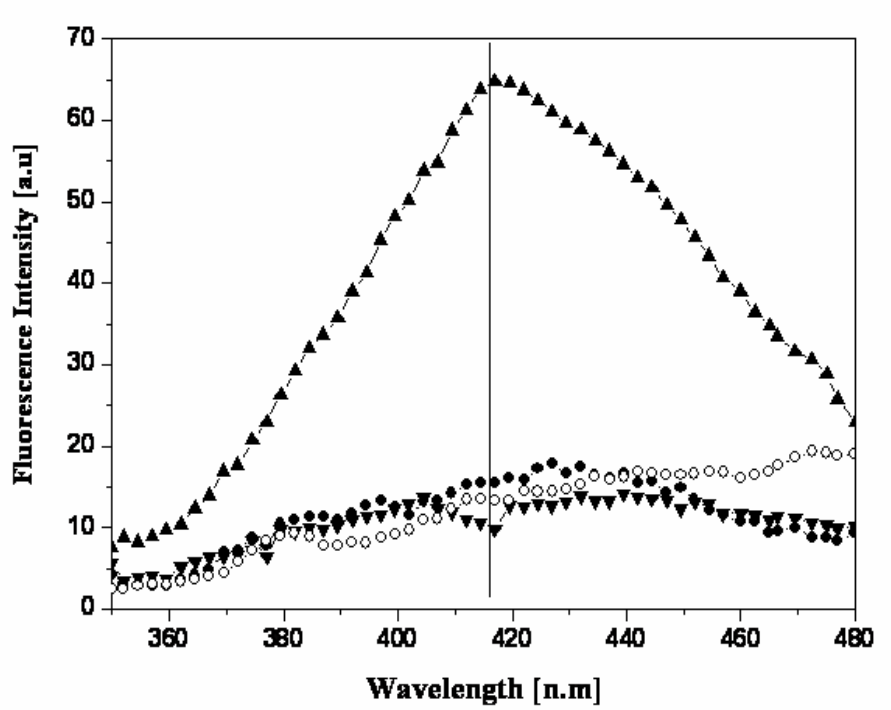

Figure 6. The formation of Xyl I-isoindole derivative was followed spectrofluorometrically by monitoring the increase in fluorescence with the excitation wavelength fixed at 330 nm. The lines represent the isoindole fluorescence of Xyl I (●), Xyl I + OPTA (▲), and Xyl I + Glycine (preincubated) + OPTA (○) and OPTA (▼), and are the average of six scans with corrections from buffer and respective controls.

DISCUSSION

Xylanases have potential applications in a wide range of industrial processes. Many of the xylanases used in industry today appear to be of mesophilic and / or neutrophilic origin, yet enzymes from extremophilic sources may be of tremendous utility in many biotechnological processes (Kulkarni et al., 1999).One of the major application of xylanases is in the pulp and paper industries where the high temperature (55-70°C) and alkaline pH of the pulp substrate needs thermo-alkalophilic enzymes for efficient biobleaching (Beg et al., 2001; Vilkari, 1994). Alkalophilic xylanases would also be required for detergent applications where high pHs are typically used (Kamal et al., 2004). In most cases, the reduced catalytic activity of xylanases at alkaline conditions appears to involve ionization or deprotonation of key amino acid residues (Nath and Rao, 2001).Therefore, to make the application of xylanases realistic the improvement of enzyme properties is of utmost importance. The introduction of Arginines into the Ser/Thr surface and modification of the protein N terminus using protein engineering techniques have improved the activity of *T. reesei* XYNII at alkaline pH (Turunen et al., 2002). Furthermore, through site directed mutagenesis, amino acid substitutions that do not involve charged amino acid residues have also increased the activity of xylanase at alkaline pH (Chen et al., 2001). In this study, without using any protein engineering techniques, the enhanced activity at alkaline pH and a shift in optimum pH of Xyl I from a *Thermomonospora* sp., using the amino acid glycine, has been demonstrated.

Structure and function of many proteins are intimately dependent on the protonation equilibria of ionizable groups. Most enzymes perform catalysis with the assistance of ionizable groups that act either as a bronsted acid or base (Harris and Turner, 2002). Glycine is a neutral amino acid with *pKa* values 2.34 and 9.60 for the carboxylate and amino groups respectively. At neutral pH although the molecule has both positive and negative charges, its net charge is zero. From pH 7 onwards glycine takes up a net negative charge in the alkaline region. The presented results well correlates with the ionization of glycine at alkaline range and its influence on Xyl I activity. Several factors have an influence on the pH-dependent properties of xylanase. The ionization states of the nucleophile and acid/base glutamates control the pH-dependent activity profile (Joshi et al., 2000). It is known that glycine can bind and interact

electrostatically with neighboring negatively charged groups on the protein (Phelps and Cann, 1957; Woods, 1958). Based on the experimental evidences, it is proposed that, glycine interacted with the catalytic carboxylic group of Xyl I (Scheme I) can facilitate the hydrolytic cleavage of the substrate at alkaline range by involving in the catalytic mechanism. The ionization of glycine and its involvement in catalysis may be the cause of shift in the pH optima of Xyl I from the neutral pH 7 to alkaline pH 8. The involvement of carboxylate group of glycine in the catalytic mechanism has been investigated using glycine derivatives such as methyl and ethyl esters of glycine, where the carboxylate group of glycine is protected by alkane groups. Both of these compound had no enhancement effect on Xyl I activity, whereas at the same concentration glycine was showing significant enhancement in Xyl I activity.

Active site labeling is a powerful technique to study the changes in microenvironment of an enzyme and also to decipher the functional groups of the active sites. Application of OPTA as a probe to ascertain the conformational flexibility and polarity of the active site of Xyl I by the formation of a fluorescent isoindole derivative with the lysine and histidine residue have been reported in our laboratory (George and Rao, 2001). OPTA contains two aldehyde groups; one of which reacts with the primary amine of lysine, while the second group reacts with the secondary amine of the imidazole ring of histidine, resulting in the formation of the isoindole derivative. When Xyl I was preincubated with glycine, OPTA failed to form the isoindole derivative as reflected by the total loss of isoindole fluorescence, which not only confirmed the presence of glycine in the active site of Xyl I but also further revealed the secondary interactions of glycine with the catalytic amino acid residues.

Based on the experimental evidences, an alternative hydrolytic mechanism of Xyl I in presence of glycine has been proposed. Scheme- I A shows the catalytic mechanism of glycoside hydrolase family. Which catalysis hydrolysis with retention of anomeric configuration with two glutamate residues being implicated in the catalytic mechanism. This indicates a double displacement mechanism in which a covalent glycosyl-enzyme intermediate is formed and subsequently hydrolysed via oxocarbenium-ion-like transition states. Two carboxylic acid residues suitably located in the active site (approximately 5.5 Å apart) are involved in the formation of the intermediate (TS I) (Rye and Withers, 2000). One acts as a general acid catalyst by

protonating the substrate, while the second performs a nucleophilic attack which results in the departure of the leaving group and formation of the α-glycosyl enzyme intermediate (inversion β to α). In the second step, the first carboxylic group now functions as a general base, abstracts a proton from the nucleophilic water molecule, which attacks the anomeric carbon. This leads to a second substitution in which the anomeric carbon again passes via an oxocarbenium-ion-like transition state to give rise to a product with the β configuration (Inversion of α toβ) (Zechel and Withers, 2000). In presence of glycine, at alkaline pH, the reaction will be mostly proceeds through an alternative pathway. Scheme I B depicts the probable interaction of glycine with the catalytic carboxylic groups of Xyl I; which further reacts with the substrate to make a transient glycosyl-enzyme-glycine intermediate (TS II). The enzyme carboxylic group acts as a general acid catalyst by protonating the substrate, while the glycine carboxyl group performs the nucleophilic attack. The secondary interactions of glycine with the active site of Xyl I can give rigidity to the catalytic residues of this TS II complex making the reaction much faster. At acidic pH range, glycine was not having any influence on Xyl I activity as expected for the proposed mechanism (Figure 3).

Scheme-I A

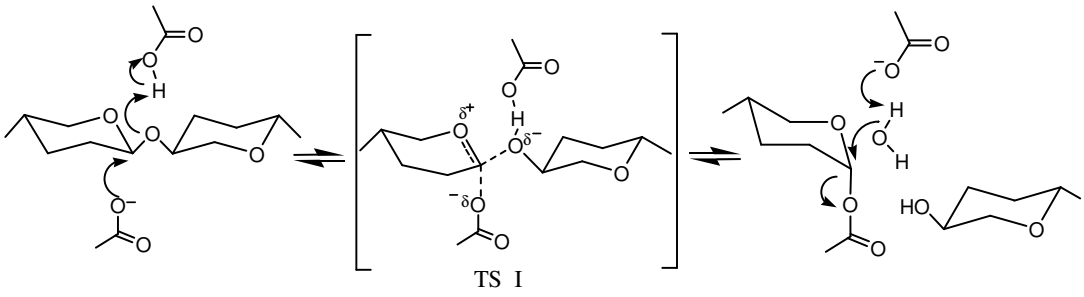

Scheme-I B

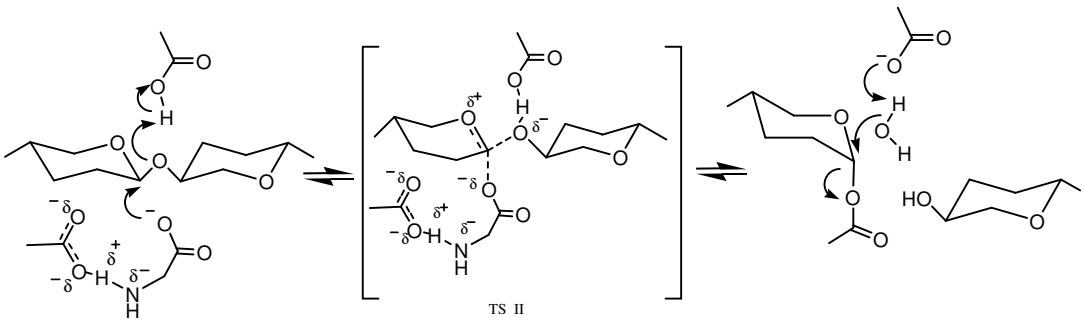

CONCLUSION

The increased Xyl I activity in presence of glycine at higher alkaline pH has been described. The pH optimum of the enzyme was shifted towards alkaline range from pH 7 to 8. The steady state kinetics revealed addition of glycine in the reaction mixture increased K_m and K_{cat} values of the enzyme. The mechanism of stimulation of Xyl I activity by glycine was deciphered by monitoring the isoindole fluorescence of the *o*-phthalaldehyde (OPTA) labeled enzyme. The enhancement of Xyl I activity in presence of glycine is due to the involvement of carboxylate ion of glycine at alkaline pH by forming a TS II intermediate and a possible mechanism of xylanase catalysis have been proposed.

REFERENCE

Beg, Q. K., Kapoor, M., Mahajan, L., and Hoondal, G. S. (2001) *Appl. Microbiol. Biotechnol.* **56,** 326-338.

Biely, P (1985) *Trends Biotechnol.* **3**, 286-290.

Bradford, M. M. (1976) *Anal. Biochem*. **72**, 248-254.

Chen, Y. L., Tang, T. Y., and Cheng, K. J (2001) *Can. J. Microbiol.* **47,** 1088-1094.

Collins, T., Gerday, C., and Feller, G. (2005) *FEMS Microbiol Rev* .**29,** 3-23.

George, S. P., Ahmad, A., and Rao, M. (2001a) *Biochem. Biophys. Res. Commun.* **282**, 48-54.

George, S. P., and Rao, M. (2001) *Eur. J. Biochem.* **268**, 2881-2888.

George, S.P., Ahmad, A., and Rao, M. (2001b) *Bioresour. Technol.* **78**, 221-224.

Goller, K and Galinski, E. A. (1999) *J. Mol. Catal. B*. **7**, 37-45.

Gupta, M. N (1991) *Biotech. and Biochem.* **14,** 1-11.

Harris, G. W., Jenkins, N. A., Connerton, I., Cummings, N., Lo Leggio, L., Scott, M., Hazlewood, G. P., Laurie, J. I., Gilbert, H. J., and Pickersgill, R. W (1994) *Structure* **2**, 1107-1116.

Harris, T. K., and Turner, G. J (2002) *IUBMB Life.* **53,** 85-98.

Joshi, M. D., Sidhu, G., Pot, I., Brayer, G.D., Withers, S. G., and McIntosh, L. P (2000) *J. Mol. Biol.* **299,** 255-279.

Kamal Kumar, B., Balakrishnan, H., and Rele, M. V. (2004) *J. Ind. Microbiol. Biotechnol.* **31,** 83-87.

Kulkarni, N., Shendye, A., and Rao, M. (1999) *FEMS Microbiol. Rev*. **23**, 411-456.

Prade, R. A. (1995) *Biotechnol Genet Eng Rev* **13**, 101–131.

Miller, G. L. (1959) *Anal. Chem*. **31**, 426-428.

Nath, D and Rao, M. (2001) *Enz. Microbiol. Technol.* 28, 397-403.

Nath, D., and Rao, M (1995) *Biotech. Lett.* **17,** 557-560.

Palczewski, K., Hargrave, P.A., and Kochman, M. (1983) *Eur. J. Biochem.* **137**, 429-435.

Pauling, L. (1946) *Chem. Eng. News.* **24**, 1375-1377.

Phelps, R. A., and Cann, J. R (1957) *J. Amer. Chem. Soc*, **79**, 4677-4678.

Rye, C. S., and Withers, S. G (2000) *Curr. Opin. Chem. Biol.* **4,** 573-580.

Santoro, M. M., Liu, Y., Khan, S. M. A., Hou, L., and Bolen, D. W (1992) *Biochemistry,* **31,** 5278-5283.

Schowen, R. L. in Transition States of Biochemical Processes, Gandour,R. D.; Schowe,R. L. Eds (Plenum,NY) (1978) p- 77-114.

Simons, S. S. Jr., Thompson, E. B., and Johnson, D. F. (1979) *Biochemistry*, **18**, 4915-4922.

Turunen, O., Vuorio, M., Fenel, F., and Leisola, M (2002) *Protein Eng.* **15,** 141-145.

Vilkari, L. (1994) *FEMS Microbiol Rev* .**13,** 335-350.

Woods, E. F (1958) *J. Phys. Chem.* **62**, 308-315.

Zechel, D. L and Withers, S. G (2000) *Acc. Chem.Res.* **33,** 11-18.

CHAPTER-4

MOLECULAR CLONING AND EXPRESSION OF AN ASPARTIC PROTEASE INHIBITOR IN *ESCHERICHIA COLI*

SUMMARY

The aspartic protease inhibitor (ATBI) purified from a *Bacillus sp*. is a potent inhibitor of recombinant HIV-1 protease, pepsin, fungal aspartic protease and xylanase. The molecule is of eleven amino acids and is peptidic in nature. The peptide sequence data of the 11-mer was exploited to synthesize the complementary oligonucleotides, which were annealed and subsequently cloned inframe with the gene for GST in to *Escherichia coli (E. coli)* BL21-A1 through the gateway cloning strategy. The expression clone was induced using arabinose which expressed the recombinant peptide as a fusion protein along with GST tag for the ease of purification. The recombinant peptide was purified using reduced glutathione column, and subsequently cleaved with Factor Xa to remove the GST-tag. The resultant product was further purified to homogeneity using *rp-HPLC*. The purified peptide was characterized using mass spectroscopy analysis. The recombinant peptide was found to be active *in vitro* against HIV-1 protease, pepsin, fungal aspartic protease and xylanase.

The cloned cells (*E coli*) expressing recombinant glutathione-S-transferase-peptidic inhibitor (GST-ATBI) gene was used as a model system to demonstrate the importance of intact cell matrix-assisted laser desorption/ionization mass spectrometry (*ICM-MS*) in drug discovery. Using ICM-MS analysis, a 28 kDa peak corresponding to the production of recombinant GST-ATBI under arabinose induced condition has been detected. The regulation of protein expression was studied using glucose as an alternative metabolite. The glucose-mediated regulation of the *ara*-operon was followed using ICM-MS technique. All these results obtained from ICM-MS data were validated using sodium dodecyl sulfate polyacrylamide gel electrophoresis (SDS-PAGE) analysis. The present technique can be extended for *in vivo* screening of drugs and it holds tremendous potential to discover novel drugs against specific protein expressions in different diseases.

PART-1

CLONING AND HYPER-EXPRESSION OF ATBI GENE IN *E. COLI*

INTRODUCTION

Aspartic proteases are found in a wide range of organisms, ranging from viruses, bacteria, fungi, and parasites to plants and animals (James, 1998). They are not only involved in many physiological processes but also can mediate the initial invasion steps of infective organisms (Stewart et al., 1999). Recently they have received enormous interest because of their significant roles in human diseases; the best-known examples are the involvement of renin in hypertension, cathepsin D in metastasis of breast cancer, and the protease of human immunodeficiency virus (HIV) in acquired immune deficiency syndrome (AIDS). In contrast to this wide spread distribution of the enzymes, gene encoded specific inhibitors of aspartic proteases are relatively uncommon and have been identified only in a few specialized locations (Bennet et al., 2000), for example an inhibitor of cathepsin D from sea anemone (Lenarcic and Turk, 1999), a 17 KDa protein from the parasite *Ascaris lumbricoids* which inhibits pepsin and cathepsin E (Ng et al., 2000), a dimeric 11 KDa protein (SQAPI) from squash phloem exudates (Christeller et al., 1998), the yeast IA3 inhibitor of protease A from *Saccharomyces cerevisiae* (Phylip et al., 2001), and a 28 KDa aspartic protease inhibitor (API) from *Ostertagia ostertagi* (Maere et al., 2005) are reported.

The major sources of aspartic protease inhibitors, that are themselves proteins, are limited in nature and the reports are from potato (Keilova and Tomasek1976), wheat (Galleschi et al., 1993), yeast (Schuand Wolf, 1991), and the nematode (*Ascaris* sp.) (Abu-Erreish and Peanasky, 1974). The well characterized of these, the potato cathepsin D inhibitor (PDI) is a bifunctional (it also inhibits serine protease inhibitor) (Keilova and Tomasek1976) and has extended similarity with soybean trypsin inhibitor family (Mares et al., 1989). Recent works have described that PDI consists of several isoforms which have been cloned and sequenced (Ritonja et al., 1990; Maganja et al., 1992; Strukelj et al., 1992; Strukelj et al., 1995). The inhibitor found in yeast IA3, has been sequenced (Schuand Wolf, 1991) but has no similarity to either PDI or the nematode inhibitor. The nematode inhibitor, which inhibits mammalian but not fungal proteases (Valler et al., 1985), has been sequenced and cloned (Martzen et al., 1990). Kageyama reported the molecular cloning of a cDNA for *Ascaris* pepsin inhibitor, and its expression in

Saccharomyces cerevisiae (Kageyama, 1998). Maere and coworkers have described the cloning and characterization of an API from *O. ostertagi* (Maere et al., 2005). Aspartic protease inhibitors from tomato was cloned and expressed in *Pichia pastoris* (Cater et al., 2002). Pepstatin is an aspartic protease inhibitor, a low molecular weight non-proteinaceous microbial hexapeptide that acts as a transition-state analogue (Umezawa, et al., 1970). To date, there are no reports on cloning of low molecular weight peptidic inhibitors for aspartic proteases from microbial sources.

In the second chapter, the inhibition of xyalanse by a peptidic aspartic protease inhibitor ATBI produced by a *Bacillus* sp has been described. Apart from xylanase inhibition, the inhibitor is well documented for its inhibitory activity towards several aspartic proteases such as pepsin, recombinant HIV-1 proteases, and fungal aspartic protease (Dash and Rao, 2001; Dash et al., 2001a; Dash et al., 2001b). Being an inhibitor of HIV-1 protease, ATBI exhibits tremendous pharmaceutical potential as a drug for the treatment of Acquired Immuno Deficiency Syndrome (AIDS). Although a synthetic approach for future clinical applications with ATBI has some advantages, large scale production may be more economical through a recombinant approach. The production of peptide for preclinical and clinical evaluation often requires multigram quantities (Kelley, 1996), and production of recombinant peptides at this scale from microbial fermentation can potentially be economical. Recently recombinant DNA technology has been used widely for obtaining and combining genes from a variety of sources, and the possibility of over expressing these genes in different host cells for its application. This technique allows researchers in the biopharmaceutical field to obtain proteins in huge quantities.

The hosts used for production of recombinant proteins range from simple prokaryotic organisms to multicellular organisms such as transgenic plants and animals, and including unicellular eukaryotic organisms such as yeast and the more complex eukaryotic insect and mammalian cells. The choice of host system depends on many factors, such as the size, structure and stability of the gene product, and the requirements for post-translational modifications for biological activity. If the protein consists of multiple subunits or requires substantial post-translational modifications, the preferred host usually is of higher eukaryotic origin. The bacterium *E. coli* has, however, also been

successfully used for production of relatively complex proteins (Rudolph, 1996). As a production host, *E. coli* has mainly been used for cost-efficient production of large amounts of proteins that are limited in size and have a relatively simple structure. Apart from that, the ability to produce foreign proteins/ peptides in *E. coli* in the form of fusion proteins with various carrier proteins has made large scale purification protocols possible (Smith and Johnson, 1988). An expressed recombinant peptide / protein may be produced intracellularly, or extracellularly. The extracellularly produced molecule can be recovered from the culture filtrate after separating the cells from the medium. An intracellularly produced recombinant protein can be accumulated in a soluble form in the cytoplasm, precipitate and form inclusion bodies, or, alternatively, be partly in the form of inclusion bodies and partly in soluble form.

Table-1

Fusion proteins used in recombinant technology

Fusion partner	**Size**	**Ligand**	**Most commonly used Elution Method**	**Reference**
GST	26 KDa	GSH	GSH	Smith and Johnson, 1988
Protein A	31 KDa	hIgG	Low pH	Nilsson and Abrahmsen, 1990
Z	7 KDa	hIgG	Low pH	Nilsson et al., 1987
ABP	5-25 KDa	HAS	Low pH	Nygren et al., 1988
Hexahistidine	6aa	Me^{2+}	Imidazole/Low pH	Porath et al., 1975
MBP	41 KDa	Amylose	Maltose	di Guan et al., 1988
FLAG peptide	8 aa	mAb M1	EDTA / Low pH	Hopp et al., 1988
Bio	13 aa	Streptavidin/ avidin	Diaminobiotin	Schatz, 1993
Pin Point	13 KDa	Streptavidin/ avidin	Biotin	Cronan, 1990

Abbreviations used: aa, amino acids; ABP, albumin-binding protein; GST, glutathione S-transferase; hIgG, human IgG; HSA, human serum albumin; mAb, monoclonal antibody; MBP, maltose-binding protein; Me^{2+}, bivalent metal ion ; FLAG, Asp- Tyr-Lys-Asp-Asp-Asp-Asp-Lys.

There are several different approaches to minimize the formation of inclusion bodies when producing heterologous proteins intracellularly in *E. coli*. Reduction of the rate of protein synthesis, which can be achieved by using a moderately strong or weak promoter, or partial induction of a strong promoter, has been found to result in a higher amount of soluble protein (Weickert et al., 1996). Other means of reducing the protein-synthesis rate is by growing the culture at lower temperature (Schein, 1993) or to add non-metabolizable carbon sources at the time of induction (Lilie et al., 1998). Fusion of the target protein to a highly soluble fusion partner, thereby increasing the overall solubility of the fusion protein, is a convenient and efficient method to increase the fraction of soluble gene product in the cytoplasm. After a successful production of a recombinant protein, different purification steps will be needed in order to recover a biologically active protein at high purity. Normally affinity purification allows a single step procedure for purification of recombinant molecule in pure form. The first example of the use of gene fusions for affinity purification was reported in 1983 (Uhlen et al., 1983). After that a large number of different affinity-fusion systems have been developed to facilitate the purification of recombinant proteins (Nilsson et al., 1997; Stevens, 2000). Some of the most commonly used affinity-fusion systems are listed in table 1.

When choosing an affinity-fusion system, it is important to note that all systems have their own characteristics, and no single system is ideal for all applications. For example, if secretion of the gene product is desired, it is necessary to choose a system with a secretable affinity tag. If the gene product needs to be purified under denaturated conditions, a system which has a tag which can bind under those conditions must be chosen, such as polyhistidine affinity tag (Porath et al., 1975; Porath, 1992). It is also important to choose an affinity-fusion system with elution conditions under which the target protein does not get denaturated (Stahl et al., 1999). In the present study, the ATBI gene was cloned inframe with the gene for GST in to *E. coli* BL21-A1 through the gateway cloning strategy.

For laboratory scale experiments affinity-fusion methods are very powerful and have achieved widespread use for easy and fast single-step purification of gene products. For large-scale pharmaceutical/industrial production affinity fusions have not been as

extensively utilized, despite the ability to replace multiple steps with one step. The main reason is most probably that, for most applications, the affinity tag needs to be removed afterwards. If the produced molecule is intended to be used as a pharmaceutical product, or if the molecule is aimed to be used for structural determination, it is necessary to remove the affinity tag after the affinity-purification step. Furthermore, proteinaceous ligands may leak from the column during elution, making it necessary to remove the ligand from the eluate. To obtain the recombinant molecule in a very pure form from the fused product, the tag should be removed after affinity purification. There are several methods, based on chemical or enzymatic treatment, available for site-specific cleavage of fusion proteins (La Vallie et al., 1994). Chemical cleavage reagents include cyanogen bromide, which cleaves at methionine residues (Itakura et al., 1977; Piers et al., 1993; Haught et al., 1998; Lee et al., 1998), N-chloro succinimide (Forsberg et al., 1989) or BNPS-skatole (Dykes et al., 1988; Knott et al., 1988) which cleaves at tryptophan residues, dilute acid which cleaves aspartyl–prolyl bonds (Marcus, 1985; Gram et al., 1994), and hydroxylamine which cleaves asparagine–glycine bonds at pH 9.0 (Moks et al., 1987; Nilsson et al., 1991).

Table-2

Enzymes used for site-specific cleavage

Enzyme	Sequence	Reference
Factor Xa	Ile-Glu-Gly-Arg-↓-Xaa	Maina et al., 1988
Enterokinase	Asp-Asp-Asp-Asp-Lys-↓-Xaa	Hopp et al., 1988
[H64A]Subtilisin	Phe-Ala-His-Tyr-↓-Xaa	Forsberg et al., 1991
IgA protease	Pro-Ala-Pro-Arg-Pro-Pro-↓-Thr	Pohlner et al., 1993
Thrombin	Leu-Val-Pro-Arg-↓-Gly-Ser	Chang, 1985
GST–protease 3C	Leu-Glu-Val-Leu-Phe-Gln-↓-Gly-Pro	Walker et al., 1994
ABP–protease 3C–His_6	Leu-Glu-Ala-Leu-Phe-Gln-↓-Gly-Pro	Graslund et al., 1997
His_6–TEV protease	Glu-Asn-Leu-Tyr-Phe-Gln-↓-Gly	Parks et al., 1994

Abbreviations used : Xaa, unspecified amino acid ; GST, glutathione S-transferase; ABP, albumin-binding protein; TEV, tobacco-etch virus ; -↓-, cleavage site ; [H64A], His^{64}→Ala; His_6, hexahistidine.

Advantages with the chemical cleavage methods are that the reagents used are inexpensive and widely available, and the reactions are generally easy to scale up. However, the harsh reaction conditions often required can lead to amino-acid-side-chain modifications or denaturation of the target protein (Carter, 1990). Furthermore, the selectivity is often rather poor, and cleavage can occur on additional sites within the target protein. For many applications, enzymatic cleavage methods are preferred to chemical ones, because of their higher selectivity, and because the cleavage often can be performed under physiological conditions. Some of the commonly used enzymes for site-specific cleavage of fusion proteins are listed below (Table 2). In the present study the recombinant ATBI was obtained in a pure form from its fusion partner (GST) through Factor Xa cleavage reaction.

By considering the potential of recombinant technology, several novel approaches have been described for the last two decades to facilitate the cloning process. Examples that take advantage of homologous recombination in *E. coli* (Bubeck et al., 1993; Oliner et al., 1993; Degryse, 1996; Zhang et al., 1998) or yeast (Lafontaine and Tollervey, 1996; Storck et al., 1996), site-specific transposition (Luckow et al., 1993), or site-specific recombination (Peakman et al., 1992; Boyd 1993; Liu et al. 1998) have been published. These have significant value for particular applications but are limited in scope by requirements for specific hosts, by selection schemes, or by the vector attributes they can effectively contribute. Hartley et al., reported a flexible approach that could provide high-efficiency, high-fidelity cloning and subcloning reactions, independent of vector function or host background (Hartley et al.,. 2000). It is a universal cloning method based on the site-specific recombination properties of bacteriophage lambda (Landy, 1989). This technology provides a rapid and highly efficient way to move DNA sequences into multiple vector systems for functional analysis and protein expression. The site-specific recombination reactions mediated by λ integrase family of recombinases are conservative (no net gain or loss of nucleotides) and highly specific. This system carries out two reactions: (1) attB × attP → attL + attR mediated by the integrase (Int) and integration host factor (IHF) proteins and (2) attL× attR → attB + attP mediated by Int, IHF, and excisionase (Xis). Thus, the direction of the reactions is controlled by providing different

combinations of proteins and sites. The *in vitro* recombination reaction initially contains two starting DNAs: an entry clone (attL1-gene-attL2), which carries the DNA segment to be transferred, and a destination vector (attR1-ccdB-attR2), the vector into which the DNA will be subcloned. Incubating these DNAs with recombination proteins (Int + Xis + IHF) results in Int-mediated recombination, first generating a cointegrate molecule and then resolving it, to accomplish transfer of the cloned DNA segment into the destination vector.

Recombination enzymes involved in the gateway recombination reactions

Lambda recombination is catalyzed by a mixture of enzymes that bind to specific sequences (*att* sites), bring together the target sites, cleave them, and covalently attach the DNA. The Clonase enzyme mixtures utilize a combination of the bacteriophage λ Integrase (Int) and Excisionase (Xis) proteins and *E. coli* Integration Host Factor (IHF) proteins.

Integrase:

It has type I topoisomerase activity. Cuts and reseals the *att* sites via covalent Int-DNA intermediate. Int binds specifically to 2 different families of DNA sequences:

1. core: CAACTTNNT
2. arm: C/AAGTCACTAT

Required for both excision (LR reaction) and integration (BP reaction) of phage

Excisionase

It is required for excision (LR) but not integration (BP) of phage. Xis inhibits integration (BP) at physiological conditions and relatively stable *in vitro* but rapidly degraded in cells. Xis promotes efficient LR recombination in presence of Int and IHF and it has no enzymatic function but rather sequence-specific cooperative binding to adjacent sites in the P arm thus introducing sharp bend in the DNA. It is also associated with cooperative interactions with DNA-bound Int.

Integration host factor

It is an *E. coli*-derived protein as opposed to phage-derived (Xis & Int), essential for both excision and integration (LR and BP reactions respectively). It is a heterodimer composed of alpha and beta subunits and similar to other type II DNA binding proteins such as histones. It has no known enzymatic function but it binds to and bends DNA at specific sites.

The gateway cloning technology takes advantage of the well-characterized bacteriophage lambda-based site-specific recombination instead of restriction enzymes and ligase. The power of the gateway cloning technology is that genes cloned into entry vectors can be subcloned in parallel into one or more destination vectors in a simple, 60-minute reaction. Moreover, a high percentage (> 95%) of the colonies obtained carries the expression clone in the desired orientation and reading frame. Illegitimate recombination does not occur since gateway cloning does not operate by homologous recombination and recombination with genomic sequence is predicted to be a rare event. The recombination sites used in gateway cloning are not wild-type sites. Several point mutations were engineered into the wild type *att* sites to generate novel specificities. For example attB1 only recombines with attP1 and not with wild type *att*P or *att*P2. As these sites differ by only a few nucleotides, the specificities of the *att* sites for the paring partners are extremely high.

The first part of the chapter describes the cloning of ATBI gene into *E. coli* for functional expression through gateway cloning approach. The recombinant peptide was found to be active *in vitro* against HIV-1 protease, pepsin, fungal aspartic protease and xylanase.

MATERIALS AND METHODS

Oligonucleotide design

The oligonucleotides for direct cloning were designed based on the peptide sequence information published earlier from our laboratory (Dash and Rao, 2001). Each amino acid of the 11-mer peptide from *Bacillus* sp. was converted to the corresponding triplet based on the preference obtained from *E. coli* codon usage table. All precautions were taken to avoid the codon bias in *E. coli* while expressing the oligonucleotide as a fusion protein.

Ala— Gly— Lys— Lys— Asp— Asp— Asp— Asp— Pro— Pro— Glu
GCG- GGC- AAA- AAA- GAT- GAT- GAT- GAT- CCG- CCG- GAA

The flanking region of the primer was constructed as per the Gateway Cloning Manual (Gateway technology Catalog nos. 12535-019 and 12535-027, Invitrogen). The primer constructed contains site for Factor Xa cleavage at the 5' end which was employed for separating the purified peptide from the recombinant GST. This construct was synthesized and obtained from Life technologies, India.

AttB1F: **[Factor Xa]**

5' GGG GAC AAG TTT GTA CAA AAA AGC AGG CTT CAT TGA GGG TCG CGC GGG CAA AAA AGA TGA TGA TGA TCC GCC GGA ATA AGA CCC AGC TTT CTT GTA CAA AGT GGT CCC C 3'

AttB1R:

5' GGG GAC CAC TTT GTA CAA GAA AGC TGG GTC TTA TTC CGG CGG ATC ATC ATC ATC TTT TTT GCC CGC GCG ACC CTC AAT GAA GCC TGC TTT TTT GTA CAA ACT TGT CCC C 3' **[Factor Xa]**

Primer annealing to produce the DNA template

The single stranded primers which are complementary each other were annealed directly for cloning purpose. The annealing reaction mixture 50 µL contained 1 µL sense oligo [100 picomoles/ µL], 1 µL anti sense oligo [100 picomoles/ µL], 5 µL 10X annealing buffer, and 43 µL nuclease free double distilled water. The reaction was carried out at 100^{o}C for 10 min and slowly cooled down to room temperature (27^{o}C).

Clonase

BP Clonase, containing Int and IHF, catalyzes the integrative (BP) reaction (*att*B × *att*P → *att*L + *att*R). LR Clonase, containing Xis, Int, and IHF, catalyzes the excisive (LR) reaction (*att*L × *att*R → attB + attP) were obtained as a part of Gateway Cloning System from Invitrogen.

BP reaction

The annealed template was used as the template for the BP reaction. 5 µL of the template was mixed with 300 ng of pDONR 221 and 4 µL of the 5X BP clonase buffer containing 25 mM Tris HCl pH 7.5, 22 mM NaCl, 5 mM EDTA, 5 mM spermidine HCl, 1 mg / mL BSA. Nuclease free double distilled water was added to make up the final reaction volume to 16 µL. The contents were mixed briefly and 4 µL of the BP clonase mix was added to the reaction mixture and the reaction was incubated at 25°C for overnight. 4 µg of Proteinase K was then added to the BP reaction and incubated at 37°C for 10 min. Half of the reaction was transformed into *E. coli* DH5-α and plated on the Kanamycine (50 µg / mL) plate for selection. The plasmids isolated from the selected colonies were screened with the help of PCR using M 13 F and M 13 R primers.

Plasmid isolation and purification

Mini preparations of plasmid DNA were carried out by alkaline lysis method. A single bacterial colony was transferred to 2 mL LB medium containing kanamycine in a loosely capped 15 mL tube. The culture was incubated at 37°C for overnight with vigorous shaking. The centrifuged (12000g) bacterial cell pellet was resuspended in Buffer P1 containing 50 mM glucose, 25 mM Tris.Cl (pH 8.0) 10 mM EDTA and 100 µg / mL RNase A. The bacterial pellet was completely dispersed in Buffer P1. Into the dispersed cells Buffer P2 (200mM NaOH and 1 % SDS) was added to lyse the cells. Buffer P3 containing 3 M potassium acetate pH 5.5 was used to precipitate genomic DNA and proteins. The precipitate was centrifuged at 10,000 rpm for 10 min. The supernatant containing plasmid DNA was transferred into a fresh 2 mL eppendorf tube and precipitated with 2 volumes of 100 % ethanol. The plasmid pellet thus obtained was washed with 70 % ethanol, air dried and dissolved in 40 µL of TE (pH 8.0). 2 µL of the

aliquot was checked on agarose ethidium bromide gel. The entry clones were sequenced using vector specific primers (using M 13 F and M 13 R primers) in a DNA analyzer 3730 of ABI.

LR reaction

Plasmid with correct template sequence was chosen as entry clone for LR reaction. Aliquot of 2 µL containing 200 ng of plasmid DNA was incubated with 300 ng of destination vector, pDEST 15 (N-terminal GST), in 20 µL of final reaction volume containing 4 µL of LR clonase, 50 mM of Tris-HCl pH 7.5, 50 mM of NaCl, 0.25 mM of EDTA, 2.5 mM of spermidine HCl, and 0.2 mg /mL of BSA. The reaction mixture was incubated for overnight at 25°C. The proteinase K (4 µg in 2 µL) was added and reaction was incubated at 37°C for 10 min. Aliquot of 2 µL of the reaction was transformed into *E. coli* DH5-α (Invitrogen) and plated on ampicillin (100 µg/ mL) plates and incubated at 37°C. Miniprep DNA was prepared as described earlier, and 2µL aliquots were applied to a 1% agarose/ethidium bromide gel. The plasmids isolated from the selected colonies were screened with the help of PCR using pET F and pET R primers and gene sequencing.

Transformation

E. coli DH 5α was used for plasmid propagation. After each recombination reaction the gene was transformed to competent *E. coli* cells (library efficient DH 5α) and the clones were selected using appropriate antibiotic. For each transformation 50 µL of library efficiency DH 5α competent cells were incubated with 1 µL of the recombination reaction. This reaction mixture was incubated on ice for 30 min. After the incubation a heat shock for 30 seconds at 42°C was given and the tube was transferred to ice. To this 450 µL of room temperature S.O.C medium was added and kept at 37°C for one hour. Aliquots were plated on LB plates containing appropriate antibiotics for selection.

Polymerized chain reaction (PCR)

All PCR reactions were set up with 1 or 2 µL of DNA template to a final reaction volume of 25 µL containing 20mM of Tris-HCl pH-8.8, 10 mM of KCl, 10 mM of $(NH_4)_2$ SO_4, 2

mM of $MgSO_4$, and 0.1% of Triton X 100. 10 picomols / µL of forward and reverse primers and 0.78 U of Taq DNA polymerase were also present in the reaction mixture. The amplification was carried out in Gene Amp PCR System 9700 with initial denaturation of 2 min and 30 cycles of one minute denaturation at 94°C, annealing for one minute at 55°C and extension for one minute at 72°C.

Protein expression

For protein expression in *E. coli*, miniprep DNAs of expression clones in pDEST 15 containing the T7 promoter was transformed into competent BL21 A1 cells. These transformed cells were plated at 37°C on LB ampicillin plates. For expression, the bacteria were grown on LB medium containing ampicillin at 30°C to limit the maximal growth rate. When the culture OD reached approximately A_{595} ~ 0.5, 0.2 % arabinose was added for the induction of recombinant peptide. The expression was continued at 30°C for 4 h and aliquots were collected in each hour for checking the expression profile.

SDS-PAGE analysis

Following growth after induction with arabinose, 100 µL of culture was centrifuged, and the pellet was resuspended in 85 µL of 1X SDS sample buffer. Samples were heated at 90 to 95°C for 15 min and subjected to SDS–PAGE analysis on 10% gels. Electrophoresis of 2 to 5 µL samples proceeded at 40 V for about 1 h. Gels were stained with Coomassie blue R250 to verify the protein expression.

Protein purification and Factor Xa treatment

After 4 h of induction the bacterial cells were harvested by centrifugation at 5000 rpm for 15 min. The cells were resuspended in Tris Buffer and disrupted by sonication at 4 °C for 5 min. The recombinant GST-ATBI protein was purified by a single-step affinity purification using Glutathione Sepharose 4B affinity column from arabinose induced *E. coli* cells according to Amersham Biosciences Instructions Manual, Code No. 17-0757-01. Factor Xa cleavage reaction was carried out in the column to remove the GST tag. The reaction was carried out as per the instructions provided by the manufacture (Sigma-Aldrich). After the reactions the cleaved fractions were collected using elution buffer (10 mM reduced glutathione, 50 mM Tris- HCl, pH 8.0), as per users instruction manual

(Amersham Biosciences). A fraction without Factor Xa cleavage was also eluted and collected for control experiments. The fractions were collected and concentrated by lyophilization.

Reverse phase HPLC

Reverse phase HPLC (*rp-HPLC*) was used to further purify the recombinant peptide. The concentrated inhibitor sample (100 µL) was loaded onto a prepacked Ultopac Lichrosorb RP-18 (LKB) column which was pre-equilibrated with 10 % acetonitrile (CH_3CN) and 0.1% trifluroacetate (TFA). The fractions detected at 210 nm were eluted on a linear gradient of 0-50% acetonitrile and water containing 0.1 % TFA. The fractions detected were collected manually and checked for its inhibitory activity against pepsin. The fractions showing the inhibitory activity were pooled and lyophilized for further studies.

Mass spectrometry analysis

PE-SCIEX Q STAR PULSAR LC-MS-MS-TOF (Applied Biosystems) was used to analyze the molecular weight and homogeneity of recombinant protease inhibitor.

Pepsin Assay

The inhibitory activity of ATBI was determined by estimating the anti-pepsin activity in 0.05 M KCl-HCl solution, pH 2.0 using casein (0.6%) as the substrate in a reaction volume of 2 mL. The reaction was stopped with equal volume of 1.7 M perchloric acid (PCA), the mixture was centrifuged (10,000 g, 5 min) and filtered, and the optical absorbance was measured at 280 nm.

Fungal protease assay

The proteolytic activity of the aspartic protease from *Aspergillus saitoi* (F-Prot) was measured by assaying the enzyme activity using hemoglobin as a substrate. 1.5 µM of F-Prot was dissolved in Glycine-HCl buffer, 0.05 M, pH 3.0, was incubated with the inhibitor for 5 min. The reaction was started by the addition of 1 mL of hemoglobin (5 mg/ ml) at 37 $^{\circ}$C for 30 min. The reaction was quenched by the addition of 2 ml of PCA (1.7 M) followed by centrifugation (10,000 g, 5 min) and filtration. The optical absorbance of the PCA soluble products n the filtrate was read at 280 nm.

HIV-1 PR activity assay

The *E. coli* strain harboring the recombinant plasmid pTδN containing the HIV-1 PR was used as a source of enzyme (Dash and Rao, 2001). The HIV-1 PR was assayed using the synthetic substrate Lys-Ala-Arg-Val-Nle-pNitro-Phe-Glu-Ala-Nle-Amide (Phylip et al., 1990; Richards et al., 1990). The HIV-PR was incubated at 37°C with the inhibitor in a reaction mixture containing 100 mM NaCl, 5 mM β-mercaptoethanol, 5 mM EDTA and 50 mM sodium acetate buffer, pH 5.6. After 15 min, the reaction was stopped by the addition of equal volume of 5 % trichloroacetate and followed by 30 min incubation at 28°C. The hydrolysis of the peptide substrate was followed by monitoring the decrease in optical absorbance at 300 nm spectrophotometrically (Dash and Rao, 2001).

Xylanase assay

Xylanase assay was carried out in phosphate buffer, 0.05 M, pH 6.0, by mixing a specified concentration of the enzyme with 0.5 ml of oat spelt xylan (10 mg/ml) in a reaction mixture of 1 ml and incubating at 50°C for 30 min. The detailed assay conditions for xylanase has been described in chapter 2.

RESULTS AND DISCUSSION

Although bioactive peptides can be produced chemically by a variety of synthetic strategies, recombinant peptides production of 5 to 50 amino acid size range offers the potential for large scale production at reasonable cost. Expression of very short polypeptide chains can sometimes be problematic in microbial systems such as *E. coli*., however some peptides have been expressed as a part of fusion proteins (Callaway et al., 1993; Piers et al., 1993). There are reports of cloning and expression of synthetic genes in *E. coli*. for functional expression of desired proteins (Howell and Blumenthal, 1989; Gavit and Better, 2000; Li et al., 2000; Brandwijk et al., 2005). To produce the recombinant inhibitor of ATBI, an artificial gene has been designed based on the amino acid sequence of the peptide (Ala-Gly-Lys-Lys-Asp-Asp-Asp-Asp-Pro-Pro-Glu). The 11 amino acid sequence was translated into 33 bp genetic code based on the preference obtained from *E. coli* codon usage table. The flanking region of the gene was constructed as per the gateway cloning manual. The single stranded primers which are complementary to each other were annealed directly for cloning purpose. This annealed primer was inserted into the entry vector pDONR 221(Figure 1) through BP reaction (Figure 3 A) and subsequently the gene was inserted into pDEST 15 (Figure 2) by LR reaction (Figure 3 B).

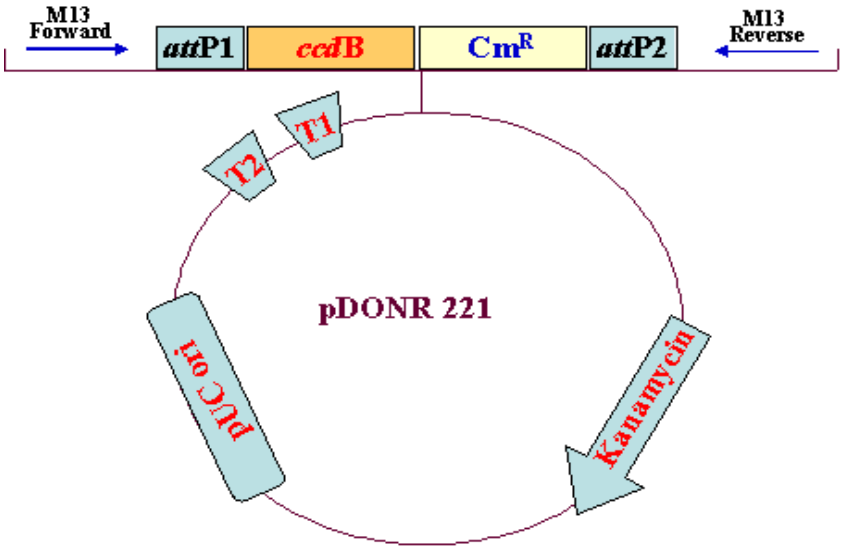

Figure 1. pDONR 221

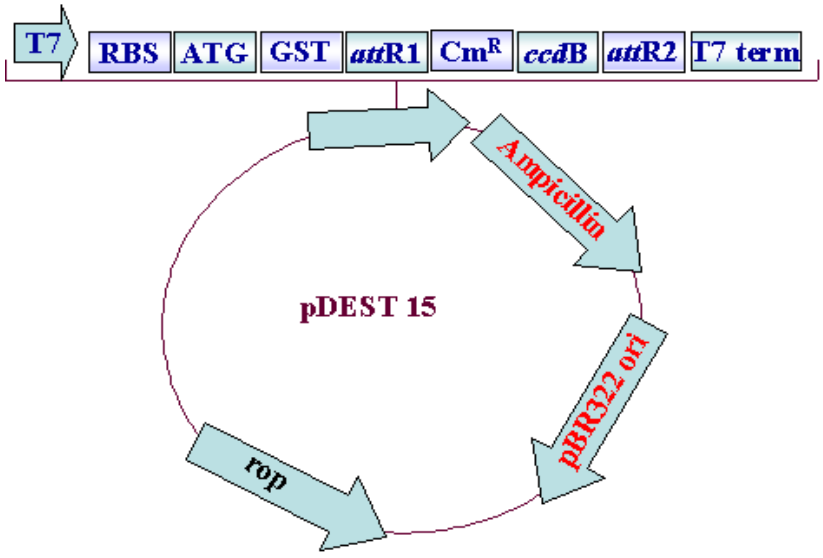

Figure 2 pDEST 15

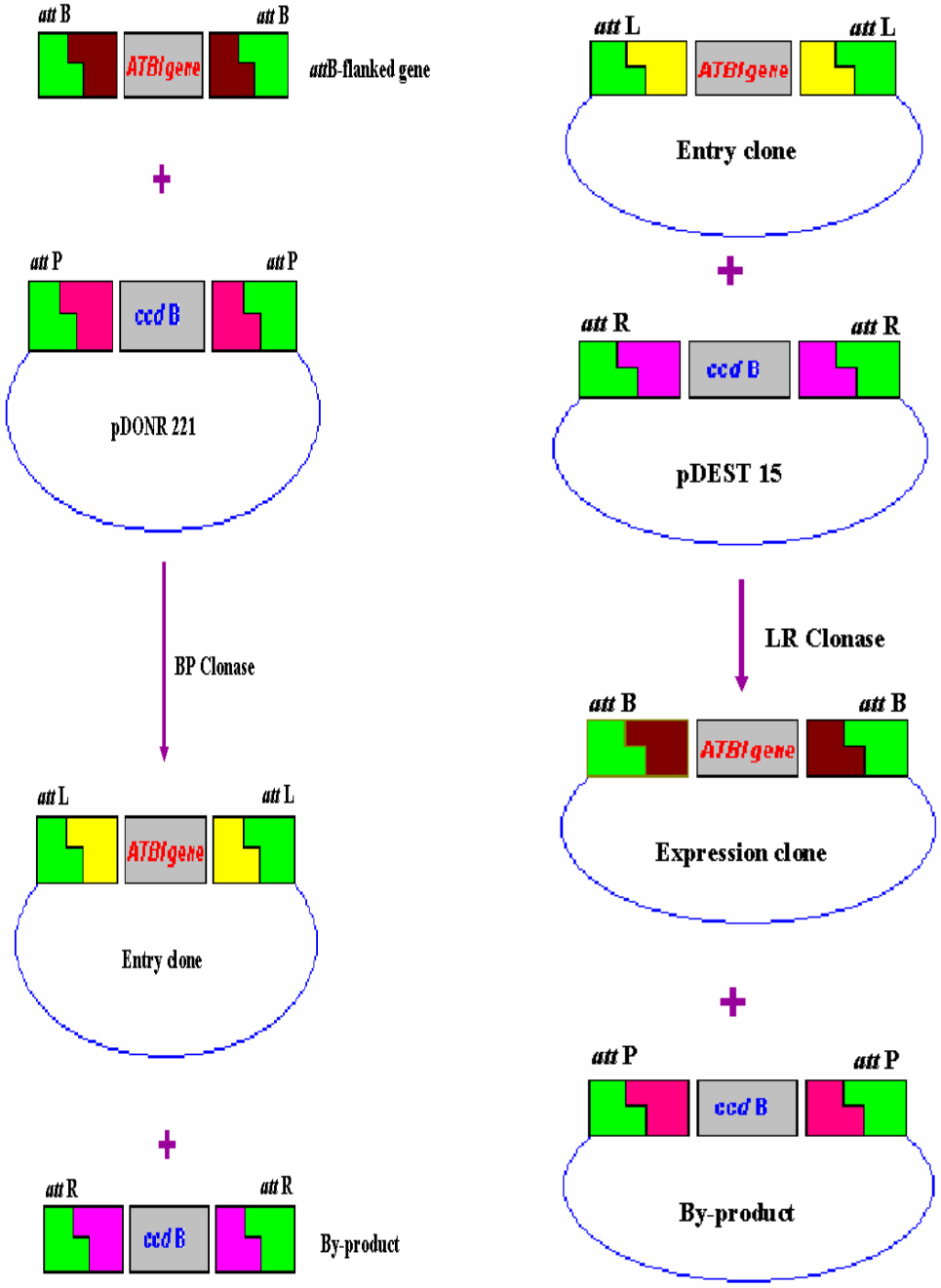

Figure 3. A. BP reaction facilitates recombination of an *att*B substrate with *att*P substrate (donor vector) to create an *att* L-containing entry clone. This reaction is catalyzed by BP clonase enzyme mix. **Figure 3. B**. LR reaction facilitates recombination of an *att*L substrate (entry clone) with *att*R substrate (destination vector) to create an *att*B-containing expression clone. This reaction is catalyzed by LR clonase enzyme mix.

There are two selection schemes to obtain the expression clone after introduction of the mixture into *E. coli* by transformation. First, the entry clone (kanamycin resistant) and the destination vector (ampicillin resistant) contain different antibiotic resistance genes. Second, the presence of the *ccd*B gene, which allows negative selection of the entry and destination vectors. The ccdB protein interferes with *E. coli* DNA gyrase (Bernard and Couturier, 1992), thereby inhibiting the growth of *E. coli* strains. When recombination occurs, the *ccd*B gene is replaced by the gene of interest. Cells that take up unreacted vectors carrying the *ccd*B gene or by-product molecules retaining the *ccd*B gene will fail to grow. This allowed high efficiency recovery of the desired clones.

Figure 4 shows the agarose gel profile of the PCR amplified gene from LR clones. The clones were sequenced with pET forward and pET reverse primers. Sequence with reverse primer was proper. The sequence obtained was reverse complemented and the resulting sequence was checked for the *att*B primer sequence along with the oligo designed for the expression of ATBI. The following electropherogram (Figure 5) shows the *att*BF primer sequence, Factor Xa site and the sequence of the oligo for inhibitor gene.

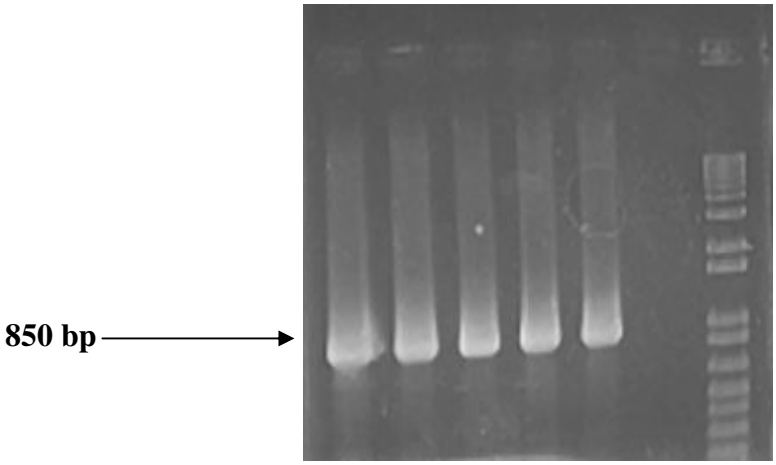

Figure 4. PCR amplified product of the gene from LR clones

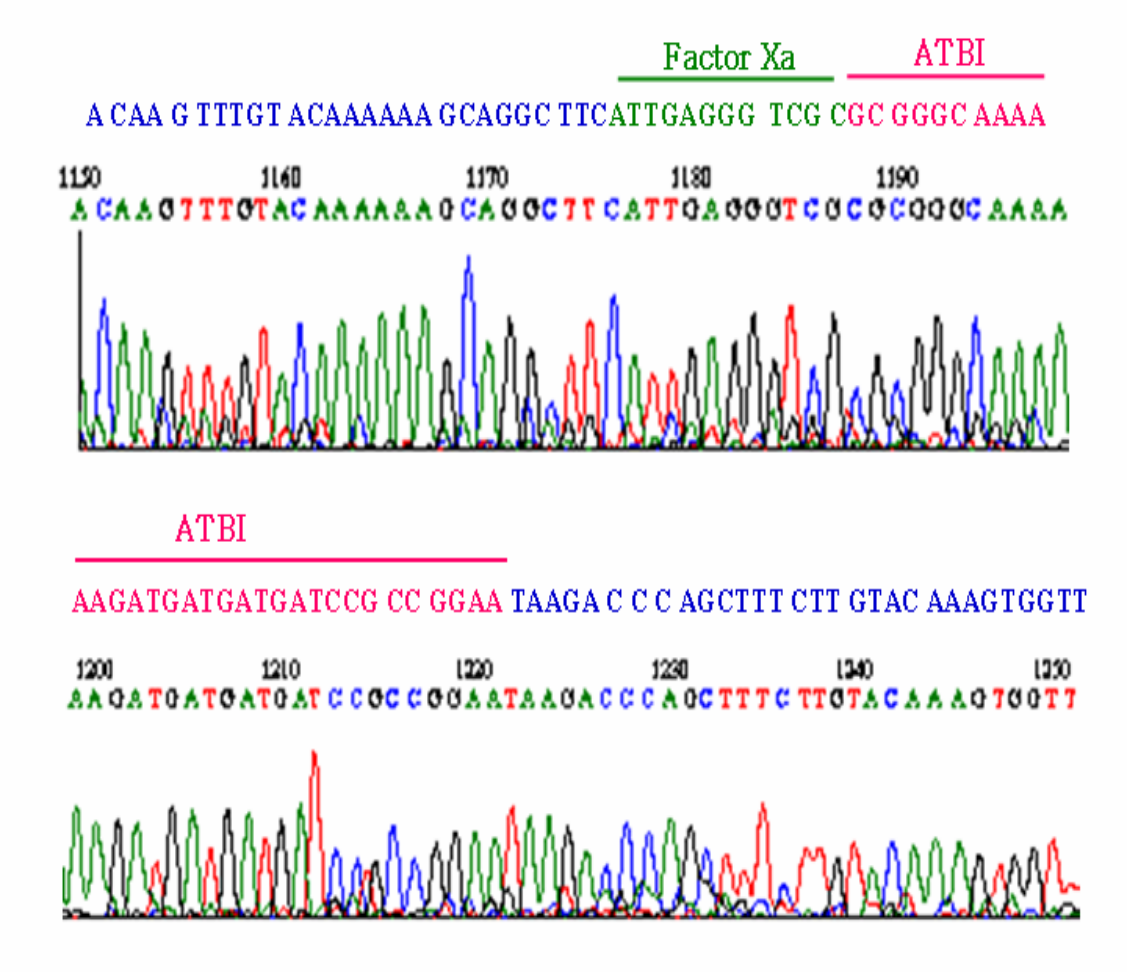

Figure 5. Electropherogram shows the factor Xa site and the sequence of the oligo for inhibitor gene

Expression of recombinant peptide in *E. coli* BL21-AI

The recombinant gene was transformed in to *E. coli* BL21-AI strain for functional expression. The BL21-AI strain is an *E. coli* B/r strain, is deficient in *lon* protease and the outer membrane protease, OmpT. The lack of these proteases reduces degradation of heterologous proteins expressed in this strain. The strain carries a chromosomal insertion of a cassette containing the T7 RNA polymerase (T7 RNAP) gene in the *ara*B locus, allowing expression of the T7 RNAP to be regulated by the *ara*BAD promoter. The transformed cells were induced with 0.2 % arabinose and the expression profile was checked on 10 % SDS PAGE (Figure 6). As a part of fusion protein, peptides may be directed to specific cellular compartments, i.e. cytoplasm, periplasm, or media, with the goal of achieving high expression yield and avoiding cellular degradative processes. The

protein profile and biological activity measurements confirmed that the recombinant peptide was expressed intracellularly. Figure 6 shows the expression of cloned protein as a function of induction time.

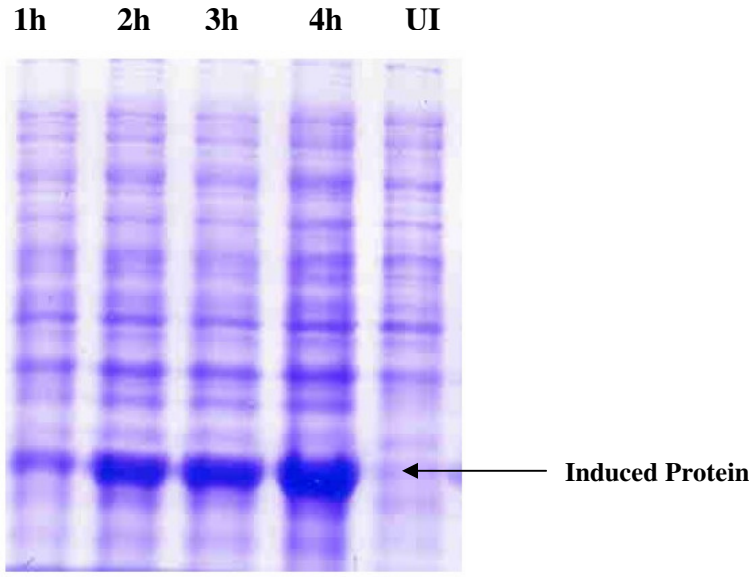

Figure 6: SDS-PAGE analysis of protein expression

Isolation and cleavage of fusion protein

The recombinant peptide was purified from arabinose induced *E. coli* cells. The cells were sonicated and the intracellular fraction was subjected to Glutathione Sepharose 4B affinity chromatography column. The unbound protein was washed with Tris buffer and Factor Xa treatment was given to the bound protein to clave the GST tag. SDS-PAGE and coomassie blue staining pattern of different samples revealed specific bands (Figure 7). The lane 1and 2 represent the uninduced and arabinose induced cells respectively. The arrow indicates the protein expression in case of 0.2% arabinose induction (Lane 2) and which was absent in arabinose uninduced cells (Lane 1). After sonication, the intracellular fraction was loaded on GST affinity column. Then the column was washed with Tris buffer to remove the unbound proteins (Lane 9 and 10). The intensity of the protein band was observed to be reduced (Lane 9 and 10) as compared with the control (Lane 2). Lane 3 and Lane 4 represent the first and second elution of bound GST-ATBI fractions. The elution was carried out using an elution buffer containing 10 mM reduced

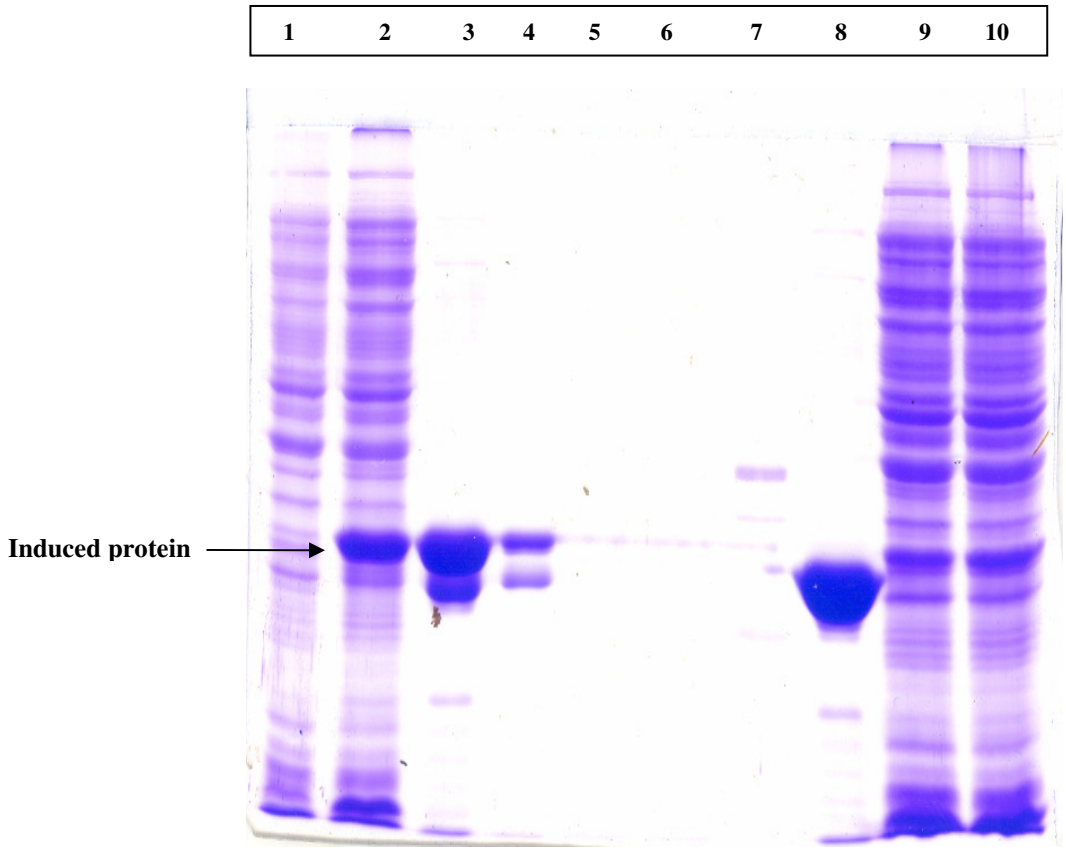

Figure 7: Lane 1-Uninduced cells, Lane 2-Induced Cells, Lane 3-GST+ATBI first elution, Lane 4-GST+ATBI second elution, Lane 5- Peptide after factor Xa cut elution 1, Lane 6- Peptide after factor Xa cut elution 2, Lane 7- Factor Xa, Lane 8- GST after Factor Xa cut and ATBI elution, Lane 9 and Lane 10 Tris Buffer wahes after binding of GST-ATBI to the column.

glutathione, 50 mM Tris- HCl, pH 8.0. The pattern of Lane 3 and 4 clearly demonstrates the purification of expressed protein from the other cellular proteins (Lane 1 and 2). Under same experimental conditions, a part of bound GST-ATBI fraction was treated with Factor Xa treatment to remove the tag and the cleaved compounds were eluted using Tris buffer. Lane 5 and 6 represents the cleaved compound from the GST tag. As the expected cleaved peptide was of a molecular weight of 1186 Da, it was not possible to detect in the 10 % SDS-PAGE analysis due to its low molecular weight but was confirmed by biological assays. Lane 7 represents a control SDS-PAGE profile of Factor Xa. After a couple of washes with Tris buffer the bound GST was eluted using elution buffer. Lane 8 represents the GST fraction in which the ATBI was removed using Factor Xa treatment prior to the elution. The band was shifted in Lane 8 in compared

with its controls such as Lane 2, 3 and 4. This is evident that it may be due to the removal of ATBI from GST-ATBI and the band shift correlates well with the molecular weight of removed ATBI.

Reverse phase HPLC

The column fractions (Lane 2, 3, 4, 5, and 6) were collected separately and the anti-pepsin activity of these fractions were evaluated. The eluted peptide fraction, which was removed from GST tag, exhibiting anti-pepsin activity was pooled (Lane 5 and 6) and concentrated by lyophilization. The other fractions (Lane 2, 3, and 4) were not showing anti-pepsin activity even though it contains ATBI. It may be due to the presence of large GST tag tailored with it. The lyophilized ATBI was loaded onto a rp-HPLC column. Figure 8 shows the rp-HPLC profile of ATBI. The peak (a) was collected manually and analyzed by mass spectrometer to confirm the molecular weight and homogeneity (Figure 9). The spectra obtained shows a peak of 1186 and which is well account for the molecular weight of recombinant peptide.

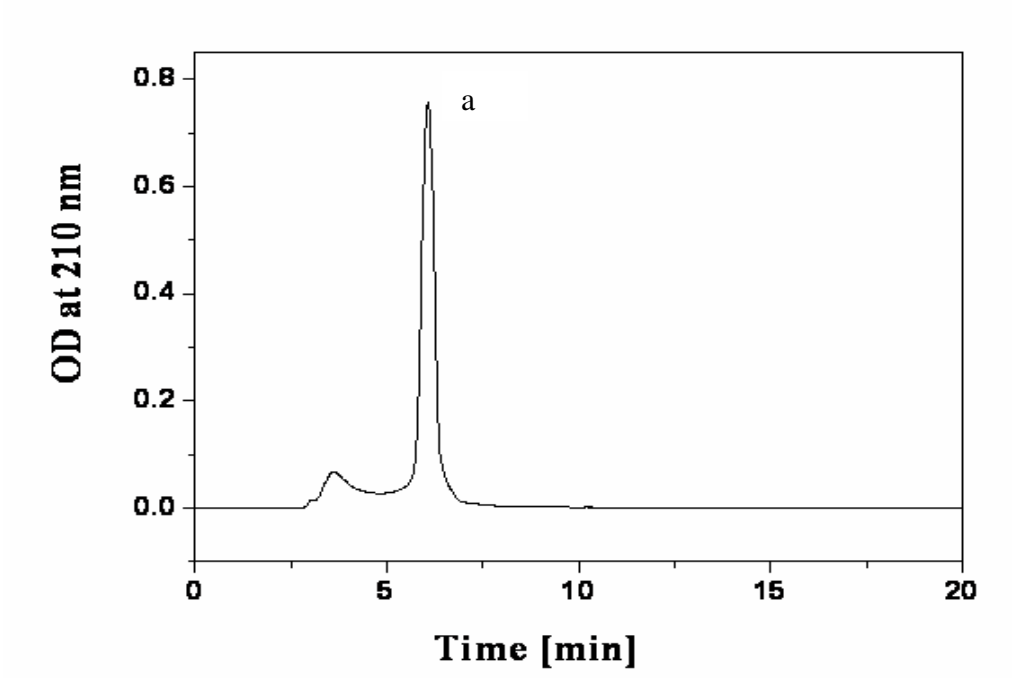

Figure 8. The rp-HPLC profile of recombinant ATBI

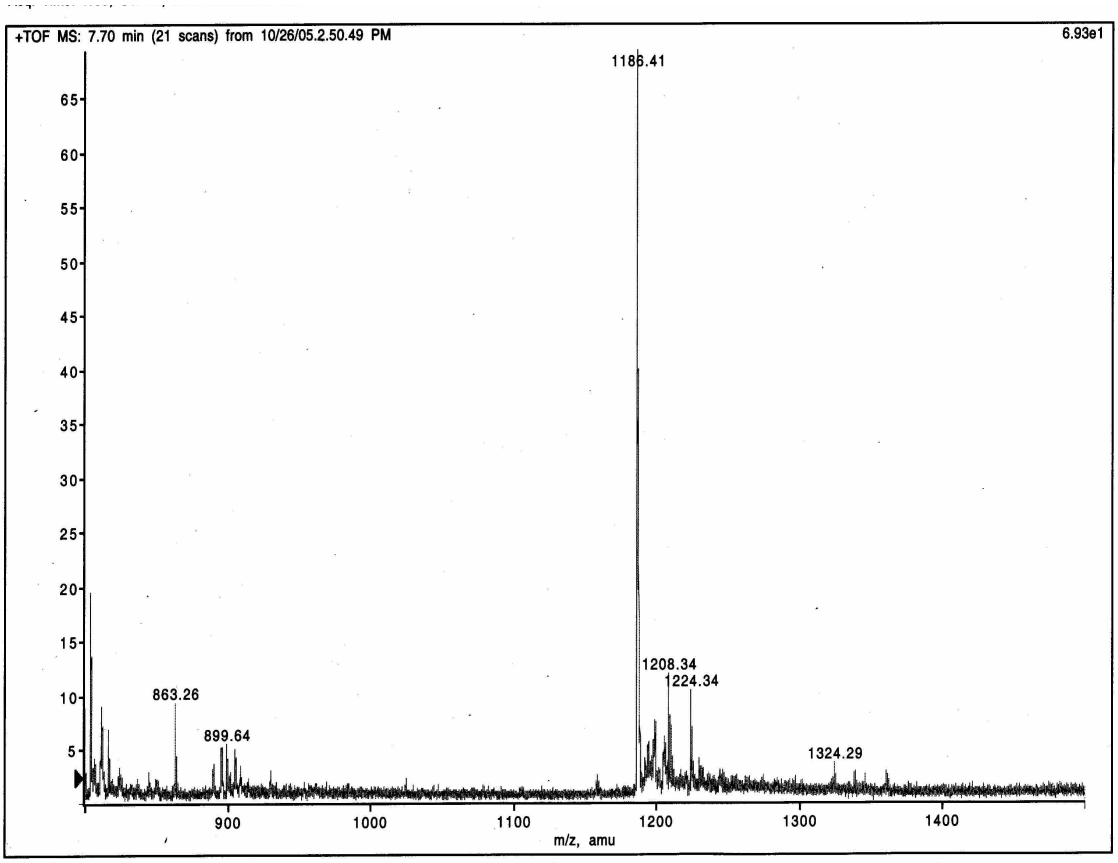

Figure 9. ESI-MS of the purified recombinant ATBI

Biological activity of the recombinant ATBI

The yield of purified inhibitor production was estimated by measuring the absorbance at 210 nm. Known concentrations of natural inhibitor were used to make the standard graph for accurate peptide quantification. The 0.2% arabinose induced inhibitor yield was ranging from 4 to 4.5 mg / L of *E. coli* culture. In case of natural peptide the yield was only 1 to 3 microgram / L of *Bacillus* sp culture. The purified recombinant peptide was tested for its inhibitory activity towards pepsin, fungal aspartic protease, recombinant HIV-1 protease and xylanase (Table 3). These results were compared with natural peptide isolated from *Bacillus* sp.

Table 3

(IC_{50} Values of ATBI)

	Natural ATBI	Recombinant ATBI
Pepsin	30 nM[1]	92 μM
Fungal aspartic protease	10 μM[1]	140 μM
HIV-1 protease	17.8 nM[2]	72 μM
Xylanase	6.5 μM	84 μM

[1] Dash et al., *Biochemistry* (2001); [2] Dash and Rao, *J. Biol. Chem* (2001)

The differences in activities between the natural and recombinant peptide may be due to the heterologous host system used for expression. When setting up a process for production of a recombinant protein, the normal approach is to first try to express the protein of interest in *E. coli*. Alternative expression systems are used only if the product is biologically inactive after production due to lack of essential post-translational modifications, incorrect folding or when the recovery of the native protein is too low (Georgiou, 1996). Parameters important for successful production of a recombinant protein in *E. coli* include transcriptional and translational efficiency, stability of the expression vector and of the transcribed mRNA, localization, proteolytic stability and folding of the gene product, as well as cell growth (Makrides, 1996; Baneyx, 1999). The observed results indicate that the recombinant peptide was active against pepsin, fungal aspartic protease, recombinant HIV-1 protease, and xylanase, however the activity was not identical to the natural peptide. The recombinant ATBI produced in *E. coli* showed decreased potency, which may be due to the lack of appropriate cellular microenvironment present in the natural host, which may be crucial for the optimal activity of the inhibitor.

CONCLUSION

The cloning of ATBI gene into *E. coli* for functional expression through gateway cloning approach has been described. The peptide sequence data of the 11-mer was exploited to synthesize the complementary oligonucleotides, which were annealed and subsequently cloned inframe with the gene for GST in to *E. coli* BL21-A1. The expression clone was induced using arabinose which expressed the recombinant peptide as a fusion protein along with GST tag for the ease of purification. The recombinant peptide was found to be active *in vitro* against HIV-1 protease, pepsin, fungal aspartic protease and xylanase. The results were not identical with the natural peptide purified from *Bacillus* sp. It may be due to the lack of lack appropriate cellular microenvironment present in the natural host. However the present results validate the use of synthetic gene of ATBI in further developing the inhibitor as a useful clinical agent as well as for sub-cloning the gene to various other host systems.

PART-2

INTACT CELL MATRIX-ASSISTED LASER DESORPTION/ IONIZATION MASS SPECTROMETRY AS A TOOL TO SCREEN DRUGS

INTRODUCTION

Protein expression can be regulated at several different levels viz. transcription, mRNA processing, mRNA turnover, and translation (Gardner et al., 1991). Currently the methods available to determine the protein expression are, by determining its activity, molecular weight, western blotting, ELISA, fluorescence imaging of GFP tagged protein or immuno histology. However, all these methods are tedious and time consuming and cannot be used for high throughput screening. The current drug discovery process relies on the availability of high quality high throughput bioassays for the selected drug target. An ideal drug discovery bioassay is one that is economic, robust, and amenable to high-throughput screening. Mass spectrometry is one such important tool that has been used extensively in the field of drug discovery. Especially, with the development of matrix assisted laser desorption / ionization (MALDI) and electrospray ionization (ESI), as well as improvements in time-of-flight mass spectrometry (TOF-MS), it has become feasible to produce and analyze gas-phase ions of biological molecules with high resolution and mass accuracy (Aebersold and Mann, 2003). Recently there has been significant research interest in the mass spectrometric analysis of whole bacterial cells called intact cell MALDI mass spectrometry (ICM-MS) to distinguish different strains of bacteria (Cain et al., 1994; Edwards-Jones et al., 2000). This technique examines the chemistry of the intact bacterial cell surface, yielding spectra consisting of a series of peaks ranging from the mass to charge ratio (m/z) of 500 to 10000 (Edwards-Jones et al., 2000). Each peak corresponds to a molecular fragment released from the cell surface during laser desorption. ICM-MS has been established for low molecular weight compounds (Erhard et al., 1997; Leenders et al., 1999; Fastner et al., 2001) and recently extended to the analysis of proteins above 20 kDa (Vaidyanathan et al., 2002). Furthermore, it was shown that the bacterial "fingerprint" profiles in the low molecular mass range obtained from ICM-MS analyses mainly originate from highly abundant intact intracellular proteins suggesting the potentiality of this method to analyze highly abundant intracellular proteins (Demirev et al., 1999; Ryzhov and Fenselau, 2001). Although, ICM-MS has a very high potential in drug discovery, its application was restricted to mainly taxonomical purpose to distinguish different microbial strains.

This study demonstrate a method with a potential for the rapid screening of drugs that regulates the protein expression, directly from an intact cell by laser desorption/ ionization, using ICM-MS. The technique described offers simple procedure for sample handling, gives specific and accurate patterns of mass spectra, and has the potential for auto sampling and the rapidity of analysis combine to meet virtually all the performance criteria required for high throughput drug screening.

MATERIALS AND METHODS

Reagents

Sinapinic acid (SA), acetonitrile (ACN), trifluoro acetic acid (TFA) were obtained from Sigma Chemicals Co., and all other chemicals used were of analytical grade.

Microorganism and growth conditions

E. coli cells expressing recombinant GST-ATBI protein were grown on LB media containing ampicillin at 37^0C. For induction of recombinant GST-ATBI, 0.2% arabinose was added. To study the regulation of GST-ATBI expression, 0.02% and 2% of glucose was added in combination with arabinose. When *E. coli* is grown in a medium containing glucose, an alternative carbon source, induction of the ***ara*** operon and utilization of the arabinose were delayed until the glucose has been consumed. Protein extraction was done by lysing the *E. coli* cells, and then separated under denaturing condition using 10% SDS- PAGE.

Sample preparation for MALDI analysis

Cells were carefully harvested to a sterile plastic tube and washed with deionized water. A final concentration of 10^6 cells was spotted on stainless steel plate, mixed with sinapinic acid (10mg /ml) prepared in 30% ACN containing 0.2 % TFA, by dried droplet method.

MALDI-TOF analysis

Mass spectral analysis was done on Voyager-De-STR (Applied Biosystems) MALDI-TOF. A nitrogen laser (337nm) was used for desorption and ionization. Spectra were acquired in the range of 10 kDa to 100 kDa, on linear mode with delayed ion extraction and with an accelerating voltage of 25kV. Low mass ion gate was set to 4500 Da. All the analysis was done in four replications. The instrument was calibrated with myoglobulin and bovine serum albumin.

Affinity purification of recombinant GST-ATBI protein

Recombinant GST-ATBI protein was purified by a single-step affinity purification using Glutathione Sepharose 4B affinity column from arabinose induced *E. coli* cells according to Amersham Biosciences Instructions Manual, Code No. 17-0757-01. The molecular weight of the purified protein was analyzed by MALDI analysis using sinapinic acid as matrix.

RESULTS AND DISCUSSION

ICM-MS approach has been used for rapid identification and characterization of clinically important microorganisms, including bacteria (Claydon et al., 1996; Holland et al., 1996; Krishnamurthy et al., 1996), fungi (Welham et al., 2000; Amiri-Eliasi and Fenselau, 2001), viruses (Kim et al., 2001) and spores (Ryzhov et al., 2000; Li et al., 2000; Elhanany et al., 2001; Dickinson et al., 2001). However, most of the studies were restricted to analysis of mass below 20000 Da, only few investigations report the detection of high mass signals by ICM-MS. Madonna et al., reported the use of ethanol application to sample spot to improve the signal content and detect high mass signals above 15 kDa (Madonna et al., 2000). Winkler et al., detected signals up to 60 kDa using *Campylobacter* and *Helicobacter* strains, but the high mass signals were less stable and lost within 1h of sample preparation (Winkler et al., 1999). Vaidyanathan et al., demonstrated ICM-MS analysis of the high molecular weight proteins above 20 kDa by employing different spotting techniques (Vaidyanathan et al., 2002).

This study demonstrates that ICM-MS can be used to study the regulation of protein expression. Furthermore it is also demonstrate that this technique can be used to screen the drugs that regulate the gene expression using *E. coli* cells expressing a recombinant GST-ATBI protein under the control of arabinose inducible promoter. The *ara* promoter is one of the well studied promoter in *E. coli* and is a classical example of gene regulation. It regulates the synthesis of the three enzymes such as arabinose isomerase, ribulokinase and ribulose-5-phosphate epimerase, which are required to catalyze the metabolism of arabinose (Gardner et al., 1991). These three structural genes are expressed only in presence of arabinose. Addition of glucose decreases the expression of these genes (Gardner et al., 1991). Using *ara* promoter, the regulation of a recombinant GST-ATBI protein expression was demonstrated in *E. coli* cells by ICM-MS.

As expected, the ICM-MS analysis showed a 28 kDa protein with highest intensity upon addition of 0.2% arabinose showing that the promoter gets activated in presence of arabinose that led to expression of its downstream gene, a recombinant 28 kDa GST – ATBI protein (Figure. 1). Only arabinose induced cells showed the induction of a 28

kDa recombinant GST-ATBI protein peak on MALDI analysis (Figure 1, spectra A), while the non-induced cells did not show the 28 kDa peak (Figure 1, spectra B).

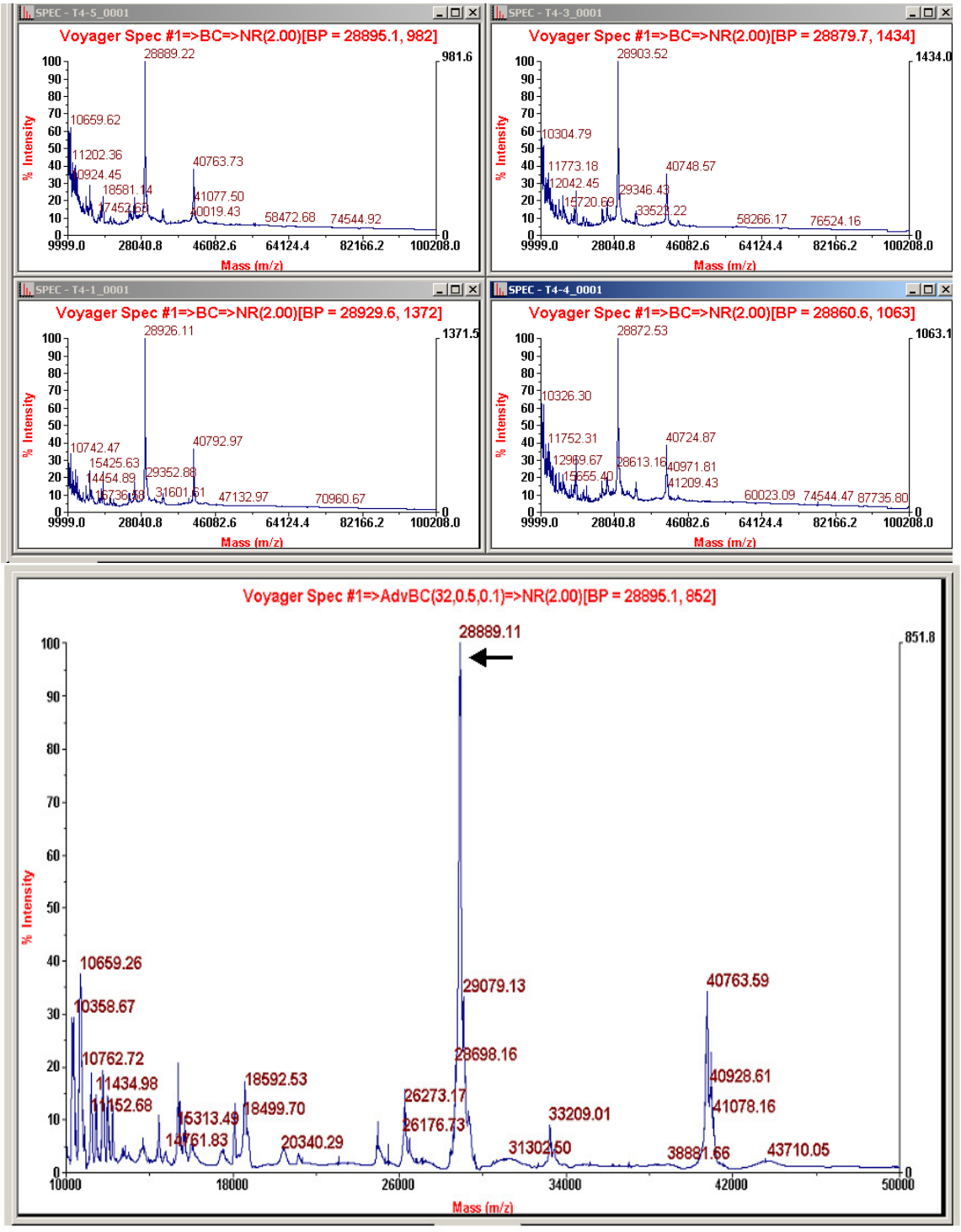

Figure 1. A. ICM-MS analysis of *E coli* cells expressing a recombinant GST-ATBI induced with 0.2% arabinose.

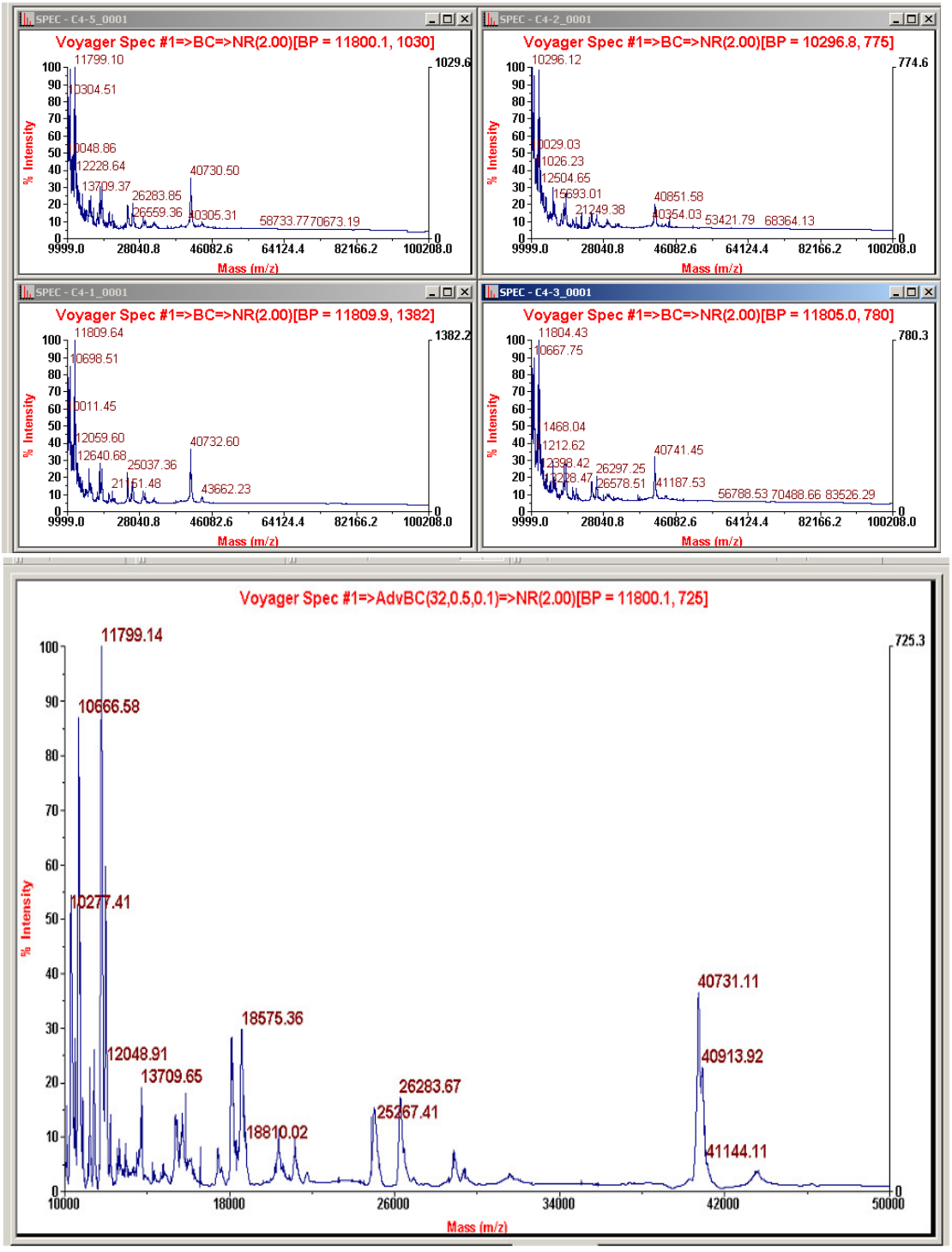

Figure 1. B. ICM-MS analysis of *E coli* cells as a control (without arabinose induction)

The SDS-PAGE analysis also showed a 28 kDa protein band only in the *E. coli* cells induced with 0.2% arabinose (Figure 3, lane 2) whereas the non–induced cells did not show the 28 kDa band (Figure 3, lane 1). The *ara* promoter is activated by arabinose and repressed by glucose. Therefore, to study the regulation of recombinant GST-ATBI expression by ICM-MS, *E. coli* cells were grown in presence or absence of 0.2% arabinose, and in combination with or without glucose. Addition of 0.02% glucose reduced the expression of GST-ATBI protein, as the intensity of the GST-ATBI peak decreased in ICM-MS, (Figure 2, spectra A). Increasing glucose to 2% increased the repression effect of GST-ATBI synthesis, with a further decrease in intensity of GST-ATBI peak in ICM-MS analysis (Figure 2, spectra B). There was no induction of GST-ATBI expression by addition of only 2% glucose (Figure 2, spectra C). Similar trend in the intensity of recombinant GST-ATBI protein bands were obtained on SDS-PAGE analysis (Figure. 3, lane 3 to lane 5) and showed good correlation with ICM-MS data. Addition of glucose repressed the GST-ATBI expression, which is well studied phenomenon in bacteria called catobolite repression or glucose effect (Gardner et al., 1991).

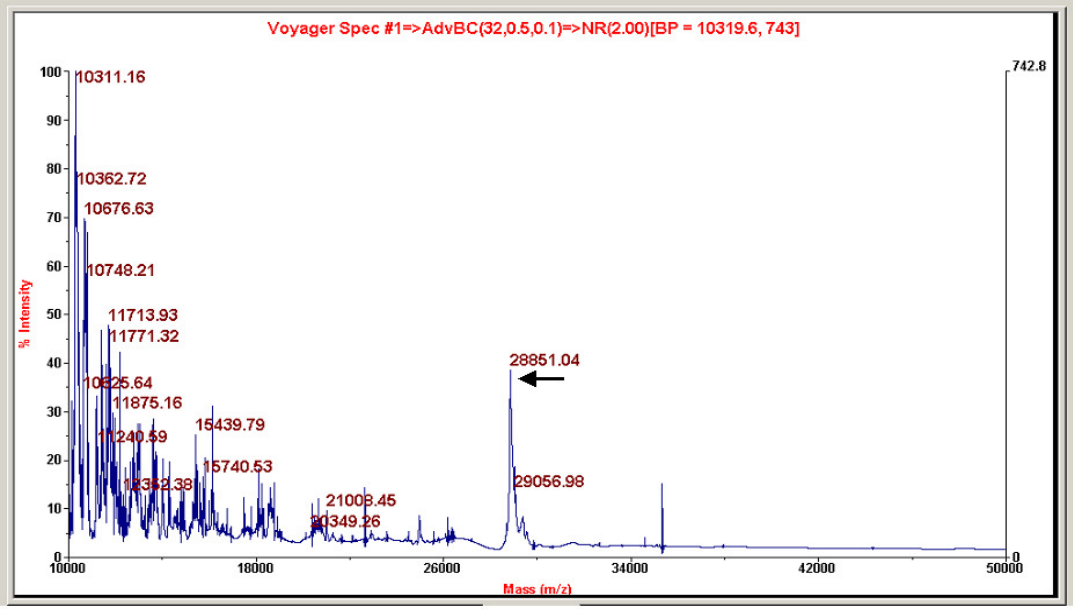

Figure 2. A. ICM-MS analysis of *E coli* cells expressing a recombinant GST-ATBI grown in 0.2% arabinose and 0.02 % glucose

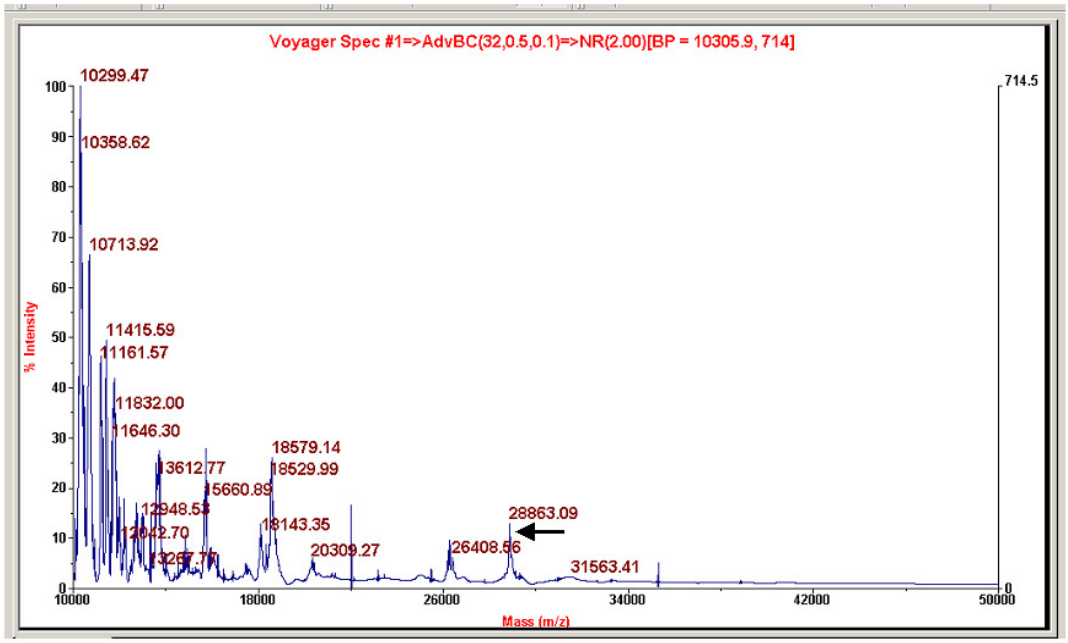

Figure 2. B. ICM-MS analysis of *E coli* cells expressing a recombinant GST-ATBI grown in 0.2% arabinose and 2 % glucose

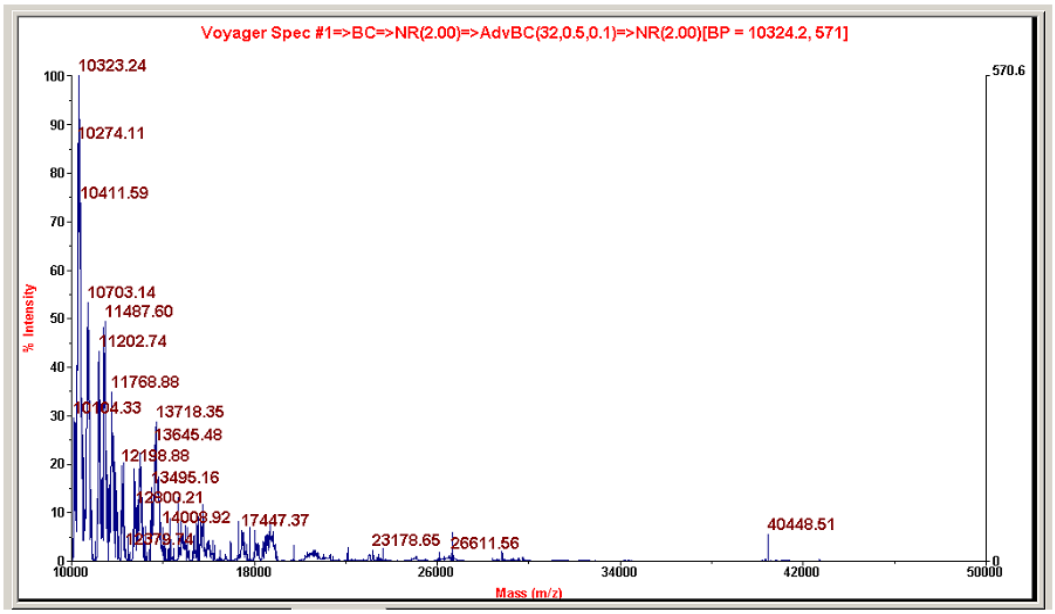

Figure 2. C. ICM-MS analysis of *E coli* cells expressing a recombinant GST-ATBI grown in 2 % glucose

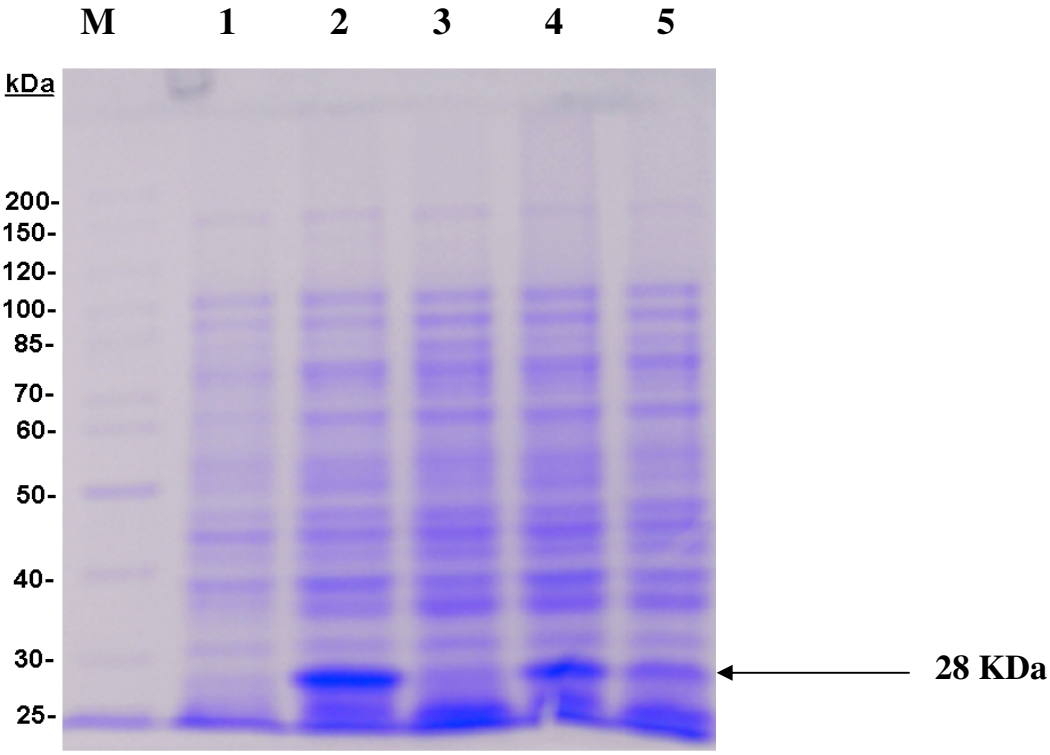

Figure 3. SDS-PAGE analysis of a 28 kDa recombinant GST-ATBI protein from *E coli* cells. Lane M- 25-200 KDa protein ladder. Lane 1, un induced *E coli* cells, Lane 2, cells were induced with 0.2% arabinose, Lane 3, induced with 2% glucose, Lane 4, Induced 0.2% Arabinose+0.02%glucose, Lane 5, Induced 0.2% Arabinose+ 2% glucose

Furthermore, the identity of arabinose induced 28 kDa proteins as GST-ATBI protein was confirmed by affinity purification using Glutathione Sepharose 4B affinity column. It has been designed for rapid single step purification of a recombinant GST proteins. The recombinant GST-ATBI protein purified from arabinose induced *E. coli* cells was found to be 28 kDa by MALDI analysis, suggesting that the arabinose induced 28 kDa protein is indeed recombinant GST-ATBI protein (Figure 4).

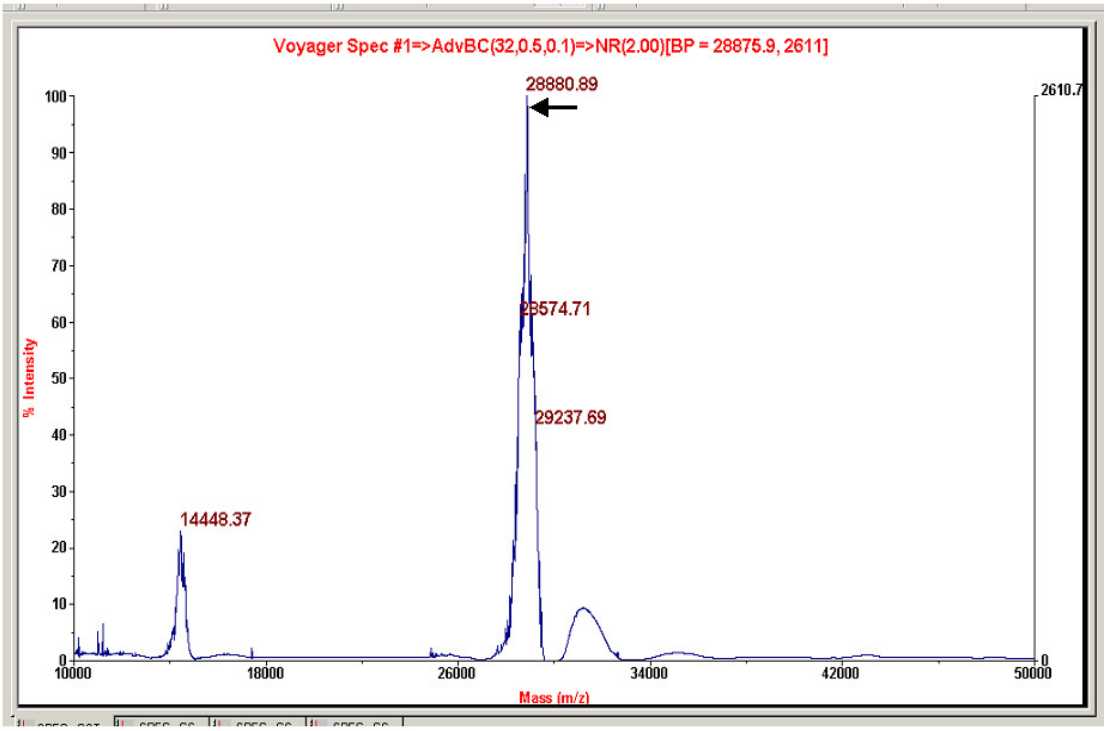

Figure 4. MALDI analysis of affinity purified recombinant GST-ATBI protein from 0.2% arabinose induced *E coli* cells

This technique has got a tremendous potential in pharmaceutical industries to screen the drugs that regulate the protein expression. Currently the methods available to assay the protein expression are tedious and time consuming, and therefore will be difficult to screen large number of combinatorial compounds. However the major limitation of this assay is the protein has to be present in abundance. With the existing limitation also, the assay has a potential for studying the regulation of proteins in some of the cell lines where the protein is over expressed. For example mammalian cell line A431, which overexpresses a 170 kD EGF receptor (Gulli et al., 1996), may be used to screen the drugs that affects its expression. Analysis of a high molecular weight protein by MALDI-TOF may be a slightly difficult task, however, with good sample preparation it should be possible to analyze high molecular weight proteins. Vaidyanathan et al., have demonstrated the use of this technique to measure the molecular weight of protein as high as 158 kDa in *Bacillus sphaericus* (Vaidyanathan et al., 2002), which is almost close to 170 kDa. Similarly there are several yeast cell lines overexpressing heterologus GPCRs

are available (Ladds et al., 2005). GPCRs upon ligand binding gets hyperphosphorylated, ubiquitinated and internalized (Ladds et al., 2005). Therefore, this assay can be used not only to screen the drugs that affect the protein expression but also to screen the drugs that affect protein conformation, internalization, translocation, etc. There are as many as 300 low molecular weight receptor proteins integral to the cell membrane in the mass range of 10 to 40 kDa listed in the Human Protein Resource Database which may perhaps be easier to analyze by ICM-MS (Available: www.hprd.org.). Very recently Schallar et al., have used ICM-MS for rapid typing of *Moraxella catarrhalis* subpopulations based on outer membrane proteins (Schaller et al., 2006). Therefore, it is possible to extend this technique to analyze the cell surface receptors such as EGFR, VEGFR, GPCRs, which are important drug targets of cancer.

It was believed that the ICM-MS analysis may be more useful to study the regulation of cell surface receptor than the intracellular proteins, as this technique relies on the chemistry of cell surface proteins. However, studies carried out by Demirey et al., and Ryzhoy and Fenselau, showed the low molecular mass range obtained from ICM-MS analyses mainly originate from highly abundant intact intracellular proteins (Demirey et al., 1999; Ryzhoy and Fenselau, 2001). The present study with intracellular recombinant GST-ATBI protein further strengthen the fact that this technique cane be used not only to study the regulation of cell surface proteins but also even intracellular protein can be studied. With the availability of this technique it would be possible to screen large number of drugs that regulate the protein expression.

CONCLUSION

The potential use of ICM-MS for screening the drugs that regulate protein expression in an intact cell using *E. coli* cells expressing recombinant glutathione-S-transferase-peptidic inhibitor as a model system has been demonstrated. Using ICM-MS analysis, a 28 kDa peak corresponding to the production of recombinant GST-ATBI under arabinose induced condition has been detected. The regulation of protein expression was studied using glucose as an alternative metabolite. All these results obtained from ICM-MS data were validated using SDS-PAGE analysis. The simple sample handling requirements, short analysis time and the specific and accurate mass spectrum suggests the possibility for using the technique in biomedical applications especially in drug discovery.

REFERENCES

Abu-Erreish, G. B., and Peanasky, R. J. (1974) *J. Biol. Chem.* **249**, 1558-1565.

Aebersold, R., and Mann, M.(2003) *Nature* **422**, 198-207.

Amiri-Eliasi, B., and Fenselau, C. (2001) *Anal Chem.***73**, 5228-5231.

Baneyx, F. (1999) *Curr. Opin. Biotechnol.* **10**, 411–421.

Bernard, P., and Couturier, M. (1992) *J. Mol. Biol.* **234**, 534-541.

Boyd, A.C. (1993) *Nucleic Acids Res.* **21**, 817–821.

Brandwijk, R. J. M. G. E., Nesmelova, I., Dings, R. P. M., Mayo, K. H., Thijssen, V. L. J. L., and Griffioen, A. J. (2005) *Biochem. Biophys. Res. Commun.* **333**, 1261-1268.

Bubeck, P., Winkler, M., and Bautsch, W. (1993) *Nucleic Acids Res.* **21**, 3601–3602.

Cain, T. C., Lubman, D.M., and Weber, W. J. (1994) *Rapid Commun Mass Spectrom.* **8**, 1026-1030.

Callaway, J.E., Lai, J., Haselbeck, B., Baltaian, M., Bonnesen, S. P., Weickmann, J., Wilcox, G., and Lei, S. P. (1993) *Antimicrob. Agents Chemother.* **37**, 1614–1619.

Carter, P. (1990) in Protein Purification: *From Molecular Mechanisms to Large-Scale Processes.* Ladish, M. R., Willson, C.-D., Painton, C.-D. C. and Builder, S. E., (Eds.), American Chemical Society, Washington, pp. 181–193.

Cater, S. A., Lees, W. E., Hill, J., Brzin, J., Kay, J., and Phylip, L. H. (2002) *Biochimica et Biophysica Acta.* **1596**, 76-82.

Chang, J.Y. (1985) *Eur. J. Biochem.* **151**, 217–224.

Christeller, J. T., Farley, P. C., Ramsay, R. J., Sullivan, P. A., and Laing, W. A. (1998) *Eur. J. Biochem.* **254**, 160-167.

Claydon, M. A., Davey, S. N., Edwards, J. V., and Gordon, D. B. (1996) *Nat Biotechnol.* **14,** 1584-1586.

Cronan, J. E. (1990) *J. Biol. Chem.* **265**, 10327–10333.

Dale, G. E., Broger, C., Langen, H., D'Arcy, A. and Stuber, D. (1994) *Protein Eng.* **7**, 933–939.

Dash C., Ahmad, A., Nath, D., and Rao, M. (2001a) *Antimicrob. Agents Chemother.* **45**, 2008-20117.

Dash, C., and Rao, M. (2001) *J. Biol. Chem.* **276**, 2487-2493.

Dash, C., Phadtare, S., Deshpande, V., and Rao, M. (2001b) *Biochemistry* **40**, 11525-11532.

Degryse, E. (1996) *Gene.* **170**, 45–50.

Demirev, P. A., Ho, Y.P., Ryzhov, V., and Fenselau, C. (1999) *Anal Chem.* **71,** 2732-2738.

di Guan, C., Li, P., Riggs, P. D. and Inouye, H. (1988) *Gene.* **67**, 21–30

Dickinson, D. N., La Duc, M. T., Haskins, W.E., Gornushkin, I, Wineforder, J. D., Powell, D. H., and Venkateswaran, K. (2004) *Appl Environ Microbiol* . **70,** 475-482.

Dykes, C.W., Bookless, A.B., Coomber, B.A., Noble, S.A., Humber, D.C., and Hobden, A.N. (1988) *Eur. J. Biochem.* **174**, 411–416.

Edwards-Jones, V., Claydon, M. A., Evason, D. J., Walker, J., Fox, A. J., and Gordon, D. B. (2000) *J Med Microbiol*. **49**, 295-300.

Elhanany, E., Barak, R., Fisher, M., Kobiler, D., and Altboum, Z. (2001) *Rapid Commun Mass Spectrom.* **15,** 2110-2116.

Erhard, M., von Dohren, H., and Jungblut, P. (1997) *Nat Biotechnol.* **15**, 906-909.

Fastner, J., Erhard, M., and von Dohren, H. (2001) *Appl Environ Microbiol.* **67,** 5069-5076.

Forsberg, G., Baastrup, B., Brobjer, M., Lake, M., Jornvall, H., Hartmanis, M. (1989) *Biofactors.* **2**, 105–112.

Forsberg, G., Brobjer, M., Holmgren, E., Bergdahl, K., Persson, P., Gautvik, K. M. and Hartmanis, M. (1991) *J. Protein. Chem.***10**, 517–526.

Galleschi, L., Friggeri, M., Repiccioli, R., and Come, D. (1993) In *Proceed. Fourth Int. Workshop Seeds*, Angers, France. 207-211.

Gardner, E. J., Simmons, M. J., and Peter, S. D. (1991) In Chapter 14 In: *Principles of Genetics* 8th Ed. John Willey and Sons. 390.

Gavit, P., and Better, M. (2000) *J. Biotech.* **79**, 127-136.

Georgiou, G. (1996) in Protein engineering: *Principles and Practice*. Cleland, J. L., and Craik, C. S. (Eds.), Wiley-Liss, New York, pp. 101–127.

Gram, H., Ramage, P., Memmert, K., Gamse, R., Kocher, H.P. (1994) *Bio:Technology* **12**, 1017–1023.

Graslund, T., Nilsson, J., Lindberg, A. M., Uhlen, M. and Nygren, P. A . (1997) *Protein Expression Purif.* **9**, 125–132

Gulli, L. F., Palmer, K. C., Chen, Y. Q., and Reddy, K. B. (1996) *Cell Growth Differ*. **7,** 173-178.

Hartley, J. L., Temple, G. F., and Brasch, M. A. (2000) *Genome Res.* **10**, 1788– 1795.

Haught, C., Davis, G.D., Subramanian, R., Jackson, K.W., Harrison, R.G. (1998) *Biotechnol. Bioeng*. **57**, 55–61.

Holland, R.D., Wilkes, J. G., Rafii, F., Sutherland, J. B., Persons, C. C., Voorhees, K. J., and Lay, J. O. (1996) *Rapid Commun Mass Spectrom*. **10,** 1227-1232.

Hopp, T. H., Prickett, K. S., Price, V. L., Libby, R. T., March, C. J., Cerretti, D. P., Urdal, D. L., and Conlon, P. J. (1988) *Bio/Technology* **6**, 1204–1210.

Howell, M. L., and Blumenthal, K. M. (1989) *J. Biol. Chem.* **264**, 15268-15273.

Itakura, K., Hirose, T., Crea, R., Riggs, A. D., Heyneker, H. L., Bolivar, F., and Boyer, H. W. (1977) *Science.* **198**, 1056–1063.

James, M. N. G. (1998) *Aspartic proteinases: Retroviral and cellular enzymes.* Plenum Press. NY, 1-499.

Jonasson, P., Liljeqvist, S., Nygren, P-A., and Stahl, S. (2002) *Biotechnol. Appl. Biochem.* **35**, 91-105.

Jonasson, P., Liljeqvist, S., Nygren, P-A., and Stahl, S. (2002) *Biotechnol. Appl. Biochem.* **35**, 91-105.

Kageyama, T. (1998) *Eur. J. Biochem.* **253**, 804-809.

Keilova, H., and Tomasek, V. (1976) *Collect. Czech. Chem. Commun.* **41**, 487-497.

Kelly, W. S. (1996) *Bio/Technology* **14**, 28-31.

Kim, Y. J., Freas, A., and Fenselau, C. (2001) *Anal Chem.* **73**, 1544-1548.

Knott, J.A., Sullivan, C.A., and Weston, A. (1988) *Eur. J. Biochem.* **174**, 405–410.

Krishnamurthy, T., Ross, P. L., and Rajamani, U. (1996) *Rapid Commun Mass Spectrom*. **10**, 883-888.

La Vallie, E. R., McCoy, J. M., Smith, D. B., and Riggs, P. (1994) In: *Current Protocols in Molecular Biology*. Ausubel, F. M., Brent, R., Kingston, R. E., Moore, D. D., Seidman, J. G., Smith, J. A. and Struhl, K., (Eds.), John Wiley and Sons, New York, pp. 16.4.5–16.4.17.

Ladds, G., Goddard, A., and Davey, J. (2005) *Trends Biotech.* **23**, 367-373.

Lafontaine, D. and Tollervey, D. (1996) *Nucleic Acids Res.* **24**, 3469–3471.

Landy, A. (1989) *Ann. Rev. Biochem.* **58**, 913–949.

Lee, J.H., Minn, I., Park, C., and Kim, S.C. (1998) *Protein Exp. Purif.* **12**, 53–60.

Leenders, F., Stein, T. H., Kablitz, B., Franke, P., and Vater, J. (1999) *Rapid Commun Mass Spectrom* . **13,** 943- 949.

Lenarcic, B., and Turk, V. (1999) *J. Biol. Chem.* **276**, 2023-2030.

Li, M., Li, L-Y., Wu, X., and Liang, S-P.(2000) *Toxocon.* **38**, 153-162.

Li, T. Y., Liu, B. H., and Chen, Y. C. (2000) *Rapid Commun Mass Spectrom.* **14**, 2393-2400.

Lilie, H., Schwarz, E. and Rudolph, R. (1998) *Curr. Opin. Biotechnol.* **9**, 497–501.

Liu, Q., Li, M.Z., Leibham, D., Cortez, D., and Elledge, S.J. (1998) *Curr. Biol.* **8**, 1300–1309.

Luckow, V.A., Lee, S.C., Barry, G.F., and Olins, P.O. (1993) *J. Virol.* **67**, 4566–4579.

Madonna, A. J., Basile, F., Ferrer, I., Meetani, A. A., Rees, J. C., and Voorhees, K. J. (2000) *Rapid Commun Mass Spectrom.* **14**: 2220-2229.

Maere, V. D., Vercauteran, I., Gevaert, K., Vercruysse, J., and Claerebout, E. (2005) *Mol. Biochem. Parasitol.* **141**, 81-88.

Maganja, D. B., Strukelj, B., Pungercar, J., Gubensek, F., Turk, V., and Kregar, I. (1992) *Plant Mol. Biol.* **20**, 311-313.

Maina, C. V., Riggs, P. D., Grandea, A. G.d., Slatko, B. E., Moran, L. S., Tagliamonte, J. A., McReynolds, L. A. and Guan, C. D. (1988) *Gene*. **74**, 365–373.

Makrides, S. C. (1996) *Microbiol. Rev.* **60**, 512–538.

Marcus, F. (1985) *Int. J. Pept. Protein Res.* **25**, 542–546.

Mares, M., Meloun, B., Pavlik, M., Kostka, V., and Baudys, M. (1989) *FEBS Lett.* **251**, 94-98.

Martzen, M. R., McMullen, B. A., Smith, N. E., Fujikawa, K., and Peanasky, R. J. (1990) *Biochemistry* **29**, 7366-7372.

Moks, T., Abrahmsen, L., Oesterlof, B., Josephson, S., Oestling, M., Enfors, S. O., Persson, I., Nilsson, B., and Uhlen, M. (1987) *Bio/ Technology* **5**, 379–382.

Murby, M., Samuelsson, E., Nguyen, T. N., Mignard, L., Power, U., Binz, H., Uhlen, M., and Stahl, S. (1995) *Eur. J. Biochem.* **230**, 38–44.

Ng, K. K. S., Petersen, J. F. W., Cherney, M. M., Garen, C., Zalatoris, J. J., Rao-Naik, C., Dunn, B. M., Martzen, M. R., Peanasky, R. J., and James, M. N. G. (2000) *Nat. Struct. Biol.* **7**, 653-657.

Nilsson, B., and Abrahmsen, L. (1990) *Methods Enzymol.* **185**, 144–161.

Nilsson, B., Forsberg, G., and Hartmanis, M. (1991) *Methods Enzymol.* **198**, 3–16.

Nilsson, B., Moks, T., Jansson, B., Abrahmsen, L., Elmblad, A., Holmgren, E., Henrichson, C., Jones, T. A., and Uhlen, M. (1987) *Protein Eng.* **1**, 107–113.

Nilsson, J., Stahl, S., Lundeberg, J., Uhlen, M., and Nygren, P.A .(1997) *Protein Expr. Purif.* **11**, 1–16.

Nygren, P. A ., Eliasson, M., Palmcrantz, E., Abrahmsen, L., and Uhlen, M. (1988) *J. Mol. Recognit.* **1**, 69–74.

Nygren, P.A., Stahl, S. and Uhlen, M. (1994) *Trends Biotechnol.* **12**, 184–188.

Oliner, J. D., Kinzler, K. W., and Vogelstein, B. (1993) *Nucleic Acids Res.* **21**, 5192–5197.

Parks, T. D., Leuther, K. K., Howard, E. D., Johnson, S. A. and Dougherty, W. G. (1994) *Anal. Biochem.* **216**, 413–417.

Peakman, T.C., Harris, R.A., and Gewert, D.R. (1992) *Nucleic Acids Res.* **20**, 495–500.

Phylip, L. H., Lees, W. E., Brownsey, B. G., Bur, D., Dunn, B. M., Winther, J.R., Gustchina, A., Li, M., Copeland, T., Wlodawer, A., and Kay, J. (2001) *J. Biol. Chem.* **276**, 2023-2030.

Phylip, L. H., Richards, A. D., Kay, J., Konvolinka, J., Strap, P., Blaha, I., Velek, J., Kostka, V., Ritchia, A. J., Farmerie, W. G., Scarborough, P. E., and Dunn, B. M. (1990) *Biochem. Biophys. Res. Com.* **171**, 439-444.

Piers, K.L., Brown, M.H., and Hancock, R.E.W. (1993) *Gene.* **134**, 7–13.

Pohlner, J., Kramer, J. and Meyer, T. F. (1993) *Gene.* **130**, 121–126.

Porath, J. (1992) *Protein Expression Purif.* **3**, 263–281.

Porath, J., Carlsson, J.,Olsson, I., and Belfrage, G. (1975) *Nature* (London) **258**, 598–599.

Richards, A. D., Phylip, L. H., Farmerie, W. G., Scarborough, P. E., Alvarez, A., Dunn, B. M., Hirel, P., Pavlickova, L. A., Kostka, V., and Kay, J. (1990) *J. Biol. Chem.* **265**, 7733-7736

Ritonja, A., Krizaj, I., Mesko, P., Kopitar, M., Lucovnik, P., Strukelj, B., Pungercar, J., Buttle, D. J., Barrett, A. J., and Turk, V. (1990) *FEBS Lett.* **267**, 13-15.

Rudolph, R. (1996) In *Protein Engineering: Principles and Practice*. Cleland, J. L., and Craik, C. S. (Eds.), Wiley-Liss, New York. pp. 283–298.

Ryzhov, V., and Fenselau, C. (2001) *Anal Chem.* **73,** 746-750.

Ryzhov, V., Hathout, Y., and Fenselau, C. (2000) *Appl Environ Microbiol*. **66,** 3828-3834.

Schaller, A., Troller, R., Molina, D., Gallati, S., Aebi, C., Stutzmann, M. P. (2006) *Proteomics.* **6**, 172-180.

Schatz, P. J. (1993) *Bio/Technology.* **11**, 1138–1143.

Schein, C. H. (1993) *Curr. Opin. Biotechnol*. **4**, 456–461.

Schu, P., and Wolf, D. H. (1991) *FEBS Lett.* **283**, 78-84.

Smith, D. B., and Johnson, K. S. (1988) *Gene.* **67**, 31-40.

Stahl, S., Nilsson, J., Hober, S., Uhlen, M. and Nygren, P.A. (1999) In: *The Encyclopedia of Bioprocess Technology: Fermentation, Biocatalysis and Bioseparation.* Flickinger, M. C., and Drew, S. W. (Eds.), John Wiley and Sons, New York, pp. 49–63.

Stevens, R. C. (2000) *Structure*. **8**, R177–R185.

Stewart, K., Goldman, R. C., and Abad-Zapatero, C. (1999) *The secreted proteinases from Candida: challenges for structure aided drug design.* In: Proteases of infectious agents. Dunn, B. M. (Ed) Academic Press, San Diego, CA, 117-138.

Storck, T., Kruth, U., Kolhekar, R., Sprengel, R., and Seeburg, P.H. (1996) *Nucleic Acids Res.* **24**, 4594–4596.

Strukelj, B., Pungercar, J., Mesko, P., Barlic-Maganja, D., Gubensek, F., Kregar, I., and Turk, V. (1992) *Biol. Chem.* **373**, 477-482.

Strukelj, B., Ravnikar, M., Mesko, P., Poljsak-Prijatelj, M., Pungercar, J., Kopitar, G., Kregar, I. & Turk, V. (1995) *Adv. Exp. Med. Biol.* **362**, 293-298.

Uhlen, M., Nilsson, B., Guss, B., Lindberg, M., Gatenbeck, S. and Philipson, L. (1983) *Gene.* **23**, 369–378.

Umezawa, H., Aoyagi, T., Morishima, H., Hamed, M., and Takeuchi, T. (1970) *J. Antibiot.* **23**, 259-253.

Vaidyanathan, S., Winder, C. L., Wade, S. C., Kell, D. B., and Goodacre, R. (2002) *Rapid Commun Mass Spectrom.* **16,** 1276-1286.

Valler,M. J., Kay, J., Aoyagi, T. & Dunn, B. M. (1985) *J. Enzyme Inhib.* **1**, 77-82.

Walker, P. A., Leong, L. E., Ng, P. W., Tan, S. H., Waller, S., Murphy, D., and Porter, A. G. (1994) *Bio/Technology.* **12**, 601–605.

Weickert, M. J., Doherty, D. H., Best, E. A., and Olins, P. O. (1996) *Curr. Opin. Biotechnol.* **7**, 494–499.

Welham, K. J., Domin, M. A., Johnson, K., Jones, L., and Ashton, D. S. (2000) *Rapid Commun Mass Spectrom*. **14,** 307-310.

Winkler, M. A., Uher, J., and Cepa, S. (1999) *Anal Chem*. **71,** 3416-3419.

Zhang, Y., Buchholz, F., Muyrers, J.P., and Stewart, A.F. (1998) *Nat. Genet.* **20**, 123–128.

CHAPTER-5

DEVELOPMENT OF GOLD NANOPARTICLE BASED BIOCONJUGATES USING FUNGAL ASPARTIC PROTEASE

INTRODUCTION

Nanotechnology

The origin of nanotechnology may be traced back to in Eric Drexler's publication, which contained a single table wherein the common devices of everyday technology were related to a biological counter part, invariably a protein molecule. Drexler compared cables and collagens, drive shafts and bacterial flagella, containers and vesicles, pipes and tubular structures, and linked glue to intermolecular forces (Drexler, 1981). Based on fundamental chemistry and physics, nanotechnology have developed over the past three decades into today's powerful disciplines, which allow the engineering of advanced technical devices and the industrial production of active substances for pharmaceutical and biomedical applications. Nanotechnology describes the creation and utilization of functional materials, devices and systems with novel functions and properties that are based either on geometrical size or on material-specific peculiarities of nano-structures. It is an area of technology where dimensions and tolerances in the range of 0.1nm to 100nm play a critical role. Generally, the nanoscale is defined from 1 to 100 nm, whereas the range from 100 to 1000 nm is named the sub micrometer scale. The nanoparticles have highly interesting optical, electronic, and catalytic properties, which are very different from those of the corresponding bulk material and which often depend strongly on the particle's size in a highly predictable way. Much of the nanotechnology is concerned with understanding the properties of materials at the nanoscale and the effect decreasing the size of materials or the structure components of materials. Nanotechnology is truly interdisciplinary, with an understanding of the physics and chemistry of matter and processes at the nanoscale being relevant to all scientific disciplines, from chemistry and physics to biology, engineering and medicine.

Nano-biotechnology

Biological sciences have taken the quickest advantage of advances in nanotechnology and developed into a highly interdisciplinary area namely 'Nano-biotechnology', a fusion of the two most glamorous prefixes in science today. Bioorganic and bioinorganic chemistry are the interdisciplinary fields that provide the basis for joining biotechnology with nanotechnology. Bioorganic model systems have long been elaborated to provide

tools for probing the mechanisms of biological principles, as well as to develop chemical means for the handling and manipulating the biological components (Dugas, 1989; Diederichsen et al., 1999). Analogously to the interactions that are abundant in many reaction centers of enzyme between the amino acid side chains and the metal centers, the interaction between organic ligands and the surface of an inorganic nanoparticle paves the way for the coupling of biomolecular recognition systems to generate novel materials. Such biomaterials have numerous applications in the area of biotechnology and biomedical applications (Rembaum and Dreyer., 1980; Wilchek and Bayer, 1990; Tischer and Wedikind, 1999). The introduction of nanotechnology in gene therapy, drug delivery, hormone therapy, magnetic imaging and vaccination is revolutionizing in the field of biomedicine. Conventional drug delivery systems face the problems like limited ability to reach the target tissue, selectivity of the target, lack of natural mimics in hormone therapies, metabolic stability, delivery of water insoluble compounds, etc. Throughout the world today, numerous researchers are exploring the potential use of nanoparticles as carriers for a wide range of drugs for therapeutic applications, especially in the area of cancer therapy and controlled delivery of drugs.

Bio-nanotechnology

Bio-nanotechnology is concerned with the molecular scale properties and applications of biological nanostructures. Bio-nanotechnology comes at the interface between the chemical, biological and physical sciences. The most complex and highly functional nanoscale machines known till date are the naturally occurring molecular assemblies that regulate and control the biological systems. Some of the examples include actin network, kinesin motor, dynein motor, myosin motor, DNA helicase, ATP synthase, bacterial flagella protein complex, etc. These are the biological nano-machines involved in the basic vital physiological activities such as cell division, muscle contraction, cell movement, vesicle transport, energy production, signal transduction, etc. Proteins, for example, are molecular nanostructures that possess highly specific functions and participate in virtually all biological, sensory, metabolic, information and molecular transport process. The volume of a single molecule bio-nanodevice such as a protein is between one-millionth and one-billionth of the volume of an individual cell. By using

nanofabrication techniques and processes of molecular self-assembly, bio-nanotechnology allows the production of materials and devices including tissue and cellular engineering scaffolds, molecular motors, and biomolecule for sensor, drug delivery and mechanical applications. The fundamental aim of bio-nanotechnology is to obtain a detailed understanding of basic biochemical and biophysical mechanism at the level of individual molecule. This knowledge will allow learning the design rules of naturally occurring molecular machines, which can lead to innovative technological applications. Thin films and crystals of the membrane protein bacteriorhodopsin have already been demonstrated to have potential photonics applications such as optically addressable spatial light modulators, holographic memories and sensors. Bacteriorhodopsin is a protein found in the cell membrane wall of *Halobacterium salinarum,* where it functions as a light-driven proton pump (Blaurock and Stoeckenius, 1971; Birge, 1990). The photosynthetic reaction centre in this protein, which is only 5 nm in size, behaves as a nanometer diode and so it may be useful in single molecule opto electronic devices (Xu et al., 2001; Bhattacharya et al., 2002; Xu et al., 2004).

Synthesis of nanoparticles

There are several methods for nanoparticle synthesis and its functionalization. The protocols for nanoparticle synthesis can be broadly classified as chemical methods, chemical vapor deposition, radiolytic methods, molecular beam epitaxy and by decompostion of organic precursors. Apart from developing special methods for the synthesis of nanoparticles or nanosized building blocks, tailoring and manipulating of the surface functionality and surface properties is a particular preparative challenge. Based on the application and of the following processing steps, it may be necessary to have a clean, ordered surface, an activated surface with dangling groups and a deactivated surface or a derivatized surface (functional organic groups). Furthermore, methods must be developed to control the surface charges and agglomeration/aggregation behavior of the nanoparticles. There is a growing need to develop environmentally benign nanoparticle synthesis protocols that do not use the toxic chemicals in the synthesis protocol.

Beveridge and coworkers have demonstrated that gold particle of nanoscale dimensions may be readily precipitated within bacterial cells by incubation of the cells with Au^{3+} ions (Beveridge and Murray, 1980; Southam and Beveridge, 1996). Nair and Pradeep have synthesized nanocrystals of gold, silver and their alloys by reaction of the corresponding metal ions within cells of lactic acid bacteria present in buttermilk (Nair and Pradeep, 2002). Klaus-Joerger and coworkers have shown that the bacteria *Pseudomonas stutzeri* AG259 isolated from silver mine when placed in a concentrated aqueous solution of $AgNO_3$ resulted in the reduction of Ag^+ ions and formation of silver nanoparticles of well defined size and distinct morphology within the periplasmic space of the bacteria (Klause et al., 1999; Joerger et al., 2000; Klaus Joerger et al., 2001). Jose- Yacaman and co-workers have shown that gold nanoparticles can be synthesized in live *alfalfa* plants by gold uptake from solid media (Gardea-Torresdey et al., 2002). Recently researchers have shown that the eukaryotes such as fungi and plants can be used to grow nanoparticles of different composition and sizes. They have shown the biosynthesis of gold (Mukherjee et al., 2001a; Mukherjee et al., 2002; Ahamed et al., 2003), silver (Mukherjee et al., 2001b) and CdS nanoparticles using eukaryotic systems (Ahamed et al., 2002).

Implication of nanoparticles in biology

The interactions between artificial nanomaterials and biological systems form an emerging research topic of broad importance. Research efforts in this area are motivated by the hope that nanomaterials will have useful applications in biology and medicine. Spherical nanoparticles are typically used for biomedical and biotechnological applications. This reflects the fact that spheres are easy to make than other shapes. Nanotubes, structure that resemble tiny drinking straws, are alternative that might offer some advantages over the spherical nanoparticles for some applications. Nanotubes have inner voids that can be filled with species ranging in size from large proteins to small molecules. In addition, nanotubes have distinct inner and outer surfaces that can be differentially functionalized. The ability to control the dimensions allows for tailoring tube size to fit accordingly for biomedical applications.

In the field of medical research, there are several methods that have been developed for *in vivo* drug delivery via nanoparticles such as nanocrystals, nanospheres, and nanocapsules. By the nature of their size, these nano delivery systems traverse membrane boundaries and can be readily adsorbed into the bloodstream. Their surface chemistry can be modified to display high concentrations of a therapeutic drug or tissue specific targeting molecules. Surface coatings can also be manipulated to exhibit fast or slow release, or for higher *in situ* stability and shelf life. In the area of cancer treatment, the removal of tumors is typically done through a combination of surgery, chemotherapy and radiation, to varying degrees of success. Similar to the target drug delivery, nanoparticles may be used as site-specific probes for tissue destruction, using light or heat to induce thermal oblation or to deposit a localized chemotherapy payload.

Recent studies have demonstrated the significance of silica nanoparticle based drug delivery system in photodynamic therapy. Silica based nanoparticles (diameter 30nm) are used for the entrapment of water insoluble photosensitizing drug *2-devinyl-2- (1-hexyloxyethyl) pyropheophorbide* in anticancer therapy (Roy et al., 2003). FeRx Inc. of San Diego has designed magnetic targeted carriers termed MTCs for site specific targeting, tissue retention, and sustained release of drugs. These MTCs are composed of elemental iron particles and activated carbon which can adsorb and desorb pharmaceutical agents. *Doxorubicin* (DOX) is an anticancer compound. MTC-DOX formulation has been found to be very effective in anticancer therapy. Other drugs delivered in this manner include antibiotics, thrombolytics, anti-inflammatories, peptides and steroids. *5-fluorouracil* is known to have remarkable anti tumor activity, but it has high toxic side effects. After acetylation PAMAM dendrimers can form dendrimer-*5-fluorouracil* conjugates, which upon hydrolysis release free *5-fluorouracil* thus minimizing its side effects (Tripati et al., 2002). Recently it has been demonstrated that poly-(butylcyanoacrylatre) nanoparticles coated with polysorbate 80, are effective in transporting the hexa-peptide *delargin* and other agents into the brain (Kreuter et al., 2003).

The advantages of nanoparticle-based dug delivery over conventional methods are

1. Nanoparticles are small in size, suitable for crossing the physiological obstacles (like blood brain barrier) to reach the target tissue
2. Nanoparticles can be formulated for targeted delivery to the lymphatic system, brain, spleen, liver, lungs and arterial walls or made for long term systemic circulation
3. Nanoparticles can be used to deliver hydrophilic and hydrophobic drugs, proteins, vaccines, biological macromolecules, etc
4. Nanoparticles can carry unstable compound at biological environment to the target site
5. Biodegradable nanoparticle-based drug delivery system could provide multi-dose drug delivery for long term treatment of conditions requiring pulsatile drug release
6. Minimizes the toxic side effects of potent drugs
7. Drug-delivery formulation involves low cost research compared to that for a discovery of a new molecule.
8. Minimizing the use of expensive drugs would reduce the cost of product

One of the characteristic functions of nanoparticles is their ability to deliver the drugs across several biological barriers to the target sites. The brain delivery of a wide variety of drugs such as anti-HIV and anti-neoplastic drug is hindered as it is to be transported through blood brain barrier. The application of nanoparticle to delivery drugs to brain is a promising way of overcoming this physiological barrier. Apart from this, magnetically guided drug targeting has been attempted to increase the efficacy and reduce the unpleasant side effects associated with the chemotherapy in cancer treatment. This method of drug delivery makes chemotherapy more effective by increasing the concentration at the tumor site, while limiting the systemic drug circulation. Nanoparticle for drug delivery may not be suitable for all drugs especially those drugs that are less potent hence the higher dose of drugs would make the drug delivery system much heavier

and larger, which would be difficult to administer. The delivery of drugs to desired target depends on the size, encapsulation efficacy, zeta potential, and release characteristics of the carrier nanoparticles. Hence there is a great need of active research in these areas for expanding these methodologies to new therapeutical applications.

Interactions of nanoparticles with biomolecules

Tailoring of biomolecules with nanoparticles is a tempting research project as it may provide new dimensions into the area of nanobiotechnology (Niemeyer, 2001). The integration of biology and medicine with nanotechnology is expected to produce major advances in medical diagnostics, therapeutics, molecular biology and bioengineering (Heller, 1992; Willner et al., 1993; Bardea et al., 1997). The miniaturization tools such as micro arrays and microchips used in clinical applications carry great promise for the future. Protein chips consist of hundreds of proteins that are directly immobilized onto arrays on a solid support with control over density and orientation. Protein chips have emerged as an exciting technology for the broad characterization of the activities and interaction of the proteins. Protein chips will prove to be essential to the researchers in biology, drug discovery and medical diagnosis. The limitation of such technology is that proteins are often immobilized in a range of orientations and usually undergo partial denaturation at the surface. DNA immobilization on planar supports and in liposomes is important in the development of DNA chips for disease diagnosis, genome sequencing and as nonviral DNA vectors in gene therapy (Lasic, 1997; Steel et al., 1998). The main requirements for the immobilization of the proteins and DNA are that the process should be relatively quick, inexpensive, biofriendly (i.e., it should not result in the degradation of the protein or DNA during entrapment), result in high loading factors and should be applicable to a large range of biomolecules. The host- matrix should be biocompatible and inert, protect the biomolecule against microbial degradation, hydrolysis and deamidation and, in the case of enzymes, should be permeable to substrates, cofactors and redox agents. There is enormous current interest in using nanoparticles for biomedical applications including enzyme encapsulation, DNA transfection, biosensors and drug delivery (Mitchell et al., 2002).

Enzyme / protein immobilization on nanoparticles

Immobilization of biomolecules can be generally defined as restricted mobility of the biomolecules. The various methods for protein immobilization that currently exist in the literature are adsorption/ attachment, covalent binding, ionic binding, biospecific binding, cross linking, encapsulation/ inclusion in membranes, polymers, gels, microcapsules, liposomes / reversed micelles, etc (Tischer and Wedikind, 1999). Proteins / enzymes are macromolecules, which are extremely sensitive to environment conditions. A number of interactions such as hydrophobic effect, hydrogen bonding are responsible for the stability of proteins. Biomolecules may easily denature or loose their catalytic activity after adsorbing on solid surfaces. This may be the primary reason for the design of a completely new class of materials, which can provide a biocompatible environment that can readily conserve the native structure of the enzyme.

Several methods have been employed for the attachment of enzymes on nanoparticles including binding through a thiol group to gold (Alivisatos et al., 1996; Mirkin et al., 1996), and maleimido modified fullerenes (Kurz et al., 1998), through amino groups to carboxyl-functionalized particle (Galow et al., 2000), through a polyhistidine tag to nickel (Bachand et al., 2001), or through electrostatic interactions to charged nanoparticles (Mattoussi et al., 2000). Carbon nanotubes are of special interest due to their unique electronic, metallic and structural characteristics (Odom et al., 2000). It has been shown that small proteins can be entrapped into the inner channel of opened nanotubes by simple adsorption (Tsang et al., 1995; Tsang et al., 1997). Attachment of small proteins on the outer surface of carbon nanotubes can be achieved either by electrostatic (Chen et al., 2001) and hydrophobic interactions (Balavoine et al., 1999), via covalent bonding (Huang et al., 2002), or by functionalization of the nanotubes sides by polymer coating (Shim et al., 2002). Chaniotakis and coworkers demonstrated the use of carbon nanotubes as immobilization matrix for the development of an amperometric biosensor (Sotiropoulou and Chaniotakis, 2003).

In a recent report Martin and coworkers have been demonstrated the differential functionalization of the silica nanotubes. They have synthesized the silica nanotubes

within the pores of alumina templates membrane using sol-gel method. This silica nanotube have differentially functionalized with the green fluorescent silane N-(triethoxysilylpropyl) dansylamide attached to their inner surfaces, and the hydrophobic octadecyl silane (C18) to their outer surfaces (Mitchell et al., 2002). One application of such differentially functionalized nanotubes is as smart nanophase extractions to remove molecules from solutions. Nanotubes with hydrophilic chemistry on their outer surfaces and hydrophobic chemistry on their inner surfaces are ideal for extracting lyophilic molecules from aqueous solution.

Encapsulation of proteins in lipid films

Cell membranes are composed of complex and dynamic patterns of lipids and proteins. The proteins serve as enzymes, transporters, receptors, and provide the membrane with distinctive structural properties. Lipids have several important biological functions, serving as structural component of the membrane, as storage and transport forms of metabolic fuel, as a protective coating on the surface of the many organisms and as cell-surface components involved in cell recognition. Lipid bilayer have been studied to a large extend as model biological membrane to gain insights into various membrane related problems such as ion transport across biomembranes, structure-functional relationship, photosynthesis, cell division and intra- and intercellular biological functions (Tanford, 1980; Fendler, 1982; Jost and Griffith, 1982; Mouritesen and Bloom, 1984). Many proteins have been immobilized within lipid bilayers, and issues such as protein orientation, biological activity, effect of salt/ions and pH on immobilization have been addressed by several groups (Hamachi et al., 1990; Hamachi et al., 1991; Hamachi et al., 1994; Hianik et al., 1996; Salamon and Tollin, 1996; Ramsden et al., 1998; Chen et al., 1999). Previous studies in our laboratory have demonstrated the interaction of an industrially important enzyme, xylanase with the, octadecylamine (ODA), a cationic lipid (George et al., 2002). The industrial importance of xylanase comes from its applications in clarification of juices and wines, conversion of renewable biomass in to liquid fuels, and development of environmentally sound prebleaching processes in paper and pulp industries. The encapsulation of enzyme with the matrix is achieved by the simple immersion of the lipid film into the enzyme xylanase precomplexed with the substrate

(xylan). On immersion of the ODA films in the enzyme solution at pH 7, attractive electrostatic interaction between the negatively charged xylanase molecules and the positively charged ODA matrix drives, to a large extend, to the diffusion of the enzyme into the lipid matrix. An important observation of this study is that the native encapsulated enzyme molecules failed to show biocatalytic activity (possibly due to blockage of the active sites during immobilization in the ODA matrix). Pre-complexing the enzyme with its substrate (Xylan) before immobilization prevents the inactivation of the enzyme in the lipid matrix. The substrate protected Xylanase-ODA biocomposite system showed biological activity compared to that of the free enzyme in the solution and was found to be reusable, enhancing its potential application in the industry. The optimum temperature of operation of the encapsulated enzyme shifts to higher values compared to that of free enzyme in the solution possibly due to the protection offered by the lipid matrix. In another study, the encapsulation of enzyme pepsin and fungal protease by electrostatically controlled diffusion from solution into thermally evaporated fatty amine films was also demonstrated (Gole et al., 2000a; Gole et al., 2000b).

Whole cell immobilization

Currently there is much interest in the synthesis of biocompatible surfaces for the immobilization of whole cells of microorganisms, which has got implications in several areas including basic cell biology (Singhvi et .al, 1994; Chen et al., 1997), biosensing (John et al., 1998), tissue engineering (Ortnwall et al., 1987), and treatment of disease by controlled delivery of biological products (Orive et al., 2002). The surfaces with which cells interacts are important for maintaining cellular viability and localization. The features of these surfaces can act as signals that influence cellular behavior. Generally self assembled monolayers are well characterized surfaces that have been used for the patterning and cell attachment (Bain et al., 1989; Stenger et al., 1992; Lopez et al., 1993; Yousaf et al., 2001). An important application of the immobilization of bacterial and fungal cells (genetically engineered and otherwise) is for the production of industrially and medically important enzymes and metabolites (Punt et al., 2002). If the enzymes of interest are unstable outside the cellular environment, the immobilization of the cells would be important to catalyze reactions that depend on the unstable enzymes. Supported

lipid membranes have been subjected to great attention because of their extraordinary ability to preserve many biological properties of the cellular membrane (Sackmann, 1996). Recent studies have shown the immobilization of *Candida bombicola* cells on lipid films as enzyme source for the transformation of arachidonic acid to 20-hydroxyeicosatetraenoic acid (20-HETE) (Phadtare et al., 2003).

Nucleic acid immobilization

The use of DNA chips is revolutionizing in many aspects of genetic analysis (Pease et al., 1994; Nollau and Wagener, 1997; Ramsay, 1998). DNA microarrays have taken advantage of many of the benefits of miniaturization, including speed of analysis, smaller sample size and decreased cost (Jakeway et al., 2000; Sanders and Manz, 2000; Quake and Scherer, 2000). Different routes are being attempted for the immobilization of DNA on planar surfaces, some of the more thoroughly studied methods being assembly at the air-water interface with langmuir monolayers (Okahata et al., 1996; Shimomura et al., 1997), self- assembly of thiolated DNA and peptide nucleic acids on gold surfaces (Wang et al., 1997; Steel et al., 1998) and attachment to terminally functionalized self-assembled monolayes via electrostatic (Higashi et al., 1997) and intercalation interactions (Higashi et al., 1999). The immobilization of single stranded DNA on planar surfaces to yield DNA chips is the focus of intense research due to its potential application in disease diagnosis and genome sequencing (Wang et al., 1997; Steel et al., 1998). Many microarray chips have DNA immobilized in a variety of polymeric surface pads to facilitate spatially localized detection of DNA hybridization (Edman et al., 1997; Belosludtsev et al., 2001). DNA molecule can be immobilized in cationic lipid films, such as octadecylamine (ODA), by simple immersion of the lipid films in DNA solution (Sastry, 2002). Entrapment of the DNA molecules in the ODA matrix is dominated by attractive electrostatic interaction between the negatively charged phosphate backbone of the DNA molecules and the protonated amine molecules in the thermally evaporated film.

The applications of DNA-functionalized gold particles were introduced recently by Mirkin and co-workers (Mirkin et al, 1996; Mucic et al., 1998). Masazo and Co-workers have been demonstrated the immobilization of DNA through intercalation at self-

assembled monolayers on gold (Higashi et al., 1999). They have demonstrated an acridine derivative containing a long alkyl chain, whose end is modified with a disulfide bond to attach to the gold surface, can form binary self-assembled monolayers together with the acridine free on gold substrates, DNA can be immobilized on these monolayer surfaces through intercalation of the acridine moiety. Tarlov and coworkers have been demonstrated a method for quantifying the density of DNA immobilized on gold (Steel et al., 1998). They have quantified the surface density of the DNA by taking the advantage of the electrostatic attraction of specific redox cations with the nucleotide phosphate backbone.

Scope of the present study

In our laboratory, aspartic proteases are used as model proteins to develop gold based bioconjugates. Protease immobilization is important in many applications such as biosensors, bioorganic synthesis and protein (or peptide) hydrolysis. Proteases offer several advantages over physical and chemical manipulations in food processing. The large success of microbial proteases in food and other biotechnological systems can be attributed to their broad substrate specificities and stability. Aspartic proteases are used commercially for hydrolysis of soyabean proteins to amino acids and in soya sauce manufacturing and exhibit milk clotting activity. They are also used in digestive aids (Kalisz, 1988). Pepsin is a proteolytic enzyme essential for the digestion process in animals, which hydrolyses the bonds formed by the carboxyl groups of amino acids such as phenylalanine, tyrosine, tryptophan and methionine. The optimal pH of its activity is 2.0. The enzyme has a total 326 amino acid residues and a maximal cross sectional length of 6.5 nm based on its crystal structure (Tang and Hartley, 1970). The immobilization of pepsin and fungal proteases onto 3-D curved surfaces such as gold nanoparticles have been studied in our laboratory (Gole et al., 2001a; Gole et al., 2001b). An important feature of this work was that the enzyme retains significant catalytic activity after adsorption on the surface of the gold nanoparticles. However a major draw back of this approach is that the gold nanoparticle bioconjugate was not easily separated from the reaction mixture under ultrahigh centrifugation conditions and hence showed poor reuse characteristics. To overcome this, we have developed a protocol for the assembly of gold

nanoparticle “shells” on massive polyurethane “cores”. These bulkier microspheres bound enzyme molecules were easily separated from the reaction mixture under mild centrifugation conditions and subsequently reused (Phadtare et al., 2004). The area of research interest of this part of the thesis is to design novel bioconjugates using gold as a template of immobilization to improve the reuse characteristics of the nano-bioconjugate. This chapter is divided into two sections; the first part discusses the assembly of the gold nanoparticles on the surface of the amine-functionalized zeolite microspheres to form zeolite-gold nanoparticle ‘core-shell’ structures and thereafter, the use of this structure in the immobilization of the enzyme fungal aspartic protease. The second section deals with the synthesis of a free-standing gold nanoparticle membrane and it was used as scaffolds for the immobilization of the enzyme fungal protease.

PART- 1

GOLD NANOPARTICLES ASSEMBLED ON AMINE-FUNCTIONALIZED NA-Y ZEOLITE: A BIOCOMPATIBLE SURFACE FOR ENZYME IMMOBILIZATION

SUMMARY

Development of simple and reliable protocols for the immobilization of enzymes is an important aspect of biotechnology. Gold nanoparticles are known to bind enzymes, but reuse characteristics of the gold nano-enzyme bioconjugates has hitherto been poor. This chapter discusses the assembly of the gold nanoparticles on the surface of the amine-functionalized zeolite microspheres to form zeolite-gold nanoparticle 'core-shell' structures and thereafter, the use of this structure in the immobilization of the enzyme fungal protease. The assembly of gold nanoparticles on the zeolite surface occurs through the amine groups present in 3-aminopropyltrimethoxysilane (3-APTS). The binding of the enzyme to the gold nanoparticles in turn occurs through the amine groups and the cysteine residue present in the enzyme. The fungal protease bound to the massive 'core-shell' structures were easily separated from the reaction medium by mild centrifugation and exhibited reuse characteristics. The proteolytic activity of fungal protease in the bioconjugate was marginally enhanced relative to the free enzyme in solution. The bioconjugate also showed significantly enhanced pH and temperature stability and a shift in the optimum temperature of operation

INTRODUCTION

Biotechnology is witnessing the impressive advances in the synthesis of biocompatible surfaces for the immobilization of a range of biomolecules (Fang et al., 1999; Loidl-Stahlhofen et al., 2001; Lei et al., 2002) with important applications in biosensing and medicine (Rembaum and Dreyer, 1980; Albers, 2001; Gilardi and Fantuzzi, 2001; Park et al., 2002). The specificity of enzymes promises great improvements in various applications such as chemical conversions, biosensing and bioremediation (Guilbault, 1984; Duran and Esposito, 2000; Koeller and Wong, 2001; Schmid et al., 2001). However, the short catalytic lifetimes of enzymes presently limits their use (Burton et al., 2002). Several approaches have been adopted to improve catalytic stability of enzymes: such as enzyme immobilization, enzyme modification, genetic modification and medium engineering (Mozhaev, 1993; DeSantis et al., 1999; Govardhan, 1999; Tischer and Wedekind, 1999; Livage et al., 2001). Insofar as enzymes are concerned, advantages of immobilized enzymes over their counterparts in solution include enhanced temperature and temporal stability of the biocatalyst and ease of separation from the reaction medium enabling multiple reuses. A number of templates have been used for enzyme immobilizations such as silica nanotubes (Mitchell et al.; 2002), phospholipid bilayers (Hamachi et al., 1994; Chen et al., 1999), self-assembled monolayers (Mrksich et al., 1995; Fang et al., 1996), Langmuir-Blodgett films (Nicolini et al., 1993; Boussand et al., 1998), polymer matrices (Yang et al., 1995; Franchina et al., 1999), galleries of α-zirconium phosphate (Kumar and McLendon, 1997), mesoporous silicates such as MCM-41 (He et al., 2000), silica nanoparticles (Qhoboshean et al., 2001) and thermally evaporated lipid films (Sastry et al., 2002), each with its characteristic pros and cons.

A number of groups have studied the adsorption of proteins on both polymer (Elgersma et al., 1990; Schmitt et al., 1997; Basinka et al., 1999; Caruso et al., 1999; Molina-Bolivar et al., 1999) and inorganic colloidal particles of oxides/metals. Recently, functionalized γ-Fe_2O_3 magnetic nanoparticles (Dyal et al., 2003) have been used as a support for the enzyme lipase. In the area of metal nanoparticle-enzyme conjugate materials, Crumbliss, Stonehuerner and co-workers have studied the formation and enzymatic activity of gold nanoparticles complexed with horseradish peroxidase

(Stonehuerner et al., 1992), xanthine oxidase (Zhao et al., 1996) as well as glucose oxidase and carbonic anhydrase molecules (Crumbliss et al., 1992). A salient feature of their work is the demonstration that enzyme molecules are bound tightly to gold colloidal particles and retain significant catalytic activity in the conjugated form while the enzyme molecules denature on adsorption to planar surfaces of gold (Crumbliss et al., 1992). In our laboratory, we have reported the conjugation of pepsin (Gole et al., 2001a) and fungal protease (Gole et al., 2001b) with gold nanoparticles. An important aspect of this study was that the enzyme retains significant catalytic activity after adsorption on the gold nanoparticle. However, one major drawback of this approach is that the gold nanoparticle bioconjugate material was not easily separated from the reaction mixture and hence showed poor reuse characteristics. Indeed, separation of the bioconjugate from the reaction medium often could not be achieved, even by ultra centrifugation. This problem may be overcome if the gold nanoparticle could be tethered at high density to a more massive surface, such as that provided by the microne-sized particles. This chapter discusses the assembly of gold nanoparticle "shells" loaded on massive amine functionalized Na-Y zeolites "cores" (pore diameter 12 A^o, average diameter of the particle ≈ 800 nm) provide a biocompatible surface for the immobilization of the enzyme fungal protease. Binding of gold nanoparticles to the zeolites occurs through the free amine groups of 3-aminopropyltrimethoxy silane (3-APTS) present on the surface and the enzyme binds strongly to the gold nanoparticle surface and shows significant proteolytic activity. The bioconjugate was showing enhanced temperature and pH stability. The fungal protease gold nanoparticle-zeolite biocatalyst could be easily removed from the reaction medium by simple sedimentation and exhibited reuse characteristics.

MATERIALS AND METHODS

Chemicals

Fungal protease (F-prot) and Hemoglobin (Hb) were obtained from Sigma Chemicals and used as-received. Chloroauric acid, sodium borohydride, sodium chloride and 3-aminopropyltrimethoxysilane (3-APTS) were obtained from Aldrich. All buffer salts were prepared from standard commercial sources.

Gold nanoparticle synthesis

In a typical experiment, 100 ml of 1.25 x 10^{-4} M concentrated aqueous solution of chloroauric acid ($HAuCl_4$) was reduced by 0.01 g of sodium borohydride ($NaBH_4$) at room temperature to yield a ruby-red solution containing 35 ± 7 Å diameter gold nanoparticles (Patil et al., 1999).

Synthesis of APTS-functionalized spherical faujasite (zeolite Y) particles

In the synthesis of micron size faujasite (zeolite Na-Y) particles, seed crystals of zeolite Na-Y were prepared separately from an aqueous mixture of Na_2SiO_3 (95 mmol, 28% SiO_2), $NaAlO_2$ (9.76 mmol, 43% Al_2O_3, 39% Na_2O), NaOH (70 mmol) and H_2O (0.55 mmol) by stirring for 1 h and then keeping the solution at rest for 18 h. The seed crystals of zeolite Na-Y thus prepared were then added to an aqueous solution of Na_2SiO_3 (355 mmol). To this mixture, 10 mmol of a non-ionic surfactant, Tween 80 (from Aldrich chemicals, marked as TW-80) with a molar ratio of SiO_2 : TW-80 of 25:1 was added under constant stirring. To this frothing gel, $NaAlO_2$ (34.2 mmol), NaOH (92.5 mmol), Al_2 $(SO_4)_3.16H_2O$ (6.02 mmol), sodium fluoride (6.4 mmol) and H_2O (1.94 mmol) was added under constant stirring for 2 h, the final pH of the gel being 13.1. The final molar composition of the reaction mixture was 12.5 SiO_2: 2.5 Al_2O_3: 12.13 Na_2O: 0.64 NaF: 0.5 TW-80: 300 H_2O. The reaction mixture for zeolite was then sealed in a polypropylene bottle and kept in an oven at 373 K for 12 h under autogenous pressure. The as-synthesized sample was filtered and washed several times with de-ionised water, dried at 383 K and then air-calcined at 813 K for 12 h.

To 1.0 g of the calcined powder Na-Y zeolite, 1 mL of 3-aminopropyl trimethoxysilane (APTS) in 30 mL of dicholoromethane (DCM) was added and the slurry stirred for 16 h at room temperature. The APTS functionalized zeolite white powder was then repeatedly washed with DCM and dried in vacuum. The samples thus obtained were used for enzyme immobilization.

Formation of gold nanoparticle- zeolite composites

10 mg of the amine-functionalized zeolite was dispersed in 50 ml of the colloidal gold solution under continuous stirring. After ca. 12 h of stirring, the originally ruby-red colloidal gold solution turned colorless, while the zeolite attained a reddish hue. The mass loading of the zeolite particles by gold nanoparticles was estimated to be 5 wt % from the decrease in the intensity of the surface plasmon resonance of gold nanoparticles in the supernatant obtained after centrifugation of the zeolite. The zeolite particles capped with gold nanoparticles were separated by mild centrifugation, washed with double distilled water and dried in air for further use. Since aggregation of the gold nanoparticles in the solution can lead to the errors in estimation of the gold loading from the UV-visible spectroscopy, atomic absorption spectrometry (AAS) was also used. 60 mg of amine functionalized Na-Y zeolite bound with gold nanoparticles was dissolved in 10 mL agua regia (conc. HCl : conc. HNO_3, 3:1) and volume was made up to 100 mL using deionized water. The solution was analyzed by CHEMITO 201 Atomic Absorption Spectrophotometer and was compared with the standard of gold solution to estimate the weight percent of gold bound to the amine-functionalized zeolite.

Formation of fungal protease-gold nanoparticle-zeolite bioconjugate

10 mg of the gold nanoparticle-zeolite powder was dispersed in 2 mL glycine-HCl buffer (0.05 M, pH 3). To this solution, 100 µl of a stock solution consisting of 50 mg/mL of fungal protease in glycine-HCl buffer (0.05 M, pH 3) was added under mild stirring. After 1 h of stirring the fungal protease-gold nano-zeolite bioconjugate material was separated by centrifugation. The loss in absorbance at 280 nm in the supernatant (arising from π-π^* transitions in tryptophan and tyrosine residues in the enzyme) (Stoscheck, 1990) was used to quantify the amount of F-prot bound to the gold nanoparticle-zeolite

for specific activity determination. The powder thus obtained was rinsed several times with glycine-HCl buffer (0.05 M, pH 3) solution and re-suspended in buffer solution (pH 3) and stored at 4 ^{0}C for further experiments. Since it is possible that the zeolite particles suspended in the supernatant would lead to an error in the quantitative analysis of the protein by UV-vis spectroscopy in the bioconjugate, fluorescence spectroscopy was also performed. Fluorescence measurements were carried out on the initial concentration of the F-prot in solution at pH 3 and supernatant of F-prot in solution after centrifugation of bioconjugate using a Perkin-Elmer Luminescence Spectrophotometer (model LS 50B). The tryptophan and tyrosine residues in the enzyme were excited at 280 nm and the emission band was monitored in the range 300 to 500 nm. The loss in fluorescence intensity (arising from π-π* transitions in tryptophan and tyrosine residues in proteins) was used to quantify the amount of F-prot bound to the gold nanoparticle-zeolite spheres (Eftink, 1981). From the calibration curve of the fluorescence intensity at different concentrations of the F-prot in solution, the amount of the enzyme in the bioconjugate was estimated. Since the amount of enzyme in the bioconjugate was known, specific activity was calculated.

UV-Vis spectroscopy studies

The binding of gold nanoparticles to the zeolite particles was monitored by UV-vis spectroscopy on a Shimadzu dual beam spectrometer (model UV-1601 PC) operated at a resolution of 1 nm. The decrease in intensity of the surface plasmon resonance in the aqueous colloidal gold solution (resonance at ca. 520 nm) (Alvarez et al., 1997; Patil et al., 1999) arising due to binding of the gold nanoparticles to the zeolite was used to estimate the weight percentage loading of gold nanoparticles.

Fourier transform infrared spectroscopy (FTIR)

FTIR was used to study the binding of gold nanoparticles to amine-functionalized zeolite particles. A film of the gold nanoparticles bound to amine-functionalized zeolite particles was prepared on a Si (111) substrate by drop-casting from solution. FTIR spectra of the films were recorded on a Perkin Elmer Spectrum One FTIR –Spectrometer instrument operated in the diffuse reflectance mode at a resolution of 4 cm^{-1}. To obtain good signal

to noise ratio, 256 scans of the film were taken in the range 450 – 4000 cm^{-1}. For comparison, an FTIR spectrum of the as-prepared amine-functionalized zeolite material on a Si (111) substrate was also recorded.

Transmission electron microscopy (TEM) measurements

TEM measurements were performed on a JEOL Model 1200EX instrument operated at an accelerating voltage of 120 kV. Samples for TEM analysis were prepared by placing drops of the amine-functionalized zeolite particle and the gold nanoparticle-capped zeolite particle solutions on carbon-coated TEM copper grids. The mixtures were allowed to dry for 1 min, and then the extra solution was removed using a blotting paper.

Scanning electron microscopy (SEM) and energy dispersive analysis of X-rays (EDAX) measurements

Samples for SEM and EDAX measurement were prepared by drop-coating a film of the gold nanoparticle-zeolite and F-prot-gold nanoparticle-zeolite solutions on a Si (111) substrate. Additional SEM measurements of the F-prot-gold nanoparticle-zeolite bioconjugate material after one reaction cycle were carried out to verify leaching of weakly bound F-prot molecules in the bioconjugate material. These measurements were performed on a Leica Stereoscan-440 scanning electron microscopy (SEM) equipped with a Phoenix EDAX attachment.

X-ray diffraction measurement (XRD)

XRD measurements of amine-functionalized zeolite and gold nanoparticles bound to zeolite powders were done on a Philips PW 1830 instrument operating at 40 kV and a current of 30 mA with Cu K_α radiation.

Enzyme activity measurements

The proteolytic activity of free F-prot in solution and of F-prot-gold nano-zeolite bioconjugate in glycine-HCl buffer (0.05 M, pH 3) was determined by reaction with 0.5 % Hb at 37 ^{o}C for 30 min. Control experiments on the proteolytic activity of F-prot immobilized directly onto amine-functionalized zeolite were also performed under identical conditions. The F-prot-gold nanoparticle-zeolite and F-prot-zeolite bioconjugate materials were separated from the reaction medium by centrifugation (2000 rpm) for recycling studies. In typical experiments to estimate the proteolytic activity of the bioconjugate, a carefully measured amount of the F-prot-gold nanoparticle-zeolite/F-prot-zeolite bioconjugate in buffer was incubated with 1 ml of 0.5 % Hb solution at 37 ^{o}C for 30 min. After the incubation time, equal volume of 1.7 M perchloric acid was added to the reaction mixture to precipitate the residual Hb. After 30 min, the precipitate was removed by centrifugation and the optical absorbance of the filtrate was measured at 280 nm. F-prot digests Hb and yields acid soluble products (such as tryptophan and tyrosine residues), which are readily detected by their strong UV signatures at 280 nm (Gole et al., 2000b). The amount of F-prot in the bioconjugate material was quantitatively estimated during the preparation of the bioconjugate as briefly discussed earlier under the subheading formation of fungal protease- gold nanoparticle-zeolite bioconjugate. For comparison, the proteolytic activity of an identical concentration of the free enzyme in solution was recorded. In order to determine the confidence limits of the catalytic activity measurements, separate measurements for 6 different F-prot-gold nanoparticle-zeolite bioconjugate solutions were carried out.

The temperature stability of the F-prot-gold nanoparticle-zeolite bioconjugate was checked by pre-incubating the bioconjugate for 1 h at different temperatures in the range 50-80 ^{0}C and was compared with an identical amount of free enzyme in the glycine-HCl buffer (0.05 M, pH 3) under similar conditions. All the reactions were carried out after pre-incubation for 1 h at the different temperatures and measuring the proteolytic activity at pH 3 and 37 ^{o}C as described earlier. Three separate measurements were done to check the reproducibility of the assay. The pH-dependent variation in the proteolytic activity of

the bioconjugate and free enzyme were studied at five different pH values (pH 3, Gly-HCl buffer; pH 4.5, 6, citrate acetate buffer; and pH 8 glycine-NaOH buffer) by pre-incubating for 1 h at 27 ^{0}C. All the reactions were carried out after pre-incubation for 1 h at the different pH and measuring the proteolytic activity at pH 3 and 37 ^{o}C as described earlier. Reproducibility of the data was tested in three separate experiments carried out under identical conditions. To determine the optimum temperature of activity of the immobilized enzyme, the bioconjugate materials was assayed at increasing temperature in the range of 35-65 ^{0}C at pH 3 for 30 min by using Hb as a substrate.

RESULTS AND DISCUSSION

Various biomolecules such as enzymes, antigens, antibodies, DNA, etc., have dimensions in the range of 2 to 100 nm. These dimensions are comparable to those of nanoparticles and thus the synthetic nanostructures and biomaterial units exhibits structural compatibility. The tailoring of nanoparticles with these biomolecules is an exciting area of research since it may provide new dimensions to the area of nanobiotechnology. This chapter demonstrates the assembly of gold nanoparticles on amine-functionalized zeolite particles and which act as biocompatible templates for the immobilization of the enzyme F-prot. The probable structure of the F-prot-gold nano-zeolite biomaterial is illustrated in Figure 1.

Preparation of the gold nanoparticle-zeolite material

Figure 2 shows UV-vis spectra recorded from the as-prepared colloidal gold solution (curve 1) and the gold solution after stirring with zeolite for 12 h and filtration (curve 2). The surface plasmon resonance in the as-prepared colloidal gold can be clearly seen at ca. 520 nm (curve 1) (Alvarez et al., 1997; Patil et al., 1999). After stirring the colloidal gold solution with the zeolite for 12 h, it is seen that there is loss in intensity of surface-

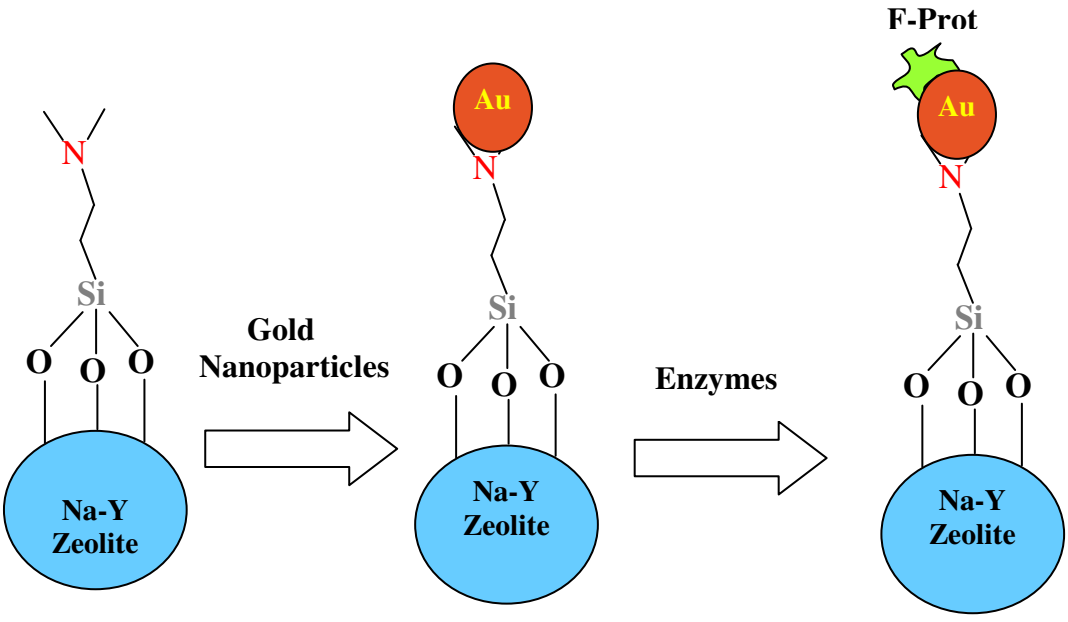

Figure 1 Schematic (not to scale) showing the binding of gold nanoparticles to APTS functionalized zeolites and thereafter their use for enzyme immobilization

plasmon resonance due to decrease in the concentration of gold nanoparticles in the aqueous solution (curve 2). This clearly indicates binding of the gold nanoparticles to the amine-functionalized zeolite through free amine groups of APTS (Brown and Hutchison et al., 1999; Kumar et al., 2000; Leff et al., 1996; Sastry, et al., 2001; Selvakannan et al., 2002). The mass loading of the gold nanoparticles on the zeolite was estimated to 5 % by weight. Since aggregation of the gold nanoparticles in solution can lead to the errors in the estimation of gold nanoparticles in the amine functionalized zeolite material from the UV-vis spectra, atomic absorption spectrometry was also used. The gold nanoparticles bound to the amine functionalized Na-Y zeolite was dissolved in aqua regia and solutions were analyzed by AAS as described in the experimental section. The mass loading of the gold nanoparticles in the amine functionalized zeolite was estimated as 5.4 weight % and is thus consistent with the estimate from the UV-vis spectroscopy.

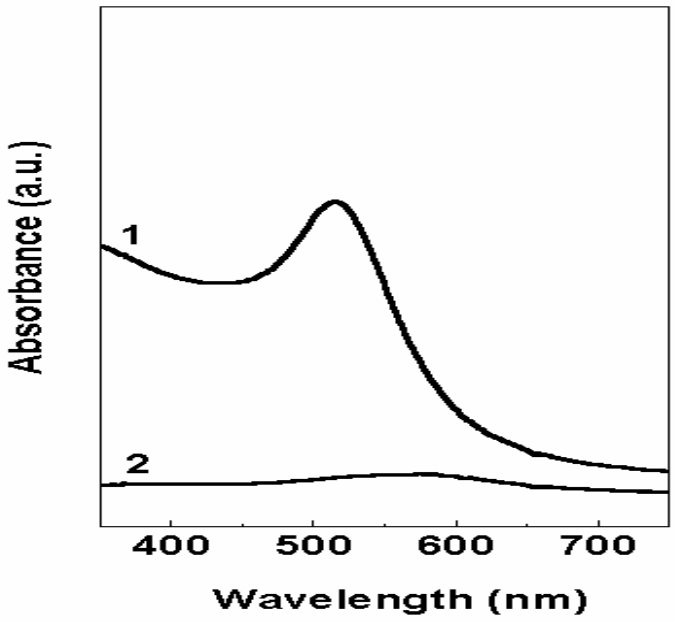

Figure 2. UV-vis spectra recorded from the as-prepared colloidal gold solution (curve 1) and gold solution after stirring with amine-functionalized zeolite for 12 h and centrifugation

FTIR studies

Drop-coated films of the amine-functionalized zeolite and the gold nano-zeolite composite material were prepared on Si (111) substrates, curves 1 and 2 in Figure 3 being the FTIR spectra recorded from these samples respectively. The FTIR spectrum of the amine-functionalized zeolite film (curve 1) shows an asymmetric, broad band centered at around 3450 cm^{-1}. This broad resonance arises from excitation of N-H stretch vibrations of the amine groups (usually centered at ca. 3350 cm^{-1}) (Bradosova, 1995) and O-H stretch vibrations from silanol groups in the zeolite material (3400 – 3600 cm^{-1} region). In the film of amine-functionalized zeolite complexed with gold nanoparticles (curve 2), a well defined band appears at ca. 3050 cm^{-1} and is assigned to the N-H stretch vibrational mode of the free amine group of APTS after binding to gold nanoparticles. The shift in the N-H stretch band from 3350 cm^{-1} to 3050 cm^{-1} after stirring with gold nanoparticles indicates binding of the gold nanoparticles to the zeolite particles through the amine groups, such shifts having been observed in Langmuir-Blodgett films of octadecylamine after formation of complexes with $PtCl^{6-}$ ions (Bradosova, 1995). Due to the shift in the N-H stretch vibration in the gold nanoparticle-capped sample (curve 2), the O-H stretch band sharpens and a well defined resonance at ca. 3350 cm^{-1} is now observed (curve 2).

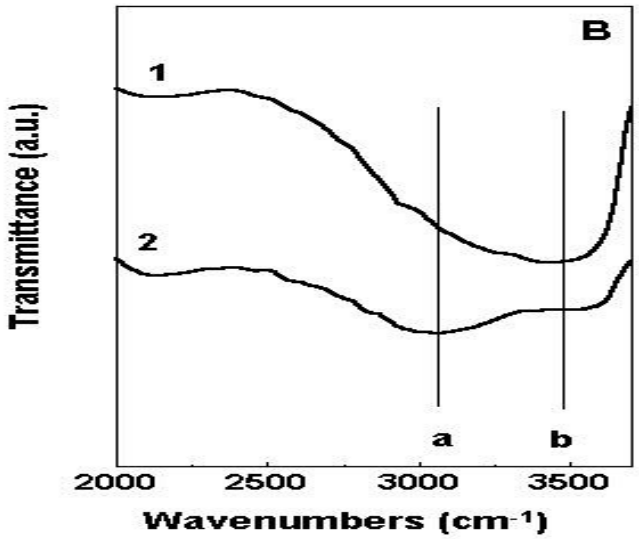

Figure 3. FTIR spectra recorded from drop-coated films of amine-functionalized zeolite (curve 1) and gold nanoparticle-bound zeolite material (curve 2) on Si (111) substrates.

TEM measurements

Figure 4A and B show representative TEM micrographs of the as-prepared amine functionalized zeolites. The particles are fairly spherical, with slightly irregular edges. Analysis of many similar TEM images indicated that the particles were quite uniform in size, with an average diameter of ca. 800 nm. TEM images recorded from the amine-functionalized zeolites particles after complexation with gold nanoparticle are shown in Figure 5A and B. In both images, gold nanoparticles (dark spots) decorating the surface of the zeolites particles can clearly be seen. This is illustrated quite beautifully in Figure 5A where the interface between three large zeolites particle is seen with a dense population of gold nanoparticle in the surface. This indicates clearly that the gold nanoparticle are bound to the zeolites at fairly high concentration. As mentioned previously and confirmed by FTIR analysis (Figure 3), the gold nanoparticle bind to the zeolite template via the primary amine groups.

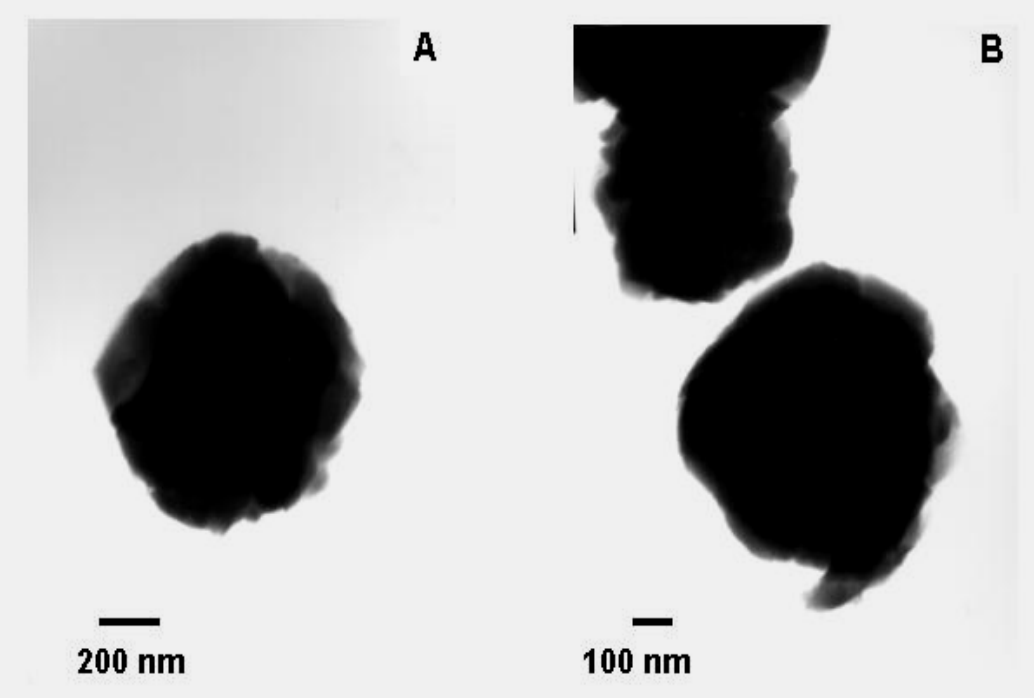

Figure 4. (A) and (B) Representative TEM images of amine-functionalized zeolite particles on a carbon-coated TEM grid

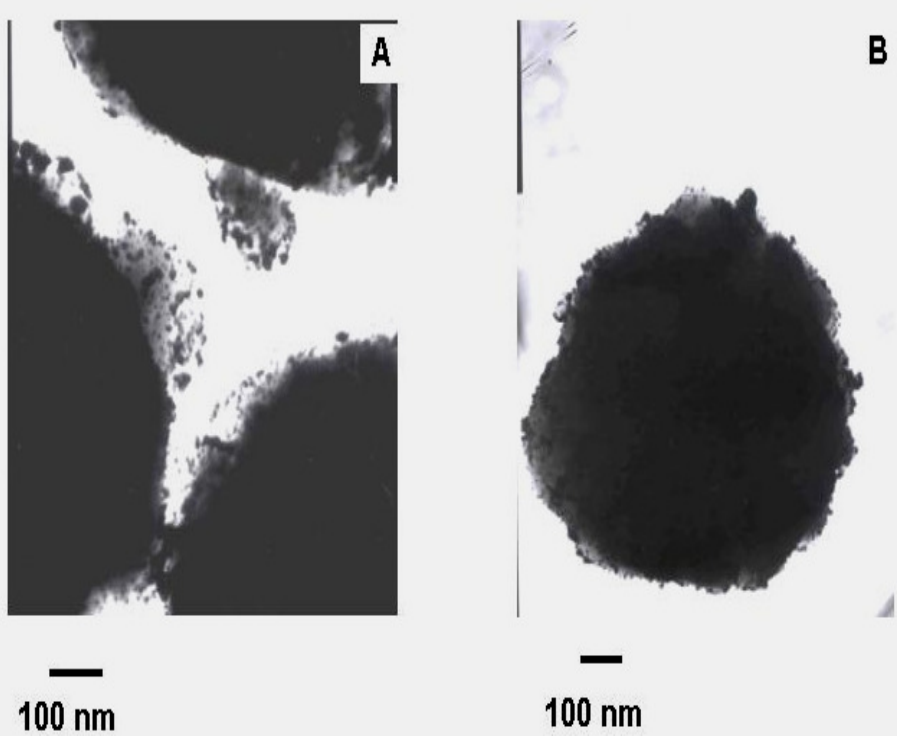

Figure 5. A and B TEM images recorded from the zeolite particles after complexation with gold nanoparticles on a carbon-coated TEM grid.

SEM studies

Figure 6A and B show SEM images of drop-cast films of the gold nanoparticle-zeolite "core-shell" particles and F-prot-gold nanoparticle-zeolite bioconjugate material (C) on Si (111) substrates. The surface texture of the zeolite particles capped with gold nanoparticles is quite smooth (Figure 6A and B). The SEM instrument is clearly unable to resolve the gold nanoparticles bound to the surface of the zeolite core. After conjugation of the gold nanoparticle-zeolite material with F-prot, thin sheets of presumably the aggregated enzyme are seen together with smooth gold nanoparticle-zeolite spheres (Figure 6C). Spot profile EDAX analysis of the sheets (marked by an '+' in Figure 6C) confirmed that they were composed of enzyme (through a strong sulfur signal from cysteine residues of F-prot). These sheets thus correspond to aggregated F-prot molecules, such protein aggregation having been observed by Caruso et al in multilayer films of polymer-anti-IgG composites (Caruso et al., 1998). Spot profile EDAX analysis of the smooth gold nanoparticle-zeolite spheres away from the F-prot

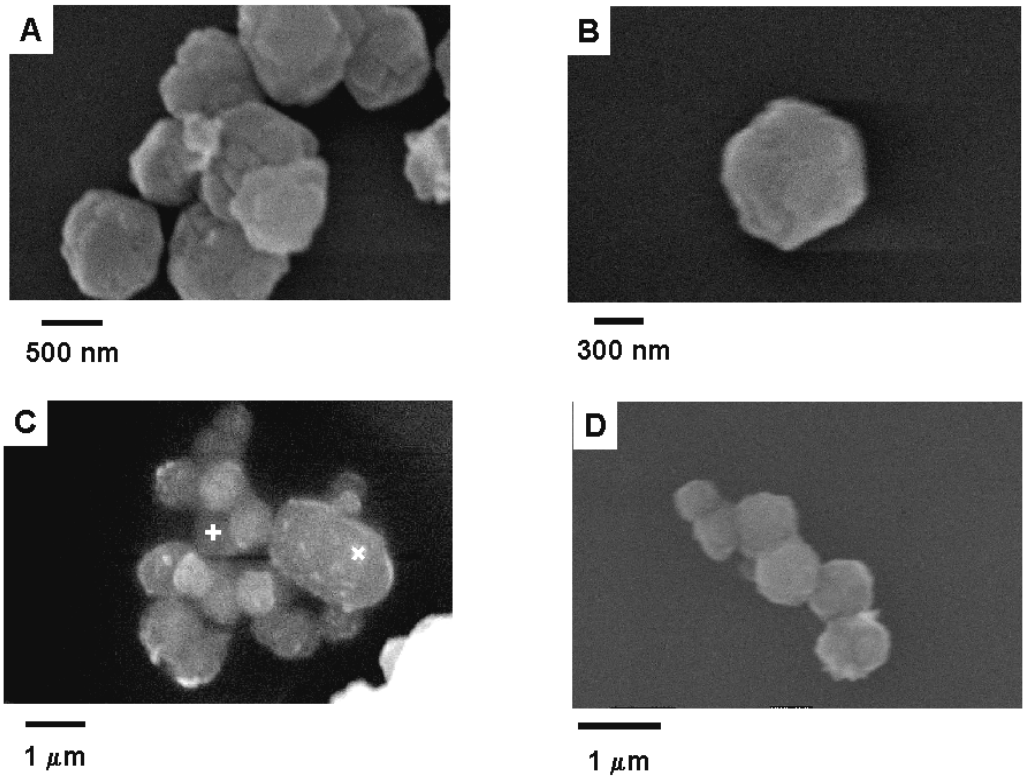

Figure 6. (A) and (B) SEM images of the gold nanoparticle-zeolite core-shell material; (C) - the F-prot-gold nanoparticle-zeolite bioconjugate material and (D) the F-prot-gold nanoparticle-zeolite bioconjugate material after one cycle of reaction with Hb as a substrate. All these films were cast as onto Si (111) wafers

sheets (marked by a 'x' in Figure 6C) also showed the presence of sulfur indicating binding of the enzyme to the gold nanoparticles even though not visible by SEM imaging. The sulfur signal was absent in the gold nanoparticle-zeolite "core-shell' particles as expected.

XRD measurements

Figure 7 shows XRD patterns recorded from the as-prepared amine-functionalized zeolite powder (curve 1) and the amine functionalized zeolite powder after complexation with gold nanoparticles (curve 2). Further to binding of gold nanoparticles to the underlying zeolite template, no changes whatsoever are seen in the peak positions and peak intensities of the Bragg reflections arising from the zeolite clearly indicating that the crystallinity of the zeolite is maintained after binding of gold nanoparticles. This is an

important result given that encapsulation of hetero polyanions in channels of Si-MCM 41 has been reported to lead to loss in crystalllinity of the mesoporous template (Kaleta, 2001). The XRD result suggests that the gold nanoparticles are bound to the surface of the zeolite particles and are not trapped within the pores of the zeolite. This is understandable since the size of the gold nanoparticles in this study is ca. 4 nm while the zeolite pore diameter is estimated to be 1.2 nm. The inset of Figure 7 is an expanded region of the patterns shown in the main part of the figure. The (111) Bragg reflection from gold nanoparticles bound to the zeolite template (curve 2) can clearly be seen, this peak is absent in the as-prepared amine-functionalized zeolite powder (curve 1). This provides additional confirmation of the binding of gold nanoparticles to the zeolite.

Enzyme quantitation studies

The amount of F-prot in the F-prot-gold nanoparticle-zeolite bioconjugate material was quantitatively estimated by UV-visible spectroscopy during preparation of the bioconjugate material as briefly mentioned earlier. The amount of the F-prot in the gold nanoparticle-zeolite was found to be 1.15 % (w/w), since amine groups and cysteine residues in the proteins are known to bind strongly with gold colloids. The protein loading in the amine functionalized zeolite was found to be 1.13 % (w/w). This may be due to the hydrogen bonding interactions between the hydroxyl and amine groups of zeolite and carbonyl or amino groups of the enzyme. The binding of the enzyme to the zeolite may also due to the electrostatic interactions between the negatively charged silanol surfaces with the positively charged F-prot enzyme (pI of F-prot~9.5).

Fluorescence spectroscopy was also used to quantify the amount of enzyme in the bioconjugate material as briefly mentioned earlier. Figure 8 shows the fluorescence emission intensity of initial concentration of free F-prot enzyme in solution at pH 3 (curve 1) and supernatant after centrifugation of gold nanoparticle-zeolite bioconjugate (curve 2). The concentration of enzyme in the bioconjugate was determined from the calibration curve (fluorescence intensity of different concentration of F-prot in solution at pH 3) shown in the inset of Figure 8. From the decrease in the intensity of the supernatant the amount of enzyme bound to gold nanoparticle-zeolite was found to be 1.12 % (w/w) and amine functionalized zeolite was 1.15 % (w/w).

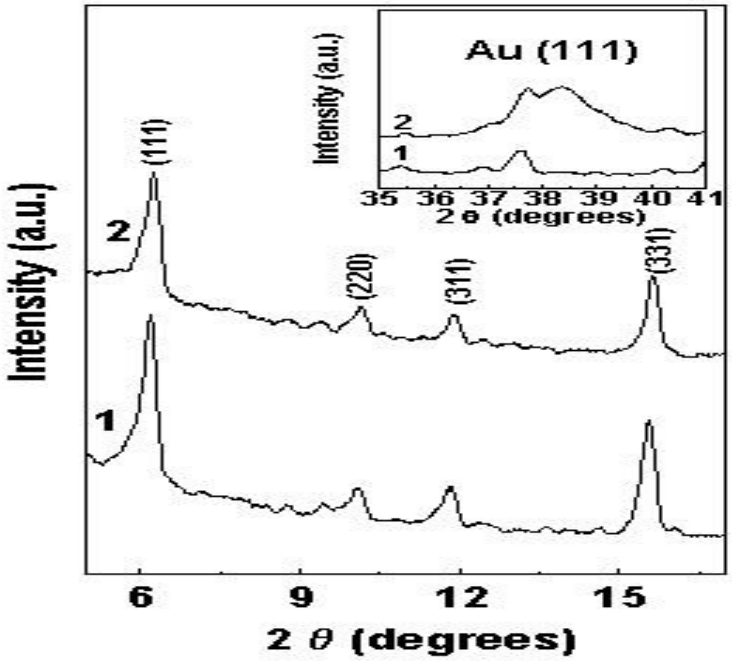

Figure 7. XRD patterns recorded from films of amine-functionalized zeolite (curve 1) and amine-functionalized zeolite after complexation with gold nanoparticles (curve 2) on Si (111) substrates. The inset shows XRD patterns recorded from films of amine-functionalized zeolite (curve 1) amine-functionalized zeolite after complexation with gold nanoparticles (curve 2) in the gold (111) Bragg reflection region.

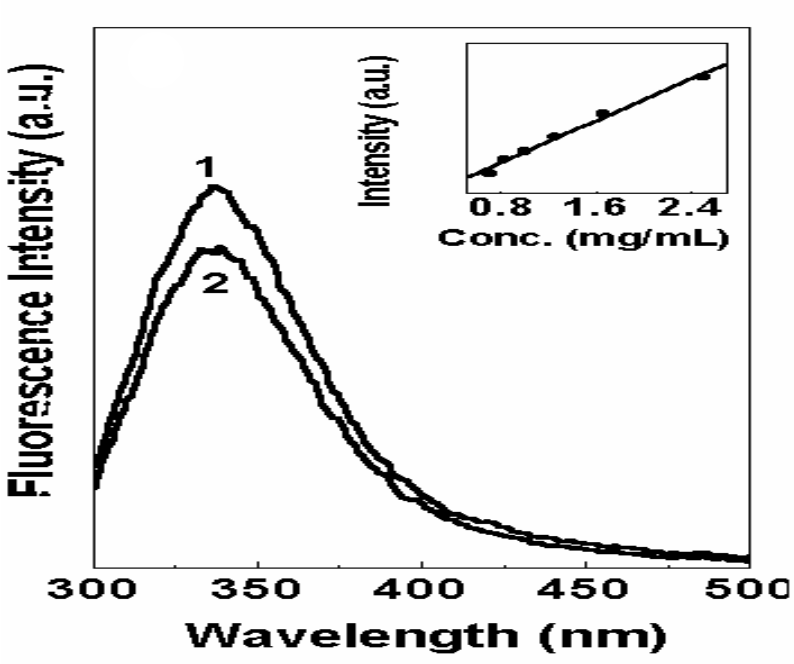

Figure 8. Fluorescence spectra of initial F-prot in solution at pH 3 (curve 1) and supernatant after centrifugation of gold nanoparticle-zeolite bioconjugate (curve 2). The inset shows the calibration curve for the fluorescence intensity at different concentration of the enzyme in solution at pH 3.

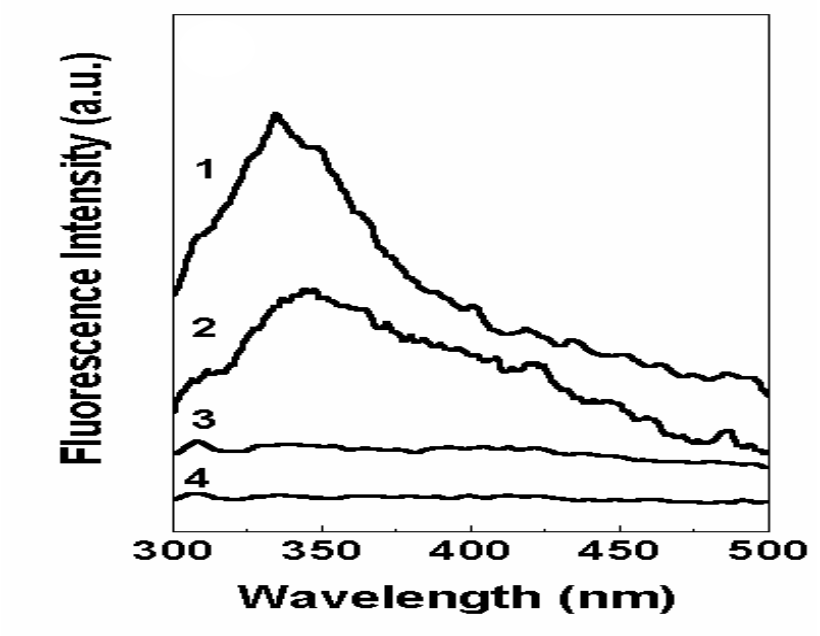

Figure 9. Fluorescence spectra of free F-prot in 10mM NaCl salt solution (curve 1), supernatants after centrifugation of amine functionalized zeolite bioconjugate (curve 2) and gold nanoparticle-zeolite bioconjugate (curve 3) dispersed in 10 mM salt solution and fluorescence spectra of 10 mM NaCl salt solution (curve 4)

In order to understand the electrostatic or covalent interactions between the enzyme with the amine functionalized zeolite and gold nanoparticle-zeolite, bioconjugate were dispersed in 2 mL, 10mM salt (NaCl) solution for 1 h. The bioconjugate were centrifuged and the supernatant was analyzed by fluorescence spectroscopy. Figure 9 shows the fluorescence spectra of the free F-prot solution prepared in 10 mM salt solution (curve 1). The F-prot solution shows a strong emission at 334 nm and as a consequence of radiative decay of the π -π^* transition from the tryptophan residues in the protein. The wavelength of this transition is a sensitive indicator of the tertiary structure of the protein. This indicates the tertiary structure of the enzyme is unperturbed. Curve 2 shows the fluorescence spectra of the supernatant of the enzyme bound to amine functionalized zeolite. It is seen that the supernatant shows a strong emission at 344 nm. This emphasizes the leaching of the weakly bound enzyme to the amine-functionalized zeolite, probably through electrostatic interactions and hydrogen bonding. Such leaching of the enzyme was not observed in gold nanoparticle-zeolite composite material, hence did not

show any emission (curve 3, Figure 9). This emphasizes the strong binding of the enzyme to the gold nanoparticles through the amine groups and cysteine residues present in the proteins. The fluorescence emission was absent in the 10 mM NaCl salt solution (curve 4, Figure 9) as expected.

Proteolytic activity measurements

The most important aspect of this study concerns retention of the proteolytic activity of F-prot after adsorption onto the gold nanoparticle-zeolite surface. Since the amount of F-prot bound to the bioconjugate could be estimated from UV-vis spectroscopy measurements quite accurately and also confirmed by fluorescence spectroscopy, it was possible to compare the proteolytic activity of the enzyme in the bioconjugate material and the free enzyme in solution under identical assay conditions. The proteolytic activity of the free F-prot in solution was determined to be 65 U/mg (Units per milligram) and that of the enzyme in the bioconjugate system was 78 U/mg. It is clear that the biological activity of the enzyme in the bioconjugate system is not compromised after immobilization on the surface of the gold nanoparticle-zeolite particles. Apart from that an enhancement of the proteolytic activity of the enzyme in the immobilized system was also observed. It may be due the microenvironment provided by the gold nanoparticles bound to the zeolite surface may be responsible for the increased activity. Such enhanced activity is also observed by organophosphorous hydrolase (OPH) enzyme immobilized on organic functionalized mesoporous silica (Lei et al., 2002).

In order to understand the role of the gold nanoparticles in the binding of the enzyme, the amine-functionalized zeolites were used directly in the immobilization of F-prot. Table 1 lists the proteolytic activities calculated from reaction of the F-prot-gold nanoparticle-zeolite and F-prot-zeolite bioconjugate materials over four sequential reuse cycles. In the first reaction, the proteolytic activity in the F-prot-zeolite material is ca. 70 % of that observed in the F-prot-gold nanoparticle-zeolite system. Thereafter, the proteolytic activity of the F-prot-zeolite material falls off rapidly losing complete activity by the 4th cycle of reaction. On the other hand, the F-prot-gold nanoparticle-zeolite system shows ca. 33 % of proteolytic activity after the 3th reuse cycle and retains 20 % of the initial

proteolytic activity after 4th cycle of reaction. These results clearly underline the remarkable reuse characteristics of the F-prot-gold nano-zeolite bioconjugate material

Table 1

Reuse characteristics of the bioconjugates

No of Cycles	Activity of F-prot immobilized on amine functionalized zeolite (U/mg)#	Activity of F-prot immobilized on gold nanoparticle- zeolite (U/mg)#
1	55	78
2	34	40
3	12	26
4	2	16

One unit of enzyme will produce a change in absorbance of 0.001 at 280 nm per minute at pH 3 and 37 ^{0}C measured as acid soluble products using Hb as the substrate

The earlier studies on immobilization of fungal protease in lipid bilayer stacks (Gole et al., 2000b), the proteolytic activity of the biocomposite lipid films fell to 15 % of the initial value by the third reuse cycle. The drop in proteolytic activity of F-prot upon reuse in the lipid films may be attributed to the inefficient release of the by-products after reaction or the presence of the unreacted/reacted trapped Hb molecules in the lipid matrix, thereby increasing the possibility of the poisoning/fouling of the biocomposite films. Such mass transport and poisoning issues are expected to be relatively unimportant in the case of the enzyme on the gold nanoparticle-zeolite surface. Moreover, the substrates are easily accessible to the enzyme immobilized on the surface of the gold nanoparticle-zeolite, thus mimicking the free enzyme in solution for all practical purposes.

The better reuse characteristics of the F-prot-gold nanoparticle-zeolite system may be due to that the F-prot molecules are bound much more strongly to the gold nanoparticles than

to the zeolite particles. This would significantly reduce the leaching out of the enzyme during the successive reaction cycles and thus, lead to improved retention of proteolytic activity. However, the monotonic and perceptible loss in proteolytic activity of the F-prot-gold nanoparticle-zeolite bioconjugate material as a function of reuse of cycles needs elaboration. It is possible that the gold nanoparticles detach from the surface of the amine functionalised zeolite during successive reaction cycles. Another possibility is the leaching out of F-prot from the bioconjugate material in successive reactions. In order to distinguish between the two mechanisms, atomic absorption spectroscopy (AAS) measurements were performed on the supernatant obtained after centrifugation of the reaction medium during each of the reaction cycles. Gold could not be detected by AAS [detection sensitivity ~ parts per million (ppm)] in any of the reaction cycles clearly shows that the nanoparticles are strongly bound to the underlying amine functionalised zeolite template. Hence the possibility of leaching of the gold nanoparticles from the surface of the zeolite is ruled out. This result indicates that the loss in activity may be related to loss of enzyme from the nanoparticle surface during reaction. UV-vis spectroscopy measurements were carried out on the supernatant from 10 mg of the F-prot-gold nanoparticle-zeolite bioconjugate material immersed in 2 mL of pH 3 buffer solution. 1 mL of the supernatant was analysed at intervals of 30 min, which is characteristic of the reaction times in the reuse measurements. After each measurement, the analyte was added back to the original buffer solution to simulate the reaction conditions precisely. It was observed that after 1 h of immersion, roughly 55 % of the total F-prot bound to the surface was released into the solution (estimated from the absorbance at 280 nm) (Stoscheck, 1990). Thereafter, only a marginal loss in the enzyme from the bioconjugate was observed. This percentage loss of enzyme correlates well with degree of loss of proteolytic activity during the first reuse cycle (Table 1). The initial loss of F-prot corresponds to loss of weakly bound enzyme from the bioconjugate. It is likely that the sheets of aggregated F-prot molecules observed in the SEM images of the F-prot-gold nanoparticle-zeolite bioconjugate (Figure 6C) correspond to the weakly bound enzyme that leaches out in the first reaction cycle. This is the possible mechanism indicated by the SEM image recorded from the F-prot-gold nanoparticle-zeolite bioconjugate material after one cycle of reuse (Figure 6D). It is clearly seen from this

figure that the percentage of aggregated F-prot sheets observed in the as-prepared bioconjugate material has reduced.

pH stability of F-prot-gold nanoparticle- zeolite bioconjugate

Figure10A shows plots of the proteolytic activity of free F-prot molecules in solution (triangles) and F-prot bound to the gold nanoparticle-zeolite template (circles) for reactions carried out after pre-incubating the enzyme/bioconjugate as a function of solution pH in the range 3 to 8. It is seen that optimum proteolytic activity in both the cases is at pH 3, with a marginal loss in proteolytic activity at pH 5. At pH 6, however, free enzyme molecules in solution retain only 7% of the proteolytic activity recorded at pH 3, while the F-prot molecules immobilized on the gold nanoparticle-zeolite template retain as much as 47% of the catalytic activity recorded at pH 3. Even at pH 8, F-prot in the bioconjugate material shows significant catalytic activity.

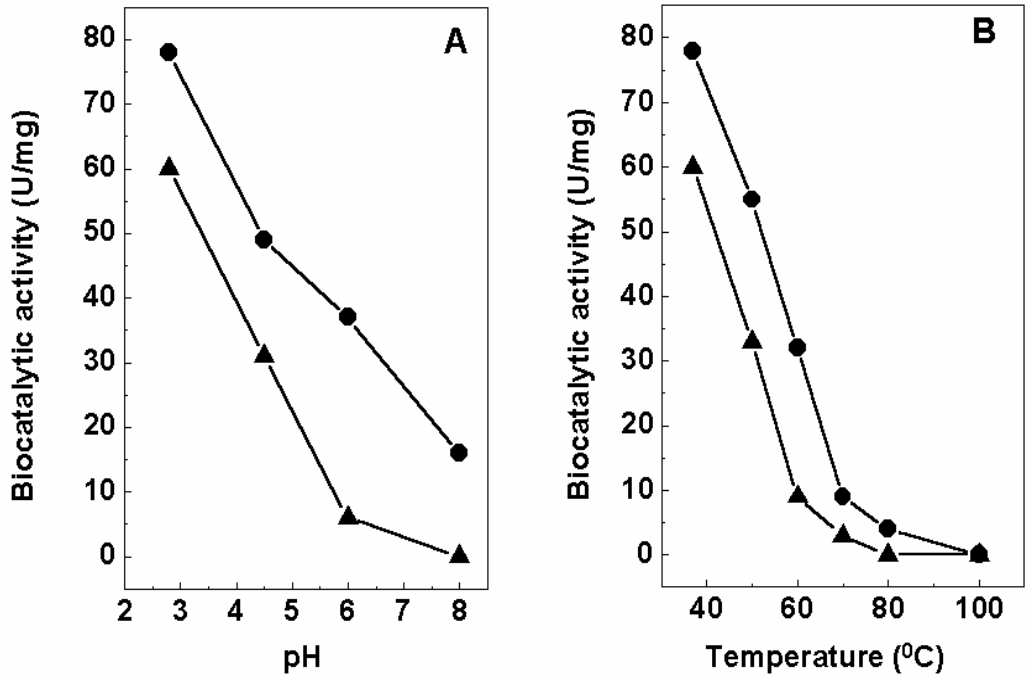

Figure 10. (A) pH-dependent proteolytic activity of free F-prot in solution (triangles) and F-prot in the gold nano-zeolite bioconjugate material (circles) preincubating for 1 h at different pH. (B) Temperature-dependent proteolytic activity of free F-prot in solution (triangles) and F-prot in the gold nano-zeolite bioconjugate material (circles) preincubating for 1 h at different temperature.

Temperature stability of F-prot-gold nanoparticle- zeolite bioconjugate

Figure10B shows plots of the variation in proteolytic activity of free F-prot molecules in solution (triangles) and F-prot immobilized on the gold nano-zeolite template (circles) as a function of temperature stability. To recollect, this reaction was carried out after preincubation for 1 h at the different temperatures and measuring the proteolytic activity at pH 3, 37 ^{o}C. At higher temperatures, dramatic differences in the proteolytic activity of the enzyme in the two cases are observed. At 50 ^{0}C, the free enzyme retains 42% of the starting proteolytic activity while the F-prot gold nano-zeolite bioconjugate retains 70% the room temperature proteolytic activity. This remarkable trend continues to higher temperatures as well with retention of 41% of initial proteolytic activity for the immobilized enzyme at 60 ^{o}C, while the free enzyme molecules in solution retains only 11% proteolytic activity. The increase in the thermal stability of the enzyme in the bioconjugate may arise from the conformational integrity of the enzyme structures after binding to the gold nanoparticles through the amine groups and cysteine residues present in the enzymes. The covalent linkage between the gold nanoparticles bound to the zeolite surface and F-prot would therefore lead to reduced conformational freedom with respect change in environmental parameters such as temperature and pH. Such enhancement in stability of immobilized enzymes as a function of temperature and pH has been observed for pepsin bound to alumina nanoparticles (Li et al., 2003) and for other enzyme within different supports (Arica et al., 1995; Akgol et al., 2002; Takahashi et al., 2000).

Temperature dependent proteolytic activity of F-prot-gold nanoparticle - zeolite bioconjugate

Figure 11 shows the effect of temperature on the proteolytic activity of free F-prot in solution (triangles) and F-prot immobilized on the gold nanoparticle-zeolite template (circles) at increasing temperature in the range of 35-65 ^{0}C at pH 3 for 30 min by using Hb as a substrate. It is seen that the proteolytic activity of the free F-prot in solution is strongly dependent on the temperature and an optimum temperature of reaction was determined to be 37 ^{o}C, whereas the optimum temperature for the F-prot immobilized on gold nanoparticle-zeolite was 45 ^{o}C. The increase in the optimum temperature is likely

due to the change in the enzyme structure upon immobilization. Such optimum temperature shift is also observed by immobilization of urease covalently attached to solid support (Akgol et al., 2002). Thus, the dynamic range of reaction of F-prot immobilized on gold nanoparticle-capped zeolite particles in terms of temperature and solution pH is considerably enhanced.

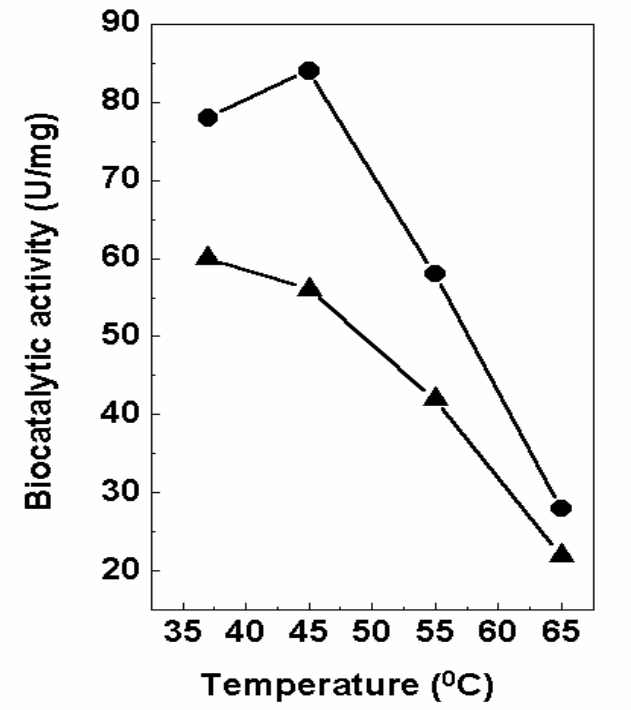

Figure 11. Variation in the proteolytic activity with temperature for free F-prot in solution (triangles) and the F-prot-gold nanoparticle-zeolite bioconjugate material (circles)

CONCLUSION

This study demonstrated the assembly of gold nanoparticles on amine-functionalized zeolite particles, the binding of the nanoparticles occurring via complexation with the free amine groups present in the zeolite. The gold nanoparticles bound to zeolite particles, act as excellent templates for the immobilization of the enzyme F-prot. F-prot in the bioconjugate system shows enhanced stability towards extreme pH and temperature conditions. The new biocatalyst material is easily separated from the reaction medium by sedimentation or mild centrifugation and exhibited reuse characteristics over four successive cycles. The optimum temperature of the bioconjugate system was observed to be higher than that of the free enzyme in solution.

PART-2

FABRICATION, CHARACTERIZATION AND ENZYMATIC ACTIVITY OF FUNGAL PROTEASE-GOLD NANOPARTICLE MEMBRANE BIOCONJUGATE

SUMMARY

Gold nanoparticles embedded in a polymeric membrane provide a biocompatible surface for the immobilization of the enzymes. This chapter deals with the synthesis of a free-standing gold nanoparticle membrane by the spontaneous reduction of aqueous chloroaurate ions by the diamine molecule DAEE (bis (2-(4-aminophenoxy) ethyl) ether) at a liquid-liquid interface. The presence of gold nanoparticles in the membrane enables facile modification of the surface properties of the membrane and this has been used to immobilize enzymes to the membrane. Fungal protease was used as a model enzyme to immobilize on the gold nanoparticle membrane leading to the formation of a new biocatalyst. A highlight of the new biocatalyst wherein the enzyme is bound to the gold nanoparticle membrane is the ease with which separation from the reaction medium may be achieved by simple filtration. In relation to the free enzyme in solution, the fungal protease in the bioconjugate material exhibited a slightly higher proteolytic activity and significantly enhanced pH and temperature stability. The fungal protease gold nanoparticle membrane bioconjugate material also exhibited proteolytic activity over ten successive reuse cycles.

INTRODUCTION

The combination of nanoscale inorganic materials with organic polymers are one of the exciting research area for designing biocompatible surfaces (Kickelbick, 2003; Liu et al., 2003; Voskerician et al., 2003; Selvakannan et al., 2004). Polymeric systems have played important roles as templates with different morphologies and tunable size for nanofabrication of a range of inorganic materials as they can be easily removed after reaction and can be further modified with different functional groups to enhance the interaction with the guest (Liu et al., 2003). These functionalized membranes have potential applications in separation of compounds, selective catalysis, artificial organs etc (Jirage et al. 1997). This method involves the synthesis of desired materials within the pores of a nanoporous membrane. Since the membrane contains cylindrical pores of uniform diameter, monodisperse nanocylinders of the desired material whose dimensions can be carefully controlled are obtained. New methods have been developed for the synthesis of various nanomaterials, which includes membrane based synthesis (Martin, 1996). Nanomaterials in the form of membranes are used as scaffolds for the binding of various biomolecules (Nienmeyer and Mirkin, 2004). Understanding the protein-membrane interactions is also important in designing matrices for efficient immobilization of biomolecules, with enhanced temporal, temperature, and pH stability, protection against degradation and intactness of natural confirmation of the immobilized biomolecule (Anvir and Braun 1996; Tischer and Kasche 1999).

In the previous section, the assembly of gold nanoparticle on zeolite microspheres and thereafter the use of gold nanoparticles for enzyme immobilization have been demonstrated. This section demonstrates the synthesis of a free-standing gold nanoparticle polymeric membrane at the interface between chloroform containing bis (2-(4-aminophenoxy) ethyl) ether (DAEE) and aqueous chloroauric acid solution and thereafter the use of gold nanoparticle embedded polymeric membrane for the immobilization of enzyme through a simple beaker-based immersion process. The objective of this work on one hand adds to development of gold based bioconjugates and on the other hand this study helps in developing robust enzyme-membrane composite materials for eventual biocatalytic and biotechnological applications.

MATERIALS AND METHODS

Chemicals

Chloroauric acid, bis (2-(4-aminophenoxy) ethyl) ether (DAEE) were obtained from Aldrich Chemicals. All other chemicals used are mentioned in the first part of this chapter.

Gold nanoparticle membrane synthesis

In a typical experiment, 100 mL of 10^{-2} M concentrated aqueous solution of chloroauric acid ($HAuCl_4$) was mixed with 100 mL of 10^{-2} M DAEE in chloroform for 4 h. A purple colored membrane was observed to form at the interface in the biphasic mixture within 1 h of reaction. This membrane was separated and repeatedly washed with deionized water and was used for enzyme immobilization. The amount of gold nanoparticles in the membrane was determined by atomic absorption spectroscopy (AAS) in the following manner. 10 mg of the gold nanoparticle membrane was dissolved in 20 mL saturated I_2 solution in KI and the volume was made up to 100 mL using deionized water. The solution was analyzed by a Varian Spectra AA 220 atomic absorption spectrometer (AAS) and was compared with a standard of gold solution to estimate the weight percent of gold nanoparticles in the membrane.

Formation of F-prot-gold nanoparticle biocatalyst

10 mg of the gold nanoparticle membrane was placed in 4.9 mL Glycine-HCl buffer (0.05 M, pH 3). To this solution, 100 μL of a stock solution consisting of 50 mg/mL of F-prot in Glycine-HCl buffer (0.05 M, pH 3) was added under mild stirring. After 1 h of stirring the F-prot-gold nanoparticle membrane, material was separated (Fig 1). The loss in absorbance at 280 nm in the supernatant (arising from π-π^* transitions in tryptophan and tyrosine residues in the enzyme) (Stoscheck, 1990; Nick Pace et al., 1995) was used to quantify the amount of F-Prot bound to the gold nanoparticle membrane for specific activity determination. The membrane thus obtained was rinsed several times with Glycine-HCl buffer (0.05 M, pH 3) solution and re-suspended in buffer solution (pH 3) and stored at 4^0C for further experiments. Since it is possible that the gold nanoparticles

leached out from the membrane and present in the supernatant could lead to an error in the quantitative analysis of the protein by UV-Vis spectroscopy in the gold nanoparticle-F-prot biocatalyst material, fluorescence spectroscopy measurements was performed. Fluorescence measurements were carried out on the initial concentration of the F-prot in solution at pH 3 and supernatant of F-prot in solution after separation of gold nanoparticle-F-Prot biocatalyst film using a Perkin-Elmer Luminescence Spectrophotometer (model LS 50B). The enzymes were excited at 280 nm and the emission band was monitored in the range 300 to 500 nm. The loss in fluorescence intensity (arising from π-π^* transitions in tryptophan and tyrosine residues in proteins) was used to quantify the amount of F-Prot bound to the gold nanoparticle membrane (Eftink and Ghiron, 1981). From the calibration curve of the fluorescence intensity for different concentrations of the F-prot in solution, the amount of the enzyme in the bioconjugate was known and used in the determination of the specific activity of gold nanoparticle-F-prot biocatalyst.

UV-Vis spectroscopy studies

UV-Vis spectra of $AuCl_4^-$ ions in the aqueous solution during the formation of gold nanoparticle membrane at the liquid-liquid interface at different time intervals (t = 0, 15, 45, 60, 120, 180 and 240 min) with DAEE in chloroform were recorded using a Jasco V570 UV/VIS/NIR spectrophotometer operated at a resolution of 1 nm. The solutions were diluted by a factor of 100 with the deionized water prior to recording the spectra. UV-Vis absorption spectra of the gold nanoparticle membrane were also recorded by placing the membrane on a quartz substrate and recording the spectra in the reflectance mode.

Transmission Electron Microscopy (TEM) measurements

TEM measurements were performed as described in the earlier section. Samples for TEM analysis were prepared by transferring the fully formed gold nanoparticle membrane from the liquid-liquid interface on carbon-coated copper TEM grids.

Energy dispersive analysis of X-rays (EDAX) measurements

Samples for EDAX measurement were prepared by transferring the fully formed gold nanoparticle membrane from the liquid-liquid interface onto a Si (111) substrate. These measurements were performed on a Leica Stereoscan-440 scanning electron microscope (SEM) equipped with a Phoenix EDAX attachment.

X-ray diffraction (XRD) measurements

XRD measurements of gold nanoparticles bound to the polymeric membrane were done on a Philips PW 1830 instrument operating at 40 kV and a current of 30 mA with Cu K_α radiation as described in the earlier section.

Proteolytic activity measurements

The proteolytic activity of free F-prot in solution and of F-prot-gold nanoparticle biocatalyst in Gly-HCl buffer (0.05 M, pH 3) was determined by reaction with 0.5 % Hb at 37 ^{0}C for 30 min as described in the earlier section. The F-prot-gold nanoparticle membrane biocatalyst was separated from the reaction medium, washed with copious amount of buffer and was used for recycling studies. In typical experiments to estimate the activity of the F-prot-gold nanoparticle biocatalyst, 10 mg of the F-prot-gold nanoparticle membrane in buffer was incubated with 1 ml of 0.5 % Hb solution at 37 ^{0}C for 30 min. After the incubation time, equal volume of 1.7 M perchloric acid was added to the reaction solution to precipitate the residual Hb. After 30 min, the precipitate was removed by centrifugation and the optical absorbance of the filtrate was measured at 280 nm. F-Prot digests Hb and yields acid soluble products (tryptophan and tyrosine residues), which are readily detected by their strong UV signatures at 280 nm (Gole et al., 2000b) The amount of F-Prot in the bioconjugate material was quantitatively estimated during the preparation of the bioconjugate as briefly discussed earlier. For comparison, the proteolytic activity of an identical concentration of the free enzyme in solution was determined. In order to determine the confidence limits of the proteolytic activity

measurements, separate measurements were done for 6 different F-prot-gold nanoparticle biocatalyst samples.

The temperature stability of the F-prot-gold nanoparticle biocatalyst was checked by pre-incubating the bioconjugate for 1 h at different temperatures in the range 40-100 ^{0}C and was compared with an identical amount of free enzyme in the Gly-HCl buffer (0.05 M, pH 3) under similar conditions. All the reactions were carried out after pre-incubation for 1 h at the different temperatures and the proteolytic activity was measured at pH 3 and 37 ^{0}C as described in the earlier section. The pH dependent variation in the proteolytic activity of the F-prot-gold nanoparticle membrane and free enzyme was studied at four different pH values (pH 3, Gly-HCl buffer; pH 4.5, 6, citrate acetate buffer; and pH 8 glycine-NaOH buffer) by pre-incubating for 1 h at 28 ^{0}C. All the reactions were carried out after pre-incubation for 1 h at the different pH and measuring the proteolytic activity at pH 3, 37 ^{0}C as described earlier. Reproducibility of the data was tested in three separate measurements carried out under identical conditions.

RESULTS AND DISCUSSION

Biocatalysts have been immobilized on a variety of supports obtained in different geometries based on their ultimate applications. Beaded forms are more useful for use in column reactors, whereas membrane forms are very useful in the fabrication of biosensors and or in membrane bioreactors. One of the important criteria for such applications of the membranes is their mechanical stability for reuse. Preparation of porous, mechanically stable membranes is also a prerequisite in the fabrication of biosensors or in membrane reactors. This chapter demonstrates the synthesis of a free standing gold nanoparticle polymeric membrane at the interface between chloroform containing bis (2-(4- aminophenoxy) ethyl) ether (DAEE) and aqueous chloroauric acid solution and thereafter the use of the gold nanoparticle embedded polymeric membrane in the immobilization of the enzyme fungal protease (Figure 1).

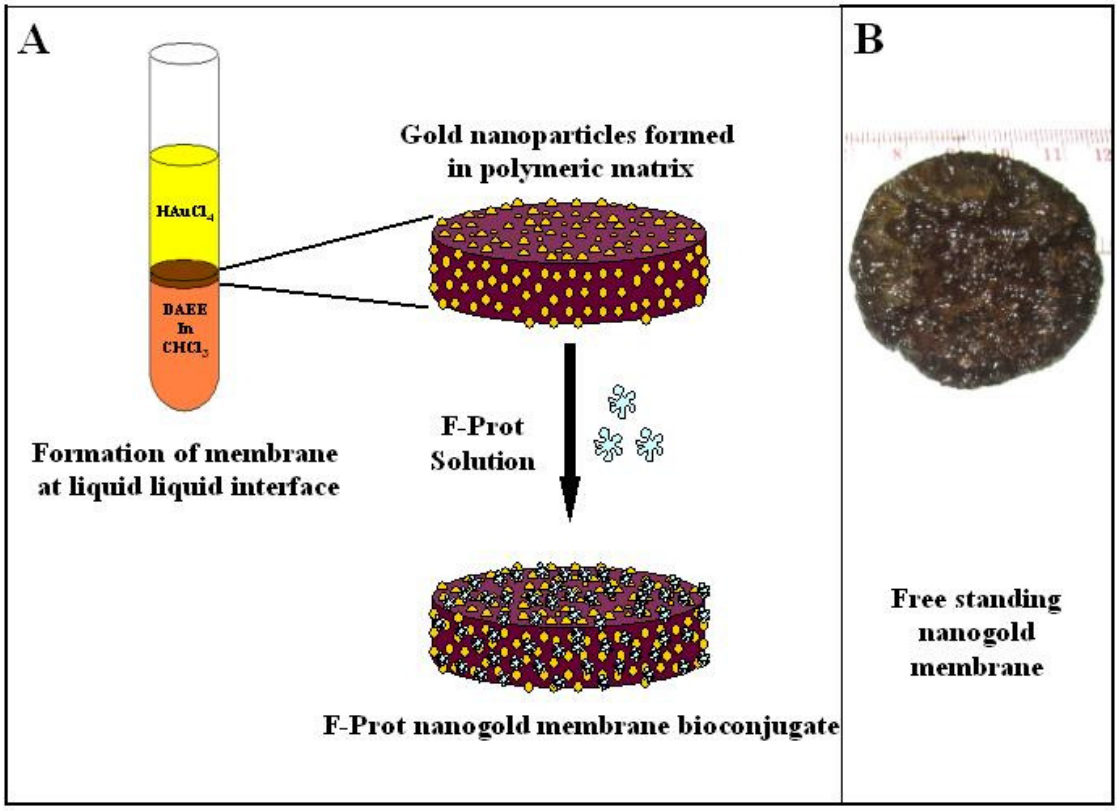

Figure 1. (A) Schematic (not to scale) showing the synthesis of gold nanoparticle polymeric membrane at the liquid-liquid interface and thereafter its use for enzyme immobilization. (B) Photograph of the air-dried, free standing gold nanoparticle membrane

Preparation of the gold nanoparticle membrane material

Figure 2A shows the UV-Vis spectrum recorded in the reflectance mode from the gold nanoparticle membrane transferred onto a quartz substrate. A strong absorption band centered at 510 nm was observed. This absorption band arises due to excitation of surface plasmons in gold nanoparticles and was responsible for their vivid pink-purple color (Patil et al., 1999). The amine groups of DAEE molecules at the interface are protonated (pH of $HAuCl_4$ solution ~ 3.2) leading to electrostatic complexation with $AuCl_4^-$ ions. That the electrostatic complexation with gold ions was a crucial step in the formation of the gold nanoparticle membrane is indicated by the control experiment where a similar interfacial reaction was carried out with the aqueous $HAuCl_4$ solution maintained at pH 9. At this pH, the amine groups in DAEE would not be protonated and no membrane formation was observed even after 12 h of reaction. Reduction of chloroaurate ions takes place at the interface and the oxidized DAEE molecules cap the spontaneously formed gold nanoparticles preventing their further aggregation. The inset of Figure 2A shows the UV-Vis spectra recorded from the $AuCl^-_4$ ions in the aqueous solution during the formation of gold nanoparticle membrane at the liquid-liquid interface for different time intervals (t = 0, 15, 45, 60, 120, 180 and 240 min). The peak position at 214 nm corresponds to light absorption by aqueous $AuCl^-_4$ ions (Li et al., 2003). It is observed that there was a steady decrease in the peak intensity at 214 nm with time indicating that the chloroaurate ions were consumed in the formation of gold nanoparticles at the liquid-liquid interface. As briefly mentioned earlier, the gold nanoparticle membrane was surprisingly robust, highly flexible and can be handled easily (Figure 1B). These membranes could be synthesized in a wide range of sizes and thickness by simple variation in the reaction time and DAEE : $AuCl_4^-$ molar ratio (Selvakannan et al., 2004). The gold nanoparticle membrane used in this study had a thickness of ca. 0.5 mm after drying.

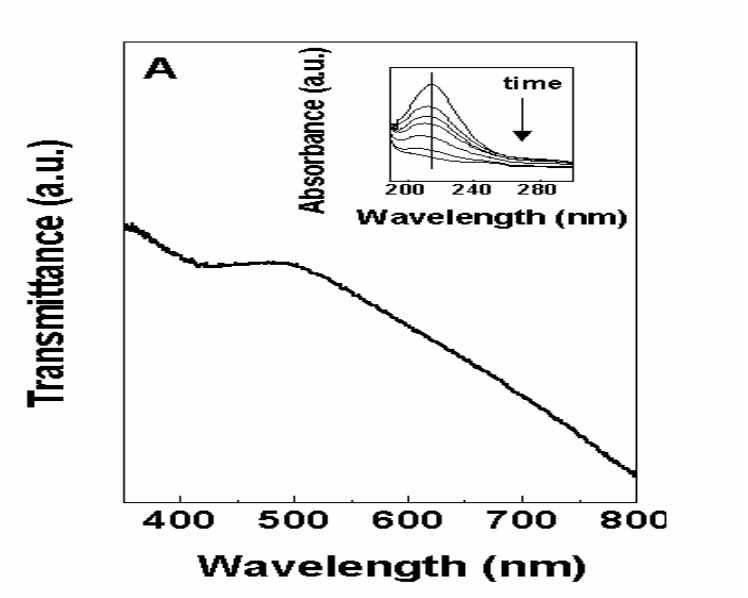

Figure 2. (A) UV-Vis spectrum recorded from the gold nanoparticle membrane on a quartz substrate. The inset shows the UV-Vis spectra recorded from the aqueous solution of chloroaurate ions during the formation of gold nanoparticle membrane at the liquid-liquid interface at different times of reaction. The curves correspond to t = 0, 15, 45, 60, 120, 180 and 240 min, the arrow of time indicated in the figure.

TEM measurements

The microstructure of the gold nanoparticle membrane was determined from TEM studies. Figure 3A and B show low and high magnification TEM micrographs of the membrane.

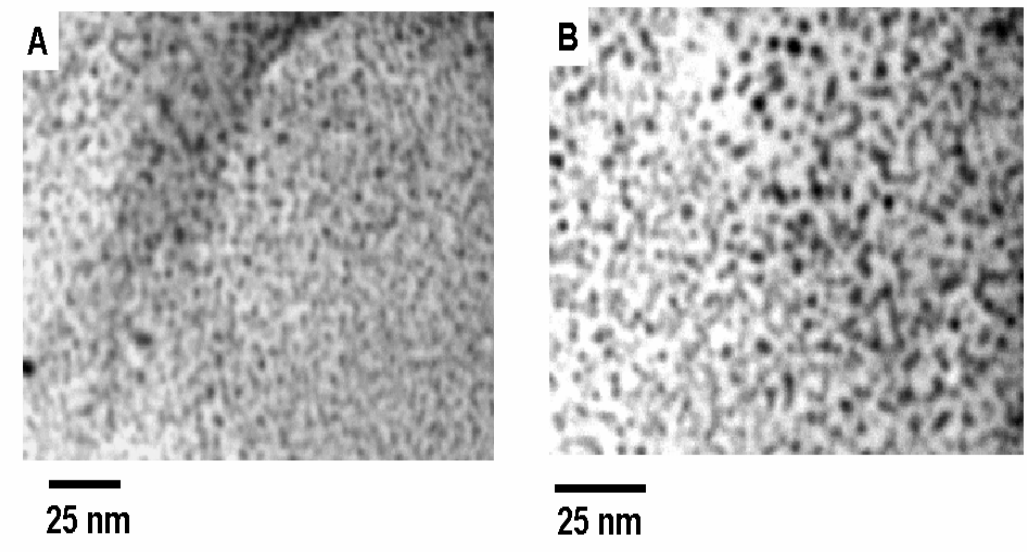

Figure 3 (A) and (B) Representative TEM images of gold nanoparticle membrane

It can be clearly seen that the gold nanoparticles (dark features) are uniformly dispersed in the polymeric membrane with little evidence for aggregation of the gold particles. The gold nanoparticles are fairly spherical and range in size from 4 to 10 nm. As mentioned previously, the chloroaurate ions form electrostatic complexes with the protonated amine groups of DAEE molecules and then are reduced. After reducing the chloroaurate ions, the oxidized DAEE molecules form a polymer and cap the spontaneously formed gold nanoparticles preventing their further aggregation. This occurs in a highly localized manner at the liquid-liquid interface leading to membrane formation at the interface. DAEE molecules possess two terminal aniline segments, which are known to be good reducing agents. Oxidation of DAEE most probably proceeds through formation of a polymeric network derived from DAEE at the liquid-liquid interface. The gold atoms formed by the reduction of $AuCl_4^-$ ions diffuse along the polymeric network, aggregate into larger gold nanoparticles as seen in the Figure 3A and B, thereby yielding a polymeric network with inclusions of gold nanoparticles at the liquid-liquid interface.

An estimation of the gold nanoparticle fraction in polymeric membrane was done by leaching out the gold nanoparticles from the membrane using a saturated I_2 solution in KI. The dissolved gold solution was analyzed by atomic absorption spectrometry (AAS) as described in the experimental section. The gold nanoparticle membrane was kept in the iodine solution for more than 5 hours. The mass loading of the gold nanoparticles in the gold nanoparticle polymeric membrane was estimated from AAS analysis to be ca. 35 weight %.

XRD measurements

Figure 4 shows the powder XRD pattern of the gold nanoparticle membrane. The sharp Bragg reflections seen in the figure underline the fact that the gold particles present in the membrane were nanocrystalline. The Bragg reflections in the gold nanoparticle membrane could be indexed on the basis of the fcc structure of gold and are identified in Figure 4. It is interesting to note that the ratios of the (311) reflection with other reflections is greater that that observed in powder diffractions patterns for gold (The XRD patterns were indexed reference to the gold structure from ASTM Chart, Card no.4-0784) indicating that there is preferred growth of the gold nanocrystals along the (311)

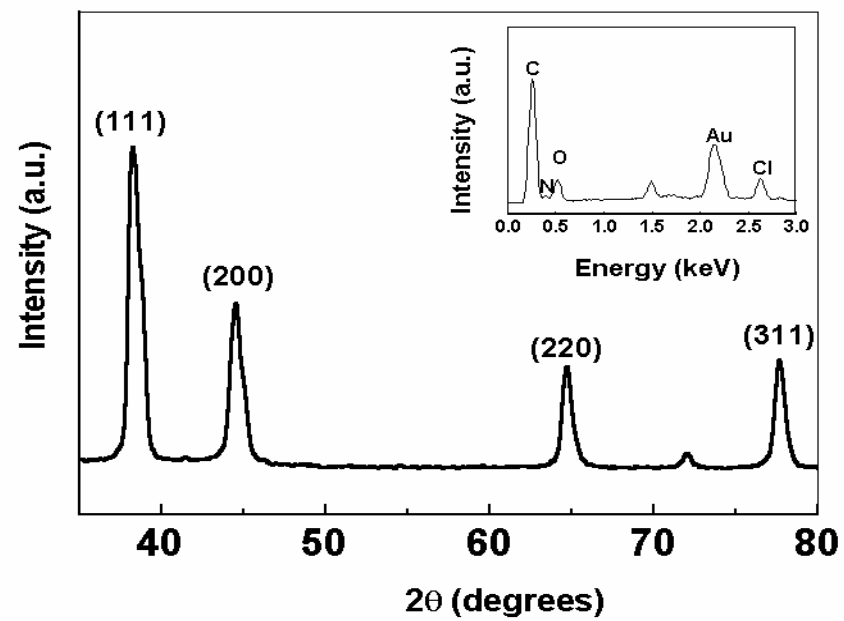

Figure 4. XRD pattern recorded from the gold nanoparticle membrane. The inset shows the spot profile EDAX spectrum recorded from the gold nanoparticle membrane

direction within the membrane. The inset of Figure 4 shows the EDAX spectrum recorded from one of the gold nanoparticles bound to the polymeric membrane. In addition to the expected prominent Au signal, a weak chlorine signal is also observed which is attributed to the presence of unreduced gold ions ($AuCl_4^-$) bound to the surface of the gold nanoparticles in membrane. As mentioned briefly earlier, the first step in the formation of the gold nanoparticle membrane is electrostatic complexation of $AuCl_4^-$ ions with protonated amine groups of DAEE molecules at the liquid-liquid interface and incomplete reduction of the gold ions would explain their presence in the membrane.

Enzyme quantitation analysis

The amount of F-prot in the F-prot-gold nanoparticle membrane bioconjugate was quantitatively estimated from UV-Vis and fluorescence spectroscopy measurements during preparation of the bioconjugate material as briefly mentioned earlier. From UV-Vis spectroscopy measurements, the amount of F-prot bound to 10 mg of the gold nanoparticle membrane was found to be 1.25 mg, the immobilization of the enzyme on the gold nanoparticles occurring via amine groups and cysteine residues in the proteins which are known to bind strongly with gold colloids (Zhao et al., 1996; Keating et al., 1998; Patolsky et al., 1999; Gole et al., 2001a; Gole et al., 2001b; Niemeyer and Ceyhan,

2001; Gole et al., 2002). It is possible that F-prot binds directly to the polymeric backbone. This contribution was estimated by first leaching out the gold fraction of the gold nanoparticle membrane by iodine treatment and then immersing the polymer membrane in F-prot under conditions identical to that employed for the as-prepared gold nanoparticle membrane. From UV-Vis spectroscopy analysis, it was determined that 10 mg of the bare membrane bound ca. 1.0 mg of F-prot, possibly through non-specific electrostatic and hydrogen bonding interactions.

The presence of small amounts of the gold nanoparticles in the supernatant could lead to an error in enzyme loading determination from UV-Vis spectroscopy measurements. In order to overcome this problem, fluorescence spectroscopy was also used to quantify the amount of enzyme in the F-prot-gold nanoparticle membrane material as described in the experimental section. Figure 5 shows the fluorescence emission spectra of different concentrations of F-prot (0.02, 0.04, 0.06, 0.08, 0.1 mg/ml) in solution at pH 3. The concentration of enzyme in the bioconjugate was determined from the calibration curve shown in the inset of Figure 5, the amount of enzyme bound to 10 mg of the gold nanoparticle membrane was found to be 1.20 mg in reasonable agreement with the UV-Vis spectroscopic estimate. From fluorescence spectroscopy measurements, direct binding of F-prot to the bare polymeric membrane was estimated to be 0.92 mg, again in agreement with UV-Vis spectroscopic estimates.

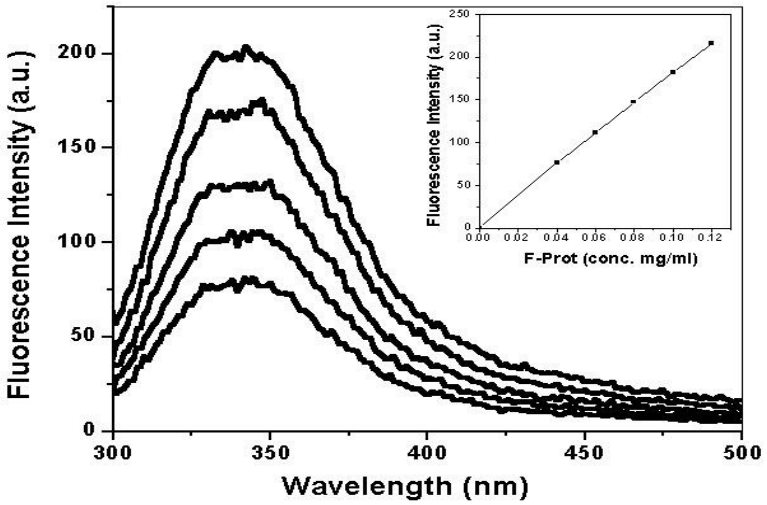

Figure 5. Fluorescence spectra of different concentration of F-prot in solution at pH 3. The inset shows the linear plot of enzyme concentration versus fluorescence intensity.

Proteolytic activity measurements

The most important aspect of this study concerns retention of the proteolytic activity of F-prot after adsorption onto the gold nanoparticle membrane. Since the amount of F-prot bound to the bioconjugate could be estimated quite accurately from independent UV-Vis and fluorescence spectroscopy measurements, it is possible to compare the specific proteolytic activity of the enzyme in the bioconjugate material and the free enzyme in solution under identical assay conditions. The proteolytic activity of the free F-prot in solution was determined to be 60 U /mg and that of the enzyme in the gold nanoparticle membrane was 68 U/mg. An analysis of the proteolytic activity of the F-prot-gold nanoparticle membrane bioconjugate material in five separate reactions yielded a standard deviation of ca.10 % and therefore, the proteolytic activity of the enzyme immobilized on the gold nanoparticle membrane bioconjugate material relative to free enzyme in solution is expected to be experimentally significant.

In order to understand the role of the gold nanoparticles in binding F-prot, the enzyme was also bound directly to the membrane after leaching out of the gold component. A small percentage of F-prot was bound to the polymeric component of the gold nanoparticle membrane through non-specific interactions and it would be important to understand the contribution of this non-specifically bound F-prot component to the overall biocatalyic behaviour of the F-prot-gold nanoparticle bioconjugate material. Figure 6 shows the results of 10 successive cycles of reuse of the F-prot-gold nanoparticle membrane (squares) and F-prot-polymeric membrane (triangles). In the first reaction, the proteolytic activity in the F-Prot-polymeric material is 60 U/mg, ca. 88 % of that observed in the F-Prot-gold nanoparticle membrane. Thereafter, the proteolytic activity of the F-Prot-polymeric material falls off rapidly losing complete activity by the 7th cycle of reaction. On the other hand, the F-prot-gold nanoparticle membrane system shows ca. 76% of proteolytic activity after the 2nd reuse cycle and retains 35% of the initial proteolytic activity after 8th cycle of reaction. These results clearly underline the remarkable reuse characteristics of the F-prot-gold nanoparticle membrane bioconjugate

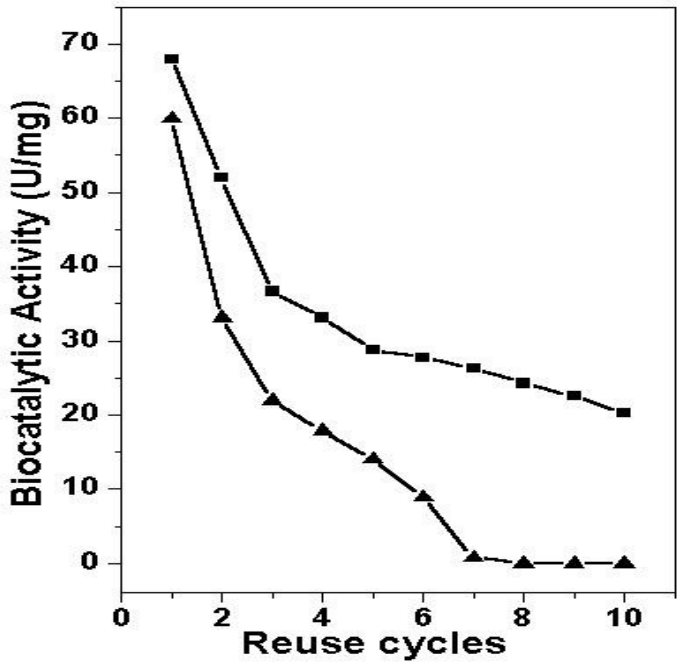

Figure 6. Proteolytic activity of F-prot-gold nanoparticle membrane bioconjugate materials (Squares) and F-prot bound to the polymeric membrane after removal of gold nanoparticles (triangles) over 10 successive reuse cycles.

material and represent a major advance in the development of gold nanoparticle based enzyme immobilization protocols.

This retention of proteolytic activity of F-prot-gold nanoparticle membrane bioconjugate during reuse is to be contrasted with the almost complete loss in activity of the same enzyme immobilized in thermally evaporated fatty amine films after just 3 cycles of reuse (Gole et al., 2000b). Clearly the blockage of diffusion pathways of substrate molecules implicated in the earlier study for loss in activity with recycling is not operative in the bioconjugation strategy presented in this work. This is a salient feature of the work with immense commercial implications. However, the monotonic and perceptible loss in proteolytic activity of the F-prot-gold nanoparticle membrane biocatalyst with reuse needs elaboration. It is possible that the gold nanoparticles detach from membrane during successive reaction cycles. Another possibility is the leaching out of F-prot from the bioconjugate material in successive reactions due to weak binding with the underlying gold nanoparticle scaffold. In order to distinguish between the two mechanisms, atomic absorption spectroscopy (AAS) measurements were performed on the supernatant

obtained after centrifugation of the reaction medium during each of the reaction cycles. Gold could not be detected by AAS [detection sensitivity ~ parts per million (ppm)] in any of the reaction cycles clearly showing that the nanoparticles are strongly bound to the underlying polymeric membrane. This results points to loss of enzyme from the gold nanoparticle membrane surface during reaction. UV-Vis spectroscopy measurements were carried out on the supernatant from 10 mg of the F-prot-gold nanoparticle membrane bioconjugate material immersed in 5 ml of pH 3 buffer solution. 1 mL of the supernatant was analysed in intervals of 30 min, which is characteristic of the reaction times in the reuse measurements. After each measurement, the analyte was added back to the original buffer solution to simulate the reaction conditions precisely. It was observed that after 2 h of immersion, roughly 50% of the total F-prot bound to the gold nanoparticle membrane was released into solution (estimated from the absorbance at 280 nm). This percentage loss of enzyme correlates well with degree of loss of proteolytic activity during the first four reuse cycle (Figure 6). Thus the initial loss of F-prot corresponds to loss of weakly bound enzyme from the bioconjugate, this being the weakly bound F-prot component bound non-specifically to the polymeric membrane and not the gold nanoparticles.

pH stability of F-prot-gold nanoparticle membrane bioconjugate

Figure 7A shows the proteolytic activity of free F-prot in solution and F-prot bound to the gold nanoparticle membrane as a function of solution pH in the range 3 to 8 by pre-incubating for 1 h at 28 ^{o}C and measuring the proteolytic activity at pH 3, 37 ^{o}C as descried in the experimental section. It is seen that optimum proteolytic activity in both the cases is at pH 3. At pH 4.5, however, the free enzyme in solution retain only 54% of the proteolytic activity recorded at pH 3, while the F-Prot immobilized on the gold nanoparticle membrane retains as much as 85% of the catalytic activity recorded at pH 3. At pH 6 the free enzyme in solution shows 13% of the proteolytic activity recorded at pH 3 but the F-prot immobilized on the gold nanoparticle membrane retains 38 % of the proteolytic activity recorded at pH 3. Even at pH 8, F-prot in the bioconjugate material shows significant catalytic activity.

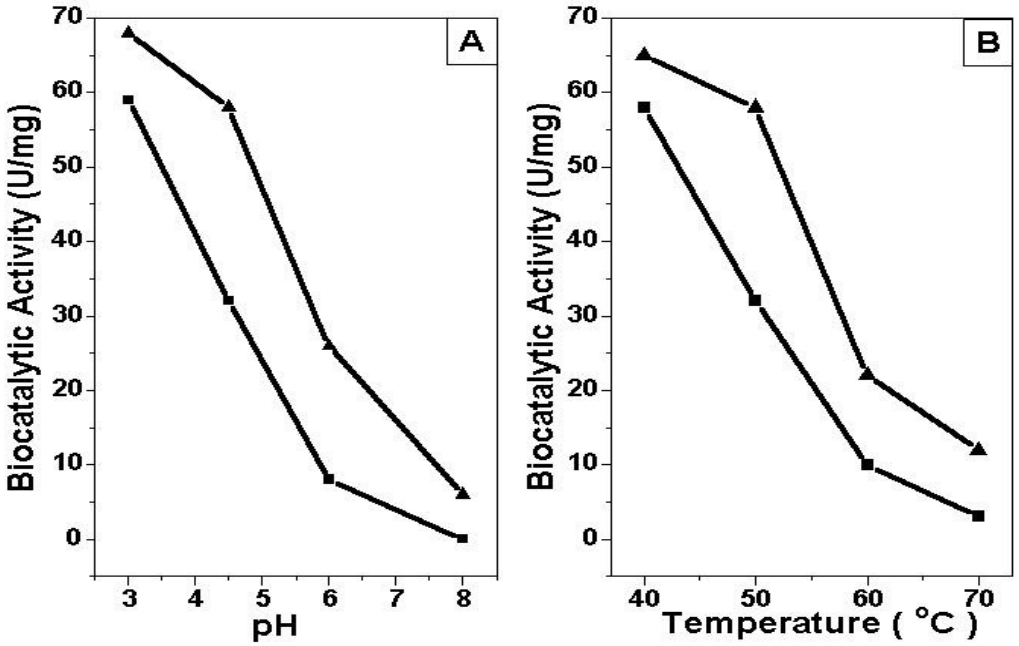

Figure 7. (A) pH-dependent proteolytic activity of free F-prot in solution (squares) and F-prot in the gold nanoparticle membrane (triangles) preincubating for 1 h at different pH. (B) Temperature-dependent proteolytic activity of free F-prot in solution (squares) and F-prot in the gold nanoparticle membrane (triangles) preincubating for 1 h at different temperature.

Temperature stability of F-prot-gold nanoparticle membrane bioconjugate

Figure 7B shows the variation in proteolytic activity of free F-prot in solution and in immobilized on the gold nanoparticle membrane as a function of temperature. To recollect, this reaction was carried out after pre-incubation of the biocatalyst for 1 h at the different temperatures and measuring the proteolytic activity at pH 3, 37 ^{o}C. At higher temperatures, dramatic differences in the proteolytic activity of the enzyme in the two cases are observed. At 50 ^{0}C, the enzyme in the F-prot-gold nanoparticle membrane shows 85% of the initial proteolytic activity, while the free enzyme in solution retains only 53% proteolytic activity. At 60 ^{0}C, the difference is much more marked with the F-prot-gold nanoparticle membrane retaining 32% of initial proteolytic activity while the free enzyme in solution retains only 16% of the initial activity. The increase in the thermal stability of the enzyme in the F-prot-gold nanoparticle bioconjugate material may

arise from the conformational integrity of the enzyme structures after binding to the gold nanoparticles through the amine and cysteine residues present in the enzymes. The covalent linkage between the gold nanoparticles in the polymeric membrane and F-prot would therefore lead to reduced conformational freedom with respect to change in environmental parameters such as temperature and pH. Such enhancement in stability of immobilized enzymes as a function of temperature and pH has been observed for pepsin bound to alumina nanoparticles (Li et al., 2003) and for other supports (Arica et al., 1995; Takahashi et al., 2000; Akgol et al., 2002).

CONCLUSION

This study demonstrated the synthesis of a free-standing gold nanoparticle membrane by the spontaneous reduction of aqueous chloroaurate ions by the diamine molecule DAEE at a liquid-liquid interface. The membrane consists of gold nanoparticles embedded in a polymeric background and was robust and malleable. The presence of gold nanoparticles in the membrane enables facile modification of the properties of the membrane, which acts as a biocompatible template for the immobilization of the enzyme F-prot leading to the formation of an interesting new biocatalyst. F-prot in the bioconjugate system shows enhanced stability towards higher pH and temperature conditions. This new biocatalyst can be easily separated from the reaction medium and exhibits reuse characteristics over ten successive cycles.

REFERENCES

Ahamed, A., Mukharjee, P., Mandal, D., Senapathi, S., khan, M.I., Kumar, R., and Sastry, M., (2002) *J. Am Chem Soc*, **124**, 12108-12109.

Akgol, S., Yalcinkaya, Y., Bayramoglu, G., Denizil, A., and Arica, M.Y. (2002) *Process Biochem.* **38,** 675-683.

Albers, W. M., Vikholm, I., Viitala, T., and Peltonen, J. (2001) *Handbook of surfaces and interfaces of materials.* **Vol. 5**, Chapter 1, Academic Press, San Diego, USA.

Alivisatos, A. P., Johnsson, K.P., Peng, X., Wilson, T.E., Loweth, C.J., Bruchez, M. P., and Schultz, P.G. (1996) *Nature* (London), **382**, 609-611.

Alvarez, M. M., Khoury, J. T., Schaaf, T. G., Shafigullin, M. N., Vezmar, I., and Whetten, R. L. (1997) *J. Phys. Chem. B* **101**, 3706-3712.

Anvir, D and Braun, S. (1996) *Biochemical Aspects of Sol-Gel Science and Technology.* Kluwer: Hingham, M. A.

Arica, M. Y., Hasirci, V., and Alaeddinoglu NG. (1995) *Biomaterials* **16**, 761-768.

Bachand, G.D., Soong, R. K., Neves, H.P., Olkhovets, A., Craighead, H.G., and Montemagno, C. D. (2001) *Nano. Lett*., **1**, 42-44.

Bain, C. D., Troughton, E. B., Tao, Y, T., Evall, J., Whitesides, G. M., and Nuzzo, R. G. (1989) *J. Am. Chem. Soc.* **111**, 321-335.

Balavoine, F., Schultz, P., Richard, C., Mallouh, V., Ebbesen, T.W., and Mioskowski, C. (1999) *Angew Chem Int Ed Engl*, **38**, 1912-1915.

Bardea, A., Katz, E., Tao, G., Buckmann, A. F., and Heller, A. (1997) J. *Am. Chem. Soc. 119*, 9114-9119.

Basinska, T., and Calwell, K. D. (1999) *ACS Symp. Ser.* **731,** 162-177.

Battacharya, P., Xu, J., Varo, G., and Birge, R. (2002) *Optics Lett*. **27**, 839-841.

Belosludtsev, Y., Iverson, B., Lemeshko, S., Eggers, R., Wiese, R., Lee, S., Powdrill, T., and Hogan, M. (2001) *Anal. Biochem*. **292**, 250-256.

Beveridge, T. J., and Murray, R. G. E. (1980) *J. Bacteriol*, **141**, 876-887.

Birge, R. R. (1990) *Ann. Rev. Phys. Chem.* **41**, 683-733.

Blaurock, A. E., and Stoeckenius, W (1971) *Nature.* **233**, 152-155.

Boussand, A., Dziri, L., Arechabaleta, N. J., Tao, N. J., and Leblanc, R. M. (1998) *Langmuir* **14**, 6215-6219.

Bradosova, M., Tregold, R. H., and Ali-Adib, Z. (1995) *Langmuir* **11**, 1273-1276.

Brown, L. O., and Hutchinson, J. E. (1999) *J. Am. Chem. Soc.* **121**, 882-883.

Burton, S. G., Cowan, D. A., and Woodley, J. M. (2002) *Nature Biotechnol.* **20**, 37-45.

Caruso, F., and Mohwald, H. (1999) *J. Am. Chem. Soc.* **121**, 6039-6046.

Caruso, F., Furlong, D. N., Airaga, K., Ichinose, I., and Kunitake, T. (1998) *Langmuir* **14**, 4559-4565.

Chen, G.S., Mrksich, M., Haung, S., Whitesides, G. M., and Ingeber, D. E. (1997) *Science*, **276**, 1425-1427.

Chen, R.J., Zhang, Y., Wang, D., and Dai, H. (2001) *J. Am Chem Soc*, **123**, 3838-3839.

Chen, X., Hu, N., Zeng, Y., Rusling, J. F., and Yang, J. (1999) *Langmuir*, **15**, 7022-7030.

Crumbliss, A. L., Perine, S. C., Stonehuerner, J., Tubergen, K. R., Zhao, J., and O'Daly, J. P. (1992) *Biotech. Bioeng.* **40**, 483-490.

DeSantis, G., and Jones, J. B. (1999) *Curr. Opin. Biotechnol.* **10**, 324-330.

Diederichsen, U., Lindhorst, T. K., Westermann, B., and Wessjohann, L. A. (1999) *Bioorganic Chemistry,* Wiley-VCH, Weinheim.

Drexler, E. K. (1981) *Proc. Natl. Acad. Sci. USA*, **78**, 5275-5278.

Dugas, H (1989) *Bioorganic Chemistry*, Springer, New York,

Duran, N., and Esposito, E. (2000) *Appl. Catal. B.* **28**, 83-99.

Dyal, A., Loos, K., Noto, M., Chang, S. W., Spagnoli, C., Shafi, K. V. P. M., Ulman, A., Cowman, M., and Gross, R. A. (2003) *J. Am. Chem. Soc.* **125**, 1684-1685.

Edman, C.F., Raymond, D.E., Wu, D.J., Tu, E.J., Sosnowski, R.G., Butler, W.F., Nerenberg, M., and Heller, M.J. (1997) *J. Nucleic Acids Res*, **25**, 4907-4914 .

Eftink, M. R., and Ghiron, C. A. (1981) *Anal. Biochem.* **114**, 199-227.

Elgersma, A. V., Zsom, R. L. J., Norde, W., and Lyklema, J. (1990) *J. Colloid and Interface Sci.* **138**, 145-156.

Fang, J., and Knobler, C. M.(1996) *Langmuir* **12**, 1368-1374.

Fang, X., Liu, X., Schuster, S., and Tan, W. (1999) *J. Am. Chem. Soc.* **121**, 2921-2922.

Fendler, J.H. 1982. Membrane mimetic Chemistry, Wiley-Interscience: New York

Franchina, J. G., Lackowski, W. M., Dermody, D. L., Crooks, R. M., Bergbreiter, D. E., Sirkar, K., Russell, R. J., and Pishko, M. V. (1999) *Anal. Chem.* **71**, 3133-3139.

Galow, T.H., Boal, A.K., and Rotello, V. M. (2000) *Adv. Mater.* **12**, 576-579.

Gardea-Torresdey, J.L., Parsons, J.G., Gomez, E., Perelta-Videa., Troiani, H.E., Santigo, P., and Yacaman, M.J. (2002) *Nano. Lett*., **2**, 397-401.

George, S. P., Gole, A., Sastry, M., and Rao. M. B. (2002) *Langmuir*, **18**, 9494-9501.

Gilardi, G., and Fantuzzi, A. (2001) *Trends. Biotechnol.* **19**, 468-476.

Gole, A., Dash, C., Mandale, A. B., Rao, M., and Sastry, M. (2000b) *Anal. Chem.* **72**, 4301-4309.

Gole, A., Dash, C., Ramakrishnan, V., Sainkar, S. R., Mandle, A. B., Rao, M., and Sastry, M. (2001a) *Langmuir* **17**, 1674-1679.

Gole, A., Dash, C., Rao, M., and Sastry, M. (2000a) *J. Chem. Soc.,Chem. Commun.* 297-298.

Gole, A., Dash, C., Soman, C., Sainkar, S. R., Rao, M., and Sastry, M. (2001b) *Bioconjugate Chem*., **12**, 684-690.

Gole, A., Vyas, S., Phadtare, S., Lachke, A., and Sastry, M. (2002) *Colloids and Surfaces B: Biointerface.* **25**, 129-138.

Govardhan, C. P. (1999) *Curr. Opin. Biotechnol.* **10**, 331-335.

Guilbault, G. (1984) *Analyticl use of immobilized enzymes,* Marcel Dekker: New York.

Hamachi, I., Fujita, A., and Kunitake, T. (1994) *J. Am. Chem. Soc.* **116**, 8811-8812.

Hamachi, I., Honda, T., Noda, S., and Kunitake, T. (1991) *Chem. Lett.* 1121-1124.

Hamachi, I., Noda, S., and Kunitake, T. (1990) *J. Am. Chem. Soc.* **112**, 6744-6745.

He, J., Li, X., Evans, D. G., Duan, X., and Li, C. (2000) *J. Molecular Catalysis. B: Enzymatic.***11**, 45-53.

Heller, A. (1992) *J. Phys. Chem*. **92**, 3579-3587.

Hianik, T., Snejdarkova, M., Passechnik, V.I., Rehak, M., and Babinkova, M. (1996) *Bioelectrochem. Bioenerg.* **41**, 221-225.

Higashi, N., Inoue, T., and Niwa, M. (1997) *J. Chem. Soc. Chem. Commun.* 1507-1508.

Higashi, N., Takahashi, M., and Niwa, M. (1999) *Langmuir*, **15**, 111-115.

Huang,W., Taylor, S., Fu, K., Lin, Y., Zhang, D., Hanks, T.W., Rao, A., and Sun, Y. (2002) *Nano Lett*, **2**, 311-314.

Jakeway,S.C., de Mello, A. J., Russel, E. L., and Fresenius. (2000) *J. Anal. Chem.* **366**, 525-539.

Jirage, K, B., Hulteen, J. C., and Martin, C. R (1997) *Science* **278**, 655-658.

Joerger,R., Klaus, T., and Granqvist, C.G.(2000) *Adv. Mater.* **12**, 407-409.

John, P.M. St., Davis, R., Cady, N., Czajka, J., Batt, C.A., and Craighead, H.G. (1998) *Anal. Chem.* **70**, 1108-1111.

Jost, P.C., and Griffith, O.H. (1982) Lipid-Protein Interactions, John Wiley & sons: New York, Vol.2

Kaleta, W., and Nowinska, K. (2001) *Chem. Commun.* 535-536.

Kalisz, H. M. *Advances in Biochemical Engineering,* Biotechnology, Springer-Verlag: New York, (1988) Vol. 86

Keating, C. D., Kovaleski, K. M., and Natan, M. J. (1998) *J. Phys. Chem. B.* **102**, 9404-9413.

Kickelbick, G (2003) *Prog. Polym. Sci.* **28**, 83-114.

Klaus,T., Joerger, R., Olsson, E., and Granqvist, C.G. (1999) *Proc. Natl. Acad. Sci.* **96**,13611-13614.

Klaus-Joerger,T., Joerger, R., Olsson, E., and Granqvist, C.G. (2001) *Trends Biotechnol.*,**19**, 15-20.

Koeller, K. M., and Wong, C. H. (2001) *Nature* **409**, 232-240.

Kreuter, J. Et al (2003) *Pharm. Res.* **20**, 409-416.

Kumar, A., Mukherjee, P., Guha, A., Adyantaya, S. D., Mandale, A. B., Kumar, R., and Sastry, M. (2000) *Langmuir* **16**, 9775-9783.

Kumar, C. V., and McLendon, G. L. (1997) *Chem. Mater.* **9**, 863-870.

Kurz, A., Halliwell, C. M., Davis, J., Hill, H. A. O., and Canters, G.W. (1998) *Chem. Commun.* **433**-434.

Lasic, D. D (1997) *Nature*, **387**, 26-27.

Leff, D. V., Brandt, L., and Heath, J. R. (1996) *Langmuir* **12**, 4723-4730.

Lei, C., Shin, Y., Lui, J., and Ackerman, E. J. (2002) *J. Am. Chem. Soc.* **124**, 11242-11243.

Li, J., Wang, J., Gavalas, V. G., Atwood, D. A., and Bachas, L. G. (2003) *Nano. Lett.* **3**, 55-58.

Liu, T., Burger, C., and Chu, B (2003) *Prog. Polym. Sci.* **28**, 5-26.

Livage, J., Coradin, T., and Roux, C. J. (2001) *J. Phys.: Condes. Matter.* **13**, R673-R691.

Loidl-Stahlhofen, A., Schmitt, J., Noller, J., Hartmann, T., Brodowsky, H., Schmitt, W., and Keldenich, J. (2001) *Adv. Mater.* **13**, 1829-1834.

Lopez, G. P., Albers, M. W., Schreiber, S. L., Carroll, R., Peralta, E., and Whitesides, G. M. (1993) *J. Am. Chem. Soc.* **115**, 5877-5878.

Martin, C. R. (1996) *Chem. Mater.* **8**, 1739-1746.

Mattoussi, H., Mauro, J.M., Goldman, E.R., Anderson, G. P., Sundar, V.C., Mukelec, F.V., and Bavendi, M.G. (2000) *J. Am. Chem. Soc.* **122**, 12142-12150.

Mirkin, C. A., Lestinger, R. L., Mucic, R.C., and Storhoff, J.J., (1996) *Nature* (London), **382**, 607-609.

Mitchell, D. T., Lee, S. B., Trofin, L., Li, N., Nevanen, T. K., Soderlund, H., and Martin, C. R. (2002) *J. Am. Chem. Soc.* **124**, 11864-11865.

Molina-Bolivar, J. A., and Ortega-Vinuesa, J. L. (1999) *Langmuir*. **15**, 2644-2653.

Mouritesen, O. G., and Bloom, M. 1984., Biophys J.,46,141-153

Mozhaev, V. V. (1993) *Trends Biotechnol.* **11**, 88-95.

Mrksich, M., Sigal, G. B., and Whitesides, G. M. (1995) *Langmuir* **11**, 4383-4385.

Mucic, R.C., Storhoff, J.J., Mirkin, C.A., and Letsinger, R.l. (1998) *J. Am. Chem. Soc.* **120**, 12674-12675.

Mukherjee, P., Senapathi, S., Mandal, D., Ahmad, A., Khan, M.I., Kumar, R., and Sastry, M. (2002) *Chem. Bio. Chem.* **3**, 461-463.

Mukherjee, P., Ahmad, A., Mandal, D., Senapathi, S., Sainkar, S. R., Khan, M.I., Parischa, R., Ajaykumar, P.V., Alam, M., Kumar, R., and Sastry, M. (2001b) *Nano. Lett.* **1**, 515-519.

Mukherjee, P., Ahmad, A., Mandal, D., Senapathi, S., Sainkar, S. R., Khan, M.I., Ramani, R., Parischa, R., Ajaykumar, P.V., Alam, M., Sastry, M., and Kumar, R. (2001a) *Angew. Chem. Int. Ed.*, **40**, 3585-3588.

Nair, B., and Pradeep, T. (2002) *Cryst. Growth Des.* **2**, 293-298.

Neimeyer, C. M., and Ceyhan, B. (2001) *Angew. Chem. Int. Ed*. **40**, 3685-3688.

Nick Pace, C., vajdos, F., Fee, L., and Grimsley, Gray, T. (1995) *Protein Science* **4**, 2411-2423.

Nicolini, C., Erokhin, V., Antolini, F., Catasti, P., and Facci, P. (1993) *Biochim. Biophys. Acta.* **1158**, 273-278.

Niemeyer, C. (2001) *Angew. Chem. Int. Ed.* **40**, 4128-4158

Niemeyer, C. M., and Mirkin C. A (Eds) (2004) *Nanobiotechnology, concepts, applications and perspectives* Wiley-VCH verlag GmbH and Co.

Odom, T.W., Huang, J.L., Kim, P., and Lieber, C. M. (2000) *J. Phys. Chem B*, **104**, 2794-2809.

Okahata, O., Kobayashi, T., and Tanak, K. (1996) *Langmuir*,**12**, 1326-1330.

Orive, G., Hernandez, R. M., Gascon, A. R., Igartua, M., and Pedraz, J. L. (2002) *Trends Biotechnol.* **9**, 382-387.

Ortnwall, P.,Wandenwick, H., Kutti, J., and Risberg, B. (1987) *J. Vasc. Surg.* **6**, 17-25.

Park, S. A., Taton, T. A., and Mirkin, C. A. (2002) *Science* **295**, 503-1506.

Patil, V., Malvankar R. B., and Sastry, M. (1999) *Langmuir* **15**, 8197-8206.

Patolsky, F., Gabriel, T., and Willner, I. (1999) *J. Electroanalytical Chem.* **479**, 69-73.

Pease, A.C., Solas, D., Sullivan, E.J., Cronin, M.T., Holmes, C.P., and Foder, S.P.A. (1994) *Proc. Natl. Acad. Sci. USA*, **91**, 5022-5026.

Phadtare, S., Kumar, A., Vinod, V. P., Dash, C., Palaskar, D. V., Rao, M., Shukla, P. G., Sivaram, S., and Sastry, M (2004) *Chem. Mater.* **15**, 1944-1949.

Phadtare, S., Parekh, P., Shash, S., Tambe, A., Joshi, R., Sainker, S. R., Prabhune, A., and Sastry, M. (2003) *Biotechnol. Progr.* **19**, 1659-1663.

Prouzet, E., and Pinnavaia, T. J. (1997) *Angew. Chem. Int. Ed.* **36,** 516-518.

Punt, P.J., van Biezen, N., Conesa, A., Albers, A., Magnus, J., and van den Hondel, C. (2002) *Trends. Biotechnol.*, **20**, 200-206.

Qhoboshean, M., Santra, S., Zhang, P., and Tan, W. (2001) *Analyst* **126**, 1274-1278.

Quake,S.R., and Scherer, A. (2000) *Science* **290**, 1536-1540.

Ramsay, G. (1998) *Nat. Biotechnol.* **16**, 40-44.

Ramsden, J.J. (1998) *Biosens. Bioelectron.* **13**, 593-598.

Rembaum, A., and Dreyer, W. J. (1980) *Science* **208**, 364-368.

Roy, I et al., (2003) *J. Am. Chem. Soc.* **125**, 7860-7865.

Sackmann, E. (1996) *Science.* **271**, 43-48.

Salamon, Z., and Tollin, G. (1996) *Biophys. J.* **71**, 848-857.

Sanders, G.H.W., and Manz, A. (2000) *Trends Anal. Chem.* **19**, 364-378.

Sastry, M. (2002) *Trends Biotech.* **20**, 185-189 and references therein.

Sastry, M., Kumar, A., and Mukherjee, P. (2001) *Coll. Surf. A.* **181**, 255-259.

Sastry, M., Rao. M., and Ganesh KN. (2002) *Acc. Chem. Res.* **35**, 847-855 and references therein.

Schimid, A., Dordick, J. S., hauer, B., Kiener, A., Wubbolts, M., and Witholts, B. (2001) *Nature* **409**, 258-268.

Schmitt, A., Fernandez-Barbero, A., Cabrerizo-Vilchez, M., and Hidalgo-Alvarez, R. (1997) *Prog. Colloid Sci.* **104**, 144-147.

Selvakannan, P. R., Mandal, S., Pasricha, R., Adyantha, S. D, and Sastry, M. (2002) *Chem. Commun.* 1334-1335.

Selvakannan, PR., Senthil Kumar, P., More, A. S., Shingte, R. D., Wadgaonkar, P.P., and Sastry, M. (2004) *Adv. Mater.* **16**, 966-971.

Shim, M., Kam, N., Chen, R.J., Li, Y., and Dai, H. (2002) *Nano Lett.* **2**, 285-288.

Shimomura, M., Nakamura, F., Ijiro, K., Taketsuna, H., Tanak, M., Nakamura, H., and Hasebe, K. (1997) *J. Am. Chem. Soc.* **119**, 2341-2342.

Singhvi, R., Kumar, A., Lopez, G. P., Stephanopoulos, G. N., Wang, D. I. C., Whitesides, G.M., and Ingeber, D.E. (1994) *Science* 264, 696-698.

Sotiropoulou, S., and Chaniotakis, N.A. (2003) *Anal Bioanal Chem*. **375**, 103-105.

Southam, G., and Beveridge, T.J. (1996) *Geochim. Cosmochim Acta.* **60**, 4369-4376.

Steel, A.B., Herne, T.M., and Tarlov, M.J. (1998) *Anal. Chem.* **70**, 4670-4677.

Stenger, D. A., Georger, J. H., Dulcey, C. S., Hickman, J. J., Rudolph, A. S., Nielsen, T. B., McCort, S. M., and Calvert, J. M. (1992) *J. Am. Chem. Soc.* **114**, 8435-8442.

Stonehuerner, J. G., Zhao, J., O'Daly, J. P., Crumbliss, A. L., and Henkens, R. W. (1992) *Biosens. Bioelectron.* **7**, 421-428.

Stoscheck, C.M. (1990) *Meth. Enzymol.* **182**, 50-68.

Takahashi, H., Li, B., Sasaki, T., Miyazaki, C., Kajino, T., and Inagaki S. (2000) *Chem. Mater.* **12**, 3301-3305.

Tanford, C., (1980) The Hydrophobic Effect: Formation of Micelles and Biological Membrane, Wiley-Interscience: New York

Tang, J., and Hartley, B.S. (1970) *Biochem. J.* **118**, 611-623.

Tischer, W., and Kasche, V (1999) *Trends. Biotechnol.* **17**, 326-335.

Tischer, W., and Wedekind, F. (1999) *Biocatalysis-from discovery to application;* Fessner, W. D., Ed; Springer-Verlag: Berlin, **200**, 95-126.

Tischer, W., and Wedekind, F. (1999) *Top. Curr. Chem.* **200**,95-126.

Tripathi, P. K., et al (2002) *Pharmazie.* **57**, 261-264.

Tsang, S.C., Davis, J.J., Green, M., Hill, A., Leung, Y.C., and Sadlor, P.J. (1995) *J Chem Soc Chem Commun.* 1803-1804.

Tsang, S.C., Guo, Z., Chen, Y.K., Green, M., Hill, A., Hambley, T. W., and Sadlor, P.J. (1997) *Angew Chem Int Ed Engl*, **36**, 2198-2200.

Voskerician, G., Shive, M. S., Shawgo, R. S., von Recum, H., Anderson, J. M., Cima, M. J., and Langer, R (2003) *Biomaterials* **24**, 1959-1967.

Wang, J., Neilsen, P.E., Jiang, M., Cai, X., Fernandez, J.R., Grant, D.H., Ozsoz, M., Begleiter, A., and Mowat, M. (1997) *Anal. Chem.*, **69**, 5200-5202.

Wilchek, M., and Bayer, E. A (1990) *Methods Enzymol.* , **184**, 51-67

Willner, I., Rikline, A., Shoham, B., Rivenzon, D., Katz, E (1993) *Adv. Mater.* **5**, 12-915

Xu, J., Battacharya, P., and Birge, R. (2001) *Electronics Lett.* **37**, 648

Xu, J., Battacharya, P., G. Varo., Hillebrecht, J., and Birge, R. (2004) *Biosensors and Bioelectronics* **19**, 885

Yang, Z., Mesiano, A. J., Venkatasubramanian, S., Gross, S. H., and Russel, A. J. (1995) *J. Am. Chem. Soc.* **117**, 4843-4850.

Yousaf, M. N., Houseman, B. T., and Mrksich. M. (2001) *Proc. Natl. Acad. Sci.* **98**, 5992-5996

Zhao, J., O'Daly, J. P., Henkens, R. W., Stonehuerner, J., and Crumbliss, A. L. (1996) *Biosens. Bioelectron.* **11**, 493-502.